THE UNIVERSITY
OF MICHIGAN
JUN 18 1959
ENGINEERING
LIBRARY

JOURNAL OF FLUID MECHANICS

VOLUME 5 PART 4

MAY 1959

PUBLISHED BY

CAMBRIDGE UNIVERSITY PRESS

BENTLEY HOUSE, 200 EUSTON ROAD, LONDON, N.W. 1

AMERICAN BRANCH: 32 EAST 57TH STREET, NEW YORK 22, N.Y.

Price 30*s.* (*U.S.A.* $5.00)

The JOURNAL OF FLUID MECHANICS exists for the publication of theoretical and experimental investigations of all aspects of the mechanics of fluids, and is issued in four parts per volume.

EDITOR

DR G. K. BATCHELOR

Cavendish Laboratory, University of Cambridge, Cambridge, England

ASSISTANT EDITORS

DR T. B. BENJAMIN, DR I. PROUDMAN, DR P. G. SAFFMAN

Cavendish Laboratory, University of Cambridge, Cambridge, England

ASSOCIATE EDITORS

PROF. G. F. CARRIER

Pierce Hall, Harvard University, Cambridge 38, *Massachusetts, U.S.A.*

DR W. C. GRIFFITH

Research and Development Laboratory, Missile Systems Division, Lockheed Aircraft Corporation, Palo Alto, California, U.S.A.

PROF. M. J. LIGHTHILL

Department of Mathematics, The University, Manchester, England

PROF. R. R. LONG

School of Engineering, The Johns Hopkins University, Baltimore 18, *Maryland, U.S.A.*

Authors wishing to have papers published in the JOURNAL should communicate them to any one of the persons named above, choosing one in their own country where possible.

Authors are urged to ensure that their papers are written clearly and attractively, in order that their work will be readily accessible to readers.

Manuscripts should be typed in double spacing on one side of the paper only, with references listed at the end in alphabetical order of authors. Drawings should be done on a large scale in Indian ink on tracing cloth or drawing paper, the lettering being shown clearly in pencil for reproduction by the printer; the list of captions should be typed at the end of the manuscript. Proofs of papers from overseas will usually be despatched to authors by airmail. There is no charge for publication. Authors are entitled to receive 50 offprints of a paper in the JOURNAL free of charge, and additional offprints can be purchased if ordered in advance.

SUBSCRIPTIONS

The subscription price for a volume of four parts is £5. 10*s*. net, post free, payable in advance; separate parts 30*s*. net, plus postage. Subscriptions may be sent to any bookseller, or to the Cambridge University Press, Bentley House, 200 Euston Road, London, N.W.1.

Subscribers in the United States should send their orders to the Cambridge University Press, American Branch, 32 East 57th Street, New York 22. The subscription price per volume is $18.50, post free, payable in advance; separate parts $5.00, plus postage.

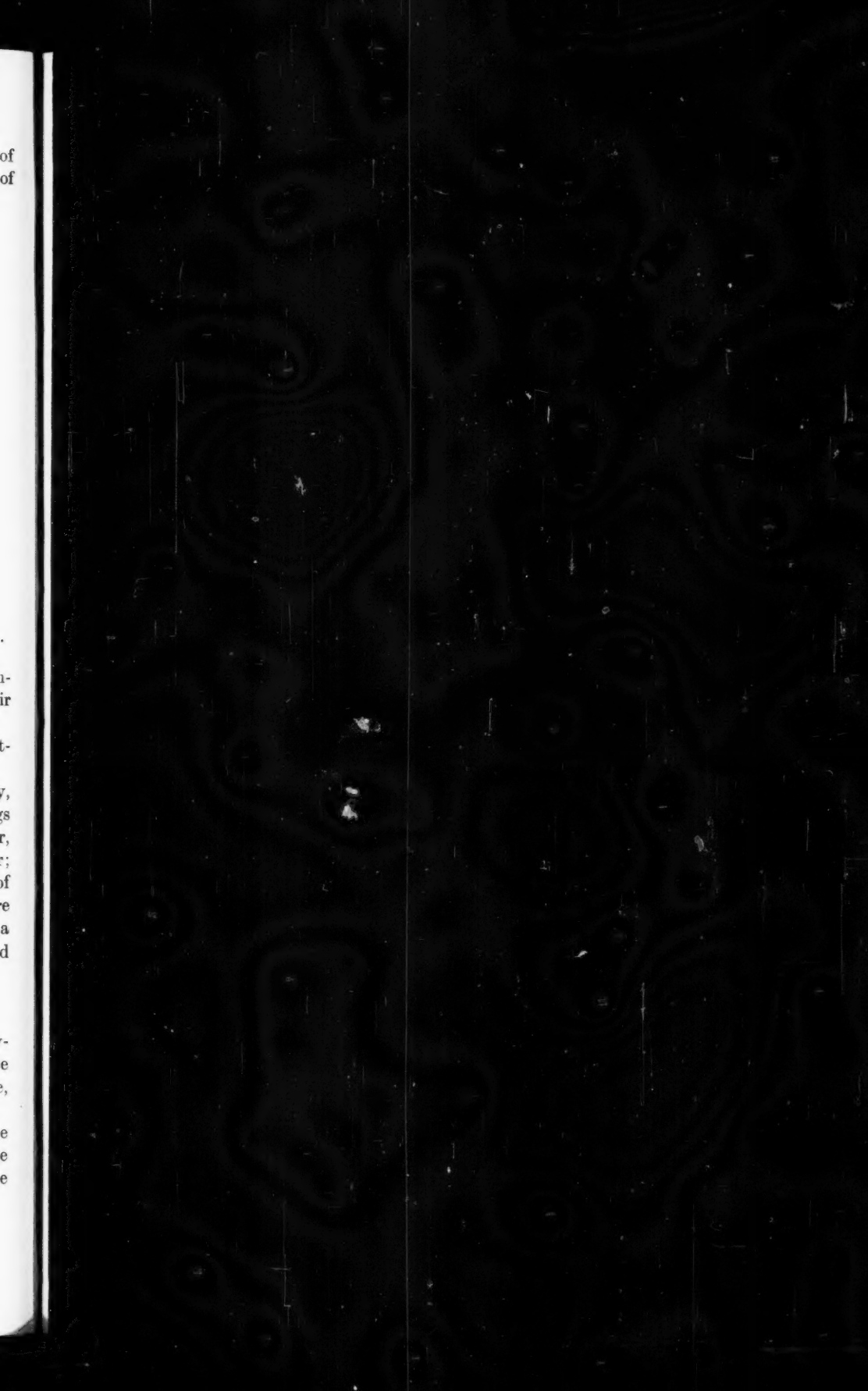

The structure of isotropic turbulence at very high Reynolds numbers

By ROBERT H. KRAICHNAN
Institute of Mathematical Sciences, New York University, New York 3

(Received 24 February 1958 and in revised form 1 October 1958)

A recapitulation is first given of a recent theory of homogeneous turbulence based on the condition that the Fourier amplitudes of the velocity field be as randomly distributed as the dynamical equations permit. This theory involves the average infinitesimal-impulse-response functions of the Fourier amplitudes and employs a new kind of perturbation method which yields what are believed to be exact expansions of third- and higher-order statistical moments of the Fourier amplitudes in terms of second-order moments and these response functions.

In the present paper the theory is applied in lowest approximation (called the direct-interaction approximation) to stationary isotropic turbulence of very high Reynolds number. The characteristic wave-number $k_0 = \epsilon/v_0^3$ and Reynolds number $R_0 = v_0 k_0^{-1}/\nu$, where v_0 is the r.m.s. velocity in any given direction, ϵ is the power dissipated per unit mass, and ν is the kinematic viscosity, are introduced. For $R_0^{\frac{1}{4}} \gg 1$, it is found that the inertial and dissipation ranges extend over wave-numbers k satisfying $k_0 \ll k \ll R_0 k_0$. The time-correlation and average infinitesimal-impulse-response functions of the Fourier amplitudes in these ranges are evaluated. They are found to be asymptotically identical and given by $J_1(2v_0 k\tau)/v_0 k\tau$, where τ is the time interval.

The energy spectrum in these ranges is determined by a non-linear integral equation, involving the time-correlation and response functions, which is suitable for solution by iteration. The solution is of the form $E(k)/v_0\nu = (k/k_d)^{-\frac{3}{2}} f(k/k_d)$, where $E(k)$ is the three-dimensional spectrum function, $k_d = R_0^{\frac{3}{4}} k_0$ is a wave-number characterizing the dissipation range, and $f(k/k_d)$ is a universal function. In the inertial range, $E(k) = f(0)(\epsilon v_0)^{\frac{1}{2}} k^{-\frac{3}{2}}$, asymptotically. The parameter $f(0)$ can be obtained by quadratures, without solving the integral equation for $E(k)$. Spectral energy transport throughout the inertial and dissipation ranges is found to proceed by a cascade process essentially local in wave-number space; the direct power delivered by all modes below k to all modes above $k' \gg k$ is of order $\epsilon(k/k')^{\frac{4}{3}}$ if k and k' both lie within the inertial range. The mean-square velocity derivatives of all orders are found to be finite. For $R_0^{\frac{1}{4}} \gg 1$ the skewness factor of the distribution of the nth-order longitudinal velocity derivative is found to have the asymptotic form $A_n R_0^{-\frac{1}{4}}$, where A_n is a universal constant.

The theory is compared with experiment and is found to be slightly better supported than the Kolmogorov theory. However, it is stressed that extreme caution must be exercised in interpreting the experimental evidence as support for either theory.

An analysis is given of the relations between the Kolmogorov theory, Heisenberg's heuristic theory, the analytical theories of Heisenberg and Chandrasekhar, the theories of Proudman & Reid and Tatsumi, and the present theory.

Contents

		PAGE
1.	Introduction	498
2.	Foundations of the theory	500
	2.1. The maximal randomness condition	500
	2.2. The weak dependence principle	503
	2.3. The perturbation method	504
	2.4. The direct-interaction approximation	508
3.	Statistical equations for stationary isotropic turbulence	510
4.	The spectral transport of energy	513
5.	Response and time-correlation functions for high wave-numbers	515
	5.1. The response function	515
	5.2. The time-correlation function	518
6.	The inertial range	519
7.	The dissipation range at huge Reynolds numbers	522
	7.1. The energy-balance integral equation	522
	7.2. Behaviour in the far dissipation range	523
	7.3. Skewness factors for the longitudinal velocity derivatives	525
	7.4. Qualitative discussion of the dynamics	526
8.	Comparison with experiment	527
	8.1. The effect of deviations from idealized conditions	527
	8.2. Wave-number spectra in turbulent pipe flow	529
	8.3. Wave-number spectra in grid turbulence	532
	8.4. The response and time-correlation functions	534
9.	Comparison with other theories	535
	9.1. The Kolmogorov theory	535
	9.2. Heisenberg's heuristic theory	538
	9.3. The analytical theories of Heisenberg and Chandrasekhar	539
	9.4. The theories of Proudman & Reid and Tatsumi	541
	References	543

1. Introduction

An attempt has been made recently to develop an exact theory of homogeneous turbulence in which all the statistical moments of the velocity field are derived analytically from the Navier–Stokes equation (Kraichnan, 1958*a*, *b*; the first reference will be cited as Paper I). In the present paper an approximation to this theory is used to examine the energy dynamics and the spectral structure, with respect to both frequency and wave-number, of the inertial and dissipation ranges of very-high-Reynolds-number stationary, isotropic turbulence. The statistical equations of motion for the stationary isotropic case obtained in Paper I are not rederived here, but we shall preface our investigation with a recapitulation, and, in part, an amplification, of the foundations of the theory. This seems especially advisable since the foundations have undergone considerable evolution since the writing of Paper I; in particular, that paper contains an important misconception. A full account of the basic theory in its present state

will be given elsewhere. In discussing it here, the emphasis will be upon illuminating the principles involved, and no attempt at rigorous or complete treatment will be made.

The essential difficulties of the turbulence problem arise from the strongly dissipative character of the dynamical system and the non-linearity of the equations of motion. The first of these two characteristics effectively precludes treatment by conventional methods of statistical mechanics. The second is responsible for the fact that the Navier–Stokes equation does not yield closed differential equations for the velocity covariance, the statistical quantity of principal interest. The equations of motion for this covariance contain third-order moments of the velocity field, the equations of motion for the third-order moments contain fourth-order moments, and so forth, *ad infinitum*. A central goal of turbulence theory is the closing of this infinite chain of coupled equations into a determinate set containing only moments below some finite order.

Closure has been obtained in a number of previous treatments of homogeneous turbulence by the assumption of expressions, in terms of second-order moments, for either third-order moments (Obukhov 1941; Heisenberg 1948; von Kármán 1948; Kovásznay 1948) or fourth-order moments (Millionshtchikov 1941; Heisenberg 1948; Proudman & Reid 1954; Chandrasekhar 1955; Tatsumi 1957). The assumptions made were justified on heuristic grounds, on the basis of experimental indications, or on grounds of mathematical simplicity.

In the present approach no *ad hoc* assumption relating higher-order to lower-order moments is made. The velocity field within a very large volume is represented by Fourier series amplitudes $u_i(\mathbf{k}, t)$, which are considered to be the fundamental dynamic variables. In addition to the moments of the many-time joint-distribution of all the Fourier amplitudes, the average impulse-response tensors of the Fourier modes are introduced. These quantities, which do not appear in the treatments cited in the last paragraph, describe the relaxation of arbitrary infinitesimal impulsive disturbances of individual vector Fourier amplitudes. The fundamental condition imposed is that the statistical dependence among the Fourier amplitudes is induced wholly by the non-linear terms in the Navier–Stokes equation and not at all by the initial conditions or by the external forces which may be acting. This condition, which we term that of maximal randomness, implies statistical homogeneity, and is more restrictive than that condition. It appears to be the simplest condition strong enough to give, in principle, a closeable statistical theory from the Navier–Stokes equation, and it seems logically indicated when the mechanism by which the turbulence is produced or maintained is not explicitly described.

Maximal randomness and certain qualitative features of the Navier–Stokes equation lead to the principle of weak dependence of the Fourier amplitudes. The essential qualitative content of this principle is that the effective dynamical coupling and statistical interdependence among any few individual Fourier amplitudes corresponding to different wave vectors is very weak when the flow volume is very large. The substantial departure from normality of the velocity distribution in x-space appears as the summed effect of very many of these very weak statistical dependence

The weak dependence principle leads to a perturbation treatment of the dynamical couplings among sets of individual Fourier amplitudes which differs importantly from conventional perturbation theory based on expansion in powers of the Reynolds number. This treatment yields what are believed to be exact infinite-series integral representations of all higher-order moments in terms of the second-order moments and the average impulse-response tensors. Integral equations fixing the second-order moments and the impulse-response tensors may then be obtained; they involve the representations for the third-order moments. If the representations are exact, these equations are also.

In order for the theory to be used, the infinite-series representations must be approximated. In the present paper, as in Paper I, the series for the third-order moments are approximated by their lowest terms. This procedure, which we term the direct-interaction approximation, has a simple dynamical significance and can be shown to lead to equations which are self-consistent in the sense that they yield rigorously realizable second-order moments. The direct-interaction approximation includes terms of all orders in an expansion in powers of the Reynolds number. It is the lowest of a sequence of self-consistent and dynamically interpretable approximations which, it is believed, should converge to yield exact and complete solutions of the statistical problem. The higher approximations involve closure of the moment-equation heirarchy at higher levels. Each successive approximation is based on new perturbation expansions, the lowest terms of which represent terms of all orders in the expansions used in the immediately preceding approximation. In each case, only these lowest terms are retained.

The reader who is not interested in the foundations of the present theory, but only in its application, may start this paper with § 3. In this case the fundamental relations (3.7) and (3.11) may be regarded simply as an assumption about the form of the triple moments, analogous to those in the theories cited previously. The essential physical interpretation of this assumption, from the point of view of its consequences for the transport of energy, is then brought out in the discussion following equation (4.3).

2. Foundations of the theory

2.1. *The maximal randomness condition*

Let us consider a fluid confined in a cubical box of side L. Instead of requiring that the velocity vanish at the walls we shall employ the well-known artifice of cyclic boundary conditions; later, this will permit the description of rigorously statistically homogeneous flows. The velocity field $\tilde{u}_i(\mathbf{x}, t)$ may be expanded in a Fourier series

$$\tilde{u}_i(\mathbf{x}, t) = \sum_{\mathbf{k}} u_i(\mathbf{k}, t)\, e^{i\mathbf{k}\cdot\mathbf{x}}, \tag{2.1}$$

where the summation is over all wave-vectors permitted by the boundary conditions. For compactness, we shall often write $\mathbf{u}(\mathbf{k})$ for $\mathbf{u}(\mathbf{k}, t)$, $\mathbf{u}'(k)$ for $\mathbf{u}(\mathbf{k}, t')$, etc. The reality of $\tilde{u}_i(\mathbf{x})$ requires $u_i(-\mathbf{k}) = u_i^*(\mathbf{k})$. In terms of the Fourier amplitudes, the Navier–Stokes equation takes the form

$$\left(\frac{\partial}{\partial t} + \nu k^2\right) u_i(\mathbf{k}) = -\frac{i}{2} P_{ijm}(\mathbf{k}) \sum_{\mathbf{k}'+\mathbf{k}''=\mathbf{k}} u_j(\mathbf{k}')\, u_m(\mathbf{k}''), \tag{2.2}$$

where ν is the kinematic viscosity and the tensor operator

$$P_{ijm}(\mathbf{k}) = k_m P_{ij}(\mathbf{k}) + k_j P_{im}(\mathbf{k}), \quad P_{ij}(\mathbf{k}) = \delta_{ij} - k^{-2} k_i k_j,$$

serves to include both Reynolds stresses and pressure forces. The latter maintain the incompressibility property

$$k_i u_i(\mathbf{k}) = 0. \tag{2.3}$$

We regard the amplitudes $\mathbf{u}(\mathbf{k})$ as the fundamental dynamic variables. Formulation of the flow problem in terms of Fourier series rather than Fourier integrals is preferred because it seems to be easier to think of dynamic variables in intuitive terms when they form a discrete set.

In all of the following we shall assume that there is no mean flow, so that $\mathbf{u}(0,t) = 0$.

Let us imagine that at $t = t_0$ an arbitrary infinitesimal solenoidal perturbing force-term $\xi_i(\mathbf{k})$ is introduced on the right side of (2.2), for a single wave-vector $\mathbf{k}$. We may expect that the perturbation induced in $\mathbf{u}(\mathbf{k})$ will be of the form

$$\delta u_i(\mathbf{k}, t) = \int_{t_0}^{t} \zeta_{ij}(\mathbf{k}; t, t') \xi_j(\mathbf{k}, t')\, dt', \tag{2.4}$$

where $\zeta_{ij}(\mathbf{k}; t, t')$ is the infinitesimal-impulse-response tensor for mode $\mathbf{k}$. (We shall sometimes use the abbreviation $\zeta_{ij}(\mathbf{k})$.) If the dynamical equations were linear and time-independent, the impulse-response would be a function only of $\mathbf{k}$ and $t - t'$. Since actually (2.2) is essentially non-linear, $\zeta_{ij}(\mathbf{k}; t, t')$ is really an implicit functional of all the Fourier amplitudes at all times between t' and t. It expresses the relaxation of an infinitesimal impulsive disturbance (imposed at t') through the joint action of viscosity and the non-linear interaction. The determination of the $\zeta_{ij}(\mathbf{k})$ is in general not less of a problem than finding the $\mathbf{u}(\mathbf{k})$ themselves. The impulse-response tensors play an essential role in the theory to be described.

Now let us take L very large compared to any characteristic length scale of the flow and consider the limit $L \to \infty$. For any flow of physical interest we may expect that in any excited wave-vector range, no matter how small, the excitation will be spread over an infinite number of individual modes in the limit. Hereafter we shall admit to consideration only such flows. This property leads to a dynamical consequence of basic importance. Any given wave-vector $\mathbf{p}$ appears in only two terms on the right of (2.2), once as $\mathbf{k}'$ and once as $\mathbf{k}''$. In the limit $L \to \infty$ these two terms can make only an infinitesimal contribution to the summation, and hence to the time dependence of $\mathbf{u}(\mathbf{k})$ and $\zeta_{ij}(\mathbf{k})$. This suggests that the effective dynamical coupling between $\mathbf{u}(\mathbf{k})$ and $\mathbf{u}(\mathbf{p})$ ($\mathbf{k} \neq \pm \mathbf{p}$) becomes infinitely weak as $L \to \infty$. By an extension of the argument, the effective dynamical coupling among any finite set of Fourier amplitudes corresponding to distinct wave-vectors becomes infinitely weak in the limit. (We shall call a set of wave-vectors distinct when they contain no pair $\mathbf{p}$, $\mathbf{q}$ such that $\mathbf{p} = \pm \mathbf{q}$.)

So far our considerations have been non-statistical. Now, in order to describe turbulence, we introduce averages $\langle\ \rangle$ over products of the $\mathbf{u}(\mathbf{k})$ and $\zeta_{ij}(\mathbf{k})$. The averages which appear in the present paper are to be interpreted as over an ensemble of flows, in accordance with the most usual practice in statistical

mechanics. However, for the statistically homogeneous systems which are to be treated we consider it more physical to define averages in terms of a single system (the actual physical one) by taking them over the infinitely many modes contained in appropriately chosen tiny neighbourhoods in k-space, in the limit $L \to \infty$. This single-system average corresponds closely to the experimental procedure of determining spectral quantities; we shall discuss its advantages further in a later paper. If the choice of ensemble is physically appropriate, the two kinds of average should be interchangeable for $L \to \infty$.

The fundamental restriction we shall impose on the flow is that the statistical dependence among the $\mathbf{u}(\mathbf{k})$ be induced wholly by the non-linear terms in (2.2) and not at all by initial conditions or any external forces, representable by additional terms in (2.2), which may be acting. We shall call this the maximal randomness condition. In the present paper we shall also include under this title the symmetry conditions that the real and imaginary parts of $\mathbf{u}(\mathbf{k})$ have zero means, identical auto-covariances, and are uncorrelated. Now complete statistical independence of the $\mathbf{u}(\mathbf{k})$, together with our symmetry conditions, implies statistical homogeneity.† Since the Navier–Stokes equation is invariant under translation it cannot of itself induce inhomogeneity. Hence, we may anticipate that maximal randomness restricts us to statistically homogeneous flows. The restriction actually is much more severe. Consider a flow consisting initially of an infinite array of identical vortices with centres placed at random. It is statistically homogeneous, but it is excluded because at any finite time of evolution it will display statistical dependencies among distinct wave-vectors due to the far-from-maximally random initial conditions.

The notion of maximal randomness seems to be implicit in many theoretical treatments of turbulence; few workers would call the flow just described 'homogeneous turbulence'. We believe, however, that *explicit* appeal to this condition, or one of equivalent strength, is necessary to pose a statistical problem which is closeable even in principle. For certainly there can exist statistically homogeneous flows with a given wave-number spectrum, at some given time in their evolution, but with widely different higher statistical structures. None of these flows is excluded simply by the usual procedure of taking averages of the Navier–Stokes equation, and the future history of the various flows surely will be influenced by the differences in higher structure. Maximally random flow is a considerable idealization of laboratory homogeneous turbulence. But unless the mechanism which generates or maintains the turbulence is explicitly described by additional terms in (2.2), our condition appears to be the most reasonable way to pose a physically and mathematically determinate problem. It should be noted that maximal randomness is *not* a condition on the Reynolds number, although the correspondence to laboratory flows probably is closer at higher Reynolds numbers.

† Invariance of averages of $\mathbf{x}$-space quantities under translation is implied by the vanishing of all averages $\langle u_i(\mathbf{k})\, u_j'(\mathbf{p}) \ldots \rangle$ unless $\mathbf{k}+\mathbf{p}+\ldots = 0$. Our symmetry conditions give $\langle u_i(\mathbf{k})\, u_j'(\mathbf{k}) \rangle = 0$. Averages in which a given $\mathbf{u}(\mathbf{k})$ appears more than bilinearly cannot contribute to $\mathbf{x}$-space averages when $L \to \infty$, for the spectrally dense flows to which we have already restricted attention.

2.2. *The weak dependence principle*

We have already noted the property of weak dynamical coupling among any finite set of Fourier amplitudes in the limit $L \to \infty$. Under the maximal randomness condition, statistical interdependence among the $\mathbf{u}(\mathbf{k})$ can arise only from these weak couplings. We are led to conjecture that in this case the statistical dependencies among any finite set of $\mathbf{u}(\mathbf{k})$ become infinitely weak in the limit. A corollary is that the statistical dependencies among both the $\mathbf{u}(\mathbf{k})$ and the $\zeta_{ij}(\mathbf{k})$ for distinct wave-vectors become infinitely weak. We shall call these conjectures the weak dependence principle and state them more formally as follows.

Let the normalized Fourier amplitudes be defined as the quantities

$$\mathbf{u}(\mathbf{k})/\langle|\mathbf{u}(\mathbf{k})|^2\rangle^{\frac{1}{2}}.$$

Then, all moments of the many-time distribution of the response tensors and normalized Fourier amplitudes belonging to any finite set of $\mathbf{k}$'s tend in the limit $L \to \infty$ to values belonging to some distribution in which all quantities associated with distinct $\mathbf{k}$'s are statistically independent.

The following typical examples will serve to illustrate the principle. Let $\mathbf{k}$, $\mathbf{p}$, $\mathbf{q}$ be three distinct wave-vectors. Then weak dependence requires

$$\frac{\langle u_i(\mathbf{k})\, u_j'(\mathbf{p})\, u_m''(\mathbf{q})\rangle}{[\langle|\mathbf{u}(\mathbf{k})|^2\rangle\langle|\mathbf{u}'(\mathbf{p})|^2\rangle\langle|\mathbf{u}''(\mathbf{q})|^2\rangle]^{\frac{1}{2}}} \to 0 \quad (L \to \infty). \tag{2.5}$$

As a second example we have

$$\langle u_i'(\mathbf{k})\, u_j(-\mathbf{k})\, u_m'(\mathbf{p})\, u_n(-\mathbf{p})\rangle \to \langle u_i'(\mathbf{k})\, u_j(-\mathbf{k})\rangle\langle u_m'(\mathbf{p})\, u_n(-\mathbf{p})\rangle \quad (L \to \infty). \tag{2.6}$$

It is extremely important to distinguish clearly between weak dependence, which can be defined only in terms of a limiting process, and independence of the Fourier amplitudes, certain restricted consequences of which have been assumed by Millionshtchikov (1941), Heisenberg (1948), Proudman & Reid (1954), Chandrasekhar (1955), Tatsumi (1957), and other authors. It is known experimentally that the full probability distribution of the velocity field is far from normal (Batchelor 1953). In particular, the skewness and flatness factors of the difference between the velocities at two points depart from normal values. As a complement to the experimental evidence, it is clear from the Navier–Stokes equation that non-vanishing triple moments are necessary for mean energy transfer, and it has been shown from this equation that the relation of fourth-order to second-order moments is non-normal (Kraichnan 1957). By the central limit theorem, these facts are inconsistent with independence of the $\mathbf{u}(\mathbf{k})$ in the limit $L \to \infty$. However, they are wholly consistent with weak dependence. Consider the moment $M = \langle(\partial\tilde{u}_1/\partial x_1)^3\rangle$ which, when normalized, gives the skewness factor of the distribution of $\partial\tilde{u}_1/\partial x_1$. Expanding, and assuming homogeneity, we have

$$M = -i \sum_{\mathbf{k}+\mathbf{p}+\mathbf{q}=0} k_1 p_1 q_1 \langle u_1(\mathbf{k})\, u_1(\mathbf{p})\, u_1(\mathbf{q})\rangle. \tag{2.7}$$

Now consider the contribution from all terms with k, p, q below some arbitrary high wave-number K. As $L \to \infty$, corresponding to a larger and larger box of

turbulence, the number of allowed wave-vectors in this range varies as L^3 and the number of such terms as L^6. The quantities $\langle|\mathbf{u}(\mathbf{k})|^2\rangle$ vary as L^{-3}, since

$$\tfrac{1}{2}\sum_{\mathbf{k}}\langle|\mathbf{u}(\mathbf{k})|^2\rangle$$

is the energy per unit mass. Thus, M can approach a non-zero limit if the left side of (2.5) varies as $L^{-\frac{3}{2}}$, for $\mathbf{k}+\mathbf{p}+\mathbf{q}=0$.

The case of the moment $N=\langle(\partial\tilde{u}_1/\partial x_1)^4\rangle$, which determines the flatness factor of the distribution of $\partial\tilde{u}_1/\partial x_1$, is somewhat more complicated. Writing

$$N=\sum_{\mathbf{k}+\mathbf{p}+\mathbf{q}+\mathbf{m}=0} k_1p_1q_1m_1\langle u_1(\mathbf{k})\,u_1(\mathbf{p})\,u_1(\mathbf{q})\,u_1(\mathbf{m})\rangle, \tag{2.8}$$

we may break the sum on the right into a part in which $\mathbf{k}$, $\mathbf{p}$, $\mathbf{q}$, $\mathbf{m}$ are equal and opposite in pairs and a part in which they are not. It follows from (2.6) that as $L\to\infty$ the first part gives a contribution to N which by itself would yield the flatness factor 3, corresponding to a normal distribution of $\partial\tilde{u}_1/\partial x_1$. In an independent distribution of the $\mathbf{u}(\mathbf{k})$ the second part would contribute zero. With weak dependence, although the terms composing this part tend individually to zero, even when normalized, their total contribution need not, just as in the case of the terms contributing to (2.7).

The examples just treated suggest that weak dependence relations of the type (2.5) may represent necessary conditions for statistical homogeneity and boundedness of x-space moments. If relations of the type (2.6) are also consequences of homogeneity,† weak dependence can be viewed as a kinematical property without reference to the Navier–Stokes equation. Our point of view here is quite different. We regard both homogeneity and weak dependence as consequences obtained by dynamical considerations from the maximal randomness condition, and, as will be discussed in § 2.3, we find weak dependence to be the key *dynamical* property which permits actual evaluation of the cross-moments of the $\mathbf{u}(\mathbf{k})$. This is also the case in certain more general applications than those to be considered here, where the maximal randomness condition is not satisfied by the initial conditions.

2.3 *The perturbation method*

The evaluation of the cross-moments of the $\mathbf{u}(\mathbf{k})$ with the aid of the considerations developed above involves a perturbation method with features that appear to be novel in fluid mechanics. In order to bring out the distinctive characteristics of the method with greater clarity, we first shall illustrate how one might attempt to evaluate cross-moments by conventional perturbation techniques. Let us consider the moment

$$S=\langle u_n(\mathbf{k})\,u_r'(\mathbf{p})\,u_s'(\mathbf{q})\rangle \quad (\mathbf{k}+\mathbf{p}+\mathbf{q}=0), \tag{2.9}$$

where $\mathbf{k}$, $\mathbf{p}$, $\mathbf{q}$ are distinct wave-vectors. Moments of this type appear in the equations of motion for the covariance $\langle u_i'(-\mathbf{k})\,u_n(\mathbf{k})\rangle$. In accord with maximal randomness, let us assume that the flow is started at time t_0 with the $\mathbf{u}(\mathbf{k},t_0)$ independently and Gaussianly distributed and with specified values of the

† There is evidence that this is the case. However, we have not found discussions of relations of this type in the literature on statistical homogeneity.

quantities $\langle u_i(\mathbf{k}, t_0)\, u_j(-\mathbf{k}, t_0)\rangle$ for all $\mathbf{k}$. Let us denote by $\bar{\mathbf{u}}(\mathbf{k})$ the amplitudes which obey $\bar{\mathbf{u}}(\mathbf{k}, t_0) = \mathbf{u}(\mathbf{k}, t_0)$ and satisfy the linearized equation of motion

$$\left(\frac{\partial}{\partial t} + \nu k^2\right) \bar{u}_i(\mathbf{k}) = 0. \tag{2.10}$$

We may immediately solve for $\bar{\mathbf{u}}(\mathbf{k}, t)$ in terms of $\mathbf{u}(\mathbf{k}, t_0)$ and then express all the moments of the many-time distribution of the dashed quantities by using the initial conditions.

Now if an appropriate Reynolds number were sufficiently low, we could proceed by treating the non-linear terms in (2.2) as a perturbation and expanding the $\mathbf{u}(\mathbf{k})$ by iteration in terms of the $\bar{\mathbf{u}}(\mathbf{k})$. Integrating (2.2), we have

$$u_i(\mathbf{k}) = \bar{u}_i(\mathbf{k}) - \frac{i}{2} P_{ijm}(\mathbf{k}) \sum_{\mathbf{k}'+\mathbf{k}''=\mathbf{k}} \int_{t_0}^{t} \exp\left[-\nu k^2 (t-t')\right] u'_j(\mathbf{k}')\, u'_m(\mathbf{k}'')\, dt'. \tag{2.11}$$

To obtain, on the left, the first-order approximation to $\mathbf{u}(\mathbf{k})$ we replace u on the right by $\bar{u}$. To continue the procedure, we successively insert on the right the expressions, for the various amplitudes, given by the previous approximation. It is clear that this results in an expansion for $\mathbf{u}(\mathbf{k})$ in ascending orders of the $\bar{\mathbf{u}}(\mathbf{k})$. For $t - t_0$ the order of some characteristic time of the turbulence this is effectively an expansion in powers of some typical Reynolds number.

The lowest-order non-vanishing contribution to S is given by

$$\bar{S}_1 = \langle \Delta u_n(\mathbf{k})\, \bar{u}'_r(\mathbf{p})\, \bar{u}'_s(\mathbf{q})\rangle + \langle \bar{u}_n(\mathbf{k})\, \Delta u'_r(\mathbf{p})\, \bar{u}'_s(\mathbf{q})\rangle + \langle \bar{u}_n(\mathbf{k})\, \bar{u}'_r(\mathbf{p})\, \Delta u'_s(\mathbf{q})\rangle, \tag{2.12}$$

where $\Delta u_n(\mathbf{k}) + \bar{u}_n(\mathbf{k})$ is the first-order approximation to $u_n(\mathbf{k})$, etc. By (2.11) we have

$$\Delta u_n(\mathbf{k}) = \int_{t_0}^{t} \bar{\xi}_{ni}(\mathbf{k}; t, t'')\, \bar{b}_i(\mathbf{k}, t'')\, dt'' + \ldots, \tag{2.13}$$

with corresponding expressions for $\Delta u'_r(\mathbf{p})$, $\Delta u'_s(\mathbf{q})$, where

$$\bar{\xi}_{ni}(\mathbf{k}; t, t'') = \delta_{ni} \exp\left[-\nu k^2 (t - t'')\right]$$

and

$$\left.\begin{aligned} \bar{b}_i(\mathbf{k}) &= -iP_{ijm}(\mathbf{k})\, \bar{u}_j(-\mathbf{p})\, \bar{u}_m(-\mathbf{q}), \\ \bar{b}_i(\mathbf{p}) &= -iP_{ijm}(\mathbf{p})\, \bar{u}_j(-\mathbf{q})\, \bar{u}_m(-\mathbf{k}), \\ \bar{b}_i(\mathbf{q}) &= -iP_{ijm}(\mathbf{q})\, \bar{u}_j(-\mathbf{k})\, \bar{u}_m(-\mathbf{p}). \end{aligned}\right\} \tag{2.14}$$

The terms denoted by dots on the right of (2.13) involve unperturbed amplitudes with wave vectors other than $\pm\mathbf{k}$, $\pm\mathbf{p}$, $\pm\mathbf{q}$. No factors of $\frac{1}{2}$ appear in (2.14) because, to take $\mathbf{b}(\mathbf{k})$, $-\mathbf{p}$ appears on the right of (2.11) once as $\mathbf{k}'$ and once as $\mathbf{k}''$. (Note that $P_{ijm}(\mathbf{k}) = P_{imj}(\mathbf{k})$.) We have written things in a rather elaborate fashion in order to facilitate later comparisons.

The $\bar{\mathbf{u}}(\mathbf{k}, t_0)$ and hence the $\bar{\mathbf{u}}(\mathbf{k}, t)$ are statistically independent for distinct $\mathbf{k}$'s. Thus it is clear that only the term shown explicitly in (2.13) can contribute to the averages in (2.12). Inserting expression (2.14) in (2.13), and again noting the statistical independence property, we find for the first term on the right of (2.12) the expression

$$-iP_{ijm}(\mathbf{k}) \int_{t_0}^{t} \bar{\xi}_{ni}(\mathbf{k}; t, t'')\, \langle \bar{u}'_r(\mathbf{p})\, \bar{u}''_j(-\mathbf{p})\rangle\, \langle \bar{u}'_s(\mathbf{q})\, \bar{u}''_m(-\mathbf{q})\rangle\, dt''. \tag{2.15}$$

This result involves only the second-order moments of the unperturbed amplitudes. Corresponding expressions may be obtained for the other two terms in (2.12).

If the appropriate Reynolds number were $\ll 1$, we should expect $\bar{S}_1$ to be a good approximation to S for all t. As this Reynolds number approached unity, however, we should expect that more terms in the expansions for the $\mathbf{u}(\mathbf{k})$ would have to be retained for substantial values of $t-t_0$. Finally, for the Reynolds number $\gtrsim 1$, it is not hard to see that the convergence of the expansions should be very poor if $t-t_0$ is larger than some characteristic time of the turbulence. Thus the perturbation technique just described would appear to be quite useless for cases of typical interest in turbulence theory.

The failure of conventional perturbation techniques at moderate and high Reynolds numbers of course simply reflects the fact that the non-linear terms in (2.2) are then not a small perturbation. However, we have seen that even when the non-linear terms are large they consist, in the limit $L \to \infty$, of an infinite sum of infinitesimal contributions from individual pairs of modes. This property makes it possible to develop new perturbation expansions which seem to be useful at all Reynolds numbers.

Let us again consider the moment S for the flow defined above. According to the maximal randomness condition, S must represent a phase correlation of the modes $\mathbf{k}$, $\mathbf{p}$, $\mathbf{q}$ induced by the dynamical interaction; according to the weak dependence principle this phase correlation is infinitesimal. We may ask how the dynamical interaction produces the weak phase correlation. The most obvious way is through the *direct interaction* of $\mathbf{u}(\mathbf{k})$, $\mathbf{u}(\mathbf{p})$, $\mathbf{u}(\mathbf{q})$, involving the terms in the equations of motion of these three amplitudes bilinear in $\mathbf{u}(\pm\mathbf{k})$, $\mathbf{u}(\pm\mathbf{p})$, $\mathbf{u}(\pm\mathbf{q})$. Denoting these terms by $\mathbf{b}(\mathbf{k})$, $\mathbf{b}(\mathbf{p})$, $\mathbf{b}(\mathbf{q})$, we have from (2.2)

$$\left.\begin{aligned} b_i(\mathbf{k}) &= -iP_{ijm}(\mathbf{k})\, u_j(-\mathbf{p})\, u_m(-\mathbf{q}), \\ b_i(\mathbf{p}) &= -iP_{ijm}(\mathbf{p})\, u_j(-\mathbf{q})\, u_m(-\mathbf{k}), \\ b_i(\mathbf{q}) &= -iP_{ijm}(\mathbf{q})\, u_j(-\mathbf{k})\, u_m(-\mathbf{p}). \end{aligned}\right\} \tag{2.16}$$

Let us denote by $\delta\mathbf{u}(\mathbf{k})$, $\delta\mathbf{u}(\mathbf{p})$, $\delta\mathbf{u}(\mathbf{q})$ the perturbations in the three amplitudes induced by the direct interaction. At this point very much hinges upon the meaning given the word 'induced'. If we were to follow the spirit of the conventional perturbation approach, we would take $\delta\mathbf{u}(\mathbf{k})$ to be the increment which must be added to $\bar{\mathbf{u}}(\mathbf{k})$ to yield the $\mathbf{u}(\mathbf{k})$ generated by retaining, of the non-linear parts of the equations of motion, *only* the terms $\mathbf{b}(\mathbf{k})$, $\mathbf{b}(\mathbf{q})$, $\mathbf{b}(\mathbf{p})$. Instead, we define $\delta\mathbf{u}(\mathbf{k})$, $\delta\mathbf{u}(\mathbf{p})$, $\delta\mathbf{u}(\mathbf{q})$ as the differences between the *exact* amplitudes $\mathbf{u}(\mathbf{k})$, $\mathbf{u}(\mathbf{p})$, $\mathbf{u}(\mathbf{q})$ and the values they would have if the terms $\mathbf{b}(\mathbf{k})$, $\mathbf{b}(\mathbf{p})$, $\mathbf{b}(\mathbf{q})$ were removed from the equations of motion *and all other non-linear terms retained*. The dynamical significance of our new procedure is that instead of treating in isolation the effect of the direct interaction of modes $\mathbf{k}$, $\mathbf{p}$, $\mathbf{q}$ we take full account of the modification of this effect due to the coupling of each of the three modes to all the rest of the system. The latter coupling is very strong at high Reynolds numbers, and we therefore expect a marked improvement over the conventional procedure.

In the limit $L \to \infty$, $\delta\mathbf{u}(\mathbf{k})$, $\delta\mathbf{u}(\mathbf{p})$, $\delta\mathbf{u}(\mathbf{q})$ represent infinitesimal perturbations according to our previous considerations. It follows that the contribution S_1 which the direct interaction makes to S in the limit is

$$S_1 = \langle \delta u_n(\mathbf{k})\, u'_r(\mathbf{p})\, u'_s(\mathbf{q})\rangle + \langle u_n(\mathbf{k})\, \delta u'_r(\mathbf{p})\, u'_s(\mathbf{q})\rangle + \langle u_n(\mathbf{k})\, u'_r(\mathbf{p})\, \delta n'_s(\mathbf{q})\rangle. \quad (2.17)$$

Now we have

$$\delta u_n(\mathbf{k}) = \int_{t_0}^{t} \zeta_{ni}(\mathbf{k}; t, t'')\, b_i(\mathbf{k}, t'')\, dt'', \quad (2.18)$$

since, by (2.4), $\zeta_{ni}(\mathbf{k}; t, t'')$ is defined as the response tensor, for arbitrary infinitesimal perturbation, associated with the exact equation of motion (2.2). Thus, noting (2.16), the first term on the right of (2.17) may be written

$$-iP_{ijm}(\mathbf{k}) \int_{t_0}^{t} \langle \zeta_{ni}(\mathbf{k}; t, t'')\, u'_r(\mathbf{p})\, u''_j(-\mathbf{p})\, u'_s(\mathbf{q})\, u''_m(-\mathbf{q})\rangle\, dt''. \quad (2.19)$$

According to the weak dependence principle, the average in (2.19) is equal, in the limit, to the product of independent averages over the factors associated with $\pm\mathbf{k}$, $\pm\mathbf{p}$, $\pm\mathbf{q}$. Hence we obtain

$$-iP_{ijm}(\mathbf{k}) \int_{t_0}^{t} \langle \zeta_{ni}(\mathbf{k}; t, t'')\rangle \langle u'_r(\mathbf{p})\, u''_j(-\mathbf{p})\rangle \langle u'_s(\mathbf{q})\, u''_m(-\mathbf{q})\rangle\, dt'', \quad (2.20)$$

with corresponding results for the other two terms in (2.17). Thus we obtain an expression for S_1 which involves the exact second-order moments and average impulse-response tensors.

The direct-interaction contribution S_1 is the first term in a new, well-defined perturbation expansion for the moment S in the limit $L \to \infty$. Each higher term corresponds to the interaction of modes $\mathbf{k}$, $\mathbf{p}$, $\mathbf{q}$ through some finite set of the modes other than $\mathbf{k}$, $\mathbf{p}$, $\mathbf{q}$. In each case the relevant set of bilinear interaction terms represents an infinitesimal perturbation on the *exact* equations of motion, and each resulting higher-order contribution to S is an integral expression involving only second-order moments and average response tensors.† We shall not be explicitly concerned with the higher-order terms in the present paper, and consequently we shall reserve the derivation of the full expansion for elsewhere (see Kraichnan 1958*b* for a preliminary and partial description).

The perturbation method just described can be extended to give well-defined expansions for all higher moments of the $\mathbf{u}(\mathbf{k})$ in terms of only second-order moments and the average response tensors. In the present paper, however, we shall be concerned only with the third-order moments.

The structure of (2.20) closely resembles that of (2.15), the expression for the first-order contribution according to the conventional perturbation theory. The difference is that (2.15) contains the unperturbed covariances and response tensors while (2.20) contains the exact covariances and response tensors. These latter quantities can be expanded, by the conventional procedure, in the form of

† It was erroneously concluded in Paper I (§5.2) that the higher-order contributions could vanish by symmetry. This is not the case, and equation (3.12) of Paper I, which led to the conclusion, is wrong.

infinite series in the unperturbed quantities. If this is done, and the results substituted into (2.20), it is easy to see that (2.20) *contains contributions of all orders in the conventional expansion for* S. It represents, in fact, a partial summation of that expansion. Consequently, we may hope that S_1 will represent a valid approximation to S at Reynolds numbers where the convergence of the conventional expansion is hopelessly poor. Each higher term in our new expansion also represents an infinite summation over terms of the old. The new expansion may be regarded formally as a regrouping and consolidation of the terms in the conventional expansion.

2.4. *The direct-interaction approximation*

From (2.2) we have the equation of motion

$$\frac{\partial}{\partial t}\langle u_n'(-\mathbf{k})\, u_i(\mathbf{k})\rangle = -\frac{i}{2} P_{ijm}(\mathbf{k}) \sum_{\mathbf{p}+\mathbf{q}=\mathbf{k}} \langle u_n'(-\mathbf{k})\, u_j(\mathbf{p})\, u_m(\mathbf{q})\rangle \tag{2.21}$$

for the covariance tensor. There is also a second equation of motion involving differentiation with respect to t'. If we substitute for the triple moments on the right the new perturbation expansions just described, we obtain an integro-differential equation which involves only the covariance tensors and the average response tensors. Further application of our new perturbation method yields an equation of motion for $\langle \zeta_{ij}(\mathbf{k})\rangle$ which also involves an expansion in only these two kinds of quantities. Thus the method yields formally complete equations for the covariance tensors and average response tensors. We shall now outline the derivation of the direct-interaction contribution to the equation of motion for $\langle \zeta_{ij}(\mathbf{k})\rangle$. The method to be followed differs somewhat from that employed in Paper I and has the advantage of being less formal.

Let us consider the effect of the impulsive disturbance represented by the addition of the terms $\xi_1(\mathbf{k}, t) = \alpha\delta(t-t')$, $\xi_2(\mathbf{k}, t) = \xi_3(\mathbf{k}, t) = 0$ on the right side of (2.2) for a single mode $\mathbf{k}$ only. Here α is an infinitesimal parameter. For $t > t'$, the averaged perturbation in (2.2) has the form

$$\left(\frac{\partial}{\partial t} + \nu k^2\right)\langle \delta u_i(\mathbf{k})\rangle = -iP_{ijm}(\mathbf{k}) \sum_{\mathbf{p}+\mathbf{q}=\mathbf{k}} \langle u_j(\mathbf{p})\, \delta u_m(\mathbf{q})\rangle, \tag{2.22}$$

where $\delta\mathbf{u}(\mathbf{k})$, $\delta\mathbf{u}(\mathbf{q})$ are the changes in $\mathbf{u}(\mathbf{k})$, $\mathbf{u}(\mathbf{q})$ induced as a result of the initial disturbance and we retain only the terms linear in α noting the symmetry of $P_{ijm}(\mathbf{k})$ in j and m. Since the disturbance was applied originally to $\mathbf{u}(\mathbf{k})$ only, we anticipate from the property of weak coupling that each $\delta\mathbf{u}(\mathbf{q})$ is infinitesimal compared to $\delta\mathbf{u}(\mathbf{k})$ when $L \to \infty$. Now we wish to evaluate the contribution to any given term on the right of (2.22) due to direct interaction of the modes $\mathbf{k}$, $\mathbf{p}$, $\mathbf{q}$. This interaction produces a perturbation

$$-iP_{nrs}(\mathbf{q})\,[u_r(-\mathbf{p})\,\delta u_s(\mathbf{k}) + u_s(\mathbf{k})\,\delta u_r(-\mathbf{p})] \tag{2.23}$$

on the right side of the equation of motion for $u_n(\mathbf{q})$. By the weak coupling property, $\delta\mathbf{u}(-\mathbf{p})$ is infinitesimal compared to $\delta\mathbf{u}(\mathbf{k})$, and we neglect it. Then, by (2.4),

$$\delta u_m(\mathbf{q}) = -iP_{nrs}(\mathbf{q}) \int_{t'}^{t} \zeta_{mn}(\mathbf{q}; t, t'')\, u_r''(-\mathbf{p})\, \delta u_s''(\mathbf{k})\, dt''. \tag{2.24}$$

whence

$$\langle u_j(\mathbf{p})\,\delta u_m(\mathbf{q})\rangle = -iP_{nrs}(\mathbf{q})\int_{t'}^{t}\langle\zeta_{mn}(\mathbf{q};t,t'')\,u_j(\mathbf{p})\,u_r''(-\mathbf{p})\,\delta u_s''(\mathbf{k})\rangle\,dt''$$

$$= -iP_{nrs}(\mathbf{q})\int_{t'}^{t}[\langle\zeta_{mn}(\mathbf{q};t,t'')\rangle\langle u_j(\mathbf{p})\,u_r''(-\mathbf{p})\rangle\langle\delta u_s''(\mathbf{k})\rangle]\,dt'' \quad (2.25)$$

by the weak dependence principle. By the definition of the response function we have $\delta u_i(\mathbf{k}) = \alpha\zeta_{i1}(\mathbf{k};t,t')$ for the impulsive disturbance chosen. Thus we have obtained the direct-interaction contribution to the equation of motion for $\langle\zeta_{i1}(\mathbf{k};\ t,\ t')\rangle$, and it involves only covariance tensors and average response functions.

The procedure we have just followed has a rather simple dynamical interpretation. The response tensor describes the relaxation of an initial impulsive disturbance through two effects: viscous decay and the energy exchange among modes. Viscous decay alone would yield the response tensor $\delta_{ij}\exp[-\nu k^2(t-t')]$ which appeared in the conventional perturbation theory. The transfer of initial excitation energy from mode $\mathbf{k}$ to mode $\mathbf{q}$ by direct interaction involves two conceptual steps. First, a perturbation is induced in mode $\mathbf{q}$. This is determined by the response tensor of mode $\mathbf{q}$ and involves the amplitude of a third mode $\mathbf{p}$ as a modulating factor because of the non-linearity of the equations of motion. Secondly, the perturbation induced in mode $\mathbf{q}$ *reacts* upon mode $\mathbf{k}$ subtracting energy out of the original excitation. The reaction again involves the amplitude of mode $\mathbf{p}$ as a modulating factor.

The full integro-differential equations for the covariance tensors and average response tensors cannot be used without either summing or approximating the infinite series of perturbation contributions they contain. In the present paper, as in Paper I, we shall make the approximation of retaining in these equations only the direct-interaction contributions. The arguments which justify this approximation and suggest the limits of its validity can be developed properly only when the complete perturbation theory is presented, which is not the object of the present paper. We shall merely state here, without proof or amplification, some of the pertinent results. First, it can be established that the direct-interaction approximation gives self-consistent equations for the covariances and average response tensors. By this we mean that the equations yield solutions which obey the initial or other boundary conditions, fall properly to zero for infinite difference times, display rigorously positive frequency spectra and are otherwise well behaved. Furthermore, the energy conservation properties of the non-linear interaction are exactly preserved so that a self-consistent energy dynamics results. These results are strong evidence for the naturalness of the approximation.

The direct-interaction approximation appears to be a useful one at all Reynolds numbers. This is suggested by the fact that no condition on the Reynolds number is invoked in the perturbation procedure and also by the fact that the direct-interaction contributions represent contributions of all orders in the Reynolds number. We shall see in the present paper that the approximation gives plausible and self-consistent results for very high Reynolds numbers, and in a later paper we shall present semiquantitative estimates of the actual errors involved.

One might expect that better approximations to the integro-differential equations would be obtained by retaining terms of successively higher perturbation orders in the expansions for the third-order moments. This, unfortunately, is not the case because the resulting equations do not have the self-consistency properties described above, and, in fact, do not seem to have solutions obeying reasonable boundary conditions. In order to obtain self-consistent higher approximations it is necessary to close off the heirarchy of moment equations at higher levels. Each such approximation depends on new perturbation expansions the lowest terms of which represent terms of all orders in the expansions for the immediately preceding approximation. In each case only these lowest terms are retained. The approximation next above the direct-interaction approximation involves expanding fourth-order moments in terms of third-order moments, second-order moments, and certain higher response functions and thereby obtaining a complete set of equations which determine the third-order and second-order moments. The complexity of the self-consistent approximations increases rapidly with order.

In concluding discussion of the foundations of the theory, we shall mention some possible generalizations and additional applications. The theory seems capable of generalization to problems like turbulent flow in an infinite uniform channel or pipe in which there is homogeneity in only one or two directions. There is no restriction to stationarity in time, and presumably the theory could then be used to investigate not only fully developed turbulence but also the development of turbulence from the laminar state under perturbations statistically homogeneous in the axial direction of the channel or pipe.

With further modification the theory seems applicable to classes of problems which display no homogeneity at all but do exhibit statistical stationarity in time. In this case, the weak dependence principle would apply to the *frequency* components of the dynamic variables. A simple example would be a damped nonlinear oscillator excited by Gaussian noise.

3. Statistical equations for stationary isotropic turbulence

The theory described in the preceding section takes its simplest form when the turbulence is isotropic in space and stationary in time. For this case each tensor involved can be expressed in terms of a single scalar, and all statistical moments depend only on difference times rather than absolute times. The remainder of the present paper will be concerned almost exclusively with the stationary isotropic case. However, we should note at the outset that this implies a considerable idealization of physical flows. For turbulence to be stationary there must be driving forces to replace energy lost by viscosity; in order to maintain isotropy the driving forces must themselves be isotropic, and this is physically unrealistic. (We may visualize such forces, perhaps, as due to a random volume distribution of stirring devices.) The physical justification for studying the stationary isotropic case (apart from its intrinsic dynamical interest) is that the structure at high wave-numbers, with which we shall be principally concerned, plausibly may be expected to differ inappreciably for stationary and freely decaying turbulence at high Reynolds numbers. We shall return to this matter after exploring the stationary theory.

In order to describe the stationary isotropic case explicitly, we replace (2.2) with the new equation of motion

$$\left(\frac{\partial}{\partial t}+\nu k^2\right) u_i(\mathbf{k},t) = -ik_m P_{ij}(\mathbf{k}) \sum_{\mathbf{p}+\mathbf{q}=\mathbf{k}} u_j(\mathbf{p},t)\, u_m(\mathbf{q},t)+f_i(\mathbf{k},t), \tag{3.1}$$

where $f_i(\mathbf{k},t)$ is a statistically stationary and isotropic solenoidal forcing term. In accord with the condition of maximal randomness, we take the $\mathbf{f}(\mathbf{k})$ statistically independent for distinct $\mathbf{k}$'s.

The conditions of stationarity and isotropy require that the covariances constructed from $\mathbf{u}(\mathbf{k})$ and $\mathbf{f}(\mathbf{k})$ have the forms

$$\left.\begin{aligned}(L/2\pi)^3 \langle u_i(\mathbf{k},t+\tau)\, u_j^*(\mathbf{k},t)\rangle &= \tfrac{1}{2}P_{ij}(\mathbf{k})\, U(k,\tau),\\ (L/2\pi)^3 \langle f_i(\mathbf{k},t+\tau) f_j^*(\mathbf{k},t)\rangle &= \tfrac{1}{2}P_{ij}(\mathbf{k})\, F(k,\tau),\\ (L/2\pi)^3\, \mathrm{Re}\,\langle f_i(\mathbf{k},t+\tau)\, u_j^*(\mathbf{k},t)\rangle &= \tfrac{1}{2}P_{ij}(\mathbf{k})\, G(k,\tau),\end{aligned}\right\} \tag{3.2}$$

where the scalars U, F, G are all real and U, F are even functions of τ.† The normalization in (3.2) is such that in the limit $L\to\infty$ (which is required for rigorous isotropy),

$$U(k,\tau) = (2\pi)^{-3} \int \breve{U}(x,\tau)\, e^{-i\mathbf{k}\cdot\mathbf{x}} d^3x, \tag{3.3}$$

where $\breve{U}(x,\tau) = \langle \tilde{u}_i(\mathbf{x}+\mathbf{y}, t+\tau)\, \tilde{u}_i(\mathbf{y},t)\rangle$, with corresponding expressions for $F(k,\tau)$ and $G(k,\tau)$.

From (3.1) we may readily obtain the equation of motion

$$\dot{U}(k,\tau)+\nu k^2 U(k,\tau) = S(k,\tau)+G(k,\tau), \tag{3.4}$$

where the dot signifies differentiation with respect to τ and

$$S(k,\tau) = (L/2\pi)^3\, \mathrm{Im}\,[k_m \sum_{\mathbf{p}+\mathbf{q}=\mathbf{k}} \langle u_i(\mathbf{p},t)\, u_m(\mathbf{q},t)\, u_i^*(\mathbf{k},t-\tau)\rangle]. \tag{3.5}$$

The perturbation method described in §2 may be used to expand the triple moment on the right side of (3.5). First, we note that the isotropy and stationarity of the turbulence imply isotropy and stationarity of the average of the infinitesimal-impulse-response tensor defined by (2.4). Thus we have

$$\langle \zeta_{ij}(\mathbf{k};\, t,t')\rangle = P_{ij}(\mathbf{k})\, g(k,t-t'). \tag{3.6}$$

The scalar $g(k,\tau)$ will be called simply the impulse-response or response function; it can be shown to be real. The factor $P_{ij}(\mathbf{k})$ in (3.6) expresses the infinite impedance of the system to non-solenoidal (compressive) forces. The direct-interaction contribution to $S(k,\tau)$ in the limit $L\to\infty$ is (see Paper I, §9.1)

$$\begin{aligned}S(k,\tau) = \pi k \iint_\Delta pq\, dp\, dq \int_0^\infty ds [&a(k,p,q)\, g(k,s)\, U(p,s+\tau)\, U(q,s+\tau)\\ &- b(k,p,q)\, g(p,s)\, U(k,s-\tau)\, U(q,s)],\end{aligned} \tag{3.7}$$

† In Paper I, the present $f_i(\mathbf{k},t)$ was denoted by $F_i(\mathbf{k},t)$ in order to avoid confusion with other notation. $F(k,\tau)$ has the same meaning in Paper I as it does here.

where the domain of integration extends over all wave-numbers p, q such that p, q, k can form the legs of a triangle. The geometrical factors $a(k,p,q)$ and $b(k,p,q)$ are given by

$$\left.\begin{aligned} a(k,p,q) &= \tfrac{1}{2}(1-xyz-2y^2z^2), \\ b(k,p,q) &= (p/k)\,(xy+z^3), \end{aligned}\right\} \tag{3.8}$$

where x, y, z are the cosines of the interior angles opposite the legs k, p, q, respectively.† They obey the trigonometric identities

$$\left.\begin{aligned} a(k,p,q) &= a(k,q,p) \geqslant 0, \\ k^2 b(k,p,q) &= p^2 b(p,k,q), \\ b(k,p,q)+b(k,q,p) &= 2a(k,p,q), \end{aligned}\right\} \tag{3.9}$$

which, as we shall see shortly, are connected with the energy conservation properties of the non-linear interaction.

Application of our perturbation technique to the evaluation of $G(k,\tau)$ yields the result‡

$$G(k,\tau) = \int_0^\infty g(k,s)\,F(k,s+\tau)\,ds. \tag{3.10}$$

Finally, as shown in Paper I, the direct-interaction approximation gives the equation of motion

$$\dot{g}(k,\tau)+\nu k^2 g(k,\tau) = -\pi k \iint_\Delta pq\,dp\,dq b(k,p,q) \times \int_0^\tau g(k,\tau-s)\,g(p,s)\,U(q,s)\,ds \quad (\tau \geqslant 0), \tag{3.11}$$

for the response function. For $\tau < 0$, $g(k,\tau) = 0$, since there is no response to a perturbation before it is applied. If $F(k,\tau)$ is prescribed, (3.4), (3.7), (3.10), (3.11) form a complete system determining $U(k,\tau)$ and $g(k,\tau)$, provided suitable boundary conditions are imposed. The condition of stationarity requires

$$\dot{U}(k,0) = 0, \tag{3.12}$$

which may be formulated by (3.4) and (3.7) as an integral condition (4.2) expressing the balance of energy. The other required boundary condition is

$$g(k,+0) = 1, \tag{3.13}$$

which follows immediately from the definition of $g(k,\tau)$ and the fact that (3.1) involves only first derivatives with respect to time.

† The expression given here for $b(k,p,q)$ is related to that in Paper I by a trigonometric identity. The author is indebted to Mr Robert Wernick for the present, simplified expression. The expressions for both $a(k,p,q)$ and $b(k,p,q)$ given in Paper I should be multiplied by $\frac{1}{2}$.

‡ The restriction on the univariate distribution of $\mathbf{f}(\mathbf{k})$ made in obtaining this result in Paper I is unnecessary. Equation (3.10) can be shown to be an exact result for $L \to \infty$ provided only that the $\mathbf{f}(\mathbf{k})$ are statistically independent for distinct $\mathbf{k}$'s.

4. The spectral transport of energy

The covariance scalars introduced in the last section may be written

$$\left.\begin{aligned} \tfrac{1}{2}U(k,\tau) &= (4\pi k^2)^{-1}E(k)\,r(k,\tau), \\ F(k,\tau) &= (4\pi k^2)^{-1}F(k)\,\mu(k,\tau), \end{aligned}\right\} \tag{4.1}$$

where $E(k)$ is the kinetic energy spectrum function and $F(k)$ the forcing spectrum function, both per unit mass of fluid. The total kinetic energy per unit mass is $\int_0^\infty E(k)\,dk$. The quantity $r(k,\tau)$ is the time correlation function of the Fourier mode, normalized so that $r(k,0) = 1$, with a corresponding interpretation for $\mu(k,\tau)$. If we rewrite (3.4) in terms of the new quantities, set $\tau = 0$, and note the symmetry of the integration domain with respect to p and q, we obtain the relation

$$2\nu k^2 E(k) = \frac{1}{2}\iint_\Delta S(k\,|\,p,q)\,dp\,dq + F(k)\int_0^\infty g(k,s)\,\mu(k,s)\,ds. \tag{4.2}$$

where

$$\begin{aligned} S(k\,|\,p,q) = (k/pq)\{&2k^2 a(k,p,q)\,\theta(k,p,q)\,E(p)\,E(q) \\ &-[p^2 b(k,p,q)\,\theta(p,k,q)\,E(q) + q^2 b(k,q,p)\,\theta(q,k,p)\,E(p)]\,E(k)\} \end{aligned} \tag{4.3}$$

and

$$\theta(k,p,q) = \int_0^\infty g(k,s)\,r(p,s)\,r(q,s)\,ds. \tag{4.4}$$

The left side of (4.2) is the mean power dissipated by viscosity, per unit mass and per unit wave-number. The second term on the right may be interpreted as the mean power input by the driving forces, per unit mass and per unit wave-number. (Hereafter, all powers will be understood to refer to unit mass.) It should be noted that the linear dependence of this term on $F(k)$ is only apparent; the response function $g(k,s)$ is an implicit functional of F and μ determined by (3.4), (3.10) and (3.11). The first term on the right may be interpreted as a mean power input due to non-linear interaction of the velocity modes. Thus,

$$S(k\,|\,p,q)\,dk\,dp\,dq$$

represents the mean power delivered to the Fourier modes in the interval dk as a consequence of their triad interactions with all pairs of modes of which one member lies in each of the intervals dp and dq. $S(k\,|\,p,q)$ is symmetric in p and q, and the factor $\frac{1}{2}$ in (4.2) occurs because each pair of modes is counted twice in the integration.

It may be deduced readily from (3.1) that the interaction of any triad of Fourier modes is individually conservative; this implies

$$S(k\,|\,p,q) + S(p\,|\,q,k) + S(q\,|\,k,p) = 0, \tag{4.5}$$

which may also be obtained easily from (4.3) by using the trigonometric identities (3.9) and the fact that $\theta(k,p,q)$ is symmetric in p and q. The overall conservation property

$$\frac{1}{2}\int_0^\infty dk \iint_\Delta S(k\,|\,p,q)\,dp\,dq = 0 \tag{4.6}$$

follows directly from the detailed conservation relation.

It should be noted that while the concept of the elementary interaction of a *triad* of Fourier modes has a particular significance because of the detailed conservation property, the same is not true of the concept of exchange of energy between *pairs* of modes, which has been used frequently in turbulence theory. There is no way to tell how much of the energy a mode **k** receives from interaction with modes **p** and **q** comes from **p** rather than from **q** (Paper I, footnote 7).

The quantities which enter expression (4.3) may be given fairly direct physical interpretations. We shall consider first the factors $\theta(k,p,q)$, $\theta(p,k,q)$, $\theta(q,k,p)$ which, from their dimensions, evidently represent characteristic times for the triad interaction. We may anticipate that these factors are essentially positive. The physical significance of the response function $g(k,s)$ is that it traces the relaxation of an initial applied excitation of mode k through the joint action of viscous decay and the energy exchange, or mixing action, with the infinitely large number of only weakly statistically inter-related other modes. We may expect that it falls to zero with increasing s in a fairly smooth fashion and that it does not exhibit strongly negative regions. The correlation function $r(k,s)$ also is determined by the general mixing action. We may expect that it, too, is essentially positive and falls fairly smoothly to zero with increase of s. Thus $\theta(k,p,q)$, $\theta(p,k,q)$ and $\theta(q,k,p)$ may be expected to be the order of characteristic correlation and relaxation times of the three modes involved.

The proportionality of the terms in $S(k\,|\,p,q)$ to the θ factors may be interpreted as follows. A non-zero mean transfer of energy among the three modes requires that certain phase relations among these modes be established in a statistical sense. These relations are built up by the direct interaction of the three modes, according to the direct-interaction approximation, but are simultaneously broken down by the viscous decay and effectively random mixing with all the other modes, as expressed by the g and r functions. Loosely speaking, we may say that $\theta(k,p,q)$ is an effective time during which the triple phase correlation can build up before it is broken down.

The first of identities (3.9) indicates that $a(k,p,q)$ is never negative, and the third that $b(k,p,q)$ is typically positive. If, as anticipated, the θ factors are positive, the term in (4.3) involving a represents a *positive* flow of energy to mode k while those involving b represent a typically *negative* flow. The net flow is the resultant of these *absorption* and *emission* terms. It will be noticed that in contrast to the absorption term the emission terms are proportional to $E(k)$. This indicates that the energy exchange acts to maintain equilibrium. If the spectrum level were suddenly raised to much higher than the equilibrium value in a narrow neighbourhood of k, the emission terms would be greatly increased while the absorption term would be little affected; thus, energy would be drained from the neighbourhood and equilibrium re-established. The structure of the emission and absorption terms is such that in general we may expect the energy flow to be from strongly to weakly excited modes, in accord with general statistical mechanical principles.

Although, as was noted above, it is impossible to define unambiguously the transfer of energy between a pair of modes, it is meaningful to define a *transport power* $\Pi(k)$ as the mean power input *to* all modes of wave-number higher than

some value k *from* all modes of wave-number less than k. For this purpose we divide all the triad interactions into four classes as shown in figure 1. Classes A and B do not transfer energy across the boundary. $\Pi(k)$ is therefore the power input to all modes $k' > k$ by all interactions in class C less the power input to all modes $k' < k$ by all interactions in class D. Thus

$$\Pi(k) = \frac{1}{2}\int_k^{2k} dk' \iint_{\Delta'}^{(p,q<k)} S(k'|p,q)\,dp\,dq - \frac{1}{2}\int_0^k dk' \iint_{\Delta'}^{(p,q>k)} S(k'|p,q)\,dp\,dq. \tag{4.7}$$

The upper limit on the first integral sign is taken as $2k$ instead of ∞ because for $k' > 2k$ there are no p and q such that $p, q < k$ and k', p, q form a triangle.

It follows from the conservation properties that the interaction power-input density appearing in (4.2) is related to $\Pi(k)$ by

$$\frac{1}{2}\iint_{\Delta} S(k\,|\,p,q)\,dp\,dq = -\frac{\partial \Pi(k)}{\partial k}. \tag{4.8}$$

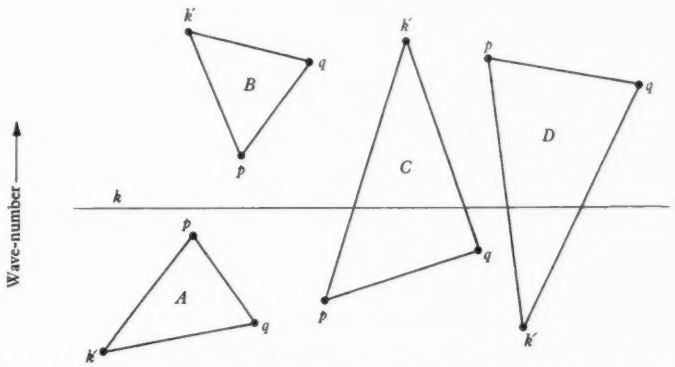

FIGURE 1. Classification of triad interactions for computing the transport power $\Pi(k)$.

5. Response and time correlation functions for high wave-numbers

5.1. *The response function*

The equations of motion (3.4) and (3.11), with $S(k,\tau)$ and $G(k,\tau)$ given by (3.7) and (3.10), are of a type which does not seem to have been studied, and it may be anticipated that in general their solution will present severe difficulties. Our procedure here will necessarily be mathematically non-rigorous. We shall surmise properties of the solution and then examine the consistency of our assumptions with the equations. Our primary purpose in this initial investigation is to see whether the equations seem to yield physically sensible results.

The simplest starting point is the equation of motion for $g(k,\tau)$. Using (4.1) we may rewrite (3.11) in the form

$$\dot{g}(k,\tau) + \nu k^2 g(k,\tau) = -\frac{k}{2}\iint_{\Delta} dp\,dq\,\frac{p}{q}\,b(k,p,q)\,E(q)\int_0^{\tau} g(k,\tau-s)\,g(p,s)\,r(q,s)\,ds \quad (\tau \geqslant 0). \tag{5.1}$$

Now let us consider a k sufficiently high that all but a very small fraction of the total energy lies very far below k. Because of the factor $E(q)$, it appears plausible to assume that the right side of (5.1) should be dominated by contributions from the principal energy containing region $q \ll k$. This assumption is supported by direct inspection of the original equation of motion (3.1). It will be noticed that the coefficient $ik_m P_{ij}(\mathbf{k})$ of the bilinear terms is independent of $|\mathbf{p}|$ and $|\mathbf{q}|$. Apart from certain angular dependence effects, the coupling of the mode $\mathbf{k}$ to modes p or $q \ll k$ appears quite as strong intrinsically as its coupling to modes $\sim k$. Thus we might expect that the contribution of the bilinear terms to the motion should be dominated by terms involving the modes which contain most of the total excitation. Also, it is clear from the appearance of the factor k_m that, in general, the rate of change of $u_i(\mathbf{k}, t)$ ascribable to the non-linear terms tends to increase with k. Thus we may anticipate that the characteristic times of the functions $g(k, s)$ and $r(k, s)$ decrease with increasing k.

Our assumptions are related to the observations in the x-space representation that the time variation of the fine structure, viewed in a fixed co-ordinate system, should be dominated by the sweeping action of the energetic large-scale motion and that small structures should be swept past fixed points more rapidly than large ones.

Returning to (5.1), we note that for $q \ll k$ the triangle relation gives $p \approx k$; then we may approximate $g(p, s)$ by $g(k, s)$, provided it is a reasonably smooth function. Since the time characterizing $r(q, s)$ should be very large compared to that of $g(k, s)$, we shall assume that in the region where $g(k, s)$ is significantly different from zero we may replace $r(q, s)$ by $r(q, 0) = 1$. Finally, we can find from the definition (3.8) that, for $k \approx p$,

$$b(k, p, q) \approx \sin^2 \beta,$$

where β is the interior angle between k and q. The wave-number integration for q in the energy range now can be readily carried out, yielding

$$\iint_{\Delta} pq^{-1} b(k, p, q)\, E(q)\, dp\, dq \approx \int_0^{k_e} dq E(q) \int_{k-q}^{k+q} pq^{-1} \sin^2 \beta\, dp \approx \tfrac{4}{3} k \int_0^{k_e} E(q)\, dq,$$

where $k_e \ll k$ is a wave-number below which lies very nearly all the energy. Then, noting

$$\int_0^{k_e} E(q)\, dq \approx \int_0^{\infty} E(q)\, dq = \tfrac{3}{2} v_0^2,$$

where v_0 is the r.m.s. velocity in any direction, we obtain the equation of motion

$$\dot{g}(k, \tau) + \nu k^2 g(k, \tau) = -v_0^2 k^2 \int_0^{\tau} g(k, \tau - s)\, g(k, s)\, ds \quad (\tau \geqslant 0). \tag{5.2}$$

If our assumptions and approximations are well-founded, this equation should be asymptotically exact, in the direct-interaction approximation, for sufficiently high k.

The solution of the Laplace transform of (5.2) for the boundary condition (3.13) is a standard form, and we thereby find

$$g(k, \tau) = \exp(-\nu k^2 \tau)\, J_1(2 v_0 k \tau)/(v_0 k \tau) \quad (\tau \geqslant 0). \tag{5.3}$$

A detailed investigation of the behaviour of the right side of (5.1), with g given by (5.3) and r estimated from the results to be derived in §5.2, indicates the consistency of our assumptions and approximations. It is found that the restriction of the integration region to $q \ll k$ can give rise to appreciable fractional error in $g(k,\tau)$ only when $\tau \gg (\nu k^2)^{-1}$. For such τ, error can arise because the integral over s may be much larger for, say, $p, q \sim \frac{1}{2}k$ than for $p \approx k$. However, $g(k,\tau)$ is very small for such τ, and the possible error is unimportant. Moreover, it decreases with increasing separation of k and the energy containing region. Our further approximations appear to be justified also.

The factor $\exp(-\nu k^2\tau)$ in (5.3) is the response function appropriate to the decay of an applied excitation by viscosity without interaction with the other modes. The factor $J_1(2v_0k\tau)/(v_0k\tau)$ (plotted in figure 2) represents the relaxation

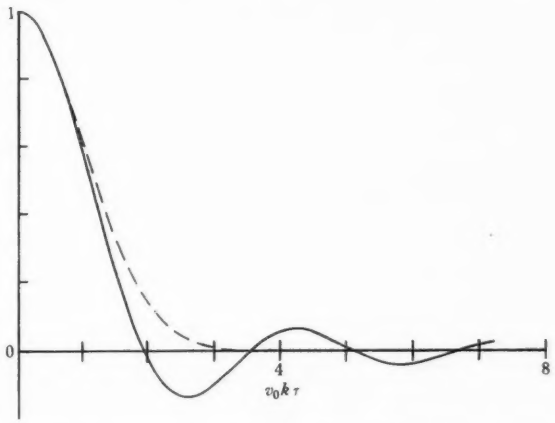

FIGURE 2. Solid curve: the asymptotic response and time-correlation function $J_1(2v_0k\tau)/v_0k\tau$ given by the direct-interaction approximation. Dashed curve: the function $\exp(-\frac{1}{2}v_0^2k^2\tau^2)$ discussed in §8.4.

associated with the energy exchange between the given mode and others with very nearly equal wave-vectors, due to the mixing action of the energy-containing region. By this process the applied excitation is mixed, or diffused, into many neighbouring (but statistically weakly dependent) modes. The characteristic time $(v_0k)^{-1}$ associated with the mixing contribution to $g(k,\tau)$ is the same order as that which would be expected from the convection of a periodic pattern of wave-number k by a uniform velocity of magnitude v_0. However, the action of the low wave-numbers in the present theory is very different from the convective action of a uniform field. Such a field does not produce mixing of neighbouring modes and therefore gives rise to 'coherent' time dependence rather than relaxation effects.

The oscillations in $g(k,\tau)$ which appear in figure 2 are probably to be ascribed to the direct-interaction approximation rather than the physical phenomenon. We shall discuss this in relation to experimental evidence in §8.4.

5.2. *The time-correlation function*

In actual stationary turbulent flows at high Reynolds numbers, the supply of energy to the turbulence seems to be concentrated principally in the energy-containing range. This suggests that in our present investigation we take $\mathbf{f}(\mathbf{k})$ to be negligible outside this range. Then for $\mathbf{k}$ well above the energy-containing range we may omit the term $G(k,\tau)$ in (3.4). In this case (3.4), (3.7) and (4.1) lead to the equation of motion

$$\dot{r}(k,\tau)+\nu k^2 r(k,\tau) = \frac{k}{2}\iint_{\Delta}\left[k^2 a(k,p,q)\frac{E(p)\,E(q)}{E(k)}\int_{\tau}^{\infty} g(k,s-\tau)\,r(p,s)\,r(q,s)\,ds - p^2 b(k,p,q)\,E(q)\int_{0}^{\infty} g(p,s)\,r(k,\tau-s)\,r(q,s)\,ds\right]\frac{dp\,dq}{pq}. \quad (5.4)$$

(In obtaining this form a slight change of time variable has been made, and it has been noted that r is an even function of time.)

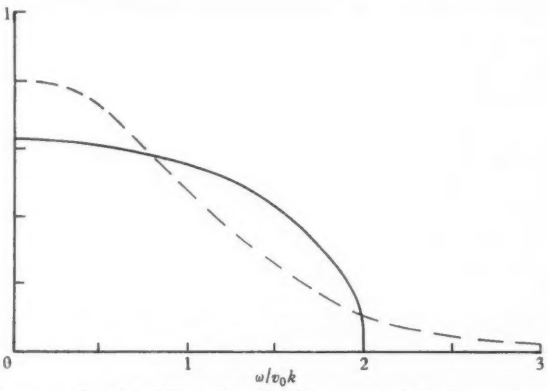

FIGURE 3. Solid curve: the (non-dimensionalized) asymptotic frequency spectrum function $(2/\pi)\,[1-\omega/2v_0k)^2]^{\frac{1}{2}}$ given by the direct-interaction approximation. Dashed curve: the function $(2/\pi)^{\frac{1}{2}}\exp(-\frac{1}{2}\omega^2/v_0^2k^2)$ discussed in § 8.4.

Now let us assume that the Reynolds number is high enough for there to be a range of k large compared to energy-containing wave-numbers but small compared to v_0/ν, so that $\nu k^2 \ll v_0 k$. For such k we may anticipate that the behaviour of $r(k,\tau)$ should be dominated by the energy range mixing action discussed previously, and consequently be characterized by a time the order of $(v_0 k)^{-1}$. If this be so, the term $\nu k^2 r(k,\tau)$ on the left of (5.4) should be negligible compared to $\dot{r}(k,\tau)$, except in the immediate vicinity of the origin. Now, following arguments similar to those used in obtaining (5.2), let us retain on the right of (5.4) only those contributions, involving $b(k,p,q)$, such that $E(q)$ refers to the energy-containing range and only those, involving $a(k,p,q)$, such that $E(p)$ or $E(q)$ refers to this range. Making the further approximations used in obtaining (5.2), taking either $E(q)/E(k)$ or $E(p)/E(k) \approx 1$, as appropriate, using the fact that

$$2a(k,p,q) \approx \sin^2\beta \quad (q \ll k)$$

and writing $$\int_0^{\infty} ds = \int_0^{\tau} ds' + \int_{\tau}^{\infty} ds, \quad \text{where} \quad s' = \tau - s,$$

we obtain the asymptotic equation

$$\dot{r}(k,\tau) = -v_0^2 k^2 \left\{ \int_0^\tau g(k,\tau-s')\, r(k,s')\, ds' + \int_\tau^\infty [r(k,\tau-s)\, g(k,s) - g(k,s-\tau)\, r(k,s)]\, ds \right\}. \quad (5.5)$$

The solution satisfying (3.12) is $r(k,\tau) = g(k,|\tau|)$, since for this choice the second integral on the right of (5.5) vanishes and the equation reduces to the asymptotic form taken by (5.2) for the case $\nu k^2 \ll v_0 k$. Thus we have the result

$$r(k,\tau) = J_1(2v_0 k\tau)/(v_0 k\tau). \quad (5.6)$$

A consistency check similar to that described after (5.3) suggests that this solution is indeed asymptotically valid if k satisfies the double inequality we have postulated. The frequency spectrum corresponding to our solution is

$$\left.\begin{aligned} \mathfrak{r}(k,\omega) &= \frac{2}{\pi}\frac{1}{v_0 k}\left[1-\left(\frac{\omega}{2v_0 k}\right)^2\right]^{\frac{1}{2}} && (\omega \leqslant 2v_0 k), \\ &= 0 && (\omega > 2v_0 k). \end{aligned}\right\} \quad (5.7)$$

This function is shown, non-dimensionalized, in figure 3.

The spectrum of a correlation function must be positive everywhere, and the fact that (5.7) exhibits this property is some evidence of the consistency of our theory. The existence of all derivatives of $\mathfrak{r}(k,\omega)$ at the origin indicates that all the moments $\int_0^\infty r(k,\tau)\,\tau^n\, d\tau$ exist. The sharp cut-off in the spectrum at $\omega = 2v_0 k$ is associated with the oscillations in $r(k,\tau)$. Almost certainly, it is a consequence of the direct-interaction approximation rather than a physical fact. We shall discuss this further in § 8.4.

6. The inertial range

Let us assume the existence of an extended range of k which satisfies all the inequalities invoked in § 5 and over which the integral of the left side of (4.2) is negligible compared to the total dissipation at higher wave-numbers. We shall call this the inertial range. If, as before, we take the driving forces to be negligible, the energy-balance equation (4.2) reduces in this range to

$$\frac{1}{2}\iint_\Delta S(k\,|\,p,q)\, dp\, dq = 0. \quad (6.1)$$

It follows according to the analysis of § 5 that the contributions to this equation for which p or q is in the energy-containing range are given asymptotically by $2E(k)$ times the right side of (5.5) for $\tau = 0$. The s integrals in this expression vanish identically (independently of the form of $r(k,s)$ and $g(k,s)$), which suggests that modes of high wave-number do not receive energy from direct interaction with the energy-containing range. This is in accord with the widely accepted intuitive notion that the transfer or energy up the spectrum proceeds by an essentially local cascade process. We shall assume that this is so, determine the spectrum in the inertial range, and then check the consistency of our assumption

by obtaining an expression for the energy transport due to interaction among distant wave-numbers.

The existence of an effectively local cascade process, together with the conservative character of the interaction, implies that in the inertial range, where dissipation is negligible, the transport power must satisfy

$$\Pi(k) = \epsilon, \tag{6.2}$$

where the parameter ϵ is the mean power eventually dissipated at very high wave-numbers. In accord with the concept of a local cascade process we shall assume that contributions to $\Pi(k)$, as given by (4.7) and (4.3), may be neglected if p, q, or k' is very large or small compared to k. For all the remaining contributions, the relevant response functions and correlation functions are of the form $J_1(2v_0k\tau)/(v_0k\tau)$. The θ factors defined by (4.4) then are symmetric in their arguments and have the dimensional form

$$[\theta(k,p,q)] = [v_0]^{-1}[k]^{-1}.$$

Consequently, $\Pi(k)$ has the dimensional form

$$[\Pi(k)] = [v_0]^{-1}[k]^3\,[E(k)]^2.$$

It seems rather clear from this that if $\Pi(k)$ is to be determined wholly by contributions with k', p and q all in some essentially local neighbourhood of k and is to have the value ϵ, which is independent of k, then one must have

$$E(k) = f(0)\,(\epsilon v_0)^{\frac{1}{2}}k^{-\frac{3}{2}}, \tag{6.3}$$

where $f(0)$ is a numerical constant. (We choose this symbol for later convenience.)

The argument just given only suggests the necessary form of $E(k)$, and we must check to see that (6.3) actually satisfies (6.1) and leads to a local cascade process. If (6.3) is substituted in (4.3) and one takes $g(k,s) = g(v_0ks)$, $r(k,s) = r(v_0ks)$ (without specifying the particular functional forms of r and g), it is not difficult to verify by formal manipulations, using the identities (3.9), that (6.1) is satisfied. This actually is rather clearly implied by the conservative nature of the theory and the dimensional considerations above. The formal property has meaning, however, only if the integrals involved converge properly, which corresponds physically to the presumed localness of cascade. We may verify the latter property by considering the total power input to all modes of wave-number $k'' > k'$ from direct interactions with all mode pairs p, q such that p or $q < k \ll k'$, where k and k' are fixed wave-numbers and all wave-numbers concerned are within the inertial range. Using $r(k,s) = g(k,|s|) = J_1(2v_0ks)/(v_0ks)$ and computing this power as

$$\Pi(k'\,|\,k) = \frac{1}{2}\int_{k'}^{\infty} dk'' \iint_{\Delta''}^{(p \text{ or } q<k)} S(k''|p,q)\,dp\,dq, \tag{6.4}$$

we find, after considerable algebra, the asymptotic result

$$\Pi(k'|k) = (\text{numerical factor})\,[f(0)]^2\epsilon(k/k')^{\frac{4}{3}} \quad (k \ll k'). \tag{6.5}$$

The triad interactions involved in the integration are shown in figure 4. $\Pi(k'|k)$ goes to zero with k/k', so that the energy transport is asymptotically local, as

originally assumed. However, the dependence on k/k' is not particularly strong, and thus the cascade is rather diffuse.

It remains to determine the constant $f(0)$. This may be done by substituting (6.3) into (4.7), taking the form $J_1(2v_0ks)/(v_0ks)$ for the response and correlation functions, evaluating the definite multiple integrals, and noting (6.2). After this is done, (5.6) and (6.3) provide a complete asymptotic solution for the inertial range.

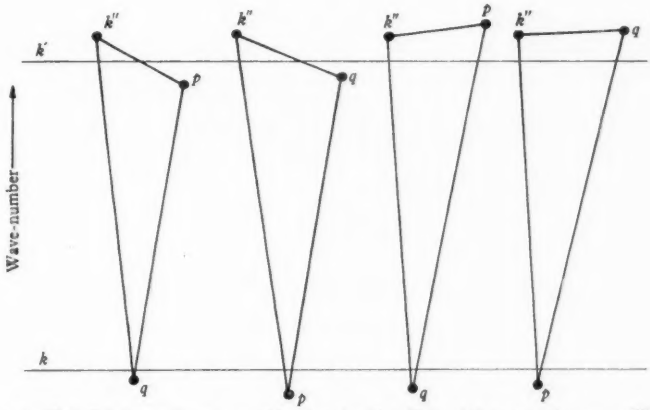

FIGURE 4. Triad interactions contributing to the distant-transport power $\Pi(k'|k)$.

If the inertial range extends through and well above the wave-number k, the total energy above k according to (6.3) is

$$\int_k^\infty E(p)\,dp \approx 2f(0)\,(\epsilon v_0)^{\frac{1}{2}}\,k^{-\frac{1}{2}}. \tag{6.6}$$

Now let us consider the extrapolation of this expression down to low k. Assuming that $f(0)$ is the order of unity, it is clear that (6.6) gives an energy the order of v_0^2 (per unit mass) when k is the order of

$$k_0 = \epsilon/v_0^3. \tag{6.7}$$

Such an extrapolation violates our conditions for the inertial range, of course, but nevertheless the result suggests strongly that k_0 is actually the order of a wave-number characteristic of the energy-containing range. It is also known empirically that this is the case (Batchelor 1953, p. 103). We therefore define a Reynolds number nominally characteristic of the energy-containing range by

$$R_0 = v_0k_0^{-1}/\nu = v_0^4/\epsilon\nu. \tag{6.8}$$

If the inertial range extends through and well below a wave-number k, the total power dissipated below k is

$$\int_0^k 2\nu p^2E(p)\,dp \approx \tfrac{4}{3}f(0)\,\nu(\epsilon v_0)^{\frac{1}{2}}\,k^{\frac{3}{2}}. \tag{6.9}$$

This expression becomes the order of ϵ for k the order of

$$k_d = \epsilon^{\frac{1}{4}}v_0^{-\frac{1}{2}}\nu^{-\frac{3}{4}} = R_0^{\frac{3}{4}}k_0. \tag{6.10}$$

It is clear, then, that necessary conditions for the validity of our asymptotic inertial range spectrum are

$$k_0 \ll k \ll R_0^{\frac{3}{4}} k_0 \tag{6.11}$$

for an extended range of k. This requires in turn that R_0 satisfy

$$R_0^{\frac{1}{4}} \gg 1. \tag{6.12}$$

Since $v_0/\nu = R_0 k_0$, it is clear that the condition $\nu k^2 \ll v_0 k$, invoked in the derivation of (5.6), is contained in (6.11).

A Reynolds number R_λ may be defined by $R_\lambda = v_0 k_\lambda^{-1}/\nu$, where $k_\lambda^2 = \epsilon/15\nu_0^2\nu$ (Batchelor 1953, p. 51). Thus,

$$\left.\begin{aligned} R_\lambda &= (15R_0)^{\frac{1}{2}}, \\ k_\lambda &= R_\lambda k_0/15. \end{aligned}\right\} \tag{6.13}$$

The condition (6.12) is equivalent to

$$R_\lambda^{\frac{3}{2}} \gg 1. \tag{6.14}$$

7. The dissipation range at huge Reynolds numbers

7.1. *The energy-balance integral equation*

The discussion at the end of §6 indicated that a major part of the dissipation takes place at wave-numbers the order of $k_d = R_0^{\frac{3}{4}} k_0$. This suggests that for $R_0^{\frac{1}{4}} \gg 1$, where the inequality is strong enough, all but a negligible fraction of the total dissipation occurs at wave-numbers $k \ll R_0 k_0 = v_0/\nu$. We shall assume that this is so and verify later that the resulting equations do yield a dissipation which falls off rapidly for $k \gg k_d$. Then for k in the dissipation as well as the inertial range, $r(k,s) \approx g(k,|s|)$ is given by (5.6). Let us anticipate, on the basis of the local cascade process already found for the inertial range, that energy transport in both inertial and dissipation ranges is negligibly dependent on direct contributions from triad interactions with modes outside both these ranges. Then the energy balance equation (4.2) takes the asymptotic form

$$2\nu k^2 E(k) = k \iint_\Delta [k^2 a(k,p,q)\, E(p) - p^2 b(k,p,q)\, E(k)]\, E(q)\, \theta_I(k,p,q) \frac{dp\,dq}{pq}, \tag{7.1}$$

where

$$\theta_I(k,p,q) = \int_0^\infty \frac{J_1(2v_0 ks)}{v_0 ks} \frac{J_1(2v_0 ps)}{v_0 ps} \frac{J_1(2v_0 qs)}{v_0 qs}\, ds. \tag{7.2}$$

As before, we have taken $F(k)$ to be negligible for $k \gg k_0$. It is clear physically that the solution of (7.1) cannot be unique, since we have not specified the power input or dissipation rate. (In effect, we have pushed the source of energy supply off to zero wave-number.) To specify a presumably unique solution we may require

$$\int_0^\infty 2\nu k^2 E(k)\, dk = \epsilon. \tag{7.3}$$

If we write

$$E(k) = (\epsilon v_0)^{\frac{1}{2}} k^{-\frac{3}{2}} f(k/k_d), \tag{7.4a}$$

which may be expressed in the dimensionless form

$$E(k)/v_0\nu = (k/k_d)^{-\frac{3}{2}} f(k/k_d), \tag{7.4b}$$

we readily find that (7.1) reduces to the universal equation

$$2u^{\frac{1}{2}}f(u) = \iint_{\Delta}\left[u^2a(u,v,w)\frac{f(v)}{v^{\frac{1}{2}}} - v^2b(u,v,w)\frac{f(u)}{u^{\frac{1}{2}}}\right]\frac{f(w)}{w^{\frac{1}{2}}}K\left(\frac{v}{u},\frac{w}{u}\right)\frac{dv\,dw}{vw}, \quad (7.5)$$

where

$$K(m,n) = \int_0^\infty \frac{J_1(2s)}{s}\frac{J_1(2ms)}{ms}\frac{J_1(2ns)}{ns}\,ds. \quad (7.6)$$

Equation (7.3) takes the form

$$\int_0^\infty u^{\frac{1}{2}}f(u)\,du = \tfrac{1}{2}. \quad (7.7)$$

Instead of imposing (7.7), we could require that $f(0)$ have the value determined in §6 from (6.2). The two conditions are equivalent because the non-linear interaction is conservative; the energy transported through the inertial range is equal to the total viscous dissipation.

The singularities in the integrand of (7.5) at $v = 0$ and $w = 0$ cancel, as may be verified, with some labour, from (3.8) and (3.9). This, again, expresses the localness of the cascade process, according to which the total contribution to the integrand from the infinitesimal neighbourhood of these points is infinitesimal. We anticipate that $f(u)$ is a well-behaved function in the entire range $0 \leqslant u \leqslant \infty$.

It was pointed out in §4 that the emission term in the energy balance equation is proportional to $E(k)$, so that if the spectrum level in the immediate neighbourhood of k were suddenly raised above its equilibrium value the result would be a decrease of the net non-linear input to the neighbourhood and a return to equilibrium. This behaviour suggests that it should be possible to solve (7.5) by a corresponding correction or iteration procedure, in which one obtains an improved trial function as an appropriate linear combination of an initial trial function $2u^{\frac{1}{2}}f(u)$ and the function generated as the right side of (7.5) upon substituting the initial function. It may be expected, however, that considerable practical difficulty will arise because of the singularities in the integrand.

It is of interest at this point to discuss further the relative roles played in (5.4) by local and by energy-containing modes. We have noted that for $k \ll R_0k_0$ the behaviour of $r(k,\tau)$ and $g(k,\tau)$ as functions of τ is determined by interactions involving the energy-containing region. However, although contributions involving the energy-containing region dominate the right side of (5.4) away from the origin, they cancel out in the immediate neighbourhood of $\tau = 0$, as indicated by (5.5). In this neighbourhood, $\dot{r}(k,\tau)$ goes to zero and the term $\nu k^2 r(k,\tau)$, which here dominates the left side, is balanced by contributions on the right nearly entirely from local triads. At $\tau = 0$, this corresponds to the localness of energy transport. As the inequalities $k_0 \ll k \ll R_0k_0$ become stronger, the range of τ about the origin in which wholly local contributions dominate becomes a smaller fraction of $(v_0k)^{-1}$.

7.2 *Behaviour in the far dissipation range*

Let us suppose that R_0 is sufficiently large that there are values of k, very large compared to k_d, for which (7.1) is still valid. There appear to be two general possibilities for the energy supply to such wave-numbers. Either they are

powered by an essentially local cascade process, or they draw power principally from wave-numbers of the order of k_d, in the region where the spectrum begins to fall below the inertial range form. We might perhaps anticipate that the first possibility is the actual fact. In the inertial range we have seen that the energy transport is essentially local. If now we imagine a part of the spectrum to be depressed by local viscous drain, it would appear that the net input from much lower wave-numbers should be affected relatively little, since to start with the local region was already very far from equipartition with these wave-numbers; on the other hand, the local decrease in the level of excitation with respect to that of closer wave-numbers should act in the direction of increasing relatively more the net input from these latter wave-numbers. These considerations actually must be considerably elaborated because of the non-linearity of the system, but it is not difficult to verify that the transport does remain essentially local in the dissipation range and to find the qualitative shape of the spectrum for $k \gg k_d$.

First, it is easy to see that no law of the form $E(k) \propto k^n$ is possible for $k \gg k_d$. Consider, to start, the assumption that the transport is essentially local so that the right side of (7.1) is dominated by contributions for which q and p are the order of k. Then in the contributing regions $\theta_I(k, p, q)$ is of order $(v_0 k)^{-1}$. Since a and b are dimensionless, one finds, counting up the wave-number factors, that (7.1) corresponds to the order-of-magnitude relation

$$2\nu k^2 E(k) \sim v_0^{-1} k^2 [E(k)]^2. \tag{7.8}$$

As k increases indefinitely this cannot be satisfied by any power law except the absurd choice $n = 0$. On the other hand, if we assume that most of the power is supplied by interactions involving modes of wave-number $\sim k_d$, then in place of (7.8) we have

$$2\nu k^2 E(k) \sim v_0^{-1} k_d k E(k_d) E(k), \tag{7.9}$$

where leading terms have been retained on the right. The expression $k_d k$ appears instead of k^2 because one of the pair p, q is of order k_d and the integration ranges of both p and q are restricted to intervals of width $\sim k_d$. Equation (7.9) cannot be satisfied by any power law at all. Thus, both (7.8) and (7.9) are inconsistent with the initial assumption of a power law, under which they were derived.

The impossibility of a power law arises from the fact that E appears linearly on the left of (7.1) and bilinearly on the right, while the equation is homogeneous in the wave-numbers. This suggests that $E(k)$ contains a factor e^{-ck/k_d} (where c is a numerical factor), since that form gives the product law

$$e^{-cp/k_d} e^{-cq/k_d} = e^{-c(p+q)/k_d}.$$

An investigation of (7.1) for $k \gg k_d$ shows that it is, in fact, satisfied asymptotically by a function of the form

$$E(k) = \text{const}\,(k/k_d)^2 e^{-ck/k_d} \quad (k \gg k_d). \tag{7.10}$$

The dominant contributions to the power input come from wave-number pairs p, q forming very flat triangles with k, as would be anticipated from the effect of the exponential factors in depressing the value of $E(p) E(q)$ for pairs not having this property. The integration thus is effectively confined to an area of the p, q plane

very much smaller than k^2, and in this area $E(p)\,E(q) \gg [E(k)]^2$. The factor $(k/k_d)^2$, which might seem surprising in view of the homogeneity of (7.1) in wave-numbers, arises because of the restriction of integration domain; its form also is affected by the behaviour of $a(k,p,q)$, which vanishes for an exactly flat triangle. As we partially anticipated on general grounds, the energy transport is local; this appears as a consequence of the fact that as k_d/k goes to zero so does the fraction of p,q pairs satisfying $p+q \approx k$ which also satisfy p or $q \sim k_d$.

The form of (7.10) confirms the assumption that the dissipation is effectively confined to wave-numbers the order of k_d. It suggests also that each decade range (to make a somewhat arbitrary division) in the region $k \gg k_d$ dissipates most of the energy supplied to it, passing on an ever-decreasing fraction to the next decade.† Corresponding to this fact, the emission terms in (7.1) are very small compared to the absorption term for $k \gg k_d$.

An important characteristic of (7.10) is that it suggests the existence of the moments $\int_0^\infty k^n E(k)\,dk$ for arbitrarily high n. In the x-space representation, this implies the existence of mean square velocity derivatives of all orders—a property which seems required by physical intuition. To establish this conclusion more fully it is necessary to investigate the behaviour of $E(k)$ for extremely high wave-numbers $k \gg R_0 k_0$. Although we have not determined the form of $r(k,\tau)$ in this range, the energy balance equation is, nevertheless, tractable because the function $\theta(k,p,q)$ appearing in the dominant absorption term is determined asymptotically by $g(k,s) \approx \exp(-\nu k^2 s)$. An analysis of the type described above shows that

$$E(k) \propto k^3 \exp[-(\text{const})\,k] \quad (k \gg R_0 k_0). \tag{7.11}$$

This result appears to be valid even for $R_0^{\frac{1}{2}} \sim 1$. The proportionality constants, however, are not independent of R_0.

7.3. *Skewness factors for the longitudinal velocity derivatives*

For $R_0^{\frac{1}{2}} \gg 1$, the skewness factor

$$S_1 = \langle(\partial\tilde{u}_1/\partial x_1)^3\rangle / \langle(\partial\tilde{u}_1/\partial x_1)^2\rangle^{\frac{3}{2}} \tag{7.12}$$

is given in terms of spectrum moments by the asymptotically valid relation (Batchelor 1953, p. 168)

$$S_1 = -\tfrac{3}{7}(30)^{\frac{1}{2}}\,\nu \left[\int_0^\infty k^2 E(k)\,dk\right]^{-\frac{3}{2}} \int_0^\infty k^4 E(k)\,dk. \tag{7.13}$$

By (7.4) and (7.7), we find

$$S_1 = -\tfrac{12}{7}(15)^{\frac{1}{2}} R_0^{-\frac{1}{2}} \int_0^\infty u^{\frac{5}{2}} f(u)\,du. \tag{7.14}$$

We can also evaluate S_1 by expressing it in terms of k space triple moments and expressing these moments in terms of $U(k,\tau)$ and $g(k,\tau)$ by the method employed in Paper I to obtain (3.7). This same procedure can be applied, in general, to the determination of the skewness factor S_n of the distribution of $\partial^n\tilde{u}_1/\partial x_1^n$. It is not difficult to show that for $R_0^{\frac{1}{2}} \gg 1$ the result depends asymptotically only on the

† We must have an *extremely* high R_0 for this to be other than a purely academic point.

dissipation range structure and that upon substituting (5.3), (5.6) and (7.4) in the resulting expressions we obtain the asymptotic result

$$S_n = A_n R_0^{-\frac{1}{2}}, \tag{7.15}$$

where the A_n are universal constants.

The R_0 dependence indicated by (7.14) and (7.15) is quite weak, and it is impossible to estimate, without further analysis, how strong the inequality $R_0^{\frac{1}{2}} \gg 1$ has to be for the asymptotic behaviour not to be masked by other effects.

7.4. *Qualitative discussion of the dynamics*

An interesting paradox arises when we attempt to interpret the dynamics of huge Reynolds number turbulence, as given by the present theory, in terms of familiar impedance concepts. Equation (6.7) implies that if the driving forces were removed the characteristic decay time for the energy-containing range of the turbulence, due to the power output to higher wave-numbers, would be of the order of $(v_0 k_0)^{-1}$; that is, the energy range is approximately critically damped by a resistive dynamical coupling to higher wave-numbers.

Now let us go up the wave-number spectrum considering each decade, say, a subsystem. (We imagine a sufficiently huge R_0 that there are many decades in each spectrum range.) As we go through the inertial range, the characteristic time of each subsystem is of order $(v_0 k)^{-1}$, the energy in each subsystem is of order $(\epsilon v_0)^{\frac{1}{2}} k^{-\frac{1}{2}}$, and the power output to the next higher subsystem is of order ϵ. The 'damping factor' of the subsystem, the fraction of energy passed on in a characteristic 'period', is of order

$$\epsilon (v_0 k)^{-1} / (\epsilon v_0)^{\frac{1}{2}} k^{-\frac{1}{2}} = (k_0/k)^{\frac{1}{2}}.$$

Thus, the damping due to dynamical coupling goes steadily down as we rise through the inertial range.

When we get into the dissipation range $k \gtrsim k_d$, a similar argument shows that the damping due to coupling with the next higher subsystem continues to go down, and with great rapidity since the coupling to higher modes becomes ineffective and transfers a rapidly decreasing fraction of the energy in a subsystem. In this range, as in the inertial range, the damping factor associated with direct viscous dissipation increases linearly with k (as $\nu k^2 / v_0 k$); however, it does not become critical until $k \sim R_0 k_0$, which is far above the range of significant dissipation for huge Reynolds numbers. Thus we have the situation that the energy-containing range, where viscosity does not act, is approximately critically damped, while the range in which viscosity disposes of the energy is very lightly damped. As we go up above $R_0 k_0$ the damping due to dynamical coupling continues to decrease rapidly (it has long since become extremely small), while the direct viscous damping becomes, finally, very large and dominates the mechanics of the subsystems.

The behaviour described seems strange, but there does not appear to be anything either physically or mathematically inconsistent about it. It arises from the non-linearity and complication of the system, and the consequent artificiality of dividing it into subsystems. The characteristic frequencies of the subsystems are

not really internal parameters, but are controlled by the energy-range mixing, as discussed before. We must also keep in mind that each subsystem serves as a kind of frequency multiplier for the energy supplied to it.

The asymptotic identity of time correlation and response functions for the inertial and dissipation ranges indicated by the present theory is of considerable fundamental interest. It has been shown for many types of conservative systems that time-correlation and averaged response functions are identical in an equilibrium (detailed-balance) ensemble. In particular, this is true for a dissipationless system closely related to turbulence (Paper I, appendix). In the present case we have found this same behaviour for modes which are very far from a state of detailed balance and which dissipate most of the energy lost by the system. It seems likely that this is significantly connected with the fact that for these modes the effective damping due to both dynamical coupling and direct dissipation is very small.

8. Comparison with experiment

8.1. *The effect of deviations from idealized conditions*

Our analysis has been based on maximal randomness, exact isotropy, and stationarity, and it has been limited to the direct-interaction approximation. Furthermore, we have indicated solutions of the resulting equations only for extremely high Reynolds numbers. In order to make a very meaningful comparison with experiment, it is necessary to have some idea of the theoretical corrections implied by the experimental deviations from the ideal conditions listed. It also is desirable to have theoretical estimates of the errors associated with the direct-interaction approximation. The latter estimates will be reserved for a future paper. The principal question is whether the qualitative results of §§6 and 7 and the spectrum form (7.4*b*) are consequences also of the exact asymptotic theory for high R_0. If they are, the errors associated with the direct-interaction approximation involve only the value of $f(0)$, the quantitative behaviour of $f(k/k_d)$, and the quantitative functional dependence of $r(k,\tau)$, $g(k,\tau)$ on their argument $v_0 k\tau$. Unfortunately, little can be said at present on the question of corrections for experimental deviations, and we shall attempt only a very qualitative discussion.

We shall not discuss here the deviation of laboratory homogeneous turbulence from maximal randomness, except to note that for grid-produced turbulence we may expect to observe downstream regularities of some kind associated with the grid spacing. We shall, however, consider briefly the relation between our stationary isotropic turbulence and freely decaying isotropic turbulence, which possibly can be closely approximated in the laboratory. For R_0 sufficiently high that the asymptotic solution developed in §7 has a range of accurate validity, it seems clear that the behaviour of this range should be negligibly affected by decay, provided enough time has elapsed for the high wave-number structure to have been fully established. This follows from the fact that the decay of v_0 is very slow compared to characteristic periods of the range. The spectrum and time correlation for the stationary case, therefore, should apply to the free decay case, provided v_0 and ϵ are measured within a time short compared to the decay time.

Since the instantaneous rate of viscous dissipation equals the instantaneous rate of decrease of kinetic energy, it should not matter whether ϵ is measured as $-\partial(\frac{3}{2}v_0^2)/\partial t$ or as $\int_0^\infty 2\nu k^2 E(k)\,dk$, if accurately isotropic and homogeneous conditions have been established.

At lower Reynolds numbers the equivalence of the stationary and decaying cases no longer follows, and we must consider also that (7.1) no longer is necessarily an accurate expression of the stationary theory. After the numerical constants are evaluated, (6.5) may be of value in the qualitative understanding of lower Reynolds numbers.

The role of anisotropy in the present theory is quite interesting. Let us consider huge Reynolds number homogeneous axisymmetric turbulence. For this case the response and time-correlation functions for high wave-vectors can be determined in close analogy to the isotropic case, yielding similar Bessel function expressions in the direct-interaction approximation. It is easy to see, however, that the effective mixing velocity, replacing v_0 in the arguments, depends on the angle between $\mathbf{k}$ and the axis of symmetry and is maximum when $\mathbf{k}$ is in the direction of maximum r.m.s. velocity. The energy transport among a triad $\mathbf{k}, \mathbf{p}, \mathbf{q}$ in the inertial or dissipation ranges has a consequent dependence on the orientations of these wave-vectors relative to the axis of symmetry. Thus, despite the localness of energy cascade, it does not appear likely that the present theory yields asymptotic isotropy of energy partition in the inertial and dissipation ranges. The geometry of the transport terms is sufficiently complicated that further investigation is needed to determine whether the anisotropy in the θ factors actually results in appreciable energy anisotropy at high wave-numbers and, if so, whether it is of the same or opposite sign as the anisotropy of the r.m.s. velocity components.

As we go to wave-numbers $k \gtrsim R_0 k_0$, the transport terms begin to be dominated by isotropic factors of the form $\exp(-\nu k^2 s)$ in the response functions. In consequence of the localness of the cascade process, we should then expect an approach to energy isotropy at these very high wave-numbers regardless of possible anisotropy lower in the spectrum.

The presence of inhomogeneity as well as anisotropy brings into question the basic assumptions of the present theory. If, for example, we consider turbulence confined within a region not large compared to k_0^{-1}, the mode density will not be high, and we cannot expect the weak dependence property to hold accurately.†

Without further investigation, extreme caution must be used in attempting to interpret shear flow experiments on the basis of homogeneous theory. Laboratory 'spectrum' measurements involve a kind of 'local Fourier analysis' and give results which depend on the position in the inhomogeneous flow. The Fourier

† However, the present theory may be adapted to give a valid description of turbulence homogeneous in only one or two directions—for example, flow in an infinitely long pipe or channel. To obtain closed, determinate covariance equations, weak dependence need be assumed only for wave-vectors differing in their axial components; the phase correlations in transverse directions may be retained and determined, along with the mean velocity profile.

components used in the present theory are *not* local quantities; they refer to the entire flow. Without further justification, we cannot divide into local regions an inhomogeneous flow, in which there are necessarily phase correlations between pairs even of high-lying Fourier modes, and attempt to treat each region more or less independently. It is conceivable that the mixing action of a strong shear velocity in one part of the flow may influence the energy balance in high wave-number Fourier components which affect a laboratory 'spectrum' measurement made in a different part of the flow.

Even apart from the interpretation of the present theory, the concept of local Fourier analysis is not a simple one. Terms like 'eddies of wave-number k', sometimes used in discussing turbulence, imply a vagueness of distinction between x-space and k-space concepts which can lead to serious inconsistencies.

We shall now proceed to disregard the cautions just presented and compare the asymptotic maximally random, stationary, isotropic theory with real experiments including shear flow experiments. It is hoped that the comparison may lead to insights regarding the questions which have been raised. A further motivation is that the only other course open at present would appear to be to ignore entirely the relation of theory to experiment.

8.2. *Wave-number spectra in turbulent pipe flow*

The highest laboratory values of R_0 ($> 10^3$) appear to have been obtained in shear flows. An experimental situation for which very careful measurements have been taken is the fully developed flow in a long circular pipe (Laufer 1954). Measurements were made by Laufer of the one-dimensional spectra $\phi_1(k_1)$, $\phi_2(k_1)$, $\phi_3(k_1)$ of (twice) the energy in the axial, radial, and circumferential velocity components, respectively, at several stations across the pipe. The results of the measurements on the axis are shown in figure 5. The one-dimensional spectrum of the total kinetic energy $\phi(k_1) = \phi_1(k_1) + \phi_2(k_1) + \phi_3(k_1)$, for two stations, is shown in figure 6. In most cases the points shown on the latter plot are not experimental points but are computed from the curves drawn by Laufer through the original experimental points for the three component-spectra. In both figures 5 and 6, wire-length corrections have been applied only to $\phi_1(k_1)$. The values of $R_0^{\frac{1}{2}}$, k_0 and k_d shown on figure 6 are computed from $v_0 = 3^{-\frac{1}{2}} \langle \tilde{u}_1^2 + \tilde{u}_2^2 + \tilde{u}_3^2 \rangle^{\frac{1}{2}}$ and estimates of local values of ϵ. The dissipation rate cannot be determined precisely from the measurements, but the computed parameters are not very sensitive to its value. $R_0^{\frac{1}{2}}$ and k_d probably are not in error by more than 10 % and k_0 probably by not more than 25 %. The accuracy of the relative values of the component spectra may be estimated as about 15 to 20 % (Laufer, private communication).

It can be seen from figure 6 that the total energy spectrum follows a $k_1^{-\frac{5}{3}}$ law quite closely for a substantial fraction of the range between k_0 and k_d. If estimated wire-length corrections (Laufer, private communication) are applied to $\phi_2(k_1)$ and $\phi_3(k_1)$, the range of adherence to the $k_1^{-\frac{5}{3}}$ law is somewhat extended. Within the range where $\phi(k_1)$ exhibits $(k_1^{-\frac{5}{3}})$-law behaviour, it can be seen from figure 5 that there are substantial differences among the slopes of the component spectra, the deficiency in excitation of u_2 and u_3 at low wave-numbers changing to an excess, above the isotropic relation to u_1, at high wave-numbers.

Superficially at least, the behaviour would seem not inconsistent with what might be expected on the basis of the asymptotic isotropic results. The total energy cascade appears to proceed according to the isotropic law. As the cascade goes on, there appears to be a drain of energy from u_1 to u_2 and u_3 so that the component spectra have respectively greater and lesser slopes than the total

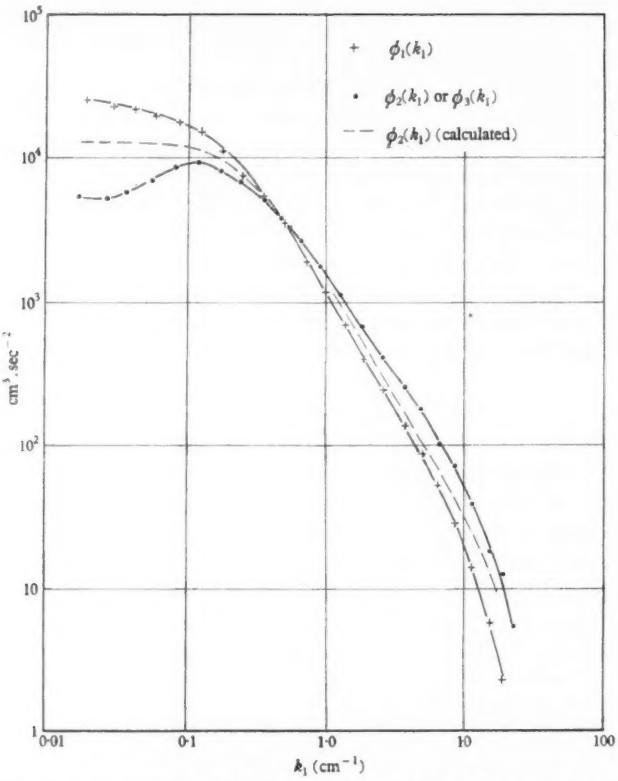

FIGURE 5. Energy-component spectra $\phi_1(k_1)$, $\phi_2(k_1)$, $\phi_3(k_1)$ on the axis of fully turbulent pipe flow. The dashed line gives $\phi_2(k_1)$ as calculated from $\phi_1(k_1)$ using isotropic relations. The pipe radius is $a = 12{\cdot}33$ cm, and the Reynolds number based on a and the mean velocity on axis is 5×10^5. After Laufer (1954).

spectrum. The eventual non-isotropic partition of energy at high wave-numbers does not appear too surprising in view of the discussion in §8.1. We may note that $R_0 k_0$, the wave-number at which the response functions must begin to become isotropic, is far above the range plotted.

In his interpretation of the measurements Laufer noted that $\phi_1(k_1)$ follows a $k_1^{-\frac{5}{3}}$ law very closely over a substantial range. This is the inertial range law predicted by the Kolmogorov theory for isotropic turbulence, and the result would seem to indicate consistency with that theory. Actually, the agreement is not very satisfying, as Laufer himself observed. In the centre of the inertial range, $\phi_1(k_1)$ represents only about 20 to 25 % of the total energy associated with k_1, and

the components $\phi_2(k_1)$, $\phi_3(k_1)$, which contain the rest of the energy, do not follow the $(-\frac{5}{3})$-law at all. In making a comparison with an isotropic theory it would appear more reasonable to consider the total energy spectrum, as we have done above. For this spectrum, the $(-\frac{3}{2})$-law appears to give an optimum straight-line fit, and the $(-\frac{5}{3})$-law appears to lie slightly outside the experimental error. It may also be noted that the very fact of the observed anisotropy at very high wave-numbers, which is not surprising on the basis of the present theory, seems a complete mystery on the Kolmogorov theory.

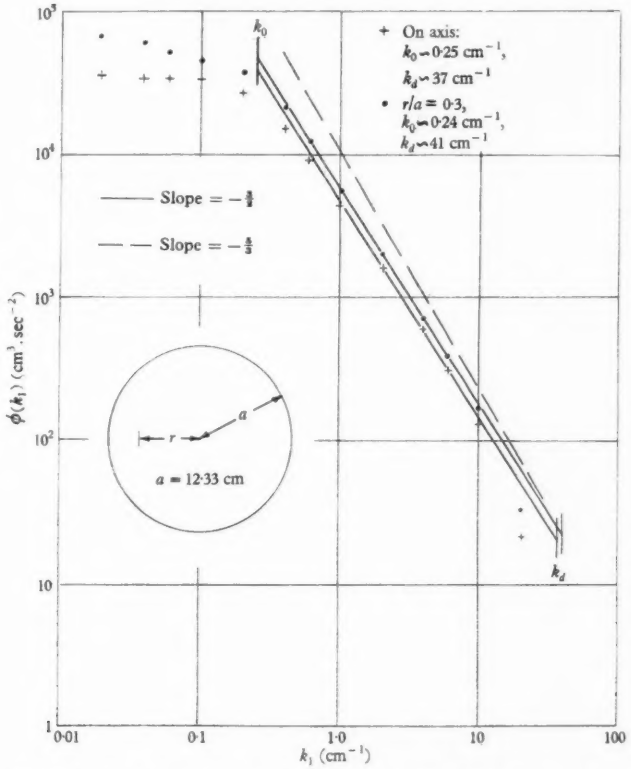

FIGURE 6. Total energy spectrum $\phi(k_1) = \phi_1(k_1) + \phi_2(k_1) + \phi_3(k_1)$ at two stations in the flow of figure 5. $R_\theta^{\frac{1}{2}} \sim 15$, on axis, ~ 17 at $r/a = 0{\cdot}3$. From data of Laufer (1954).

It should be emphasized that the discussion above is merely suggestive. The cautions expressed in § 8.1 must be kept firmly in mind in evaluating the arguments we have just advanced.

Measurements in the boundary layer on a flat plate at values of $R_\theta^{\frac{1}{2}}$ similar to those in the pipe-flow experiment have been reported by Klebanoff (1955). In the outer part of the boundary layer a behaviour qualitatively similar to that described above was found; the slope of $\phi_1(k_1)$ was steeper, and that of $\phi_2(k_1)$ flatter, than $-\frac{3}{2}$. Unfortunately, measurements of $\phi_3(k_1)$ were not made. It is

of interest that the anisotropy at very high wave-numbers found in the pipe flow measurements did not appear in this experiment.

Betchov (1957) has also reported measurements at closely comparable $R_\theta^{\frac{1}{2}}$, made in a shear flow of novel character. Only $\phi_1(k_1)$ was measured, and it resembled closely the corresponding function for the pipe flow. No detailed comparison with isotropic theory seems possible in the absence of data on $\phi_2(k_1)$ and $\phi_3(k_1)$.

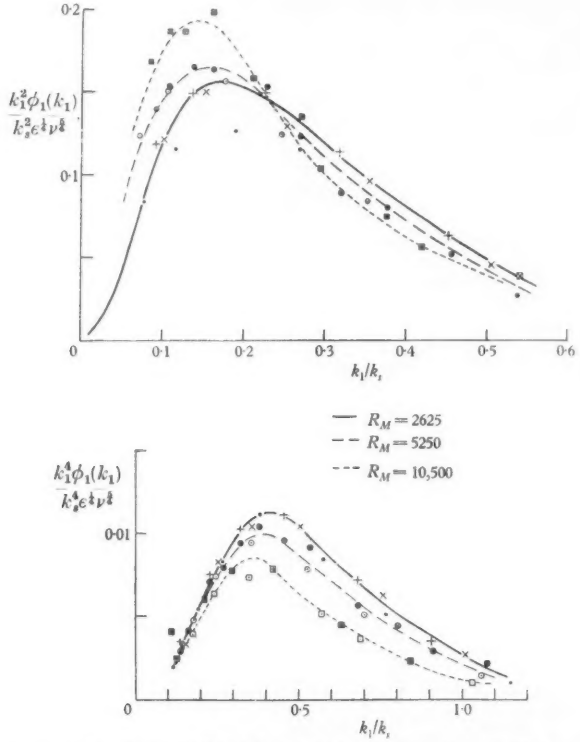

FIGURE 7. Dimensionless plots of $k_1^3\phi_1(k_1)$ and $k_1^4\phi_1(k_1)$ according to Kolmogorov scaling ($k_s = R_\theta^{\frac{1}{2}}k_0 = \epsilon^{\frac{1}{4}}\nu^{-\frac{1}{2}}$), for several grid Reynolds numbers R_M. R_M is defined as (mean stream velocity) × (grid spacing)/ν. After Stewart & Townsend (1951).

8.3. *Wave-number spectra in grid turbulence*

Grid-produced turbulence appears to represent at present the closest laboratory approach to homogeneity and isotropy. Although Reynolds numbers high enough to produce an inertial range have not been described in the literature, it is of some interest to examine to what extent the dissipation range spectrum at moderate Reynolds numbers obeys the scaling indicated by (7.4*b*). Figure 7 shows the results of one-dimensional spectrum measurements by Stewart & Townsend (1951) as plotted and drawn by these authors on the basis of scaling indicated by the Kolmogorov theory. Similar measurements have been reported by Liepmann, Laufer & Liepmann (1951). Figure 8 shows the curves drawn by

Stewart & Townsend through their data points, rescaled according to (7.4*b*). The plots have been prepared so that the curves for $R_M = 5250$ are congruent in each case. The values of R_M correspond to the values of relevant parameters shown in the table below:

R_M	R_0	$R_0^{\frac{1}{2}} = R_0 k_0/k_d$	$R_0^{-\frac{3}{2}} = k_0/k_d$
2625	13	2·35	0·18
5250	26	2·95	0·11
10500	53	3·75	0·07

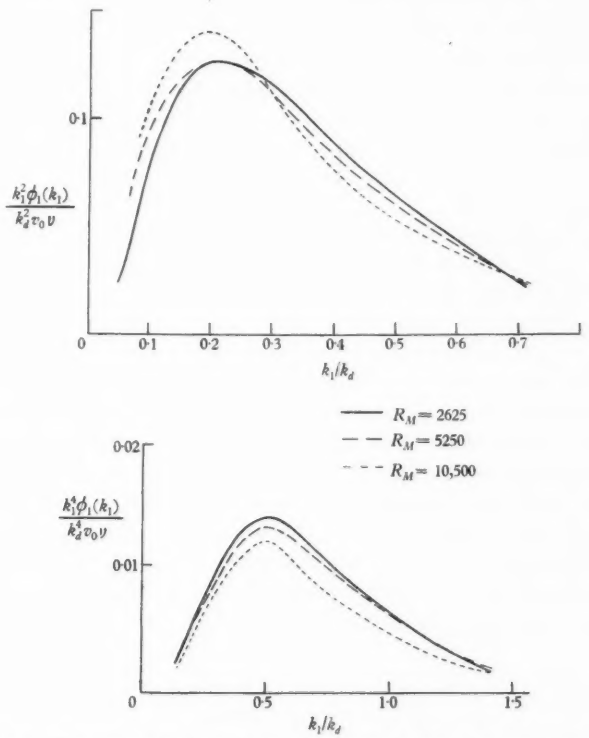

FIGURE 8. The curves in figure 7 rescaled according to the present theory. The rescaling is defined by $k_s = R_0^{\frac{1}{2}} k_d$, $\epsilon^{\frac{1}{4}}\nu^{\frac{3}{4}} = R_0^{-\frac{1}{2}} v_0 \nu$.

It will be noticed that the curves of both $k_1^2\phi_1(k_1)$ and $k_1^4\phi(k_1)$ fall substantially closer together with the new scaling than with the old. In particular, the systematic shift with R_M of the horizontal position of the maxima seems largely absent with the new scaling. It should be noted that, while $R_0 k_0$ has a definite theoretical significance as the wave-number at which $\nu k^2 = v_0 k$, k_0 is only nominally the wave-number characterizing the energy-containing range. In this experiment most of the energy lies below k_0 in each case. From the values given in the table it would seem not implausible that, particularly in the case of $k_1^4\phi_1(k_1)$, the functions should bear some relation to the asymptotic forms for a substantial part of the k-range plotted. However, the values of $R_0^{\frac{1}{2}}$ are too low, and the experimental

scatter too high, to permit attaching very much significance to the comparison. It must also be noted that detailed measurements on the isotropy of the flow were not presented.

8.4. *The response and time-correlation functions*

Direct experimental measurements on the modal impulse-response and time-correlation functions $g(k,\tau)$ and $r(k,\tau)$ do not appear to have been made. Indirect information about $r(k,\tau)$ is obtainable, in principle, from measurements of acoustic and electro-magnetic scattering from turbulence, but existing data of this kind appear to involve too many unknowns to provide useful estimates. However, it appears possible to re-express $g(k,\tau)$ and $r(k,\tau)$ so that fairly good indirect estimates of both these quantities for $k_0 \ll k \ll R_0 k_0$ can be made from measurements of the one-point, one-time velocity distribution. Work on this is still incomplete, but it seems pertinent to include a brief report of the tentative conclusions in the present paper. Our discussion here will be confined to the isotropic case.

It seems almost certain on intuitive grounds that for $k_0 \ll k \ll R_0 k_0$ both $g(k,\tau)$ and $r(k,\tau)$ are determined by the energy-range mixing action. That is to say, they are determined by the non-linear terms in (2.2) for which $\mathbf{k}'$ or $\mathbf{k}''$ falls in the energy-containing range. Now if our double inequality holds, the characteristic fluctuation and relaxation times for energy-range modes will be extremely long compared to those for wave-numbers the order of k. Therefore, if we retain in (2.2) only the terms cited, we have equations of motion for $\mathbf{u}(\mathbf{k})$ and the amplitudes in the neighbourhood of $\mathbf{k}$ which are linear in the amplitudes in this neighbourhood and in which the energy-range amplitudes appear as effectively constant coefficients. These equations then may be handled by the general methods for linear systems with constant coefficients.

The analysis suggested by the last paragraph leads without much difficulty to a simple exact asymptotic expression for $g(k,\tau)$. The result is

$$g(k,\tau) = M(k\tau) \quad (\tau \geqslant 0,\ k_0 \ll k \ll R_0 k_0), \tag{8.1}$$

where M is the characteristic function associated with the one-point, one-time distribution function of any velocity component $\tilde{u}_1$ of the turbulence. M is defined by

$$M(\alpha) = \int_{-\infty}^{\infty} \exp(i\alpha\tilde{u}_1)\, P(\tilde{u}_1)\, d\tilde{u}_1 = \langle \exp(i\alpha\tilde{u}_1) \rangle, \tag{8.2}$$

where $P(\tilde{u}_1)$ is this distribution function (Batchelor 1953, §2.3).

The evaluation of $r(k,\tau)$ by these methods is not so direct. It appears to be necessary to appeal explicitly to the maximal randomness condition, which need not be invoked to obtain (8.1). The tentative asymptotic result which we have obtained is

$$r(k,\tau) = M(k\tau) \quad (k_0 \ll k \ll R_0 k_0), \tag{8.3}$$

which might have been anticipated from (8.1). Neither (8.1) nor (8.3) involve the direct-interaction approximation.

It follows from (8.3) that the frequency spectrum function for wave-number k is given by

$$\mathfrak{r}(k,\omega) = 2k^{-1} P(\omega/k) \quad (k_0 \ll k \ll R_0 k_0). \tag{8.4}$$

This result has a very simple interpretation: the weight with which any frequency ω appears in the spectrum function is proportional to the probability of occurrence of the velocity at which a harmonic component of wave-number k would have to be convected to give oscillations of this frequency at a fixed point in space. This interpretation must not be taken too literally, however. The energy-range mixing is not a simple convection process.

Measurements indicate that $P(\tilde{u}_1)$ is close to Gaussian in a variety of turbulent flows (Batchelor 1953, §8.1). For a Gaussian distribution,

$$P(\tilde{u}_1) = (2\pi)^{-\frac{1}{2}} v_0^{-1} \exp(-\tfrac{1}{2}\tilde{u}_1^2/v_0^2)$$

and

$$M(\alpha) = \exp(-\tfrac{1}{2}v_0^2\alpha^2).$$

For this case (8.3) and (8.4) yield

$$r(k,\tau) = \exp(-\tfrac{1}{2}v_0^2k^2\tau^2), \tag{8.5}$$

$$\mathfrak{r}(k,\omega) = (2/\pi)^{\frac{1}{2}}(v_0k)^{-1}\exp(-\tfrac{1}{2}\omega^2/v_0^2k^2), \tag{8.6}$$

for the range of k considered. These functions are compared in figures 2 and 3 with the results we have previously obtained by the direct-interaction approximation. It seems likely that the deviations which appear are large compared to those associated with departure of the relevant empirical distribution function from exact Gaussian form and give a fairly good picture of the error due to the direct-interaction approximation. The comparisons suggest that the oscillations in $r(k,\tau)$ and the sharp cut-off in $\mathfrak{r}(k,\omega)$ found in §5 are to be ascribed to the direct-interaction approximation rather than the physical phenomenon.

It is of interest that replacing the integrand factors in (7.2) with the corresponding Gaussian functions (8.5) induces only a small change in $\theta_I(k,p,q)$. For either $p = q = k$ or $p = k$, $q = 0$ the substitution increases $\theta_I(k,p,q)$ by 5 % and for $p = q = \frac{1}{2}k$, by 10 %. This might seem to suggest that the direct-interaction approximation gives rather accurate results for $f(k/k_d)$. However, in order to decide this, the error in the functional form (4.3) for $S(k|p,q)$ must also be estimated. We shall discuss this in a future paper.

9. Comparison with other theories

9.1. *The Kolmogorov theory*

The Kolmogorov theory† has occupied a central place in thinking on turbulence in the past decade because of the intuitive appeal of its assumptions, the economy of its methods, and the approximate empirical support for its predictions. Certain results of the present theory appear to differ only slightly from those of the Kolmogorov theory: the spectrum law in the inertial range by $(k/k_0)^{\frac{1}{2}}$ and the characteristic scaling wave-number in the dissipation range by $R_0^{-\frac{1}{4}}$. However, we shall see that the two theories are in fundamental conflict. First, we shall point out that the observed structure of turbulence at high Reynolds numbers does not seem to support very well the fundamental physical assumptions of the Kolmogorov theory, as distinct from the conclusions of the theory.

† A review of this theory is given by Batchelor 1953, Chapter 6.

Kolmogorov's basic assumption (Kolmogorov 1941) is essentially that the internal dynamics of the sufficiently fine-scale structure (in x-space) at high Reynolds numbers should be independent of the large-scale motion. The latter should, in effect, merely convect, bodily, regions small compared to the macroscale. According to the restatement of this hypothesis by v. Weizsäcker (1948), the dynamical interaction of the $\mathbf{u}(\mathbf{k})$ is effectively local in wave-number space. The direct action of low-k modes on sufficiently high-k modes is assumed to be only a trivial convection effect which does not influence high-k energy dynamics. This implies that the transport of energy from the energy-containing range to the dissipation range depends on a cascade process whose mechanism is independent of the energy-containing range. An intimately related further assumption is that the cascade acts like a diffusion process in k-space. This has the consequence that, whatever the situation at low k, the **k**-spectrum should be isotropic and universal in form at sufficiently high k. The equivalent assumption in the x-space picture is that the velocity structure within any region sufficiently small compared to the macroscale should be isotropic and universal in a reference frame moving at the mean velocity of the region ('local isotropy'). If the assumptions are all valid, the dynamical equilibrium at wave-numbers well above the energy-containing range must be determined solely by two local parameters: the rate of cascade ϵ and the viscosity ν. In the inertial range, where one assumes $E(k)$ is independent of ν, simple dimensional arguments then yield the Kolmogorov law $E(k) \propto \epsilon^{\frac{2}{3}} k^{-\frac{5}{3}}$.

Let us suppose that the fine-structure of turbulence consisted of little patches of velocity corrugation, well separated from each other, superimposed on a macrostructure which varied slowly and smoothly with position. Then it would be very hard to see physically how the Kolmogorov assumption about the action of large-scale structure on small-scale could be incorrect. In the limit of the macroscale very large compared to the patch size the action would of necessity be a simple convection. The empirical evidence, however, is quite opposite to this picture. A prominent feature of turbulence at high Reynolds numbers is the presence of sharply defined, extended, and tangled vortex sheets and filaments (Batchelor 1953, §8.4). The high-wave-number Fourier amplitudes are in substantial measure associated with these structures, and the transfer of energy appears to involve, in part, the stretching and thinning of the sheets and filaments by the flow. This behaviour is easily observed by stirring ink into a bathtub of water ($R_0 > 10^4$ is readily achieved). A typical filament extends throughout a substantial part of the turbulent domain. Thus the fine structure does not appear to be 'local' in a three-dimensional sense, and the stretching actions indicate that the fine-scale dynamics may actually depend on the structure of the velocity field over rather large regions.

The vortex sheets may be thought of as internal 'boundary layers' across which occur sharp and major changes in velocity. If these structures form a prominent feature of the turbulence it seems difficult to attach a definite physical meaning to the Kolmogorov notion of a co-ordinate system moving with the local mean velocity. It is hard to know what to take as the velocity of this frame in the regions of rapid change, which, we have noted, contribute importantly to the high-k spectrum. The concept of local isotropy also does not seem well supported

by this physical picture. The vortex sheets are intrinsically anisotropic and inhomogeneous structures. It is only when averages are taken over substantial volumes of the flow, large enough to include many sheets in all orientations, that homogeneity and isotropy can appear, if they do at all. It is very important to note here that *isotropy of space-correlations, for separations small compared to the macroscale, does not imply isotropy within typical regions of the flow which are small compared to the macroscale.* The correlation functions, even for very small separations, are defined by averages over large space regions, or over equivalent ensembles (the former average being the one related to experimental procedure).

Now let us interpret the Kolmogorov theory in the light of the weak dependence principle. Let $\mathbf{k}$, $\mathbf{p}$, $\mathbf{q}$ be three distinct modes, all high above the energy-containing range, such that $\mathbf{k}+\mathbf{p}+\mathbf{q}=0$. The energy exchange among these modes is determined by quantities of the type $Q = u_i(\mathbf{k})\, u_j(\mathbf{p})\, u_m(\mathbf{q})$. Let us examine how Q changes with time. By the weak dependence principle

$$\begin{aligned}\langle Q^* Q' \rangle &= \langle u_i^*(\mathbf{k})\, u_j^*(\mathbf{p})\, u_m^*(\mathbf{q})\, u_i'(\mathbf{k})\, u_j'(\mathbf{p})\, u_m'(\mathbf{q}) \rangle \\ &= \langle u_i^*(\mathbf{k})\, u_i'(\mathbf{k}) \rangle \langle u_j^*(\mathbf{p})\, u_j'(\mathbf{p}) \rangle \langle u_m^*(\mathbf{q})\, u_m'(\mathbf{q}) \rangle \quad \text{(indices not summed).} \quad (9.1)\end{aligned}$$

It follows that the time characterizing the variation of Q must be of the order of one of the individual characteristic times for the amplitudes $\mathbf{u}(\mathbf{k})$, $\mathbf{u}(\mathbf{p})$, $\mathbf{u}(\mathbf{q})$. The latter times would seem necessarily to be of order $(v_0 k)^{-1}$, $(v_0 p)^{-1}$, $(v_0 q)^{-1}$, respectively, corresponding to the sweeping of structures of the given wave-numbers by the macro-motion. Thus the weak dependence principle leads immediately to the conclusion that the time-variation of the rate of energy-transfer among high-lying modes is strongly dependent on the parameter v_0, which measures the excitation in the energy-containing range.

The Kolmogorov theory implies that the fluctuations in Q induced by the energy-containing range, although strong, do not affect appreciably the value of $\langle Q \rangle$, which is related to the *mean* energy-transfer among modes $\mathbf{k}$, $\mathbf{p}$, and $\mathbf{q}$. If so, the fluctuations simply reflect the dynamically insignificant distortion of small-scale structures by the slight shear associated with the macro-motion. That they arise at all is then an indication of the essential awkwardness of representing, in Eulerian k-space, phenomena which are more naturally described in quasi-Lagrangian co-ordinates.

In the direct-interaction approximation, on the other hand, these fluctuations represent the dominant contribution to a *relaxation* process acting on the phase correlation among modes $\mathbf{k}$, $\mathbf{p}$, and $\mathbf{q}$ built up by their direct coupling. Thus, they depress the magnitude of $\langle Q \rangle$ and inhibit mean energy-transfer. This difference underlies the divergence between the predictions of the two theories. As an illustration, we may replace v_0 in expression (7.2) by $[kE(k)]^{\frac{1}{2}}$, which is a measure of the r.m.s. velocity associated with wave-numbers of order k only. This has the effect of eliminating the influence of the energy-containing range on the relaxation time $\theta_I(k, p, q)$. With the change, it may be verified that (7.1) leads to the inertial-range law and dissipation-range scaling of the Kolmogorov theory.

It is hardly surprising that the direct-interaction approximation does not reproduce the Kolmogorov theory. The convection-without-appreciable-distortion appealed to by that theory involves the 'co-operative' action of the

very many triad interactions which link the energy-containing modes with pairs of the high-wave-number Fourier components of the convected small-scale structures. It is likely to be described poorly in an approximation where the various triad interactions are related only through relaxation effects. More surprising is the small difference between the spectrum laws of the two theories. Whatever may turn out to be the exact inertial range law, this in itself perhaps justifies a degree of confidence in the essential soundness of the direct-interaction approximation. It implies that even in the situation assumed by Kolmogorov, where the convection effects which the direct-interaction approximation cannot represent are very strong, their neglect does not much affect the ultimate energy equilibrium. From this point of view our application to the high-wave-number range at large R_0 constitutes a rather severe trial of the approximation. One might expect improved results at wave-numbers below the inertial range, where convection-without-distortion clearly does not occur in any event.

At the present time it seems difficult to decide between the two sets of inertial and dissipation range predictions. In fact, the exact inertial range law may be neither $k^{-\frac{5}{3}}$ nor $k^{-\frac{7}{3}}$. We have pointed out earlier some unrealistic aspects of the physical picture usually associated with the Kolmogorov theory. Perhaps a more serious drawback to this approach is the difficulty of developing it to the point of yielding quantitative predictions beyond the existing dimensional results. On the other hand, if the influence of v_0 on the inertial-range mean-energy-dynamics turns out to be an artifact of the direct-interaction approximation, the absolute inertial and dissipation range spectrum levels obtainable by this approximation may be considerably in error at sufficiently high R_0. It should be possible to shed some light on these questions by examining the next approximation in the sequence described briefly at the end of § 2.4.

9.2. *Heisenberg's heuristic theory*

Several authors have proposed models for the transport power $\Pi(k)$ based on simple physical analogies (Batchelor 1953, Chapter 6). Of these the heuristic theory of Heisenberg (1948) has aroused the most interest. Heisenberg assumed that $\Pi(k)$ could be represented as a power dissipation by all wave-numbers smaller than k due to the action of an effective 'eddy viscosity' which represented their coupling to all wave-numbers larger than k. In analogy to the expression for dissipation by real viscosity, he took

$$\Pi(k) = \int_0^k 2\left\{\kappa \int_k^\infty [q^{-3}E(q)]^{\frac{1}{2}}\,dq\right\} p^2 E(p)\,dp, \tag{9.2}$$

where κ is a disposable numerical constant. The eddy viscosity $\{\ \}$ was obtained by dimensional arguments on the basis of the Kolmogorov–v. Weizsäcker hypothesis of the localness of k-space dynamics. Because of its dimensional structure, (9.2) leads to a $k^{-\frac{5}{3}}$-inertial range spectrum law. At very high k it leads to a k^{-7}-law, implying the non-existence of mean-square third- and higher-order velocity derivatives.

The comparison of the eddy viscosity and the present theories is made more

illuminating by first modifying (9.2) to yield a $k^{-\frac{5}{3}}$ inertial range law; Heisenberg's basic physical assumption seems independent of the conflict between the direct-interaction approximation and the Kolmogorov theory. Accordingly, we shall consider the transport function

$$\Pi(k) = \int_0^k 2\left\{\kappa' v_0^{-1} \int_k^\infty q^{-1} E(q)\, dq\right\} p^2 E(p)\, dp, \tag{9.3}$$

where κ' is a new disposable numerical constant. The eddy viscosity $\{\}$ is here obtained by dimensional considerations under the requirement that it depend inversely on v_0. The algebraic rationality of (9.3) makes it perhaps more satisfying intuitively than (9.2).

From (9.3) we immediately obtain

$$-\frac{\partial \Pi(k)}{\partial k} = 2\kappa' k (v_0 k)^{-1} \left[\int_0^k \frac{p^3}{k} E(k)\, E(p) \frac{dp}{p} - \int_k^\infty k^2 E(k)\, E(p) \frac{dp}{p}\right]. \tag{9.4}$$

This equation has been written in a form to facilitate comparison with $-\partial \Pi(k)/\partial k$ as given by the right side of (7.1). The time factor $(v_0 k)^{-1}$ corresponds to the θ_I factor in (7.1). The most immediate qualitative difference between the two expressions is that (9.4) expresses the total interaction as an integral over *pair* interactions (k, p), rather than the *triad* interactions (k, p, q) which enter (7.1), and which are fundamental to the structure of the original equation of motion (3.1). A further difference concerns the sharp distinction in (9.4) between the interactions with modes higher than or lower than k. The absorption term involves only $p < k$ and the emission term only $p > k$. In (7.1) both sorts of modes enter both terms, and the net input appears as the balance of both ingoing and outgoing contributions from every triad interaction; this more closely resembles other dissipative equilibrium situations in statistical physics.

$E(k)$ appears as a factor in both the absorption and emission terms of (9.4), suggesting that this transport expression does not give the tendency to return to equilibrium, upon a perturbation of the spectrum in the neighbourhood of k, that was noted in the discussion of (7.1). This peculiarity shows up more clearly in (9.3) and also in the unmodified form (9.2). If the equilibrium is disturbed by an initial increase of spectrum level of wave-numbers above k, then by (9.2) or (9.3) the effective eddy viscosity acting on wave-numbers below k is increased. This will lead to an increased flow of energy from wave-numbers below k to those above k which will tend to increase further the eddy viscosity acting on the lower wave-numbers. A kind of instability seems to be indicated. On general statistical mechanical grounds we should expect precisely contrary behaviour; an increase of excitation in modes above k should lead to a decreased flow of energy to them from modes below k, as found in §4.

The comparisons made above can also be made on the basis of (9.2) but with less clarity. For this case the algebraic irrationality of the eddy viscosity expression results in greater asymmetry between absorption and emission terms.

9.3. *The analytical theories of Heisenberg and Chandrasekhar*

Heisenberg (1948, §5) and Chandrasekhar (1955) have developed analytical theories of turbulence based on the approximation that fourth-order moments

of the two-time distribution of the $\mathbf{u}(\mathbf{k})$ are related to second-order moments as if the $\mathbf{u}(\mathbf{k})$ were independent or, equivalently, that the corresponding x-space moments are related as in a normal distribution. We shall call this the quasi-normality approximation. It is far more drastic than the direct-interaction approximation, for the cross-moments involved. Consequently, we may surmise immediately, on the basis of the discussion in §9.1, that these theories should not yield the Kolmogorov theory. This seems to be supported by the attempt of Chandrasekhar (1956) to reconcile his theory with the $k^{-\frac{5}{3}}$ inertial range law. In order to obtain the formal possibility of a space correlation function consistent with this law, Chandrasekhar found it necessary to assume that the full space-time correlation function for small space-time separations was independent of v_0 in ordinary Eulerian co-ordinates. The Kolmogorov theory requires, instead, that this be true in a quasi-Lagrangian system moving with the macro-motion (Kolmogorov 1941), and therefore not true in Eulerian co-ordinates. As we shall note below a related situation arises in Heisenberg's theory.

Heisenberg's theory properly is appropriate to freely decaying turbulence, but its essential structure may be discussed in terms of our present specialization to the stationary case. The two cases should be equivalent, in any event, for treatment of the inertial and dissipation ranges at high Reynolds numbers. The theory first involves expressing the triple moment $S(k,\tau)$, defined by (3.5), in terms of fourth-order moments by substituting for $u_m(\mathbf{q},t)$ a bilinear integral expression obtained by integrating (2.2) (with $\mathbf{k}\to\mathbf{q}$, $i\to m$) with respect to time. Next, the fourth-order moments are expressed in terms of $U(k,\tau)$ by means of the quasi-normality approximation. This results in a closed equation for $U(k,\tau)$. The analysis was carried out for $\nu = 0$, but can be straightforwardly generalized to $\nu \neq 0$.

The expression which results for $S(k,\tau)$ can be obtained from our result (3.7) by (*a*) replacing the response functions $g(p,s)$, $g(q,s)$ with $\exp(-\nu p^2 s)$, $\exp(-\nu q^2 s)$; (*b*) discarding the terms involving $a(k,p,q)$; (*c*) retaining from the terms involving $b(k,p,q)$ only a particular linear combination of the parts which are antisymmetric in k and p for $\tau = 0$. The alteration of the response functions is equivalent to ignoring the effect on them of the non-linear interaction. The discarding of terms amounts, on the basis of the present theory, to throwing out most of the interaction altogether. This shows up strikingly if one evaluates the contribution to $r(k,\tau)$, for high k, due to energy-range mixing, after the fashion in which (5.5) and (5.6) were obtained. One finds that the dependence of $r(k,\tau)$ on v_0 disappears as $k/k_0 \to \infty$. This result apparently led Heisenberg to the following conjecture: Independence of $r(k,\tau)$ on v_0 is physically unreasonable in Eulerian co-ordinates, and moreover conflicts with the Kolmogorov theory. However, it is just the behaviour one would expect, on the Kolmogorov theory, in a quasi-Lagrangian system moving with the low-k motion. Therefore, possibly the quasi-normality approximation, and the resulting equation of motion (Heisenberg 1948, equation (83)), may be appropriate to such a co-ordinate system. The difficulty with this conjecture would seem to be that, aside from whether or not the quasi-normality approximation is appropriate to a Kolmogorov-type co-ordinate system, it is hard to see how making the approximation could automatically effect a transformation to such co-ordinates.

The theory of Chandrasekhar (1955) was developed by analysis in x-space. Expressed in k-space, it differs from that of Heisenberg, as generalized above, only in that $S(k,\tau)$ is expressed in terms of fourth-order moments by substituting a bi-linear expression for $u_i^*(\mathbf{k}, t-\tau)$ rather than for $u_m(\mathbf{q}, t)$. This gives, however, quite a different result from Heisenberg's, thereby indicating the intrinsic inconsistency of the quasi-normality approximation. Chandrasekhar's result may be obtained from (3.7) by replacing $g(k,s)$ with $\exp(-\nu k^2 s)$ and discarding all the contributions involving $b(k,p,q)$. The terms retained are all rigourously non-negative for $\tau = 0$, and, in contrast to Heisenberg's prescription, the theory consequently does not yield conservation of energy by the Reynolds stresses and pressure forces (Kraichnan 1957).

Our brief discussion has indicated that in both Heisenberg's and Chandrasekhar's theories the use of the quasi-normality approximation is equivalent to discarding essential parts of the dynamical coupling of the Fourier modes. The unphysical result for $r(k,\tau)$ on Heisenberg's theory and the major violation of energy conservation on Chandrasekhar's seem, in some respects, almost as serious as the unphysical time-dependence and violation of energy conservation implied by neglect of the third-order moments at the outset. We conjecture that this points towards a basic property of the dynamical system and that significant improvement should not be expected from theories made determinate by ignoring higher-order cumulants instead of fourth-order. As the order increases, the number of individual cross-moments of the $\mathbf{u}(\mathbf{k})$ entering the dynamically relevant expressions rises rapidly, and their total importance cannot be expected to decrease with increase of order, except for a very short time after a statistically independent initial state of the $\mathbf{u}(\mathbf{k})$, or at very low Reynolds numbers. This situation is connected with the non-linearity of (2.2) which results in phase relations among large groups of modes being established by networks of triad interactions. The direct-interaction approximation, on the other hand, is not equivalent to neglect of cumulants of any finite order. It is an approximation on the dynamics, rather than directly on the statistical distribution resulting from the dynamics.

9.4. *The theories of Proudman & Reid and Tatsumi*

Proudman & Reid (1954) and Tatsumi (1957) make the quasi-normality approximation only for the distribution of simultaneous values of the $\mathbf{u}(\mathbf{k}, t)$. They are able, thereby, to obtain closed equations for the time change of $E(k)$ in freely decaying isotropic turbulence. No predictions are obtained concerning time correlations. The analytical structure of these authors' theories is complicated, and we shall only indicate very briefly the nature of the relation with the present theory for the inertial range at very high Reynolds numbers. It should be noted that these theories were primarily intended to describe the energy-containing range.

We shall assume that there exists an inertial range, far above the energy-containing range, in which energy transport takes place by local cascade and in which the direct effects of viscosity are negligible. In this range we shall assume that the spectrum obeys a k^{-n}-law. Then it is not difficult to verify that the

approximation of Proudman & Reid and Tatsumi can be used to obtain an asymptotic expression for $-\partial\Pi(k)/\partial k$ at time t which differs from the right side of (7.1) only in that $\theta_I(k,p,q)$ is replaced by

$$\tau_0 = \int_t^\infty \frac{E(k,s)}{E(k,t)}\,ds, \tag{9.5}$$

where $E(k,t)$ is the value of $E(k)$ at time t.

From empirical knowledge we know that τ_0 must be of order $(v_0 k_0)^{-1}$, the overall decay time of the turbulence, whereas we have found that θ_I is of order $(v_0 k)^{-1}$ for significant triad interactions. If arguments are followed similar to those which led to and verified (6.3), we now find instead

$$E(k) \sim (\epsilon v_0 k_0)^{\frac{1}{2}} k^{-2} \tag{9.6}$$

for the asymptotic inertial range spectrum.† With this spectrum, however, $2\nu k^2 E(k)$ is independent of k. This is not inconsistent with the concept of an inertial range (which requires $1 < n < 3$), but it does seem an unlikely asymptotic property according to present experimental indications.

The results suggested above are not too surprising. The quasi-normality approximation for the one-time distribution is known empirically to be considerably in error for high wave-numbers (Batchelor 1953, §8.2). The appearance of τ_0 instead of θ_I in the transport expression would seem to indicate that, as in the case of the two-time quasi-normality approximation, the effect of ignoring fourth-order cumulants is to discard most of the effect of the dynamical interaction on the time-correlation functions and response functions. The theories of Proudman & Reid and Tatsumi do yield exact conservation of energy by the non-linear interaction.

The author would like to thank the many persons whose valuable comments and criticism contributed to this paper. Particular thanks are due to Dr G. K. Batchelor, Dr W. V. R. Malkus, Dr I. Proudman and Dr R. A. Silverman for discussions of the foundations of the theory. Mr R. Wernick and Dr M. Yanowitch have contributed to the mathematical analysis. Dr J. Laufer has kindly provided information on experimental errors and wire-length corrections associated with the measurements discussed in §8.2. Several authors have kindly given permission for the reproduction of figures from their published papers. Finally, the author would like to express his indebtedness to the authors whose theories are analysed in §9. The concepts developed in these theories played an essential role in forming the ideas underlying the present paper.

The research reported herein received support from the Geophysics Research Directorate, Air Force Cambridge Research Center, Air Research and Development Command, United States Air Force under contract AF 19(604)2138.

† Dr Tatsumi has recently informed the author that he also has obtained a spectrum which varies as $k^{-\frac{3}{2}}$, working from the equations of motion of his theory.

REFERENCES

BATCHELOR, G. K. 1953 *The Theory of Homogeneous Turbulence.* Cambridge University Press.

BETCHOV, R. 1957 *J. Fluid Mech.* **3**, 205.

CHANDRASEKHAR, S. 1955 *Proc. Roy. Soc.* A, **229**, 1.

CHANDRASEKHAR, S. 1956 *Phys. Rev.* **102**, 941.

HEISENBERG, W. 1948 *Z. Physik*, **124**, 628.

VON KÁRMÁN, T. 1948 *C.R. Acad. Sci., Paris*, **226**, 2108.

KLEBANOFF, P. S. 1955 *Nat. Adv. Comm. Aero., Wash.*, Rep. 1247.

KOLMOGOROV, A. N. 1941 *C.R. Acad. Sci. U.S.S.R.* **30**, 301; **32**, 16.

KOVÁSZNAY, L. S. G. 1948 *J. Aero. Sci.* **15**, 745.

KRAICHNAN, R. H. 1957 *Phys. Rev.* **107**, 1485.

KRAICHNAN, R. H. 1958*a* *Phys. Rev.* **109**, 1407. [Cited as Paper I.] Errata: **111**, 1747.

KRAICHNAN, R. H. 1958*b* *Physics of Fluids*, **1**, 358.

LAUFER, J. 1954 *Nat. Adv. Comm. Aero., Wash.*, Rep. 1174.

LIEPMANN, H. W., LAUFER, J. & LIEPMANN, K. 1951 *Nat. Adv. Comm. Aero., Wash.*, Tech. Note 2473.

MILLIONSHTCHIKOV, M. 1941 *C.R. Acad. Sci. U.S.S.R.* **32**, 615, 619.

OBUKHOV, A. M. 1941 *C.R. Acad. Sci. U.S.S.R.* **32**, 19.

PROUDMAN, I. & REID, W. H. 1954 *Phil. Trans.* A, **247**, 163.

STEWART, R. W. & TOWNSEND, A. A. 1951 *Phil. Trans.* A, **243**, 359.

TATSUMI, T. 1957 *Proc. Roy. Soc.* A, **239**, 16.

v. WEIZSÄCKER, C. F. 1948 *Z. Physik*, **124**, 614.

The dispersion of marked fluid in turbulent shear flow

By J. W. ELDER†
Cavendish Laboratory, University of Cambridge

(Received 24 September 1958)

The analysis used by Taylor (1954) and based on the Reynolds analogy has been extended to describe the diffusion of marked fluid in the turbulent flow in an open channel. The coefficient of longitudinal diffusion arising from the combined action of turbulent lateral diffusion and convection by the mean flow is computed to be $5{\cdot}9u_\tau h$, where h is the depth of fluid and u_τ the friction velocity. This is in agreement with experiments described herein. The lateral diffusion coefficient is found by experiment to be $0{\cdot}23u_\tau h$, which is three times larger than the value obtained by the assumption of isotropy. The same analysis can be used to describe the longitudinal dispersion of discrete particles, both of zero buoyancy and of finite buoyancy, and comparison is made with observations by Batchelor, Binnie & Phillips (1955) and Binnie & Phillips (1958).

1. Introduction

This paper describes the application of the analysis used by Taylor (1953, 1954), in his work on diffusion in a circular pipe, to the case of turbulent flow in a wide channel with a free surface. For pipe flow, fluid particles are laterally restrained, whereas in such a channel this is not so. This extra degree of freedom allows a direct investigation of the validity of the assumptions made by Taylor in calculating the small contribution to the longitudinal dispersion due to longitudinal turbulent diffusion. The investigation is of some practical importance in connexion with the disposal of industrial wastes and particularly of radioactive material in estuaries and the ocean.

At the present time there are two general approaches to the problem of diffusion. The first is the Lagrangian approach, an essentially kinematic formulation originally developed by Taylor (1922) in his theory of continuous movements. A recent survey has been given by Batchelor & Townsend (1956). The second method uses a Eulerian formulation and is the method used in the calculation below. This calculation is identical in principle to that used by Taylor (1954) for longitudinal diffusion in a pipe. It relies on the fact that the flow in a pipe or channel, under the action of a steady pressure gradient, is statistically steady and a function of a single co-ordinate y only. The dispersion process is controlled by the combined action of the longitudinal convection of fluid elements

† Present address: Department of Scientific and Industrial Research, Wellington, New Zealand.

at speeds depending on their lateral positions, and the lateral diffusion of fluid elements produced by turbulent mixing or molecular diffusion.

Consider the dispersion of those fluid particles which are labelled at some initial instant by injecting a dye or solute into the flow. The resulting mixture of fluid and dye is assumed to be of the same density ρ and kinematic viscosity ν as the original fluid, and the dye particles are assumed to be of zero size. Particles of finite size are discussed in § 5. Thus we have a solute which is hydrodynamically indistinguishable from the channel fluid. For this reason the term self-diffusion has much to recommend it. The process of diffusion we study here is going on all the time in the flow. At the moment of injection we merely label some of the fluid particles so that we may see how fluid particles are being moved about.

A conclusion of some importance immediately follows from the fact that the labelled fluid particles are hydrodynamically indistinguishable from a normal fluid particle. It is that the mean velocity of a marked particle in a pipe or a channel is the same as the discharge velocity; because the discharge velocity is the average particle velocity taken over all realizations of the flow. Alternatively, the result follows the fact that the probability of a particle passing through an element of area of a given flow cross-section is independent of the position of that element on the cross-section. The result was first given by Batchelor *et al.* (1955), who accurately confirmed it by experiments in a circular pipe. Further it is clear that the mean velocity of the centre of mass of a cloud of labelled particles is also equal to the discharge velocity. Since the cloud is made up of many fluid particles, we may expect in practice that even in a single realization (or experiment) the centre of mass will have a velocity very nearly equal to the discharge velocity. This was found to be so by Taylor (1954) in his experiments in a circular pipe and is further confirmed below for the flow in a channel.

Having established the importance of the discharge velocity, it is of interest to see how marked particles are dispersed relative to a point moving with the discharge velocity. Dr G. K. Batchelor pointed out (Taylor 1954) that the original considerations by Taylor for a particle whose velocity is a stationary random function of the time also applied to particles in the statistically steady flow in a pipe or channel. It follows that the mean-square of the fluctuation in (one component of) the position of a fluid particle after a time t is

$$\overline{X^2}(t) = 2\overline{u'^2}\int_0^t (t-p)\,R(p)\,dp. \tag{1}$$

where u' is the fluctuation, about the mean, of the particle velocity, and $R(p)$ is the correlation between $u'(t)$ and $u'(t+p)$. For t sufficiently large to make $R(p) = 0$ the relation becomes

$$\overline{X^2} \to 2\overline{u'^2}\,t\int_0^\infty R(p)\,dp. \tag{2}$$

If an effective diffusion coefficient for the longitudinal dispersion of solute exists, we must have an equation for the rate of change of mean solute concentration of the form

$$\partial S/\partial t = D_1 \partial^2 S/\partial \xi^2,$$

where ξ is a position co-ordinate in the direction of mean flow, relative to an origin moving with the mean velocity of a fluid particle. The solution corresponding to diffusion from an initial concentration at $\xi = 0$ is

$$S = \frac{q}{2(\pi D_1 t)^{\frac{1}{2}}} \exp(-\xi^2/4D_1 t) \quad (q = \text{constant}), \tag{3}$$

for which the dispersion of solute is measured by

$$\int_{-\infty}^{\infty} S\xi^2 d\xi = 2D_1 t.$$

This expression has the same t-dependence as (2) and suggests the existence of a diffusion coefficient $\overline{u'^2}\int_0^\infty R(p)\,dp$. The existence of a diffusion coefficient would be proved if it could be shown that the probability distribution of the particle displacement was Gaussian, but such a proof would require a central limit theorem for a stationary continuous process. Although this theorem is not yet available there is widespread belief in its validity. The above analysis is therefore merely suggestive and at the present stage we rely on the experimental observation that the probability distribution of the particle displacement is Gaussian.

2. The longitudinal diffusion coefficient

Consider the dispersion of a solute of neutral particles of concentration s gm/cm^3 of solvent in the steady flow in a channel. Solute is conserved, so that for an incompressible fluid with molecular diffusivity κ,

$$Ds/Dt = \kappa\nabla^2 s.$$

For dispersion in a turbulent velocity field, write $s = S + s'$, $\mathbf{u} = \mathbf{U} + \mathbf{u}'$, where S, $\mathbf{U}$ are mean values of concentration and velocity at a given position, and the fluctuation in velocity is $\mathbf{u}' = (u', v', w')$. Expanding Ds/Dt and averaging the resulting equation with respect to all realizations,

$$DS/Dt + \nabla.(\overline{\mathbf{u}'s'}) = \kappa\nabla^2 S,$$

where from now on D/Dt is the rate of change following the mean motion. Choose a co-ordinate system (x, y, z) so that the x-co-ordinate line is parallel to the mean flow and the mean velocity is a function of y alone. For flow in an open channel of depth h, (x, y, z) are Cartesian co-ordinates, whereas for the flow in a circular pipe of radius h they are cylindrical polars. Components in the directions of the three co-ordinate lines are given subscripts 1, 2, 3, respectively.

It is convenient to define the three diffusivities e_1, e_2, e_3 by

$$\overline{u's'} = -e_1 \partial S/\partial x, \text{ etc.},$$

so that in Cartesian co-ordinates

$$\frac{DS}{Dt} = \frac{\partial}{\partial x}\left(e_1\frac{\partial S}{\partial x}\right) + \frac{\partial}{\partial y}\left(e_2\frac{\partial S}{\partial y}\right) + \frac{\partial}{\partial z}\left(e_3\frac{\partial S}{\partial z}\right) + \kappa\nabla^2 S. \tag{4}$$

For a flow in which the local mean velocity is $U(y)$ the mean concentration S will also be a function of y. In practice this variation is not of primary importance

because of the presence of the channel walls. It is the net diffusive and convective transport longitudinally (x-direction) and the diffusion laterally in the z-direction that is important. To describe this net longitudinal transport we search for a simple solution of the transport equation (4) from which to identify a diffusion coefficient.

Let $e = e_2 + \kappa$ be a given function of y. Consider a distribution of concentration in which no lateral dispersion occurs so that $\partial S/\partial z = 0$. In all cases, terms like $\partial/\partial x$ make only a small contribution to the diffusion coefficient since the marked fluid is extended greatly in the x-direction, so that for the moment they may be neglected. From (4) therefore,

$$y^{-n}\frac{\partial}{\partial y}\left(ey^n\frac{\partial S}{\partial y}\right) = \frac{DS}{Dt}, \tag{5}$$

where $n = 0$ in a two-dimensional channel, $n = 1$ in a circular pipe (Taylor's case), and y is measured from the free surface or the centre of the pipe. Since we are interested in dispersion about a point moving with the discharge velocity $\overline{U}$, write

$$\frac{DS}{Dt} = \frac{\partial S}{\partial t} + \overline{U}\frac{\partial S}{\partial \xi} + U^*\frac{\partial S}{\partial \xi},$$

where $U = \overline{U} + U^*$ and $\xi = x - \overline{U}t$. Seek a solution of (5) for which, since fluid elements are rapidly extended in the x-direction,

$$\frac{\partial S}{\partial t} + \overline{U}\frac{\partial S}{\partial \xi} = 0$$

is a good approximation and the transport of S across a plane at ξ depends only on the small variation of S with y; in this case (5) becomes

$$w^{-n}\frac{\partial}{\partial w}\left(ew^n\frac{\partial S}{\partial w}\right) = h^2U^*\frac{\partial S}{\partial \xi}, \tag{6}$$

where $w = y/h$. Now put $S = P + Q$, where $\partial P/\partial w = 0$, $\partial P/\partial \xi =$ constant, so that the total transport of P across a plane at ξ is zero. If further, following Taylor (1954) and subsequently justifying the procedure by the agreement with measurements, we assume $\partial Q/\partial \xi = 0$, equation (6) is then integrable and we find

$$Q = h^2\frac{\partial P}{\partial \xi}\int_0^w e^{-1}w^{-n}\left(\int_0^w w^nU^*\,dw\right)dw. \tag{7}$$

which satisfies $\partial S/\partial w = 0$ on $w = 0, 1$.

If the longitudinal dispersion can also be described by a diffusion coefficient the rate of transfer of solute across a section of area A at ξ is

$$\int_A U^*Q\,dA \equiv -D_1A\frac{\partial P}{\partial \xi}. \tag{8}$$

The relation (7) then requires

$$D_1 = -h^2\int_0^1 (2w)^n\,U^*\,dw\left[\int_0^w e^{-1}w^{-n}\left(\int_0^w w^nU^*\,dw\right)dw\right]. \tag{9}$$

This expression applies to both laminar and turbulent flows, provided the time scale of the convective effect is much greater than the time scale of the diffusion of variations of S with y (Taylor 1954). It will also be shown in § 5 to apply to particles of finite size provided U and e are replaced by their mean values over the cross-sectional area of the particle.

3. Turbulent dispersion in an open channel

At the present stage of research it is necessary to deduce the form of the e_i by comparison with experiment. It is fairly well established that near a wall the transfer of momentum and mass are analogous. That is,

$$e_2 = -\overline{v's'}\Big/\frac{\partial S}{\partial y} = -\overline{v'u'}\Big/\frac{\partial U}{\partial y}. \tag{10}$$

This relation will be assumed to hold over the whole channel. For the flow in a channel or pipe in which the velocity field is a function of y only and is otherwise homogeneous, only one such relation (10) can be written down. Hence Reynolds analogy only allows us to calculate directly the longitudinal diffusion coefficient.

For a pipe or channel the Reynolds equations for the mean flow can be integrated to give $\tau = \tau_0 w$, where τ is the stress in the fluid and τ_0 is the stress at the wall. The friction velocity u_τ is defined by $(\tau_0/\rho)^{\frac{1}{2}}$. The velocity distribution satisfies the defect law

$$\left.\begin{aligned} U &= U_1 - u_\tau f(w) \\ \text{and} \quad \bar{U} &= U_1 - u_\tau \bar{f}, \end{aligned}\right\} \tag{11}$$

where U_1 is the maximum velocity. Hence, by (10) and neglecting the molecular diffusion coefficient which is normally only about $10^{-4} e_2$,

$$e = h u_\tau w/f'. \tag{12}$$

The velocity distribution is specified by the function $f(w)$. Taylor, in his calculation for dispersion in a pipe, used an empirical function based on experiment. For flow in an open channel $f(w)$ is given closely by the logarithmic law of the wall

$$kf(w) = -\log(1-w), \tag{13}$$

where $k = 0{\cdot}41$ is an absolute constant.

Hence D_1 is determined by (11), (12), (13) and (9) and for $n = 0$ the first two integrations for D_1 can be performed to give

$$k^3 D_1/h u_\tau = \int_0^1 w^{-1}(1-w)[\log(1-w)]^2 dw. \tag{14}$$

The integral can be evaluated as a series of gamma functions to give a value $2\sum_{n=2}^{\infty} n^{-3} \doteq 0{\cdot}4041$, so that, on using $k = 0{\cdot}410$, we have

$$D_1 = 5{\cdot}86\, h u_\tau.$$

Turbulent diffusion in the x-direction

So far we have neglected the contribution from the longitudinal turbulent diffusion by ignoring the term $\partial/\partial x(e_1 \partial S/\partial x)$. Taylor showed that the contribution was normally insignificant for laminar flow and even for turbulent flow was small.

He was able to make a reasonable estimate by assuming $e_1 = e$, which is strictly true in isotropic turbulence. The additional diffusive transport is

$$h\int_0^1 e\frac{\partial S}{\partial \xi}dw \equiv D^*h\frac{\partial S}{\partial \xi}, \tag{15}$$

where D^* is the diffusion coefficient due to the longitudinal turbulent diffusion. Hence

$$D^*/hu_\tau = \int_0^1 w\,dw/f' = k/6 = 0{\cdot}068. \tag{16}$$

The total longitudinal coefficient is thus $(5{\cdot}86 + 0{\cdot}07)\,u_\tau h = 5{\cdot}93\,u_\tau h$. Although the use of the Reynolds analogy by itself does not allow the lateral diffusion coefficient to be calculated, the above calculation for D^* equally well evaluates, on the assumption of isotropy, the diffusion coefficient for lateral diffusion, D_3. Notice that D_3 is linearly related to e, whereas D_1 is linearly related to $1/e$.

4. Experimental results in an open channel

The experimental arrangement

The experimental investigation was performed in the 14-inch water flume of the Engineering Laboratory, Cambridge. The flume is described by Binnie, Davies & Orkney (1955). It was the only suitable channel available in Cambridge, and it severely restricted the range of the experiments. A roof tank was kept full by pumping water from a sink, placed beneath the outlet to the working section. Water from the tank ran through a valve into a reservoir behind the working section. The working section was 10 ft. long, rectangular in section and inclined at 0·046° to the horizontal. A sheet of white, self-adhesive plastic on which had been drawn a grid of black lines spaced 10 cm apart longitudinally and 5 cm apart transversely was stuck to the bottom of the working section.

Turbulent flow did not occur naturally in the channel. Transition to turbulence was stimulated by placing two trip fences of 4 mm height, 20 cm apart, at the beginning of the working section. Dye-injection tests revealed the efficiency of the device. Experiments were always performed more than 50 cm downstream of the trip fences.

The possible experimental range was limited by three factors, the occurrence of waves near Froude number 0·7, the need for the turbulent boundary layer thickness of the flow near the wall to exceed the channel depth and the need for the flow to be turbulent. In the flume used, the inclination was fixed and the weir height was set at zero, since otherwise the experimental range was even more restricted. Then U_1 is an increasing function of h. In the channel used here, $U_1 = 23h^{0{\cdot}63}$ cm/sec, for h in cm. The mean velocity profile was determined with a total head tube and an inclined tube manometer. The profile was directly confirmed to be the same throughout the working section. All the profiles measured satisfied (13), except very near the wall and very near the surface, for $h < 1{\cdot}5$ cm. Thus the experiments were limited to a depth of 1·0 to 1·5 cm, corresponding to a Reynolds number range of 2300 to 4500. The viscous sublayer caused departures from a logarithmic profile for $w < 0{\cdot}05$. The friction velocity

determined from the experimental profiles agreed to within $\pm 1\,\%$ with values obtained by using a Reynolds number based on the so-called hydraulic mean depth and pipe data for the friction velocity (Nikuradse 1930). Over the range considered here

$$\overline{U}/u_\tau = 5{\cdot}09(\overline{U}h/\nu)^{\frac{1}{8}}.$$

The depth of flow was determined with a pricker gauge and the discharge velocity from the rate of discharge of water volume at the end of the channel.

It was not permissible to use salt as the solute because the recirculated water was also used in other machines in the Laboratory, but permanganate solution is both harmless and intensely coloured. A stock solution was made up to a density $1{\cdot}033\,\mathrm{g/cm^3}$. Normally measurements encountered concentrations smaller by a factor 10^{-3} to 10^{-4}. Most of the measurements were made photographically. The working section was uniformly illuminated through the glass sides, photographed from above on Ilford FP3 film and developed in Ergol at 25 °C to a Weston rating of 400. This allowed a short exposure time and fine grain. Conditions of illumination, exposure and development were carefully standardized. Up to 80 strip photographs could be obtained on a single film. Each film was directly calibrated first by taking a photo with no dye in the channel, and secondly with a series of pots, filled with dye of known concentration, placed in the channel.

The film blackness is described by the density $d = -\log_{10} T$, where T is the proportion of light transmitted through the film. Over a considerable portion of the film characteristic there is a linear relation between d and the logarithm of the exposure. For a fixed exposure time the exposure is proportional to the intensity of illumination which the camera is viewing. Let the illumination with no dye in the channel be I_0. Hence if the light scattering is small and the presence of dye does not alter I_0, the observed illumination I is given by the usual relation

$$I = I_0 \exp\left(-\beta \int_0^h s\,dy\right),$$

where s is the instantaneous concentration, β is a constant related to the particular dye and the channel fluid, and it is assumed that the camera is at infinity in the y-direction. When the film is read we obtain Δd, the difference of density between that with dye in the flow and that without dye in the flow. Hence

$$\Delta d \propto C, \quad \text{where} \quad C = \int_0^h s\,dy.$$

The relation between concentration C and density was linear up to $\Delta d = 0{\cdot}7$, and although allowance was made for the non-linearity of this relation it was normally quite small. As the bulk of the observations had a density of less than 0·5, corrections due to non-linearity were not often used. The film was automatically read and plotted on the J.L.C. Walker Microdensitometer of the Medical Research Unit, Cavendish Laboratory. Normally the instrument was used with $d = 0{\cdot}5$ corresponding to the full scale of 19 cm. Plotting reproducibility was $\pm 0{\cdot}2$ mm.

There is an important advantage of the photographic or fixed time method over probe or fixed distance method. If the diffusion rate is high, the concentration

distribution may change sufficiently quickly while the cloud is passing over a probe to produce a long tail (Levenspiel & Smith 1957). Consider the simple example of injecting a small volume q of dye at unit concentration at $t = 0$ into a pipe of unit cross-section in which the fluid has a discharge velocity $\overline{U}$. At a later time the concentration is given by (3). For observations at $x = X$, S is not a Gaussian function of time unless $X^2/Dt \doteqdot \overline{U}X/D$ is large. Even for $\overline{U}X/D = 50$ a tail twice as long as for a Gaussian curve is found. In my experiments this corresponds to $X \doteqdot 40$ cm. Thus the use of the photographic method in this experiment is very desirable.

The method of injecting the dye was designed to be as simple and reproducible as possible. For continuous injection a constant head of dye was maintained above a 1·0 mm circular jet. The wall of the jet was held 1 mm from the surface so

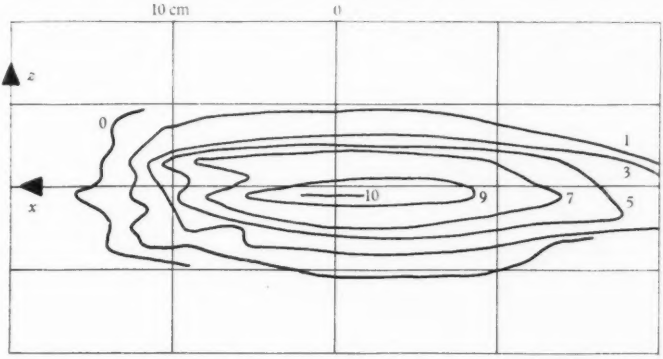

FIGURE 1. Plan view of a drop of dye diffusing in the turbulent flow in an open channel. Distribution of concentration C, normalized to have a maximum of 10. The flow is to the left. $h = 1{\cdot}43$ cm, $X/h = 90$.

that the dye was injected normal to the surface at a rate between 0·1–0·4 cm^3/sec. For the injection of drops a tube of 4 mm internal diameter was attached to a small chamber ending in a rubber diaphragm. A 1 cm length of the tube was filled with dye and the tube end held 1 cm from the surface. When the diaphragm was tapped the dye was shot into the water in the channel.

The experimental results

If a drop of dye is injected and observed at some later time the drop appears as shown in figure 1. Lines of equal values of the concentration C, with a maximum of 10, are shown. The longitudinal dispersion is some 5 times the lateral dispersion. The curves are much more disturbed in front and a pronounced tail is seen behind.

The mean position of the drop averaged over all realizations was directly verified to correspond to the position of a point moving with the discharge velocity to better than the experimental accuracy of 0·2 %. First, direct observations were made with a stop-watch, giving an accuracy over several runs of $\pm 0{\cdot}1$ sec in about 10 sec. Secondly, at the same instant as the drop of dye was released, a stop-watch was started and also a piece of paper, 2 cm in diameter, was placed on the water surface at a known position some distance upstream of the

injection point. The piece of paper moves downstream with the surface velocity. At a later time a photograph was taken showing the stop-watch, the piece of paper and the diffusing drop. The shutter speed was 0·003 sec. The accuracy is now determined by the measurements of a small length in a total length of 350 cm. No significant departure from the assumption could be found.

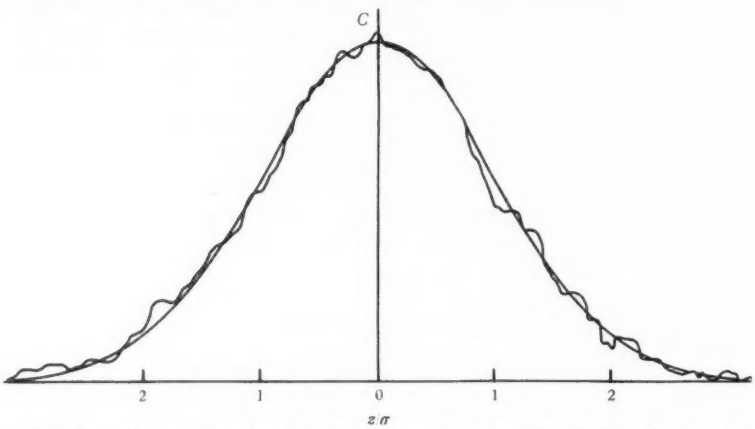

FIGURE 2. Lateral concentration distribution across the middle of a diffusing drop and the Gaussian curve of best fit. $h = 1{\cdot}34$ cm, $X/h = 110$, σ = standard deviation.

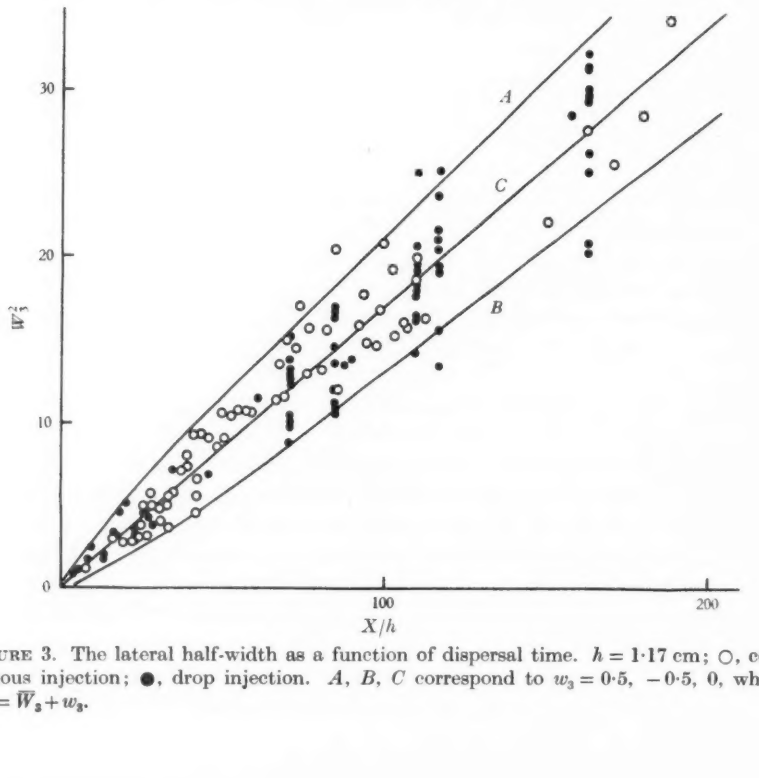

FIGURE 3. The lateral half-width as a function of dispersal time. $h = 1{\cdot}17$ cm; ○, continuous injection; ●, drop injection. *A*, *B*, *C* correspond to $w_3 = 0{\cdot}5$, $-0{\cdot}5$, 0, where $W_3 = \overline{W}_3 + w_3$.

Figure 2 shows a direct tracing of a microdensitometer traverse laterally across the middle of such a drop together with the Gaussian curve of best fit. The variations are directly due to variations of the concentration in the stream and are not due to grain on the film. The closeness of fit even in the tails is remarkable. Evidently the lateral dispersion can be described by a diffusion coefficient since a Gaussian distribution of concentration implies the existence of a diffusion coefficient. Figure 3 shows that the diffusion coefficient is independent of X for large X, where X is the mean position of the drop at any instant, this figure (based on 133 measurements both from drops and continuous injection) gives experimental values of W_3^2 as a function of X, where

$$W_3 = (\text{lateral half-width})/h,$$

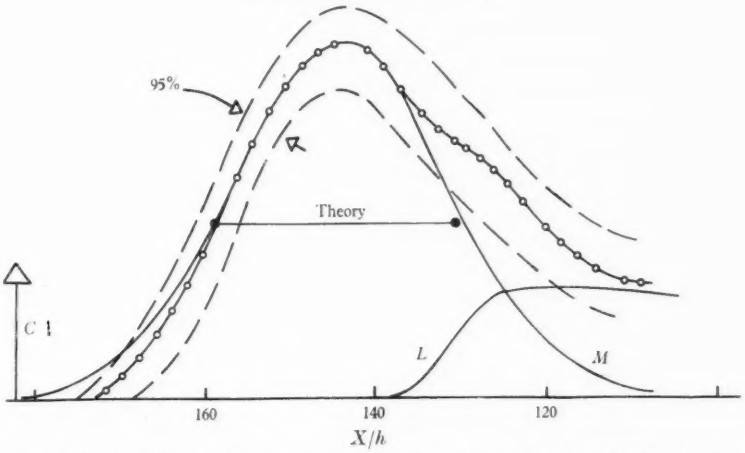

FIGURE 4. The mean longitudinal concentration distribution and the 95 % limits along the centre line of a diffusing drop. $h = 1{\cdot}27$ cm, $R = 3{\cdot}41 \times 10^3$. M, turbulent component; L, sublayer component.

and the half-width is the distance between the points at which the concentration is half the maximum value. The points lie about a mean line C for which $\overline{W_3^2} \propto X/h$, corresponding to a lateral diffusion coefficient $D_3 = 0{\cdot}228 u_\tau h$, about three times the value given by (16). If we write $W_3 = \overline{W}_3 + w_3$, the lines A, B, C correspond to $w_3 = 0$, $\frac{1}{2}$, $-\frac{1}{2}$ respectively. The probability distribution of w_3, $P(w_3)$, is symmetrical about $w_3 = 0$, has a standard deviation of 0·204, and at $w_3 = 0{\cdot}05$, 0·15, 0·25, 0·35, 0·45, 0·60 has the values $P(w_3) = 0{\cdot}119$, 0·119, 0·109, 0·072, 0·050, 0·018. $P(w_3)$ is much more rectangular than Gaussian. Notice that w_3 is independent of X so that the proportional scatter decreases as $X^{-\frac{1}{2}}$. Even at $X/h = 100$ the scatter is ± 5 % S.D.

The longitudinal dispersion can also be described by a diffusion coefficient. From the photographs, taken at the same dispersion time, from 20 different drops, a mean and a 95 % concentration curve have been derived from traverses along the centre line of the drop, and are shown in figure 4. The 95 % curve defines the region outside which 5 % of the points lie. The mean curve can be considered to consist of two components. The first and main component corresponds to solute

which is being carried in the fully turbulent part of the channel, whereas the second component arises from solute which is being carried near the wall in the viscous sub-layer. Since $C = \int_0^h s\,dy$, the total observed concentration is the sum of the two concentrations. In figure 4 an attempt has been made to separate the two components into a Gaussian curve, M, and another curve, L, by obtaining as good a fit as possible to the Gaussian curve over the forward portion of the experimental curve. From this Gaussian curve we obtain the experimental value 6·3 for D_1/hu_τ, about 8 % higher than that given by the calculation. The measurements were made at a Reynolds number of $3{\cdot}5 \times 10^3$. At such low Reynolds numbers it has already been noticed by Taylor (1954) that experimental values exceed those of calculation. The longitudinal half-width ($= W_1 h$) is given in figure 5 as a function of X/h. For the larger values of X/h the behaviour is similar to that of the lateral half-width. Writing $W_1 = \overline{W}_1 + w_1$, lines A, B, C in the figure correspond to $w_1 = 1, -1, 0$. The standard deviation of w_1 is 0·48, some 2·4 times larger than for the lateral scatter.

Notice that (figure 4) the distribution of concentration in the sublayer component L quickly rises to a peak, at a distance of about $2(2D_1 t)^{\frac{1}{2}}$ upstream of the centre of the drop, beyond which a long tail extends upstream. It is possible to obtain experimental values of the ratio of the length scales of the L and M distributions by comparing the distances between the maxima and the upstream point at which the concentration C has dropped to half its maximum value. This ratio was found to lie between 5 and 7 for the data of figure 4.

Departures from the simple theory due to the eddy structure

The most novel feature of the observations presented above is the simple manner in which the half-width for each realization varied about the mean half-width. If $W = \overline{W} + w$, the probability distribution of w, $P(w)$, is symmetrical about $w = 0$ and independent of W or X. For the lateral half-width the standard deviation of w_3 was 0·20. Thus ± 3 standard deviations extend over a width of $1{\cdot}2h$. The photographs show that the edge of the drop is distorted on a scale of order h. Thus we identify the spread of W as due to large eddy motions whose planes of circulation extend over an appreciable portion of the channel depth. These large eddies have been studied recently by Grant (1958). Similar remarks apply to the variation in the longitudinal width.

Taylor's expression (1) can be written as

$$\overline{X^2} = A_1 t - B_1,$$

where, as $t \to \infty$,

$$A_1 \to 2\overline{u'^2} \int_0^\infty R(p)\,dp, \quad B_1 \to 2\overline{u'^2} \int_0^\infty pR(p)\,dp,$$

with similar expressions relating the mean-square particle displacement in the y- and z-directions, $\overline{Y^2}$, $\overline{Z^2}$, to A_2, B_2 and A_3, B_3. Using this relation to extrapolate the data of figures 3 and 5 shows that for lateral diffusion $|B_3| < 0{\cdot}05h^2$, and for longitudinal diffusion $B_1 \doteq 30h^2$. The small value of B_3 suggests that the Lagrangian correlation $R_{33}(0, 0, t)$ reverses sign while the large value of B_1 suggests that

$R_{11}(t, 0, 0)$ is of constant sign and very extensive. This behaviour is seen to be similar to that of the corresponding Eulerian correlations recently measured by Grant (1958) in a boundary layer and suggests that the eddy motions responsible for these correlations persist for a considerable time.

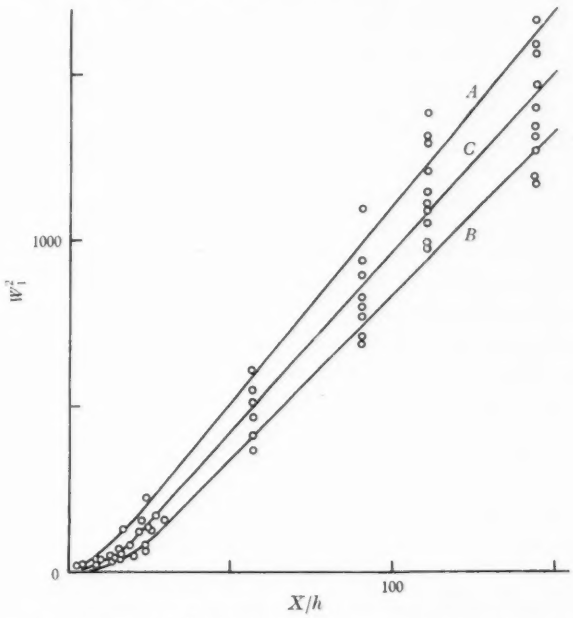

FIGURE 5. The longitudinal half-width as a function of dispersal time. $h = 1{\cdot}27$ cm. A, B, C corresponds to $w_1 = 1$, -1, 0, where $W_1 = \overline{W}_1 + w_1$.

Departures from the simple theory due to the wall sublayer

It is already well known that the distribution of concentration is found experimentally to be asymmetric for small Reynolds number and small dispersal time. I have mentioned that this can occur due to observations being made at a fixed point, at small values of $\overline{U}X/D$. This spurious effect is not responsible for the long tails found by Taylor (1954) in experiments in which $\overline{U}X/D \gg 100$. Nor, of course, does it apply to the present method. But we have so far considered the channel as completely filled by fully turbulent motion and have ignored the influence of the flow in the viscous sublayer next to the wall. This layer extends to

$$y_s/h \doteq 10\nu/u_\tau h = 50R^{-\frac{7}{8}},$$

at which position the mean velocity is

$$U_s/U_1 \doteq 10u_\tau/U_1 = 2R^{-\frac{1}{8}}.$$

Subscripts s refer to the edge of the sublayer, $R = U_1 h/\nu$ and $U_1/u_\tau \doteq 5R^{\frac{1}{8}}$. It seems reasonable to assume that the flow field is sharply divided into laminar and turbulent regions by the sublayer surface at $y = y_s$ and that marked particles can be exchanged between the two regions only by molecular diffusion. We have

already seen that a diffusion coefficient can be defined in the turbulent region. The same method can by employed to calculate the value of the diffusion coefficient D_s appropriate to the linear velocity profile of the sublayer (Couette flow). It is easily shown from (9) that $D_s = y_s^2 U_s^2/120\kappa$.

Thus the two layers can both be described by diffusion equations. The diffusion in the turbulent layer occurs about a point moving with the discharge velocity $\bar{U}$, but the diffusion in the sublayer occurs about a point moving with the velocity $\frac{1}{2}U_s$. While a diffusing drop is passing over a point in the sublayer, marked particles enter the sublayer, and as the drop passes downstream these particles disperse, by longitudinal dispersion in the sublayer and by molecular diffusion back across the sublayer surface into a well-stirred region of nearly zero concentration.

The derivation of the form of D_s relies on the assumption that the rate of transport of solute in the y-direction, and in particular the transport of solute across the plane $y = y_s$ is small compared with the transport longitudinally (Taylor 1954). That this is normally the case is seen by noting that the time for a particle in the sublayer to move (by molecular diffusion) a distance y_s in the y-direction is $y_s^2/2\kappa$, a time much larger than even the total dispersion time available in the present experiments.

The assumption that the transport of solute across y_s out of the sublayer has a much smaller effect on the distribution of solute in the sublayer, once the turbulent cloud has passed, than longitudinal dispersion in the sublayer, is supported by a comparison of the measured length scale of the tail with values computed from D_s. It is convenient to do this by comparing the length scale of the longitudinal dispersion in the turbulent layer, X_1, with the length scale of that in the sublayer, X_s. We have for the ratio of these length scales $X_s/X_1 = (D_s/D_1)^{\frac{1}{2}}$; but

$$D_1/\nu = 1{\cdot}16R^{\frac{7}{8}}, \quad D_s/\nu = \left(\frac{y_s}{h}\right)^2 \left(\frac{U_s}{\bar{U}_1}\right)^2 \frac{R^2}{120\kappa} = 83\,\nu/\kappa,$$

so that

$$X_s/X = 8{\cdot}6R^{-\frac{7}{16}}(\nu/\kappa)^{\frac{1}{2}}.$$

For the data of figure 4 we have $R = 3{\cdot}4 \times 10^3$, $\kappa = 1{\cdot}5 \times 10^{-5}$ cm^2/sec and therefore $X_s/X_1 = 6{\cdot}3$. Experimental values lay between 5 and 7. This verification of the assumption of the independence of the two layers provides some justification of the analysis of the data of figure 4 into two components.

The isotropic assumption

The isotropic assumption involved in calculating the lateral diffusion is in error by a factor of 3. Particles disperse laterally some 70 % faster than for the isotropic case. It was to be expected that the isotropic assumption produces too low a value of D_3, since the lateral turbulent intensity always exceeds the vertical intensity ($\overline{w'^2} - \overline{v'^2} \doteqdot \tau_0/\rho$; see Klebanoff 1954). It may therefore be supposed that the contribution of the turbulent fluctuating motion to the longitudinal dispersion is also in error. Assume that this contribution equals the lateral diffusion coefficient, thus giving $D_1 = (5{\cdot}86 + 0{\cdot}23)\,hu_\tau = 6{\cdot}1hu_\tau$, with $D_3 = 0{\cdot}23u_\tau h$. The experimental value of D_1, viz. $6{\cdot}3hu_\tau$, about 3 % high, is in reasonable agreement with theory, despite unfortunately low values of the Reynolds number and small dispersion times imposed by the apparatus.

5. The dispersion of discrete particles

The dispersion of non-buoyant particles

Before analysis similar to that of § 2 can be applied to the dispersion of finite solid particles of radius αh it is necessary to establish the appropriate form of both the particle velocity and the particle diffusivity. First, the mean velocity of discrete particles in the flow in a circular pipe has been shown by Batchelor *et al.* (1955)—and in an extension of the investigation by Binnie & Phillips (1958)—to be given accurately, provided α is less than about 0·15, by the discharge velocity obtained from the discharge due to the part of the pipe cross-section that is accessible to the particle centre. For larger particles ($0{\cdot}15 < \alpha < 0{\cdot}3$) it was found to be more accurate to estimate the mean particle speed on the assumption that the velocity of the particle, when its centre is at position y, is equal to the average of the mean fluid speed over a circle of radius αh centred at y. Secondly, in the theory of the transport of suspended sediment (Rouse 1937, and improved by Hunt 1954), the assumption that very small discrete particles ($\alpha \doteq 0{\cdot}002$) are dispersed at the same rate as fluid particles leads to good agreement with experiment. Thus we may expect that (9) will also apply to discrete particles, provided some account is taken of the finite size of the particle. The following discussion applies to pipe flow and to particles of size such that $\alpha < 0{\cdot}15$.

The mean particle velocity $\overline{U}(\alpha)$ has to be evaluated over the accessible area $\pi(1-\alpha)^2h^2$ as described above, so that

$$U^*(\alpha, w) = U - \overline{U}(\alpha) = U - \frac{2}{(1-\alpha)^2}\int_0^{1-\alpha} wU\,dw, \tag{17}$$

and this takes the place of U^* in (9).

An estimate of the diffusivity $e(\alpha, w)$ of a particle of finite size can be made by observing that in evaluating (9) the bulk of the contribution to D_1 arises from the region near the wall. In this region the velocity profile is logarithmic, so that by (12) and (13), $e \doteq khu_\tau w(1-w)$. Hence,

$$e(\alpha, w) \doteq e(0, w) - \tfrac{1}{3}khu_\tau\alpha^2, \tag{18}$$

so that provided α is small the error in writing $e(\alpha, w) = e(0, w)$ is small (the expression does not apply near $w = 0$ or 1). In fact the mean diffusivity $\bar{e}(0) = 4khu_\tau/15$, and the extra term in (18) represents a proportional error of $5\alpha^2/4$.

Observe also that in (8), although D_1 is defined in terms of the transport through an area πh^2, the transport occurs only over an area $\pi(1-\alpha)^2h^2$, so that in (9) the upper terminal of the integral becomes $1-\alpha$.

Equation (9) can be written in the form

$$\left.\begin{aligned} D_1(\alpha) &= -2h^2\int_0^{1-\alpha} wU^*(\alpha, w)\,A(\alpha, w)\,dw, \\ \text{where}\quad A(\alpha, w) &= \int_0^w (ew)^{-1}\left[\int_0^w wU^*(\alpha, w)\,dw\right]dw, \end{aligned}\right\} \tag{19}$$

$U^*(\alpha, w)$ is given by (17) and $e = e(0, w) = hu_\tau w/f'$ by (12). The function $f(w)$ which defines U by means of (11) has been tabulated by Taylor (1954), and throughout the subsequent calculations we use his values. On performing the integration (17) and writing

$$U^*(\alpha, w) = u_\tau[\bar{f}(0) - f(0, w)] + u_\tau[\bar{f}(\alpha) - \bar{f}(0)], \tag{20}$$

we find $$A(\alpha, w) = A(0, w) + \frac{1}{2h}[\bar{f}(\alpha) - \bar{f}(0)] f(0, w). \tag{21}$$

The final integration in (19) performed numerically for three values of α gave the values shown below.

α	0 (Taylor)	0·04	0·10	0·15
$\bar{U}(\alpha)$	4·25	3·60	2·98	2·56
$D_1(\alpha)/hu_\tau$	10·1	4·80	2·22	1·21

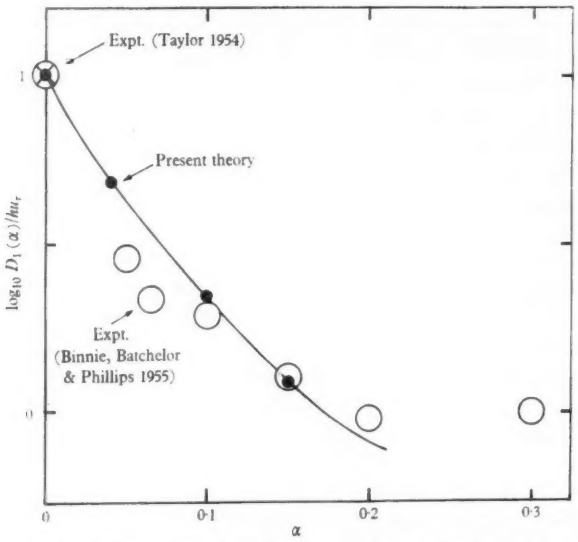

FIGURE 6. Longitudinal dispersion of non-buoyant spheres of radius αh in a circular pipe. Experimental values from Batchelor *et al.* (1955).

These points are shown in figure 6, together with the experimental values obtained by Batchelor *et al.* (1955). The experimental points have a standard error of about 5 %. The radii of the circles correspond to an error of 10 % in D_1. The agreement is quite good. The departure for large α is expected because of the neglect of the curvature of the diffusivity and velocity distributions. The mean error in neglecting the curvature of the diffusivity seems likely to be the greater, and is shown by (18) to be 11 % at $\alpha = 0{\cdot}3$. Thus, for α large, as opposed to the behaviour for α small, the principal effect arises through the diffusivity distribution, and since D_1 is linearly related to $1/e(\alpha, w)$ the neglect of the curvature of $e(\alpha, w)$ as shown by (18) leads to an underestimate of D_1. This is the case for the experimental point at $\alpha = 0{\cdot}3$. There is also significant departure for small values of α. Such an effect has also been observed in Vanoni's (1946) experiments on the transport of suspended sediment. This effect is undoubtedly due to the sublayer near the wall. In this region the tabulated values of $f(w)$ and the computed diffusivity are not necessarily reliable. It should be noticed that the computation of D_1 requires four successive integrations, so that D_1 is sensitive to the form of $f(w)$ and that the bulk of the contribution to D_1 arises near the wall, particularly for the smaller particles. The departure is therefore to be expected.

The dispersion of buoyant and heavy particles

The above discussion applies to particles of density equal to that of the surrounding fluid. In view of the success of the discussion of Binnie & Phillips (1958) in evaluating the mean velocity of buoyant and heavy particles in a circular pipe by means of the hypothesis of sedimentation theory, it appears likely that (9) can again be easily modified to apply to heavy particles. For example, consider the flow in a channel. It is assumed that the probability density $P(w)$ of the position of particles is determined by a balance between the transport due to a settling velocity V and the turbulent transport, so that

$$VP - e\frac{dP}{dy} = 0.$$

This is readily integrated by using (12) and (13) to give

$$P = \left[\frac{w}{1-w}\right]^{\beta} \frac{\sin \pi\beta}{\pi\beta} \quad (\beta \neq 1, 2, \ldots), \tag{22}$$

where $\beta = V/ku_\tau$ (Rouse 1937). The mean particle velocity $\overline{U}(\alpha, \beta)$ is then

$$\overline{U}(\alpha, \beta) = \int_0^{1-\alpha} P(w)\, U\, dw. \tag{23}$$

Equation (9) may now be used as before with $U^* = U - \overline{U}(\alpha,\beta)$ and $e(\beta) = e(0)$.

A rough idea of the variation of D_1 with β can be obtained by considering the artificial example of a parabolic velocity distribution in a channel, in which the probability distribution is given by (22), and the molecular diffusivity is a constant of value κ. From (23) and (9) with $\alpha = 0$ it is easily shown that

$$D_1(\beta) = \frac{U_1^2 h^2}{7560\kappa}(64 + 21\beta - 308\beta^2 - 210\beta^3 - 35\beta^4). \tag{24}$$

$D_1(\beta)$ rises by 0·55 % above $D(0)$ to a weak maximum at $\beta \doteqdot 1/30$ and decreases relatively quickly to zero near $\beta = \pm 0{\cdot}5$. This behaviour is typical only of the very small particles which normally utilize all the available velocity variation across the channel—unless inhibited by buoyancy—so that the convective effect is large and consequently so also is D_1.

For finite particles the available velocity variation is much reduced so that D_1 is less sensitive to buoyancy. Binnie & Phillips (1958) have already evaluated the expression corresponding to (23) for a circular pipe and find

$$\overline{U}(\alpha, \gamma) = (1 - B\gamma^2)\,\overline{U}(\alpha, 0), \tag{25}$$

where $\gamma = V/\overline{U}$ and B is given by their equation (8). For $\alpha = 0{\cdot}1$, $B = 15{\cdot}7$. $D_1(\alpha, \gamma)$ can now be evaluated from (9) and (25) using Taylor's data for $f(w)$. In figure 7, $D_1(\alpha, \gamma)/hu_\tau$ is given for $\alpha = 0{\cdot}1$, together with the experimental values, of accuracy about ± 10 % S.D., obtained by Binnie & Phillips (1958). Theory predicts only a slow change of D_1 with γ, in agreement with experiment. The experiments are not sufficiently accurate to confirm the small theoretical decrease in D_1 with increasing $|\gamma|$ which would be more apparent for smaller values of α.

Thus, it is seen that (9) can be used whenever the velocity and diffusivity distributions of the dispersed entity are known, although the expression is only valid for large dispersal times. The principal departure from the simple theory for small particles occurs at low Reynolds numbers, owing to the effect of the viscous region near the walls.

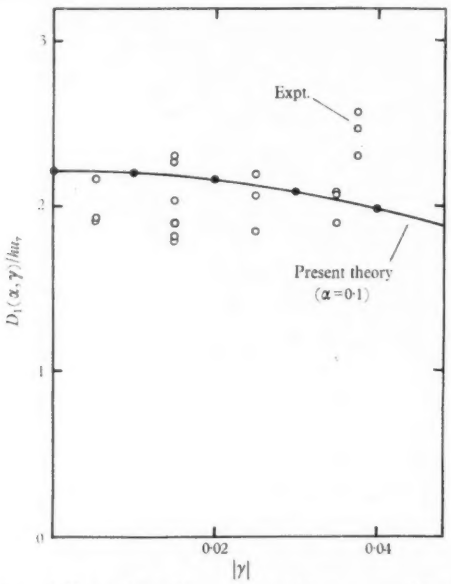

FIGURE 7. Longitudinal dispersion of buoyant and heavy particles in a circular pipe. Experimental values from Binnie & Phillips (1958).

I gratefully acknowledge that my period of research at Cambridge has been made possible by my employers, the New Zealand Defence Scientific Corps.

REFERENCES

BATCHELOR, G. K., BINNIE, A. M. & PHILLIPS, O. M. 1955 *Proc. Phys. Soc.* B, **68**, 1095.

BATCHELOR, G. K. & TOWNSEND, A. A. 1956 Article in *Surveys in Mechanics* (eds. G. K. Batchelor and R. M. Davies). Cambridge University Press.

BINNIE, A. M., DAVIES, P. A. O. L. & ORKNEY, J. C. 1955 *Proc. Roy. Soc.* A, **230**, 225.

BINNIE, A. M. & PHILLIPS, O. M. 1958 *J. Fluid Mech.* **4**, 87.

GRANT, H. 1958 *J. Fluid Mech.* **4**, 149.

HUNT, J. N. 1954 *Proc. Roy. Soc.* A, **224**, 322.

KLEBANOFF, P. S. 1954 NACA Tech. Note 3178.

LEVENSPIEL, O. & SMITH, W. K. 1957 *Chem. Engng Sci.* **6**, 227.

NIKURADSE, J. 1930 *Ing. Arch.* **1**, 306.

ROUSE, H. 1937 *Trans. Amer. Soc. Civ. Engrs*, **102**, 534.

TAYLOR, G. I. 1922 *Proc. Lond. Math. Soc.* (2), **20**, 196.

TAYLOR, G. I. 1953 *Proc. Roy. Soc.* A, **219**, 186; see also **225**, 473.

TAYLOR, G. I. 1954 *Proc. Roy. Soc.* A, **223**, 446.

VANONI, V. A. 1946 *Trans. Amer. Soc. Civ. Engrs*, **111**, 67.

Instability in a slightly inclined water channel

By A. M. BINNIE
Engineering Laboratory, Cambridge

(Received 13 October 1958)

An examination was made of the laminar travelling waves that disturbed the glassy surface in an open water channel, fitted with a trumpet entry and inclined downwards over the range 1 to $2\frac{3}{4}°$. The Reynolds number at their first appearance was observed, and measurements were obtained of their velocities and lengths, the latter being highly irregular. Comparison was made with the theoretical values after corrections had been introduced to allow for the higher velocities of flow near the walls due to the increased depth caused by surface tension. At greater discharges the onset of turbulence occurred in a random manner, leading to the production of intermittent bores moving more slowly than the laminar stream. Transition was found to have usually begun at a Reynolds number $R = 2500$, R being defined as the discharge per unit width divided by the kinematic viscosity. Except close to the inlet, the channel was continuously occupied by turbulent water when R was in the range 4000 to 4500.

1. Introduction

Two different kinds of instability can be observed in a long open water channel, fitted with a trumpet entry and inclined at a few degrees below the horizontal. As the supply is slowly increased from zero, the nature of the flow is found to change in the following sequence. As soon as a continuous film is formed covering the whole bottom, the motion is laminar, and the surface is glassy and undisturbed. This surface then becomes unstable, and transverse travelling waves appear, the theory of which has been given by Brooke Benjamin (1957, 1958). These waves increase in size; and when the velocity of the surface exceeds about 9 in./sec, stationary capillary waves spring from irregularities in the wetting of the walls in the manner mentioned by several investigators, e.g. Jeffreys (1925). At once, the travelling waves are apparently suppressed, and the surface again becomes seemingly almost motionless though covered by a diagonal pattern of stationary ripples. The next change is the irregular appearance of spots of turbulence, which immediately give rise to turbulent bores moving down the channel slower than the laminar stream. These spots become more and more numerous and originate nearer the entry, until finally the turbulence extends continuously throughout the entire channel except close to the trumpet.

In the following pages an account is given of these occurrences, as seen in apparatus described in § 2. The theory of the laminar travelling waves is outlined in § 3, and this is followed in § 4 by an account of the experiments on them. Details of the development of turbulence are explained in § 5.

2. Description of apparatus

The channel, which was made for general laboratory purposes, is composed of three sheets of plate glass 16 ft. long. For constructional reasons, each bottom joint consists of a teak strip as shown in the inset to figure 2. The clear distance between the strips is 3·30 in.; and for depths not exceeding $\frac{1}{20}$ in., as in many of the laminar wave experiments, the sides of the stream were vertical. At somewhat greater depths the walls at the free surface were inclined at 45°; but in view of the imprecise nature of the observations, it was thought unnecessary to attempt the awkward depth measurements, from which the slight widening of the stream could be calculated.

The bottom glass plate is fixed to a Dural channel placed web uppermost, a small gap being left between them that permits the insertion of graduated scales, and of white surfaces to assist observations. This channel is supported on a journal bearing close to the supply reservoir and on a jack near the outlet end, which allows the channel to be set at downward inclinations as far as $2\frac{3}{4}°$. A plywood trumpet, protruding into the reservoir, is rigidly attached to the channel, and a joint of flexible material between the reservoir wall and the exterior of the trumpet provides the necessary freedom of movement. The reservoir is 4×4 ft. in plan, and it extends about 28 in. below the level of the channel entry. It is fed by a submerged pipe from the laboratory circulating system; and to avoid the settlement of dust, the apparatus was run continuously for weeks on end while the observations were in progress. The water temperature was not under control; and, measured in the reservoir, it altered slowly between the extremes 13 and 19 °C. The discharge was determined by means of graduated glass cylinders and a small tank, into which the water fell after passing through the channel. The few depth measurements made were obtained with a point gauge mounted on a travelling carriage. The apparatus rested on a concrete floor, and the more delicate observations were postponed until no machinery in the building was audible.

3. The theory of wave formation in a laminar stream of infinite width

For reference, a summary of the properties of the undisturbed flow, free from the influence of side walls, will first be given in a form that will be wanted in § 4. The well-known analysis due to Nusselt (1916) shows that, if Q is the discharge per unit width of a stream of liquid of kinematic viscosity ν on a plane inclined at an angle θ to the horizontal, the surface velocity u_0 can be calculated from Q by means of the relation

$$u_0 = \left(\frac{9}{8}\frac{Q^2}{\nu} g \sin\theta\right)^{\frac{1}{3}}. \tag{3.1}$$

Likewise, the depth h of the stream is given by

$$h = \left(\frac{3\nu Q}{g \sin\theta}\right)^{\frac{1}{3}}. \tag{3.2}$$

The Reynolds number R will be defined by

$$R = \frac{Q}{\nu}. \tag{3.3}$$

The stability of this motion was examined in great detail by Brooke Benjamin (1957, 1958), who introduced the dimensionless phase velocity c and wave-number $\alpha = 2\pi h/\text{wavelength}$, and assumed R and α to be fairly small. Supposing that (with u_0 as the unit) $c = c_r + ic_i$, where c_r and c_i are wholly real, he found by means of a simplified theory, valid for long waves of infinitely small amplitude, that

$$c_r = 2, \tag{3.4}$$

$$c_i = \tfrac{1}{2}R\left(\tfrac{8}{5}\alpha - \frac{\alpha^3\Gamma}{hu_0^2} - \frac{\alpha h}{u_0^2}g\cos\theta\right). \tag{3.5}$$

Here Γ is the kinematic surface-tension, defined as the usual surface tension divided by the density. It is seen from (3.5) that the condition for instability is

$$\frac{8}{5} > \frac{\alpha^2\Gamma}{hu_0^2} + \frac{h}{u_0^2}g\cos\theta. \tag{3.6}$$

Following the method that he applied to the case $\theta = 90°$, we will find α for the most unstable wave by maximizing

$$\alpha c_i = \tfrac{1}{2}R\left(\tfrac{8}{5}\alpha^2 - \frac{\alpha^4\Gamma}{hu_0^2} - \frac{\alpha^2 h}{u_0^2}g\cos\theta\right). \tag{3.7}$$

Hence, the optimum value a_m of α is given by

$$\alpha_m^2 = \frac{hu_0^2}{\Gamma}\left(\frac{4}{5} - \frac{h}{2u_0^2}g\cos\theta\right). \tag{3.8}$$

With the aid of the primary-flow equations (3.1) to (3.3) this result can be expressed in terms of the Reynolds number as

$$\alpha_m = \frac{3^{\frac{1}{2}}}{2}\left(\frac{4}{5} - \frac{2}{3}\frac{\cot\theta}{R}\right)^{\frac{1}{2}}\frac{\nu^{\frac{3}{4}}}{\Gamma^{\frac{1}{4}}}(g\sin\theta)^{\frac{1}{4}}R^{\frac{1}{4}}. \tag{3.9}$$

We then have from (3.5) that the maximum value of c_i is

$$(c_i)_m = \frac{3^{\frac{1}{2}}}{4}\left(\frac{4}{5} - \frac{2}{3}\frac{\cot\theta}{R}\right)^{\frac{3}{2}}\frac{\nu^{\frac{3}{4}}}{\Gamma^{\frac{1}{4}}}(g\sin\theta)^{\frac{1}{4}}R^{\frac{11}{4}}. \tag{3.10}$$

Brooke Benjamin calculated the amplification factor

$$\mathscr{A} = \exp\{10\alpha_m(c_i)_m/2h\}, \tag{3.11}$$

where h is in cm, experienced by the wave of maximum instability on a vertical water film at 19 °C as it travels 10 cm. For a plane inclined at an angle θ and with his values $\nu = 0{\cdot}0103\ \text{cm}^2/\text{sec}$, $\Gamma = 72{\cdot}9\ \text{cm}^3/\text{sec}^2$, $g = 981\ \text{cm}/\text{sec}^2$, it appears from (3.2), (3.3), (3.9) and (3.10) that (3.11) becomes

$$\mathscr{A} = \exp\left\{0{\cdot}0434\left(\frac{8}{5} - \frac{4}{3}\frac{\cot\theta}{R}\right)^2(\sin^{\frac{3}{4}}\theta)\,R^{\frac{7}{4}}\right\}. \tag{3.12}$$

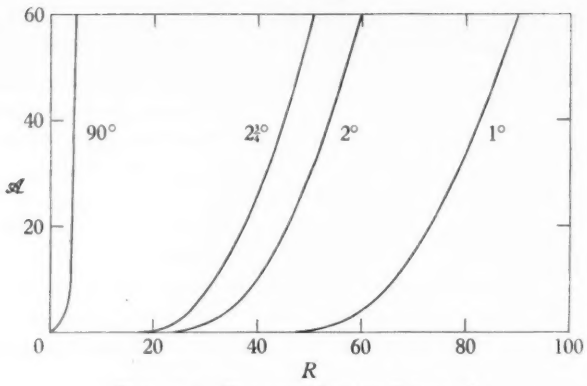

FIGURE 1. The amplification factor $\mathscr{A}$.

For the three values $\theta = 2\frac{3}{4}, 2, 1°$ that were used in the experiments, the relation (3.12) is plotted in figure 1, to which Brooke Benjamin's curve for $\theta = 90°$ has been added. As is clear from (3.5), for $\theta < 90°$ a definite value of $R > 0$ exists below which waves cannot develop, whereas for $\theta = 90°$ the flow is always unstable. The diagram indicates an important tendency. For $\theta = 90°$ the onset of large values of $\mathscr{A}$ is very sudden, and the theory did in fact confirm Binnie's experimental result (1957) that waves were just visible at $R = 4{\cdot}4$. On the other hand, the curves for small values of θ are far from steep; and it is not to be expected that the first appearance of waves as R is increased will be well defined.

4. Experiments on laminar travelling waves in the channel

The object of these experiments was to determine the Reynolds number at which the waves were just visible, together with the velocity and length of these waves. Preliminary observations showed that the waves formed near the inlet and were influenced by the sharp outlet edge where draw-down and surface-tension had some influence. In between, although some died away and fresh ones appeared, the general effect was independent of position in the channel. Measurements were therefore confined to a region about 8 ft. from the inlet, and this was illuminated by a 750 W projector, which produced a beam free from heat and inclined upstream at about 30° to the water surface. At low values of R the waves moved in an orderly manner with none of the obvious overtaking of small waves by large that was seen in the vertical film experiments. As in that investigation the wavelength was irregular, but now the waves were much less steep, and the shadows that they cast on a white surface below the glass bottom were diffuse and not easy to observe.

One effect of the side walls was immediately evident, namely, the waves did not extend right across the channel. The film thickness was too small to be accurately determined with a point gauge, and the matter was investigated by measurements of the surface velocity. Straight hairs about $\frac{1}{4}$ in. long were floated down, and their passage over 22 in. timed with a stop-watch; rotation of the hair was rarely noticed. It was found that over most of the width the surface velocity was almost uniform, but that near the walls a narrow band existed having a higher velocity.

With very thin films this velocity was as much as twice the central velocity. The cause of this effect was surface tension, which increased the depth near the walls and thereby permitted a rise in speed. Therefore, in order that a comparison could be made with the theory of § 3, it was necessary to apply a negative correction to the value of R deduced from the measured discharge. This correction was larger than the theoretical effect of the walls due to viscous action alone, and it lay in the opposite sense. For Cornish's analysis (1928) reveals that, for a stream of viscous liquid devoid of surface tension, the reduction of discharge due to the walls is only $1\frac{1}{4}\%$ when the ratio of depth to breadth is 1 %, a value representative of the experiments. We shall use the terms 'net u_0' and 'net R' to refer to the observed central surface velocity and to the Reynolds number calculated from it by means of (3.1) and (3.3), and the terms 'gross u_0' and 'gross R' to refer to the surface velocity and the Reynolds number calculated from the measured discharge by means of the same equations.

Hair measurements of the central velocity were made over the ranges required for the various wave observations, the mean of at least ten timings being taken. At the higher velocities, the uniformity of the hair's travel was slightly disturbed by the waves which had developed, and for the 1° slope the accuracy of the method fell away because the time of passage became rather short. The results are displayed in figures 2 and 3. The former, which gives the ratio of the net to the gross values of u_0, indicates that the difference between the two was large for the thin films existing at the $2\frac{3}{4}$° slope, but became only 10 % at 1° slope. This tendency is in accord with (3.2) and (3.3), which show that at a fixed value of R the stream becomes deeper as the inclination is diminished, therefore the consequencies of surface tension at the walls are proportionately smaller. The latter diagram is of more immediate use in that it provides the net value of R when the gross R has been determined. Again, the 1° results lie above the others, being less disturbed by wall effects.

Three methods were used of discerning the onset of wave formation more sensitively than observation of the shadows (mentioned above) on the white surface beneath the bottom.

A. A vertical screen was set up that intercepted the beam from the projector after reflexion from the water surface. On this, disturbances showed as moving irregularities in the intensity of illumination.

B. Direct but necessarily distant scrutiny was made from the outlet end of the channel at a small incident angle.

C. An electronic capacity indicator was devised by connecting the output from a Feilden Proximity Meter through an amplifier to a cathode-ray oscilloscope, the apparatus being connected to an electrode of diameter 1 in. held just above the water. When a balance had been obtained, a steady curve was visible on the screen. The passage of waves was indicated by momentary disturbances in the curve, the agreement between the frequencies of their occurrence and of waves actually seen in the channel being very convincing. No attempt was made to determine the sensitivity of the arrangement, but it was found that, when the electrode was raised 0·01 in. from its working position, the disturbances became so enormous that their peaks were thrown far off the screen.

An estimate of the first appearance of waves was obtained by increasing and decreasing the discharge until it was thought that the best assessment had been made. Methods *A* and *B* gave almost identical results, and the gross values of *R* produced by the former are shown in table 1. Method *C* was employed on a later occasion; and, as will be seen in the table, for the $2\frac{3}{4}°$ slope it yielded virtually the same result as *A*. This suggests that, as the discharge was increased, the development of the waves was rapid. In contrast, at 1° method *C* detected waves at

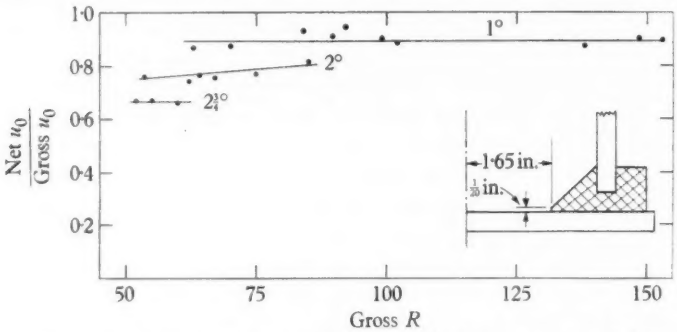

FIGURE 2. The ratio of net to gross u_0. Inset: half cross-section of channel.

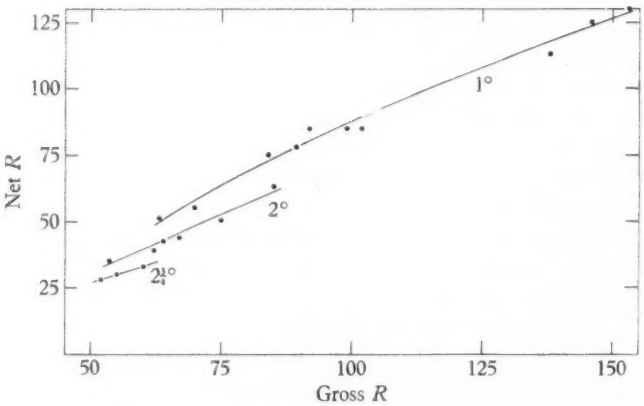

FIGURE 3. The net Reynolds number.

rather smaller discharges than *A*; thus the wave growth was now slower if it may be assumed that the sensitivity of *A* remained constant. The table also gives for method *C* the values of net *R* obtained from figure 3 and, for comparison, the Reynolds number for zero amplification calculated from the relation $R = \frac{5}{6}\cot\theta$, which follows from (3.11). The differences between these last two columns are roughly the same, the discrepancy at 1° being least, both actually and proportionately.

The disturbances shown on the vertical screen could not be interpreted to yield the velocity and length of the waves; therefore, to determine these quantities, vertical photographs were taken of the shadows thrown on the white surface

below the bottom. A 16 mm cine camera was used with a clock and a scale in the field of view. In order to obtain waves big enough to be photographed, it was necessary to raise R above the values given in table 1. As will be seen in table 2, at $2\frac{3}{4}°$ the required increase of gross R was only from 54 to 59, whereas at 1° the waves were so ill defined and developed so slowly that the gross R had to be raised from 69 to as much as 145 before measurable photographs could be secured. Thus the tendency shown up by the differences between the results of methods A and C in table 1 was found again.

The wave velocity was measured by following the passage of individual waves for distances up to 13·2 in., and taking the mean. To compare it with the central surface velocity, the values of net u_0 have been added to table 2, together with the ratios of the observed wave velocity to net u_0. Equation (4.3) indicates that theoretically the ratio is 2; thus there are discrepancies here, which are in the

Slope	Method A, gross R	Method C		Theoretical minimum R
		Gross R	Net R	
$2\frac{3}{4}°$	55	54	29	17
2°	64	57	37	24
1°	90	69	56	48

TABLE 1. The onset of wave formation.

Slope	Gross R	Net R	Wave velocity (in./sec)	Net u_0 (in./sec)	Wave velocity ÷ net u_0	Observed wave-length (in.)	Theoretical wave-length (in.)	α_m
$2\frac{3}{4}°$	59	32	6·24	3·30	1·89	1·15	1·42	0·143
2°	79	56	7·37	4·27	1·73	1·15	1·12	0·242
1°	145	123	9·83	5·68	1·73	1·11	1·04	0·429

TABLE 2. Photographic observations and comparison with theory.

opposite direction to that found in Binnie's vertical experiments (1957) where the ratio was 2·34, but in that investigation u_0 was calculated from the discharge and was not measured directly. The best agreement was at $2\frac{3}{4}°$, where the increase of discharge required for satisfactory photographs was least. Whenever a fairly regular train of at least 5 waves was noticed, the length was measured, the greatest number of waves being 7, but the mean values must be treated with reserve because the spacing of the waves was generally erratic. For comparison, the theoretical wavelength has been calculated from the net R with the aid of (3.9), h being found from (3.2) and (3.3). As in the vertical experiments, the agreement is surprisingly good, and it may be added that at $2\frac{3}{4}°$ a train of 3 waves of length 1·45 in. was also observed. The last column in table 2 gives the values of α_m obtained from (3.9) which are included to show that, although R was rather high for the theory to be valid, yet α_m remained small, and the assumption that the waves were long compared with h was not violated. In the vertical experiments α_m was 0·067.

A trial was also made with the channel set at an inclination of only 10′. As the

discharge was increased from zero, the first disturbance of the stream was due to the stationary ripples springing from the walls, and later turbulence set in. No laminar travelling waves could be discerned.

5. The development of turbulence

When the supply was raised beyond the range considered in the previous section, the amplitude of the waves increased with little alteration in their distances apart. They were soon obscured by the stationary ripples inclined to the walls at angles which diminished with rising discharge. The first sign of turbulence was an obvious commotion in the surface starting at a fixed point on one wall and spreading diagonally across to the other. This kind of disturbance was clearly the same as the turbulent spots developing into triangular shape, which were seen by Emmons (1951) on an inclined plate 3 ft. wide. In the present circumstances, however, the lateral development of the disturbance was limited by the far wall; and blocks of agitated water travelled down the channel each with a normal front and a diagonal tail, their length depending on the duration of the originating outbreak. Evidently they had much in common with the flashes, which were seen by Reynolds (1883) in his classical research on pipe flow, and which have recently been investigated in great detail by Lindgren (1953, 1954, 1957) by means of birefringence and pressure measurements. But, whereas in the pipe experiments the liquid in a flash was forced onward with its mean axial velocity virtually unimpaired, in the channel the disturbance had a depth greater than that of the adjacent laminar stream and its velocity was less. Indeed, sometimes the discharge from the channel momentarily stopped altogether as the turbulent front approached the end. The length of the disturbance increased as it travelled down the channel; and the tail, which remained sharply defined, was fed by the laminar stream behind it under conditions resembling those in an ordinary hydraulic jump. Thus the development of a disturbance differed from that of a pipe flash, for which at the higher Reynolds numbers the velocities of the front and tail were found by Lindgren (1957, figure 5.12) to be respectively greater and less than the mean flow velocity.

Usually, but by no means always, the first disturbances occurred far down the channel. At a higher supply their origin moved nearer the inlet, and they became longer and more numerous. At a fixed supply some of the fronts moved faster than others, and occasionally they formed so violently that they were preceded and later outdistanced by a short group of waves on the laminar stream. In the early stages, two kinds of apparently spurious disturbances were noticed: (i) The supply being increased in small steps, disturbances sometimes occurred soon after the valve was opened; but after a few minutes had elapsed and the supply had become steady, the surface remained unruffled for a long time. It appeared that the flow was in so unstable a state that it was upset by the wetting of surfaces previously dry. (ii) On a few occasions the work was impeded by the deposit of minute air bubbles on the bottom. When seen, they were at once brushed off; nevertheless, a disturbance could occur which carried down in front of it a single large bubble, evidently formed by the sweeping action of the bore. These occurrences were rejected as being possibly caused by the minute bubbles.

Observations with increasing supply were made at slopes of $2\frac{3}{4}$, 2, 1°, and no significant change was noticed on repetition with a decreasing supply. The process of transition was random both in time and place; and if the changes of slope did in fact influence it, their power to do so was obscured by the capricious nature of the disturbances. The observations may be summarized by stating that over a period of minutes at least one disturbance usually appeared when R was 2500. This value, like those given in this section, is a mean, calculated from the discharge, the irregularities in which were short compared with the time of measurement.

At $2\frac{3}{4}$° slope the bores were more conspicuous than at the lesser slopes. The depth of a typical disturbance at 1° slope and $R = 3100$ had a maximum value about 0·28 in. and diminished towards the ends; after a wait for a quiet period of sufficient duration the depth of the laminar stream was found to be 0·18 in. Additional evidence concerning the large difference between the depths in turbulent and laminar flow is provided in figure 4, which shows the results when

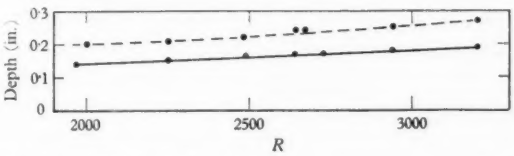

FIGURE 4. The depths at 1° slope: —— laminar, – – – – turbulent.

turbulence, probably fully developed, was induced throughout the channel by means of a brass post, $\frac{5}{8}$ in. in diameter, placed on the centre line of the channel at its inlet. The diagram extends as far as $R = 3200$, beyond which the periods of laminar motion were too brief for measurements of its depth to be made. These depths were much larger than those encountered in the laminar wave experiments, and corrections of the kind described in § 4 were not required. The observation 0·28 in., mentioned above, lies close to the turbulent curve, but evidence produced in the next paragraph suggests that in self-induced disturbances at greater values of R the turbulence was not quite fully developed.

The supply being further increased, the disturbances became still more frequent and all began between 1 and 2 ft. from the channel inlet. Their origin extended right across the channel, hence their tails as well as their fronts were normal to the walls. Again, the effect of altering the slope was not clear, and it is impossible to give precise numerical results, though at $R = 3500$ there was almost always at least one disturbance in the channel and at $R = 4000$ to 4500 the disturbances were generated continuously. But even in this range the discharge was made slightly irregular by the occasional appearance of roll waves in the downstream half of the channel. At 1° slope and $R = 4100$, these waves vanished when the turbulence stimulator was placed at the channel inlet, the depth increasing from 0·33 in. by roughly 0·01 in. This observation is in agreement with Rouse's remark (1938) that roll waves can be suppressed by roughening the walls, although at first sight it is surprising that so small an increase in the apparent turbulence was effective. However, on the assumption that the Chézy resistance law holds good, the criterion for the existence of roll waves put forward by Jeffreys (1925) and

Dressler (1952) is $\tan\theta > 4r^2$, the friction force per unit mass being r^2 multiplied by the square of the mean velocity and divided by the depth. From the measurements of depth and discharge without turbulence stimulation, $4r^2$ was estimated to be 0·018, which is not far from $\tan 1^\circ = 0{\cdot}0175$. When R was raised to 5500, roll waves were absent. Thus the transition to turbulence was an ill-defined process, and the numerical results obtained might well have been different had the channel been supplied from a larger reservoir through a contraction of still better design.

The surface near the inlet which was never troubled by turbulence could be examined by watching the reflexion of a roof light through the network of stationary ripples. Even when R was less than 2000 the surface quivered as a commotion boiled up from below and was quickly damped out. At higher values of R, the agitation was more marked; nevertheless, some conspicuous heaves in the surface faded away after travelling a short distance, their suppression probably being influenced by surface tension as well as by gravity and viscosity. When attention was concentrated on a point a foot or two downstream from the inlet, sometimes a heave in the surface was seen to be succeeded by the appearance of turbulence. Presumably the surface turbulence was caused, not by the passage of the water through the stationary ripples, but by eddies diffused from the bottom. At the highest Reynolds numbers the surface in the channel, that was free from turbulence but shaken continuously in an irregular manner, extended up to the inlet itself, and it could be seen that eddies were generated in the contraction also.

REFERENCES

Binnie, A. M. 1957 *J. Fluid Mech.* **2**, 551.

Brooke Benjamin, T. 1957 *J. Fluid Mech.* **2**, 554. Numerical corrections, *ibid.* (1958) **3**, 657.

Cornish, R. J. 1928 *Proc. Roy. Soc.* A, **120**, 700.

Dressler, R. F. 1952 *Gravity Waves*, p. 237. *Circular* 521, *National Bureau of Standards, Washington, D.C.*

Emmons, H. W. 1951 *J. Aero. Sci.* **18**, 490.

Jeffreys, H. 1925 *Phil. Mag.* (6), **49**, 793.

Lindgren, E. R. 1953 *Ark. Fys.* **7**, 293.

Lindgren, E. R. 1954 *Appl. Sci. Res., Hague*, A, **4**, 313.

Lindgren, E. R. 1957 *Ark. Fys.* **12**, 1.

Nusselt, W. 1916 *Z. ver. dtsch. Ing.* **60**, 541.

Reynolds, O. 1883 *Phil. Trans.* **174**, 935.

Rouse, H. 1938 *Fluid Mechanics for Hydraulic Engineers*, p. 388. New York: McGraw-Hill.

A pulsating sphere in a rotating fluid

By ALAR TOOMRE
Mechanics of Fluids Department, University of Manchester

(Received 11 November 1958)

A pulsating sphere, which performs a sequence of virtually impulsive changes in its radius with time, is completely surrounded by an inviscid, incompressible fluid whose velocity field is generally rotational. This paper indicates how it is possible, by means of Helmholtz's theorem, to relate the corresponding vorticity and velocity fields immediately before and after such expansions or contractions.

The method is then applied to the case of a spherical mass of fluid initially in uniform rotation in which a spherical core undergoes a single sudden expansion, followed after a short interval by an equally rapid contraction back to the original radius. An interesting meridional flow is thereby induced, which tends to decrease the angular velocity of rotation of the fluid near the poles at the outer surface, relative to that of the equatorial fluid. It is perhaps significant that this is in qualitative agreement with the variation of angular velocities observed at the surface of the sun.

1. Introduction

A mass of inviscid, incompressible fluid contains a solid (or possibly fluid) sphere, centred about $\mathbf{r} = 0$, whose radius, $a(t)$, varies with time. The sphere is said to be *pulsating*. Suppose from the outset that these pulsations consist of expansions and/or contractions which occur almost instantaneously, interspersed among intervals during which the radius remains constant. This restriction is hardly a severe one, for any time-history can be approximated by a suitably chosen series of such 'jumps'. The sphere radius can be written as

$$\left.\begin{array}{lll} a = a_0 & \text{when} & t_0 < t < t_1, \\ \quad \cdots & \cdots \quad \cdots \quad \cdots & \cdots \quad \cdots \\ a = a_n & \text{when} & t_n < t < t_{n+1}, \text{ etc.} \end{array}\right\} \tag{1}$$

Assume also that the surrounding fluid does not cavitate during the sudden motions.

The velocity field, $\mathbf{v}(\mathbf{r}, t)$, and hence the vorticity field, $\mathbf{w} = \operatorname{curl} \mathbf{v}$, is arbitrarily specified throughout this fluid at some particular time. If the fluid is of infinite extent, it is desirable that $\mathbf{w}$ should approach a constant $\mathbf{w}_\infty$ sufficiently rapidly as $r \to \infty$, so that a vector potential

$$\mathbf{A}(\mathbf{r}) = \int_V \frac{\mathbf{w}(\mathbf{r}') - \mathbf{w}_\infty}{|\mathbf{r}' - \mathbf{r}|}\, d\mathbf{r}'$$

can exist. If it is bounded, then $\mathbf{n}.\mathbf{v}$ should vanish at the surfaces, except during the sudden changes in the radius of the sphere, when the boundaries would adjust to keep the fluid volume constant.

$\mathbf{v}(\mathbf{r})$ is generally not steady, even in the absence of any motion by the sphere. However, its behaviour during the quiescent intervals can at least in principle be calculated by standard methods, and does not therefore concern us here; only what happens to $\mathbf{v}$ and $\mathbf{w}$ as a result of the quasi-impulsive changes in radius appears to be in question. It will now be shown how the values of $\mathbf{v}$ and $\mathbf{w}$ just following an expansion are related to those that existed immediately before.

2. Effect on the vorticity field of a sudden expansion

Consider a sudden increase in the radius of the sphere from a_0 to a_1 which occurs at time t_1. Take any two infinitesimally separated fluid particles lying outside the sphere, say those at P and Q, which at t_1- are joined by a particular vortex filament Ω (see figure 1). Clearly, the expansion displaces them outwards to positions P' and Q' respectively. PP' and QQ' may be called the 'drifts' of these particles caused by the expansion.

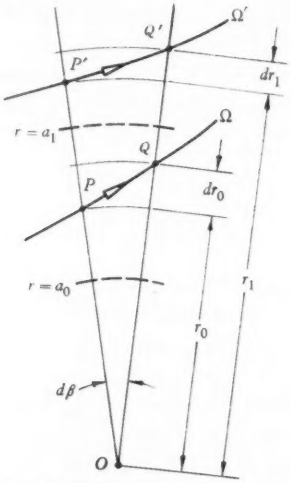

FIGURE 1. Positions of a typical vortex filament immediately before and after an expansion of the sphere.

Since the expansion takes place in virtually an instant, the velocities associated with it must be immensely larger than the original velocities of the fluid. It follows that the 'drifts' are just the same as if the body had instead expanded less rapidly into an initially stationary fluid. The instantaneous displacements of the fluid particles are radial and they will obey the increase-of-volume condition:

$$r_1^3 - r_0^3 = a_1^3 - a_0^3 = A_1^3 = \text{const.} \tag{2}$$

Helmholtz's theorem states that vortex filaments move with the fluid. There is no reason to suspect an exception in the present case, for it has been assumed that the expansion, though fast, is not quite instantaneous. P' and Q' are therefore on the same vortex line, Ω'. Referring again to figure 1, the sudden expansion

of the sphere has thus the following effect on the components of *vorticity*, which are proportional to the infinitesimal distance increments:

The radial component is *decreased* by the ratio $dr_1/dr_0 = r_0^2/r_1^2$; whereas the lateral components are *increased* $r_1 d\beta/r_0 d\beta = r_1/r_0$ times. Or, in spherical polar co-ordinates (r = radius; θ = co-latitude; ϕ = longitude),

$$\mathbf{w}(t_1+) = \{w'_r;\, w'_\theta;\, w'_\phi\} = \left\{\frac{r_0^2}{r_1^2} w_r;\, \frac{r_1}{r_0} w_\theta;\, \frac{r_1}{r_0} w_\phi\right\}, \tag{3}$$

the unprimed w's being the components of $\mathbf{w}(t_1-)$.

It does not appear possible to relate the before-and-after components of *velocity* quite so directly. Though $\mathbf{v}(t_1+)$ is strictly determinate from $\mathbf{w}(t_1+)$ and the boundary conditions,† it will generally have to be calculated by means of the vector potential. There is, however, one case where the transformation is simplified and that is when the component of velocity tangential to the circles r and θ constant, i.e. v_ϕ, is independent of the angle ϕ. Then it is easy to prove, since such rings at $t = t_1-$ have been shifted into larger circles by the time t_1+, and since the circulation theorem is obeyed, that

$$\mathbf{v}(t_1+) = \left\{v'_r;\, v'_\theta;\, v'_\phi = \frac{r_0}{r_1} v_\phi\right\}. \tag{4}$$

Equations (3) and (4) apply of course without change to a contraction by the sphere; only then $r_1 < r_0$.

3. Uniformly rotating fluid

Let us now apply the considerations of the previous section to a relatively simple example. Take the original flow to be one of uniform rotation, that is,

$$\mathbf{v}(t < t_1) = \tfrac{1}{2}\mathbf{w}_0 \times \mathbf{r}_0 = \{0;\, 0;\, \tfrac{1}{2} w_0 r_0 \sin\theta\}. \tag{5}$$

the vorticity for $t < t_1$ is

$$\mathbf{w}(t < t_1) = \{w_0 \cos\theta;\, -w_0 \sin\theta;\, 0\}. \tag{6}$$

from which equation (3) gives immediately

$$\mathbf{w}(t_1+) = \{w_0 (r_0/r_1)^2 \cos\theta;\, -w_0 (r_1/r_0) \sin\theta;\, 0\}. \tag{7}$$

This happens to be the kind of special case in which equation (4) applies; thus we know v'_ϕ immediately. Now it is quickly seen that v'_ϕ itself already possesses the vorticity given by equation (7) required of the velocity field. Hence, as long as the normal velocity at the sphere surface is zero, it follows that

$$\mathbf{v}(t_1+) = \{0;\, 0;\, \tfrac{1}{2} w_0 r_1 (r_0/r_1)^2 \sin\theta\}. \tag{8}$$

Let us examine the effect of these velocities upon the vortex filaments over a short interval of time, Δt, after t_1. For the fluid to continue rotating rigidly, v_ϕ would have to equal $v_{\phi\,\mathrm{rigid}} = \tfrac{1}{2} w_0 r_1 \sin\theta$. But this is not the case here, for $v_\phi < v_{\phi\,\mathrm{rigid}}$. In fact, all particles, particularly those in the vicinity of the sphere, will increasingly 'lag' behind their would-be positions of uniform rotation as time goes on, and the vortex lines consequently suffer a certain distortion. This is illustrated in figure 2.

† If the fluid extends to infinity, the boundary condition $\mathbf{v}(\mathbf{r}_0; t_1-) = \mathbf{v}(\mathbf{r}_1; t_1+)$ applies there.

Note that since $\mathbf{v}.\mathbf{w} = 0$ at t_1+ the motion cannot in the first instance stretch the vortex lines in the direction of $\mathbf{w}(t_1+)$. Rather, any stretching that does occur gives rise to a lateral component of vorticity, $\Delta w'_\phi$. At $t_1+\Delta t$, one can therefore separate the vorticity field into a *primary field*, $\mathbf{w}^*$, which in the first approximation is unchanged from $\mathbf{w}$ at $t = t_1+$, and a *secondary or induced field*, $\Delta\mathbf{w}'$, composed of vortex rings that are concentric with the axis of symmetry. The

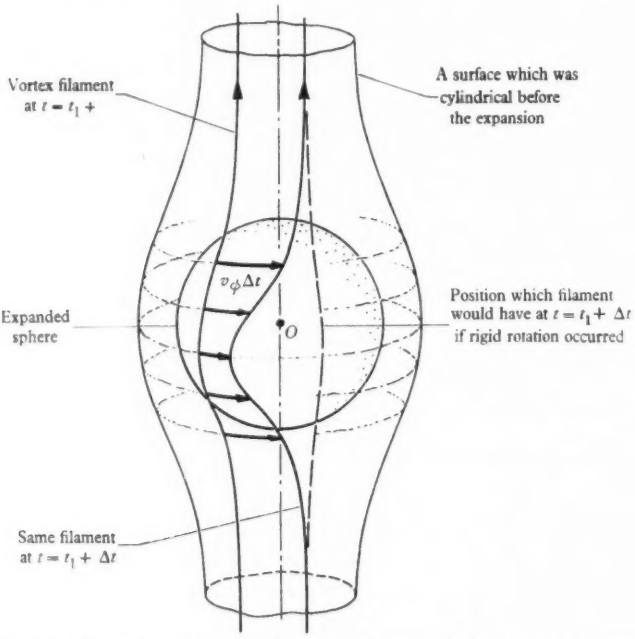

FIGURE 2. The distortion of a typical vortex filament during a short interval after an expansion.

intensity of the latter grows very nearly linearly with time, and it is anti-symmetric about the equatorial plane. These rings of vorticity represent a meridional flow directed inwards near the equatorial plane, and outwards near the axis.

Suppose now, further, that at $t = t_1+\Delta t = t_2$ the sphere undergoes a rapid contraction back to the original radius a_0. Reversing the previous procedure, we see that the primary vorticity field transforms back to the constant $\mathbf{w}_0$ which existed before t_1. However, the contraction cannot cause the vanishing of the secondary vorticity, which sprang up during the interval Δt. In other words, the expansion-contraction cycle of the sphere (i.e. the single pulsation) leaves as an immediate after-effect a vortex field $\Delta\mathbf{w}''(r_0,\theta) = (r_0/r_1)\,\Delta\mathbf{w}'(r_1,\theta)$, together with its associated flow in the originally uniformly rotating fluid, and the motion is not steady any more.

This secondary vorticity field, $\Delta\mathbf{w}''$, can be calculated from the distortion of the vortex lines at t_2+. If g represents the 'lag' of fluid particles at that time behind

the positions which they would have reached in the absence of the pulsation, then

$$\Delta w''_\phi = -w_0 \frac{\partial g}{\partial z}, \tag{9}$$

z being measured along the axis of rotation. Now g equals (r_0/r_1) times Δt multiplied by the velocity deficiency during the expanded phase, which is $\frac{1}{2}w_0 r_1[1-(r_0/r_1)^2]\sin\theta$. Differentiating, one finds that

$$\Delta w''_\phi = \tfrac{1}{2}A_1^3 w_0^2 \Delta t (r_0^2/r_1^5)\sin 2\theta, \tag{10}$$

where $r_1^3 = r_0^3 + A_1^3$.

In trying to find velocities to match $\Delta w''_\phi$, assume that $r_0^3 \gg A_1^3$. This means that the solutions are not going to be accurate for small radii, but, fortunately, this is unimportant. In this case equation (10) can be written in the expanded form

$$\Delta w''_\phi \cong A_1^3 w_0^2 \Delta t\, r_0^{-3} \sin 2\theta\,[1-\tfrac{5}{3}(A_1/r_0)^3+\ldots]. \tag{11}$$

It can then be established that

$$q_r(t_2+) \cong \tfrac{1}{2}A_1^3 w_0^2 \Delta t\, r_0^{-2}[1+\tfrac{5}{3}(A_1/r_0)^3][\cos^2\theta - \tfrac{1}{3}] \tag{12a}$$

and

$$q_\theta(t_2+) \cong \tfrac{5}{12}A_1^6 w_0^2 \Delta t\, r_0^{-5}\sin 2\theta \tag{12b}$$

are divergence-free and consistent with (11). Together with a potential-derived velocity field, which will be chosen to satisfy the boundary conditions (if any), (12*a*) and (12*b*) describe the induced flow immediately after a single pulsation.

4. Sphere of rotating fluid with a pulsating core

An interesting situation arises when the pulsating sphere is at the centre of a rotating mass of fluid which itself is spherical. In this case, there are two boundary conditions at t_2+. The normal velocity must vanish at the outer boundary, where $r = b$, say, and perhaps at the core where $r = a_0$. However, it is reasonable to disregard the latter, for the resulting irrotational velocities would drop off with distance as rapidly as r_0^{-4}, and if the core were fluid, such a condition would be unrealistic anyway. To be accurate, we assume that $a_0^3 \ll b^3$.

The boundary condition at $r = b$ is satisfied by our superimposing upon the q's the velocities derived from the potential $\phi = Kr_0^2[\cos^2\theta - \frac{1}{3}]$. The constant K is determined from $-(-\partial\phi/\partial r_0)_{r_0=b} = q_r(b)$, the latter being given by equation (12*a*). The resulting complete induced flow in the meridional planes immediately after the re-contraction, except near the centre, is very nearly

$$v_r(t_2+) \cong \tfrac{1}{2}A_1^3 w_0^2 \Delta t\, r_0^{-2}[1-(r_0/b)^3][\cos^2\theta - \tfrac{1}{3}] \tag{13a}$$

and

$$v_\theta(t_2+) \cong \tfrac{1}{4}A_1^3 w_0^2 \Delta t\, r_0 b^{-3}\sin 2\theta. \tag{13b}$$

Higher-order terms have been omitted from these equations.

Now it must be emphasized that these velocities are transient, for they will gradually distort the primary vortex filaments with resulting complications to the flow, which we cannot consider here. Moreover, in a real fluid viscosity will at the same time tend to destroy meridional motions and to restore the entire sphere to uniform rotation (assuming that the surface at $r = b$ is frictionless) with the initial angular velocity.

But neither of these effects is likely to contradict our conclusion that one of the effects of an expansion-contraction of the sphere within the sphere of rotating

fluid is a flow along the surface from both poles towards the equator. In fact, we might go one step further and postulate that the core pulsates periodically, expanding and then contracting, perhaps with sufficient quiescent intervals between a contraction and the next expansion to permit what viscosity there may exist to restore the rotation to nearly uniform. In this case, a one-way surface flow away from the poles will be present throughout, though it will fluctuate in intensity.

It is possible to show that such a meridional flow along the surface cannot help but exercise a perhaps disproportionate effect upon the main peripheral velocities there, namely, the v_ϕ's. Consider any ring of constant latitude fluid on this sphere at some given time. It has a certain circulation, say Γ. If we now assume negligible viscosity, as the meridional velocities displace this ring of fluid towards the equator and its radius increases, Γ remains constant owing to the circulation theorem. Therefore the peripheral velocities, v_ϕ, along it are decreased. By such arguments, if carried to the limit, it would follow that the fluid at the poles would cease revolving altogether! In reality, the situation will not be so drastic, but clearly if we start with a sphere rotating uniformly with the angular velocity $\frac{1}{2}w_0$ and superimpose meridional velocities such as we have described upon it, the angular velocity at the poles will soon be less than $\frac{1}{2}w_0$.

At the low latitudes, however, fluid rings increase less in radius, and because particles on the surface must remain there, a similar reasoning would reveal that the rotational speed is unaltered at the equator. One would expect the combined trend to be held in check, both by higher-order effects here neglected, and by the action of viscosity. Nevertheless, qualitatively, the regular pulsation of the core will have an effect whereby fluid at increasing latitudes will have a progressively smaller *angular* velocity, and thus take longer to complete a rotation.

This remarkable effect has been observed on the sun. Whereas its equatorial (sidereal) period of rotation has been measured at about 25 days, this period is known to grow with latitude, reaching about 29 days at the 60° latitude. This phenomenon seems to have remained virtually unexplained.

There is one aspect of a typical pulsation which has been taken rather for granted so far. We have really only considered pulsations where the core expands and then contracts, followed and preceded by periods of quiescence. It should be noted that if the behaviour were the reverse—that is, the core first contracting, then expanding—our deductions, too, would be exactly the opposite, and in the case of the spherical mass of fluid surface currents would be directed towards the poles. That its attendant effects are not evidenced in the sun's rotation suggests, according to this theory, that the hypothetical pulsations of its core are of an explosive, and not an implosive, nature.

An apologia is perhaps due for citing as a possible example the sun, which hardly consists of incompressible fluid. However, the reasons for restricting direct analysis to such fluids are obvious; and so are those for idealizing the pulsations as quasi-impulsive. It is reasonable to suppose that the qualitative conclusions are valid no matter whether the fluid is incompressible or not. Finally, we may observe that expanding spherical shock-waves have an effect somewhat analogous to the expansions–contractions of a core; both displace fluid temporarily outwards to an extent varying with distance from the centre.

On the stability of a spinning top containing liquid

By K. STEWARTSON
Department of Mathematics, The Durham Colleges in the University of Durham

With an Appendix by G. N. Ward

(Received 26 September 1958)

The stability of a heavy top, containing a cylindrical cavity partly full of liquid, for small displacements from the sleeping position is studied. It is shown theoretically that instability can occur when any one of the periods of free oscillation of the liquid, which are doubly infinite in number, is sufficiently near to the period of nutation of the empty top. In experiments carried out by Prof. Ward, only the two principal instabilities could be distinguished.

1. Introduction

Consider an axisymmetrical solid top of mass M rotating about a fixed point O of its axis at a distance d from its centre of gravity G. It is well known that the top is stable in a sleeping position with G vertically above O provided that

$$L^2\Omega^2 > 4MgdT, \tag{1.1}$$

where L, T are the moments of inertia of the top about longitudinal and transverse axes through O and Ω is the angular velocity of the top about OG.

If, however, the top has a cavity containing fluid, this simple criterion is no longer adequate. It was in fact shown by Kelvin (1877) that the top could be made unstable by choosing a suitable cavity. He exhibited a thin-walled spheroidal top full of liquid. Originally its shape was just oblate and it was stable in the sleeping position if spun fast enough. However, on hammering it into a slightly prolate form and releasing it from the sleeping position, it became violently unstable to the extent of damaging the bearings on which it was spinning. The mathematical explanation of this phenomemon was given by Greenhill (1880). He assumed that the fluid inside the top was rotating with the casing as if solid to begin with, and studied the perturbations in the motion of the fluid consequent to a small disturbance being applied to the top. The perturbed motion produces pressure variations on the inner surface of the casing leading to a couple which may augment the destabilizing couple due to gravity. However, the new couple is proportional to Ω^2, and so it is possible that no matter how rapidly the top is rotated it will still be unstable. It is thus a different kind of instability from that occurring with a solid top, which can always be removed by choosing a sufficiently high angular velocity. In particular, Greenhill was able to show that when the casing has negligible mass and is pivoted at the centre of the cavity, the top is unstable if $a < c < 3a$, where $2a$, $2a$, $2c$ are the lengths of the

principal axes of the spheroidal cavity. As the mass of the casing is increased, the unstable range of c is narrowed until in the limit body instability occurs at only one value of c given by

$$\tau_{\mathrm{nu}} = \frac{c^2 - a^2}{c^2 + a^2}, \tag{1.2}$$

where $2\pi/\Omega\tau_{\mathrm{nu}}$ is the period of nutation of the top when the cavity is empty.

Similar results have been obtained by Hough (1898) when the cavity is ellipsoidal with one principal axis along the axis of symmetry of the empty top. The restriction that the centre of the cavity coincide with the centre of rotation, which was assumed by all three writers mentioned so far, has been removed in unpublished work by S. N. Barua, E. A. Milne and the present author. The modification necessary is not difficult and does not affect the general nature of the theory.

In practice, however, it is difficult to ensure that the cavity in the top is completely full of liquid; accordingly, it is of interest to study the top's stability when the cavity is only partly full. The liquid now has a free surface whose shape depends on the relative strength of the gravitational and centrifugal forces. In this paper we shall assume that the top is rotating sufficiently rapidly that the gravitational forces may be neglected, so that the free surface is taken to be a cylinder parallel to the axis of symmetry. The condition to be satisfied is $a^2\Omega^2 \gg gc$, where a, c are now representative lengths in the cavity across and along the axis of symmetry.

The gain in simplicity obtained by choosing a spheroidal cavity, which is so clear in Greenhill's work, is now lost. Instead we shall suppose that the cavity is a finite cylinder, whereupon the boundary conditions take on a particularly convenient form and lead to a comparatively simple solution. This problem has also been considered by Narimanov (1957) who assumes, however, that the cavity is nearly empty and neglects the variation of the velocities with r, the distance from the axis. No results comparable with those of the present paper were given, but it is likely that Narimanov's assumption is very restrictive.

It is assumed throughout the paper that the liquid is compressible and inviscid, and is initially rotating with the top as if solid. Strictly speaking, an inviscid liquid cannot be given vorticity by any motion of its boundaries, and it may be argued that for consistency the liquid should be assumed to be at rest initially inside the cavity. Such an approach has been used by Chetayev (1957). However, no real liquid is completely inviscid, and so any liquid will be dragged round to some extent by the rotating casing. From considerations of diffusivity, the liquid in the top can be expected to rotate substantially as if solid after a time of the order of a^2/ν, where a is a representative length and ν the kinematic viscosity of the liquid. Chetayev's theory may then be thought of as applying at the initial stages of the motion of the top. As the liquid slowly speeds up, acquiring vorticity from the motion of the casing, the criteria for instability will change, tending ultimately to those of the present paper.

The stability equation for a top with a spheroidal cavity completely full of liquid is particularly simple, leading to a single range of values of c/a in which the

top is unstable. When the cavity is a cylinder of length $2c$ and radius a, with or without an air space, it is found that the stability equation is much more complicated, and leads to an enumerable infinity of ranges of values of c/a in any of which the top is unstable. The total length of all these ranges is probably of the same order as the length of the single range occurring with a spheroidal cavity; the fragmentation means that instability is liable to occur unexpectedly, on making apparently trivial changes in the properties of the top.

The reason is that in general the liquid in the cavity has an infinite number of normal modes, each having a different period of oscillation. The motion of the liquid in a normal mode gives rise to a fluctuating couple on the casing of the top which acts as a disturbing force on the motion of the solid part of the top. There is also a reverse mechanism in which the motion of the casing induces a motion of the liquid in the cavity. Instability occurs when the period of nutation of the casing is sufficiently near to any one of the periods of normal modes of the liquid. It turns out that the period of precession is not directly associated with instability. The theory of the cylindrical cavity is an example of this argument. The completely filled spheroidal cavity is a special case, however, because although there are an infinite number of normal modes of oscillation of the liquid, in only one is there induced a resultant couple on the casing. Further, the motion of the casing induces only one normal mode of oscillation of the liquid. Hence, instead of an infinite number of resonances, there is only one; but, on the other hand, it has a broader band-width than any of the corresponding resonances for another shape of cavity. If the spheroidal cavity is not completely filled, these special considerations no longer apply, and presumably fragmentation of the band-width again occurs although the problem is too difficult to solve completely at present.

Experiments to check the theory of the present paper were carried out by Prof. Ward who discusses them in the Appendix. He was able to confirm the presence of the principal mode of resonance, but found that its band-width was much larger than predicted by the theory. One other mode of resonance was detected, but the apparatus apparently was not sufficiently sensitive to detect any more of the weak secondary modes.

2. Equations of motion and boundary conditions

Suppose that in dynamic equilibrium the top is rotating about a fixed point O on its axis of symmetry; it has an angular velocity Ω about its axis of symmetry which is vertical and the centre of gravity of the top is above O. The top contains a cylindrical cavity of radius a and length $2c$, whose axis is the axis of symmetry and whose centre is at a distance h from O. It is partly filled with a volume $2\pi c(a^2-b^2)$ of inviscid liquid of density ρ which is rotating with the top as if solid. Thus, when the conclusions of the theory are compared with experiment, we must assume that before being disturbed the top has been rotating sufficiently long for the liquid to have taken up its angular velocity, but that in the subsequent disturbed motion viscosity may be neglected. Further, it is assumed that gravitational forces in the liquid may be neglected in comparison with the centrifugal forces. The gravitational forces on the solid casing of the top are not

negligible, however, and so the assumption is equivalent to saying that the mass of liquid is small compared with the mass of the casing. There is no formal difficulty in including the effect of gravitational forces provided that the inner surface of the liquid is effectively a cylinder concentric with the cavity, i.e. $a^2\Omega^2 \gg gc$, where g is gravity.

It is convenient to introduce two systems of rotating orthogonal triads each with origin O: (a) the triad $Oxyz$ in which Oz is vertically upwards and Ox, Oy rotate about it with angular velocity Ω; (b) the triad $Ox'y'z'$ in which Oz' lies along the axis of symmetry and Ox', Oy' rotate about it with angular velocity Ω. The components of a property with respect to $Ox'y'z'$ are distinguished from the components of the same property with respect to $Oxyz$ by primes.

Let there be a small disturbance in the motion of the top in which Oz' has at any time direction cosines (l, m, n) with respect to $Oxyz$. Since in equilibrium $l = m = 0$, $n = 1$, and $l^2+m^2+n^2 = 1$, it follows that in the disturbed motion $n-1$ is of second order. Let the velocity of the liquid at (x, y, z) be (u, v, w), where again u, v, w are small. Then, neglecting the gravitational body force in the liquid and writing

$$p = \rho P + \tfrac{1}{2}\rho\Omega^2(x^2+y^2), \tag{2.1}$$

where p is the pressure, we have, following Proudman (1916),

$$\frac{\partial u}{\partial t} - 2\Omega v = -\frac{\partial P}{\partial x}, \qquad \frac{\partial v}{\partial t} + 2\Omega u = -\frac{\partial P}{\partial y},$$
$$\frac{\partial w}{\partial t} = -\frac{\partial P}{\partial z}, \quad \frac{\partial u}{\partial x} + \frac{\partial v}{\partial y} + \frac{\partial w}{\partial z} = 0. \tag{2.2}$$

Here and subsequently we neglect all second-order quantities.

In order to study the stability of the equilibrium position, we now assume that l, m, u, v, w, P are each proportional to e^{st}, where s is a constant. The coefficient of e^{st} in each case is denoted by a suffix s, so that for example

$$u(x, y, z, t) = u_s(x, y, z, s)\, e^{st}. \tag{2.3}$$

The method is then to determine the motion of the liquid due to the perturbation of the casing and the reaction of the liquid on the motion of the casing. It is found that the assumption is only justified if s satisfies a certain transcendental equation, and the condition of stability is that no roots of this equation should have positive real parts.

In terms of s, equations (2.2) reduce to

$$\frac{\partial^2 P_s}{\partial x^2} + \frac{\partial^2 P_s}{\partial y^2} = \alpha^2 \frac{\partial^2 P_s}{\partial z^2}, \quad \text{where} \quad \alpha^2 = -\frac{s^2+4\Omega^2}{s^2}, \tag{2.4}$$

$$\alpha^2 s^2 u_s = s\frac{\partial P_s}{\partial x} + 2\Omega\frac{\partial P_s}{\partial y}, \quad \alpha^2 s^2 v_s = -2\Omega\frac{\partial P_s}{\partial x} + s\frac{\partial P_s}{\partial y}, \tag{2.5}$$
$$s w_s = -\frac{\partial P_s}{\partial z}.$$

The condition on any surface $F(x, y, z, t) = 0$ bounding the liquid is that

$$\frac{\partial F}{\partial t} + u\frac{\partial F}{\partial x} + v\frac{\partial F}{\partial y} + w\frac{\partial F}{\partial z} = 0 \quad \text{when} \quad F = 0, \tag{2.6}$$

since it always consists of the same particles of liquid. Further, the coordinates of any point satisfy

$$z' = z + lx + my. \tag{2.7}$$

The two formulae (2.5) and (2.7) are now applied to the plane and curved boundaries of the liquid. First, since the equations to the plane faces of the cavities are $z' = h \pm c$, it follows that

$$w_s = -s(l_s x + m_s y) \quad \text{when} \quad z' = h \pm c. \tag{2.8}$$

Secondly, the curved part of the cavity is distant a from Oz'; and hence, for any point on it,

$$a^2 + z'^2 = x^2 + y^2 + z^2,$$

i.e.
$$x^2 + y^2 - 2lxz - 2myz - a^2 = 0. \tag{2.9}$$

The boundary condition is therefore

$$u_s x + v_s y = sz(l_s x + m_s y) \quad \text{when} \quad x^2 + y^2 = a^2. \tag{2.10}$$

Thirdly, the pressure is constant on the free boundary, which in equilibrium is distant b from Oz'. Hence, from (2.1), the boundary condition is

$$sP_s + \Omega^2(u_s x + v_s y) = 0 \quad \text{when} \quad x^2 + y^2 = b^2. \tag{2.11}$$

The inner boundary is not exactly a cylinder, and if necessary its equation may be found in terms of P. Let the distance of any point on it from Oz' be $b + \eta'$. Then

$$(b + \eta')^2 + z'^2 = x^2 + y^2 + z^2,$$

whence, from (2.6) and (2.7),

$$b\Omega^2\eta' = -P - \Omega^2(lx + my), \tag{2.12}$$

the right-hand side being evaluated at $x^2 + y^2 = b^2$.

These boundary conditions may be expressed in terms of a new variable Q_s, defined by

$$Q_s = P_s - s^2 z(l_s x + m_s y), \tag{2.13}$$

and which satisfies the same equation as P_s. We have, writing

$$r\cos\theta = x, \quad r\sin\theta = y,$$

$$\frac{\partial Q_s}{\partial z} = 0 \tag{2.14}$$

when $z = h \pm c$,

$$sr\frac{\partial Q_s}{\partial r} + 2\Omega\frac{\partial Q_s}{\partial \theta} = -2sza(l_s\cos\theta + m_s\sin\theta)(s^2 + 2\Omega^2) + 2\Omega s^2 za(l_s\sin\theta - m_s\cos\theta) \tag{2.15}$$

when $r = a$, and

$$sr\frac{\partial Q_s}{\partial r} + 2\Omega\frac{\partial Q_s}{\partial \theta} - s(s^2 + 4\Omega^2)Q_s = s^3 zb(s^2 + 3\Omega^2)(l_s\cos\theta + m_s\sin\theta) + 2\Omega^2 s^3 zb(l_s\sin\theta - m_s\cos\theta) \tag{2.16}$$

when $r = b$.

3. The motion of the liquid

The boundary conditions suggest that we look for solutions of the differential equation (2.4) satisfied by Q_s which are proportional to $\cos\theta$, $\sin\theta$. The most general solution of this form is

$$Q_s = \sum_k C_k\{A_k(r)\cos\theta + B_k(r)\sin\theta\}\cos k(z-h+c), \tag{3.1}$$

where the summation is over a range of values of k to be determined, C_k are constants introduced for convenience, and $A_k(r)$, $B_k(r)$ are Bessel's functions of order one with argument αkr. There are other solutions of (2.4), but none of them can depend on l_s, m_s, nor can they contribute to the couple exerted by the liquid on the casing of the top.

From (2.14) it follows that

$$k = 0 \quad \text{or} \quad k = \frac{\pi}{2c}(2j+1), \tag{3.2}$$

where j is a positive integer including zero.

We now expand z as a Fourier cosine series in the range $h-c \leqslant z \leqslant h+c$, obtaining

$$z = h - \frac{8c}{\pi^2}\sum_{j=0}^{\infty}\frac{1}{(2j+1)^2}\cos\left\{\frac{\pi}{2c}(2j+1)(z-h+c)\right\} = \sum_k C_k\cos k(z-h+c) \tag{3.3}$$

on setting $C_0 = h$ and $C_k = -2(ck^2)^{-1}$ when $k \neq 0$. Substituting (3.1) and (3.3) into (2.15), we find that when $r = a$

$$sa\frac{dA_k}{dr} + 2\Omega\frac{dB_k}{dr} = -2as(s^2+2\Omega^2)l_s - 2as^2\Omega m_s, \tag{3.4}$$

$$-2\Omega A_k + sa\frac{dB_k}{dr} = 2as^2\Omega l_s - 2as(s^2+2\Omega^2)m_s, \tag{3.5}$$

i.e.
$$\left(sa\frac{d}{dr} - 2i\Omega\right)(A_k + iB_k) = -2as(s+i\Omega)(s-2i\Omega)(l_s+im_s). \tag{3.6}$$

Similarly, when $r = b$,

$$\left(sb\Omega^2\frac{d}{dr} - 2i\Omega^3 - s(s^2+4\Omega^2)\right)(A_k+iB_k) = -bs^2(s-2i\Omega)(s+i\Omega)^2(l_s+im_s). \tag{3.7}$$

First consider the special case when $k = 0$. Here

$$A_0 + iB_0 = (l_s+im_s)(X_0 r + Z_0/r), \tag{3.8}$$

where X_0, Z_0 are independent of r. On substituting into (3.6) and (3.7), it is found, after some algebra, that

$$X_0 a + Z_0/a = -2as(s+i\Omega) + \frac{2s^2ab^2(s+i\Omega)^2}{b^2(s+i\Omega)^2 + a^2(s^2+\Omega^2-2i\Omega s)}. \tag{3.9}$$

This is the only combination of X_0 and Z_0 needed in the argument.

Next consider the general case $k \neq 0$. Write

$$\frac{A_k+iB_k}{l_s+im_s} = X_k J_1(\alpha kr) + Z_k Y_1(\alpha kr) = \mathscr{C}_1(\alpha kr), \tag{3.10}$$

where X_k, Z_k are constants and J, Y are Bessel's functions of the first and second kind with real argument. Let us also write

$$X_k J_0(\alpha kr) + Z_k Y_0(\alpha kr) = \mathscr{C}_0(\alpha kr). \tag{3.11}$$

Then the boundary conditions become

$$\left.\begin{aligned} \alpha sb\Omega^2 \mathscr{C}_0(\alpha kb) - (s+2i\Omega)(s^2-2i\Omega s+\Omega^2)\mathscr{C}_1(\alpha kb) &= bs^2(s-2i\Omega)(s+i\Omega)^2, \\ \alpha sa\mathscr{C}_0(\alpha ka) - (s+2i\Omega)\mathscr{C}_1(\alpha ka) &= -2sa(s+i\Omega)(s-2i\Omega). \end{aligned}\right\} \tag{3.12}$$

4. The couple on the casing

In this section we calculate the couple on the casing exerted by the motion of the liquid described in the previous section. Contributions to the couple come from the curved surface and the plane parts of the cavity, and we shall consider them separately. The pressure in the liquid is

$$p = \tfrac{1}{2}\rho\Omega^2(x^2+y^2) - \tfrac{1}{2}\rho\Omega^2 b^2 + p_0 + \rho P, \tag{4.1}$$

where p_0 is the constant pressure in the air space ($r' < b$).

Let the components of the couple exerted on the curved surface be (E_c, F_c, G_c) referred to $Oxyz$ and (E'_c, F'_c, G'_c) referred to $Ox'y'z'$. Then $G'_c = 0$; and, since all other components are first order,

$$E_c = E'_c, \quad F_c = F'_c. \tag{4.2}$$

Now
$$E'_c + iF'_c = \frac{i}{a}\iint z'(x'+iy')\,p\,dS', \tag{4.3}$$

where the integral is taken over the curved surface $r' = a$, $|z'-h| \leqslant c$. From (4.1) and (2.9), $p = \rho P + \rho\Omega^2(lx'z' + my'z') + \text{const.}$ on this surface, and therefore

$$E'_c + iF'_c = \frac{i\rho}{a}\iint \{P + \Omega^2(lx'z' + my'z')\}\, z'(x'+iy')\,dS'. \tag{4.4}$$

Substituting from (3.1), (3.9), (3.10) and dropping the primes, we get

$$\begin{aligned} \frac{(E_c+iF_c)_s}{l_s+im_s} = {} & \tfrac{2}{3}i\rho\pi a^2c^3(s^2+\Omega^2) - 2i\pi\rho ca^2h^2(s+i\Omega)^2 + i\pi\rho ac\sum_{j=0}^{\infty} C_k^2 \mathscr{C}_1(\alpha ka) \\ & - \frac{4i\pi ca^2h^2(s+i\Omega)^2(s^2-2i\Omega s+\Omega^2)(a^2-b^2)}{b^2(s+i\Omega)^2 + a^2(s^2-2i\Omega s+\Omega^2)}. \end{aligned} \tag{4.5}$$

The couple exerted by the liquid on the plane faces of the cavity may be found on the assumption that the liquid extends from $r' = b$ to $r' = a$. This is not strictly correct, of course, for the inner boundary of the liquid is $r' = b + \eta'$, where η' is defined in (2.12). However, since the pressure perturbation in $b < r' < b + \eta'$ is first-order, the couple exerted on that part of the plane faces is of second-order and negligible.

Relative to $Ox'y'z'$, let the components of the couple exerted on the plane face $z' = h + c$ be $(E'_+, F'_+, 0)$. Then

$$E'_+ + iF'_+ = -i\rho\int_0^{2\pi} d\theta' \int_b^a (x'+iy')\,[P + \tfrac{1}{2}\Omega^2(r'^2 + 2lx'z' + 2my'z')]\,dr'. \tag{4.6}$$

Again the primes may be dropped. After some reduction it is found that

$$\frac{(E_+ + iF_+)_s}{l_s + im_s} = i\pi\rho \sum_{j=0}^{\infty} C_k \int_b^a r^2 \mathscr{C}_1(\alpha k r)\, dr - \tfrac{1}{4} i\rho\pi (a^4 - b^4)(h+c)(s^2+\Omega^2) + i\pi\rho h \int_b^a r^2 (X_0 r + Z_0/r)\, dr. \quad (4.7)$$

Similarly, if the couple exerted by the liquid on the plane face $z' = h - c$ is $(E'_-, F'_-, 0)$, then

$$\frac{(E_- + iF_-)_s}{l_s + im_s} = i\pi\rho \sum_{n=0}^{\infty} C_k \int_b^a r^2 \mathscr{C}_1(\alpha k r)\, dr - \tfrac{1}{4} i\rho\pi (a^4 - b^4)(h-c)(s^2+\Omega^2) - i\pi\rho h \int_b^a r^2 (X_0 r + Z_0/r)\, dr. \quad (4.8)$$

Now
$$\int_b^a r^2 \mathscr{C}_1(\alpha k r)\, dr = \frac{1}{\alpha^2 k^2} [2r\mathscr{C}_1(\alpha k r) - \alpha k r^2 \mathscr{C}_0(\alpha k r)]_b^a, \quad (4.9)$$

and we may use the boundary conditions (3.4) to eliminate $\mathscr{C}_0(\alpha k b)$ and $\mathscr{C}_0(\alpha k a)$.

Hence finally, if F, G are the components of the couple about Ox, Oy, we have, adding (4.5), (4.7) and (4.8),

$$\frac{F_s + iG_s}{l_s + im_s} = \tfrac{2}{3} i\pi\rho a^2 c^3 \frac{(s+i\Omega)(3s-2i\Omega)}{(s+2i\Omega)} + \tfrac{2}{3} i\pi\rho b^2 c^3 \frac{s^3 (s+i\Omega)^2}{\Omega^2 (s+2i\Omega)} - \tfrac{1}{2} i\pi\rho c (a^4 - b^4)(s^2+\Omega^2) - \frac{2i\pi\rho c a^2 b^2 (a^2-b^2)(s+i\Omega)(s^2 - 2i\Omega s + \Omega^2)}{b^2(s+i\Omega)^2 + a^2(s^2 - 2i\Omega s + \Omega^2)} + \frac{2i\pi\rho c a (s+i\Omega)}{s+2i\Omega} \sum_{j=0}^{\infty} C_k^2 \mathscr{C}_1(\alpha k a) + \frac{i\pi\rho c b s (s+i\Omega)^2}{\Omega^2 (s+2i\Omega)} \sum_{j=0}^{\infty} C_k^2 \mathscr{C}_1(\alpha k b). \quad (4.10)$$

A partial check on the validity of this rather complicated expression is obtained by setting $b = a$. Then

$$\mathscr{C}_1(\alpha k a) = \mathscr{C}_1(\alpha k b) = -a(s^2 + \Omega^2) \quad (4.11)$$

from (3.12). On substituting (4.11) into (4.10) and noting that

$$\sum_{j=0}^{\infty} C_k^2 = \tfrac{2}{3} c^2,$$

it follows that $F_s + iG_s = 0$, as would be expected because the cavity is empty.

5. The motion of the top

Let H_x, H_y be the moments, about Ox, Oy respectively, of the rate of change of the momentum of the casing of the top, and let T, T, L be the principal moments of inertia of the casing about O. Then from dynamical considerations,

$$\left.\begin{aligned} H_x &= T(\dot{m} + 2\Omega\dot{l} - \Omega^2 m) - \Omega L(\dot{l} - \Omega m), \\ H_y &= T(\dot{l} - 2\Omega\dot{m} - \Omega^2 l) + \Omega L(\dot{m} + \Omega l). \end{aligned}\right\} \quad (5.1)$$

The disturbing couple consists of two parts. First, there is a contribution from the liquid in the cavity which has been calculated in the preceding section. Secondly,

there is a contribution from the gravitational forces on the casing, their effect on the liquid being neglected. The equations of motion of the casing are therefore

$$H_x = E - Mg\,dm, \quad H_y = F + Mg\,dl, \tag{5.2}$$

where M is the mass of the casing and d the distance of its centre of gravity from O. These equations may be combined to give

$$(l_s + im_s)\,[T(s+i\Omega)^2 - i\Omega L(s+i\Omega)] = \frac{\Omega^2 L^2}{4T}\beta(l_s + im_s) - i(E_s + iF_s), \tag{5.3}$$

where for convenience we have set

$$4Mg\,dT = L^2\Omega^2\beta. \tag{5.4}$$

It is noted that the condition for the stability of the empty top is $\beta < 1$. On substituting for $E_s + iF_s$ from (4.10), $l_s + im_s$ cancels throughout and we obtain an equation for s in terms of the physical properties of the top. The equation must be satisfied if the assumption concerning the nature of the motion made in §2 (i.e. $l, m \propto e^{st}$), is to be justified. Corresponding to the roots of this equation are the normal modes of the hydrodynamic-dynamic system, which is stable therefore only if in none of the roots of the equation is $\mathscr{R}\{s\} > 0$. On writing $s = i\Omega(1+\tau)$, the equation for τ becomes

$$\begin{aligned} T\tau^2 - L\tau + \frac{L}{4\tau}\beta = {} & -\tfrac{1}{2}\pi\rho c\tau(\tau-2)\,(a^4 - b^4) - \tfrac{2}{3}\rho\pi b^2 c^3\,\frac{\tau^2(\tau-1)}{\tau+1} \\ & + \tfrac{2}{3}\pi\rho a^2 c^3\,\frac{\tau^2(3\tau-5)}{\tau+1} - \frac{2\pi\rho c a^2 b^2 (a^2-b^2)\,\tau^2(\tau^2-4\tau+2)}{a^2(\tau^2-4\tau+2) + b^2\tau^2} \\ & - \frac{\pi\rho c}{\Omega^2(1+\tau)} \sum_{j=0}^{\infty} C_k^2\{2a\tau\mathscr{C}_1(\alpha ka) + \tau^2(1-\tau)\,b\mathscr{C}_1(\alpha kb)\}, \end{aligned} \tag{5.5}$$

where $\alpha^2 = (3-\tau)\,(1+\tau)/(1-\tau)^2$, and k, C_k, are defined in (3.2) and (3.3).

Further, in (5.5),

$$\mathscr{C}_1(\alpha kr) = X_k J_1(\alpha kr) + Z_k Y_1(\alpha kr), \tag{5.6}$$

where from (3.12)

$$\left.\begin{aligned} & X_k\{\alpha ka(1-\tau)\,J_0(\alpha ka) + (1+\tau)\,J_1(\alpha ka)\} \\ & \quad + Z_k\{\alpha ka(1-\tau)\,Y_0(\alpha ka) + (1+\tau)\,Y_1(\alpha ka)\} = -2a\Omega^2(3-\tau)\,(1-\tau), \\ & X_k\{\alpha kb(1-\tau)\,J_0(\alpha kb) - (1+\tau)\,(2-4\tau+\tau^2)\,J_1(\alpha kb)\} \\ & \quad + Z_k\{\alpha kb(1-\tau)\,Y_0(\alpha kb) - (1+\tau)\,(2-4\tau+\tau^2)\,Y_1(\alpha kb)\} \\ & \quad = b\Omega^2\tau^2(3-\tau)\,(1-\tau)^2. \end{aligned}\right\} \tag{5.7}$$

It is noted that (5.5) is a real equation for τ, and hence the roots are either real or are complex conjugates. The condition for stability is therefore that the roots are all real. Further, $\mathscr{C}_1(\alpha kr)$ is regular *qua* function of τ, except at a discrete set of poles which we can expect to be real. Otherwise the motion of the liquid would be unstable if the casing were fixed. In numerical calculations by Dr D. C. Gilles of the Scientific Computing Service, the poles of X_k, Z_k found were all real.

A complete discussion of (5.5) would be exceedingly complicated in view of the number of parameters, and here we shall restrict attention only to the stability

of a heavy top with a small cavity. In fact a system of this kind is necessary to justify the neglect of the gravitational forces on the liquid but not on the casing. In this special case the right-hand side of (5.5) is small except at the poles of X_k, Z_k and when $b^2\tau^2 + a^2(\tau^2 - 4\tau + 2) = 0$. If a zero of (5.5) is not near a pole of the right-hand side, it may be neglected, so that the equation reduces to

$$T\tau^2 - L\tau + \frac{L^2}{4T}\beta = 0, \tag{5.8}$$

which has the solution $\tau = (L/2T)[1 \pm (1-\beta)^{\frac{1}{2}}]$. Hence, the top is unstable if $\beta > 1$ and none of the poles of the right-hand side of (5.5) are near

$$\tau_{\rm pr} = \frac{L}{2T}[1-(1-\beta)^{\frac{1}{2}}] \quad \text{or} \quad \tau_{\rm nu} = \frac{L}{2T}[1+(1-\beta)^{\frac{1}{2}}]. \tag{5.9}$$

Now let us suppose that a root of (5.5) occurs near a pole $\tau = \tau_0$ of the right-hand side. Near $\tau = \tau_0$, (5.5) reduces to

$$T\tau^2 - L\tau + \frac{L^2}{4T}\beta = \frac{D(\tau_0)}{\tau - \tau_0} + \text{small terms}, \tag{5.10}$$

where $D(\tau_0)$ is a small known parameter, the residue at the pole. Then if

$$T\tau_0^2 - L\tau_0 + \frac{L^2}{4T}\beta \gg D, \tag{5.11}$$

the root in question is

$$\tau = \tau_0 + \frac{D}{T\tau_0^2 - L\tau_0 + L^2\beta/4T},$$

and is real since τ_0 is real.

An exception arises if (5.11) is not satisfied. Suppose, for example, that $\tau_0 \doteqdot \tau_{\rm nu}$. Then, near $\tau = \tau_{\rm nu}$, (5.5) reduces to

$$T(\tau_{\rm nu} - \tau_{\rm pr})(\tau - \tau_{\rm nu}) = \frac{D}{\tau - \tau_0}.$$

with real roots only if

$$T(\tau_{\rm nu} - \tau_{\rm pr})\left(\frac{\tau_0 - \tau_{\rm nu}}{2}\right)^2 + D \geqslant 0.$$

Hence, even if $\beta < 1$, the top is unstable if $D < 0$ and

$$|\tau_0 - \tau_{\rm nu}| \leqslant \left[\frac{-D(\tau_0)}{L(1-\beta)^{\frac{1}{2}}}\right]^{\frac{1}{2}}. \tag{5.12}$$

Similarly, the top is unstable if $D > 0$ and

$$|\tau_0 - \tau_{\rm pr}| \leqslant \left[\frac{D(\tau_0)}{L(1-\beta)^{\frac{1}{2}}}\right]^{\frac{1}{2}}. \tag{5.13}$$

Thus, if the empty top is stable, it is theoretically possible to render it unstable by introducing a small quantity of liquid. It is also possible to render an unstable top stable if $\beta - 1$ is small, but the conditions are complicated and not of great interest. In most cases the only poles which can lead to instability are those of X_k, Z_k, and the residues at these poles are always real and negative so that only

(5.12) is relevant. A slightly more convenient function than D for practical applications is $R > 0$, where $\rho a^6 R^2 + cD = 0$. Thus, R is a positive real number which depends, like the position of the poles, only on c/a, b/a. The theoretical condition (5.12) may thus be restated as follows. The top is unstable if any pole τ_0 of X_k, Z_k satisfies

$$\frac{|\tau_0 - \tau_{\mathrm{nu}}|}{R}\left(\frac{cL(1-\beta)^{\frac{1}{2}}}{\rho a^6}\right)^{\frac{1}{2}} \leqslant 1. \tag{5.14}$$

In the calculations connected with (5.14), there are actually a double infinite set of poles to be considered, because to each integer j the determinant of the coefficients of X_k, Z_k in (5.7) and (5.8) has an infinite number of zeroes. Fortunately, however, k can be absorbed into c/a, and so it is only necessary to tabulate the poles with $j = 0$. Tables from which the leading poles and the corresponding values of R may be determined for given values of b/a, $c/\{(2j+1)a\}$ have been computed on behalf of the author by Dr Gilles and some of them are displayed here (tables 1–5). In the computation it was assumed that poles in which $\tau_0 < 0$, or $\tau_0 > 0{\cdot}20$ were not of great interest. The way in which the tables are to be used

τ_0	$\frac{c}{(2j+1)a}$	R	$\frac{c}{(2j+1)a}$	R	$\frac{c}{(2j+1)a}$	R
				0·0		0·0
0·00	0·995	0·000	0·478	000	0·310	000
0·02	1·018	0·058	0·490	070	0·319	019
0·04	1·042	0·118	0·503	144	0·327	040
0·06	1·066	0·181	0·516	223	0·336	062
0·08	1·091	0·246	0·530	307	0·345	086
0·10	1·117	0·313	0·544	396	0·355	111
0·12	1·144	0·382	0·559	491	0·364	139
0·14	1·172	0·454	0·574	591	0·375	168
0·16	1·201	0·528	0·590	697	0·385	198
0·18	1·231	0·604	0·607	809	0·397	231
0·20	1·262	0·682	0·624	928	0·408	266

TABLES 1–5. Tables from which the leading poles τ_0 of X_k, Z_k and the corresponding residues may be calculated as functions of $c/(2j+1)a$, b/a.

TABLE 1. $b = 0$

τ_0	$\frac{c}{(2j+1)a}$	R	$\frac{c}{(2j+1)a}$	R	$\frac{c}{(2j+1)a}$	R
				0·0		0·0
0·00	0·947	0·000	0·387	000	0·224	000
0·02	0·968	0·055	0·398	047	0·230	010
0·04	0·991	0·113	0·408	096	0·236	020
0·06	1·015	0·172	0·419	148	0·242	031
0·08	1·039	0·234	0·430	202	0·249	044
0·10	1·065	0·298	0·442	259	0·256	057
0·12	1·092	0·365	0·454	319	0·263	071
0·14	1·120	0·434	0·467	383	0·271	086
0·16	1·149	0·506	0·480	450	0·279	103
0·18	1·181	0·580	0·494	521	0·287	121
0·20	1·214	0·657	0·509	597	0·295	140

TABLE 2. $b^2/a^2 = 0{\cdot}20$

τ_0	$\frac{c}{(2j+1)\,a}$	R	$\frac{c}{(2j+1)\,a}$	R	$\frac{c}{(2j+1)\,a}$	R
				0·0		0·00
0·00	0·842	0·000	0·281	000	0·154	000
0·02	0·861	0·047	0·288	023	0·158	039
0·04	0·881	0·097	0·296	046	0·162	081
0·06	0·901	0·148	0·304	071	0·166	127
0·08	0·923	0·201	0·312	098	0·171	177
0·10	0·945	0·256	0·320	125	0·176	231
0·12	0·969	0·314	0·329	154	0·181	289
0·14	0·994	0·374	0·338	185	0·186	352
0·16	1·020	0·437	0·348	218	0·191	419
0·18	1·048	0·503	0·358	252	0·197	492
0·20	1·077	0·572	0·369	289	0·203	571

TABLE 3. $b^2/a^2 = 0{\cdot}40$

τ_0	$\frac{c}{(2j+1)\,a}$	R	$\frac{c}{(2j+1)\,a}$	R	$\frac{c}{(2j+1)\,a}$	R
				0·0		0·00
0·00	0·697	0·000	0·182	0000	0·096	000
0·02	0·712	0·035	0·186	0080	0·098	012
0·04	0·728	0·071	0·191	0164	0·101	025
0·06	0·744	0·109	0·196	0252	0·104	040
0·08	0·762	0·149	0·202	0345	0·107	055
0·10	0·780	0·190	0·207	0444	0·110	072
0·12	0·799	0·233	0·213	0547	0·113	091
0·14	0·819	0·278	0·219	0657	0·116	111
0·16	0·840	0·326	0·225	0773	0·119	132
0·18	0·862	0·375	0·232	0896	0·123	155
0·20	0·886	0·427	0·239	1027	0·126	180

TABLE 4. $b^2/a^2 = 0{\cdot}60$

τ_0	$\frac{c}{(2j+1)\,a}$	R	$\frac{c}{(2j+1)\,a}$	R	$\frac{c}{(2j+1)\,a}$	R
				0·00		0·000
0·00	0·496	0·000	0·088	000	0·045	000
0·02	0·506	0·019	0·091	014	0·047	019
0·04	0·517	0·039	0·093	028	0·048	040
0·06	0·529	0·060	0·096	043	0·049	062
0·08	0·541	0·081	0·098	059	0·050	087
0·10	0·553	0·104	0·101	077	0·052	113
0·12	0·566	0·127	0·104	094	0·053	142
0·14	0·580	0·152	0·107	113	0·055	174
0·16	0·594	0·178	0·110	134	0·057	207
0·18	0·609	0·205	0·113	155	0·058	244
0·20	0·625	0·234	0·117	178	0·060	284

TABLE 5. $b^2/a^2 = 0{\cdot}80$

may be exemplified as follows. Suppose that $\tau_{\mathrm{nu}} = 0{\cdot}1$, $c/a = 3$, $b^2/a^2 = 0{\cdot}20$. In order to test for instability, we use the table in which $b^2/a^2 = 0{\cdot}20$, and to begin with look for any poles in $0 \leqslant \tau_0 \leqslant 0{\cdot}2$ with $j = 0$ and therefore with $c/\{(2j+1)\,a\} = 3$. There are none. Next we try $j = 1$ so that $c/\{(2j+1)\,a\} = 1$.

There is a zero in the first table at $\tau \doteq 0{\cdot}047$ and at which $R = 0{\cdot}13$. Thirdly, try $j = 2$, so that $c/\{(2j+1)a\} = 0{\cdot}600$. There are no poles in $0 \leqslant \tau_0 \leqslant 0{\cdot}2$. Further values of j may be considered in the same way. Having found all the relevant τ_0, the modified form of (5.14) may now be used to test for instability.

In the Appendix below, Prof. Ward describes some experiments which he has carried out to check the stability criterion in (5.14). It was observed that there was a range of filling ratios on either side of the filling ratio, which corresponded to the theoretical value of principal mode of instability for which the top was violently unstable. However, this range corresponds to a stability criterion

$$-3{\cdot}9 < \frac{(\tau_0 - \tau_{\mathrm{nu}})}{R}\left[\frac{cL(1-\beta)^{\frac{1}{2}}}{\rho a^6}\right]^{\frac{1}{2}} < 2{\cdot}7, \tag{5.15}$$

instead of (5.14) as required by the theory. Possible reasons for this discrepancy are discussed by Ward, but without positive conclusions. In any practical application it may be wiser at this stage to use (5.15) instead of (5.14), but it must be admitted that the supporting evidence is not sufficient to be convincing.

Only one other theoretical mode of instability could be detected with certainty in Ward's experiments, which may possibly have been due to the difficulty of designing an apparatus both strong enough to withstand the large forces at the principal mode of instability and yet sensitive enough to show up the weak secondary modes.

REFERENCES

Chetayev, N. 1957 *Prikl. Mat. i. Mex.* **21**.

Greenhill, A. G. 1880 *Proc. Camb. Phil. Soc.* **4**, 4.

Hough, S. S. 1898 *Phil. Trans.* A, **186**, pt. 1, 297.

Lord Kelvin 1877 *Nature, Lond.*, **15**, 297.

Narimanov, C. S. 1957 *Prikl. Mat. i. Mex.* **21**, 696.

Proudman, J. 1916. *Proc. Roy. Soc.* A, **92**, 408.

APPENDIX

BY G. N. WARD

In order to test Prof. Stewartson's theory of the stability of a rotating cylindrical shell which is partially filled with liquid, experiments were made with a constant-speed gyrostat. The rotor had a cavity $1\frac{1}{8}$ in. in diameter and $3\frac{3}{8}$ in. long, and was supported by two ball races mounted in a cage. The rotor was driven through a flexible coupling by a small 3-phase induction motor which was also mounted in the cage, and was fed from a variable frequency alternator, the electrical connexions being through some special woven copper wire of great flexibility. The cage was connected by gymbal bearings to a comparatively massive support, the inner gymbal ring having small lead weights attached so that the equivalent moments of inertia of the system were the same about both gymbal axes. The cage was adjustable in the inner gymbal and was positioned in such a way that the centre of mass of the whole system (without liquid) coincided with the centre of rotation, thus making the system into a gyrostat, and in this state the moment of inertia about the gymbal axes was 8·95 lb. in.^{2}. The equivalent moment of inertia

of the rotating parts about the axis of symmetry was inferred from a dynamic experiment in which the frequencies of nutation and rotation were measured by stroboscopic means: the ratio of these frequencies was 0·112, from which it follows that the required equivalent moment of inertia was

$$0{\cdot}112 \times 8{\cdot}95 = 1{\cdot}002 \text{ lb. in.}^2.$$

The frequency of precession was very small, being less than 1 cycle/min at a rotor speed of 6000 r.p.m. with the cavity full of liquid, which was the state of maximum unbalance.

The liquid used for the experiment was a mixture of light lubricating oil and liquid paraffin, which had a kinematic viscosity of 23·9 centistokes at 70 °F and 12·8 centistokes at 100 °F, and 47·5 g of this liquid were required to fill the cavity completely. The experimental procedure was to weigh the rotor plus any residual liquid, determine the mass of the residual liquid by subtracting the weight of the empty rotor, and then add the liquid 1 cm^3 at a time, observing the stability or instability after each addition. To make quantitative estimates of the instability, use was made of the fact that a light far up in the laboratory roof was reflected conveniently in the cap of the upper rotor bearings, and that this reflexion appeared to trace out a small circle whose diameter was proportional to the amplitude of the nutational motion. This circle was observed through a slot, cut in thin metal sheet, which was $\frac{1}{8}$ in. wide over half its length and $\frac{1}{4}$ in. wide over the other half, and by moving this slot along its length, and measuring the time taken for the circle to increase in diameter from just filling the narrow portion of the slot to just filling the wider portion, the rate of increase of the amplitude of the oscillation could be determined. This rather crude but effective method of instrumentation proved to be most convenient in use; precautions were taken to ensure that the relative positions of the slot, the gyrostat, and the observer's eye were maintained during an observation. In this way observations of instability were made with a rotor speed of 6000 r.p.m., this being considered to be the highest speed at which it was desirable to run the gyrostat. Even at this speed, the violent instabilities at resonance and in the subsequent tests at large amplitudes, mentioned below, proved to be too much for the gymbal bearings, which suffered some damage, and also for the rotor bearings, which were thrown slightly out of alignment.

The results of the tests are shown in figure 1, where the reciprocal of the time to double the amplitude (for small amplitudes) is plotted against the filling-ratio. In the notation of this paper, when

$$\gamma_n = \frac{\text{nutational frequency}}{\text{rotational frequency}} = 0{\cdot}112,$$

$$n = \text{number of waves radially},$$

$$j + \tfrac{1}{2} = \text{number of waves axially},$$

the theoretical filling-ratios $(1 - b^2/a^2)$ for resonance are shown in table 6.

It will be seen from figure 1 that the main resonance $(n, j) = (1, 1)$ at filling-ratio 0·66, and the second resonance $(1, 2)$ at filling-ratio 0·23 can be detected with certainty, and that the experimental values of the filling-ratio agree well with the

theoretical predictions. Other minor resonances appear to occur, but their positions do not agree with any of the filling-ratios in table 6, and it is possible that these resonances may be spurious. However, there is no doubt about the existence of the main resonance at filling-ratio 0·06, and the results at and near this resonance can be used to rest the theoretical predictions for the range of filling-ratios in which instability occurs.

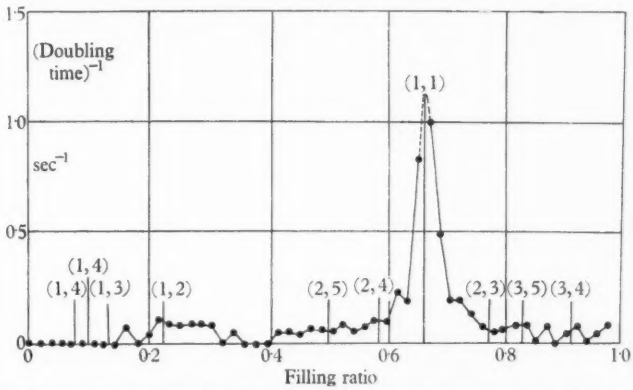

FIGURE 1. Experimental results. Filling ratio against reciprocal of time (in seconds) for amplitude to be doubled, at rotor speed of 6000 r.p.m.

	n		
j	1	2	3
0	—	—	—
1	0·66	—	—
2	0·23	—	—
3	0·14	0·78	—
4	0·10	0·60	0·92
5	0·08	0·50	0·83

TABLE 6

The limits of filling-ratio for instability are very vague in figure 1, but it seems that the gyrostat is definitely unstable between filling-ratios of 0·63 and 0·70. If we define a number A by

$$A = \frac{(\tau_0 - \tau_{nu})}{R}\left[\frac{cL(1-\beta)^{\frac{1}{2}}}{\rho a^6}\right]^{\frac{1}{2}},$$

then the theoretical criterion given in equation (5.14) becomes $-1 \leqslant A \leqslant 1$ for instability. In the present case, the values of A corresponding to the filling-ratios 0·63 and 0·70 are respectively 2·7 and $-3{\cdot}9$, so the experimental range of A for instability is $-3{\cdot}9 < A < 2{\cdot}7$, which is considerably greater than the theoretical range.

It is interesting to speculate on possible reasons for this disagreement. It seems that there are four major factors which would affect the motion and which are neglected in the present theory, namely, the effect of gravity on the liquid filling,

the displacement of the axis of rotation from the axis of the cylinder, the effect of non-linear terms, and the effect of friction in the gymbal bearings. As to the effect of gravity, some qualitative experiments at lower rotational speeds (4000 and 5000 r.p.m.) showed that it was appreciable, but the ranges of instability were smaller at the lower rotational speeds, so the effect will not provide an explanation for the discrepancy between the theory and experiment. The effect of the second factor should be small provided that displacement of the axis of symmetry is kept small, and in the experiments the axis of symmetry never made an initial angle of more than about 3° with the axis of nutation (which was approximately vertical in all tests), so the resultant axis of rotation never made an initial angle of more than about 0·3° with the axis of symmetry; nevertheless, the extra inertia forces might have been significant, and to test for this, some large initial displacements in nutation were applied. It was found that the range of instability was increased by doing this, and in fact the gyrostat could be made unstable for almost all filling-ratios tested by giving it a sufficiently violent initial impulse. Unfortunately these tests have not been made systematically owing to the bearing failures described above. The effects of non-linearities are difficult to estimate and must play their part in the increased instability at large displacements noted above; it is difficult to believe that they are of great importance for the small displacements used in the quantitative tests. The fourth possibility is that friction in the gymbal bearings added an appreciable amount of instability to the system. The gymbal bearings were hard conical pivots bearing on ball races; although such bearings leave something to be desired from the frictional point of view, they were adopted to withstand the large forces which were anticipated at the main resonance, and even then they were damaged. Friction in these bearings would be expected to be de-stabilizing, and the fact that the oscillations were never damped at any filling-ratio might lend support to the view that friction there was the cause of the disagreement between the theoretical and experimental ranges of instability; however, the theory indicates that the liquid filling should never give rise to damping of the oscillations, and the results for small filling-ratios show that any de-stabilization caused by bearing friction must have been very small and unlikely to produce the comparatively large effects under discussion.

The authors wish to thank Brigadier G. H. Hinds, Mr F. M. Herbert and Dr G. R. Higginson for their support and assistance, Dr D. C. Gilles for carrying out the computation of the tables, Mr W. G. Holloway for designing the gyroscope, and Mr S. H. Lilley for his assistance during the experiments.

On the forced motion due to heating of a deep rotating liquid in an annulus

By T. V. DAVIES
King's College, London†

(Received 14 August 1958 and in revised form 7 November 1958)

In the laboratory experiments by Fultz & Riehl (1957) and by Hide (1958) on heated rotating liquids contained in the annulus between two cylinders, it has been observed that a strongly marked jet stream appears on the free surface of the liquid under certain conditions of rotating and heating. This jet stream meanders around the annulus in a regular wave-like pattern alternately approaching the outer and inner cylindrical boundaries. The present paper puts forward an analytical theory for this jet, or Rossby regime, in the course of which exact solutions are presented of certain fundamental non-linear partial differential equations. The assumption is made that the flow is geostrophic at the first approximation and that the heat transfer across the stream lines of geostrophic flow (that is, the isobars) is due to molecular conduction. From a calculation of the heat flow it appears that this leads to values of the heat transfer which are too small, so that the ageostrophic terms must be of importance in the actual heat transfer; nevertheless, the exact solution obtained here probably reveals the mechanism of the change from one wave pattern to another and certainly provides an explanation for the observed upper limit to the number of waves in a given geometrical configuration, as discussed by Hide. It has been established that the mean zonal flow and mean zonal temperature field are dependent upon the amplitude function of a finite amplitude wave solution. In this exact solution it is found that the amplitude and phase functions of the wave patterns are themselves interdependent and that the shape of the wave depends on the quantity of heat and angular momentum being transferred. It is shown that the wave pattern consisting of an integral number m lobes or petals can exist only in a restricted range of the Rossby number S—this is well-known from the experimental work of Fultz and Hide.

Introduction

In the laboratory experiments by Fultz & Riehl (1957) and Hide (1958), liquid contained in the annulus between two concentric circular cylinders (radii b and a ($< b$): see figure 1) is bounded below by a horizontal smooth surface and bounded above by a free surface. The cylinders are constrained to rotate steadily about their common axis, the outer cylinder being maintained at a temperature T_b and the inner at a temperature T_a ($< T_b$). Under certain circumstances of rotation and heating, the forced flow of the liquid relative to the cylinders consists of a well-marked wave pattern in which the fluid motion is principally horizontal and in

† Now at University College of Wales, Aberystwyth.

which a clearly defined jet stream can be observed on the free upper surface. The jet meanders regularly around the wave pattern, and the whole wave pattern plus the jet rotates relatively to the cylinders. A particular m-lobed wave pattern may be maintained indefinitely under constant conditions of rotation and temperature difference $T_b - T_a$, but can be changed by variation of either of these quantities. A discussion of the stability of the wave pattern has been made by the present author in an earlier paper (1956), and in this paper it was shown theoretically that the stability of the wave pattern is dependent principally upon one parameter known as the Rossby number S. In such stability analyses one is forced to assume that the wave amplitudes of the perturbation are infinitesimal compared, say, with the annulus radius $(b-a)$, and the results of such analyses will apply only to the initial stages of the wave growth under unstable conditions. The waves have an amplitude which is almost as large as the distance $(b-a)$, and this finiteness of amplitude can no longer be ignored in the investigation of the jet stream problem. This implies that the analytical investigation of the jet stream problem is necessarily one involving non-linear equations; until recently the only attempts which had been made to understand the jet stream structures mathematically were by numerical methods (Phillips 1956).

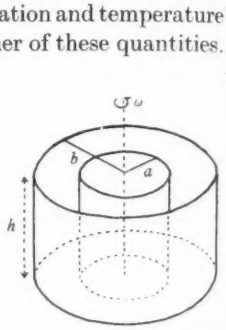

FIGURE 1. Definition sketch.

An analytical approach to the problem is possible, however, and the first step in this direction has been made by Miss Ruth Rogers (1959) who has investigated rectilinear jets using thermal boundary layer concepts in the heat transfer equation. The existence of such a rectilinear jet solution suggested to the present author that it might be profitable to investigate the corresponding jet problem in cylindrical co-ordinates and the present paper is a summary of the findings. It is interesting to note, however, that the boundary layer type of approximation made by Miss Rogers is not necessary in dealing with the present cylinder problem, and the solutions are correspondingly more valuable.

In the solution presented here it is found convenient to introduce amplitude and phase functions for the wave, and it then emerges that the zonal temperature field and the zonal flow can be expressed in terms of the amplitude and phase functions, which is something one would have expected from the many qualitative discussions of the corresponding meteorological problem (see, for instance, Lorenz 1957). It is found that the amplitude function and phase function are interdependent: one of these functions must be postulated before the complete solution can be obtained. Some guidance in postulating the nature of the phase function can be obtained from investigating the angular momentum and heat transfer associated with the wave. Particular examples illustrating different types of transfer have been included in this paper. One of the important results obtained is that the shape of the wave is dependent upon not only the amount of angular momentum transferred but also the amount of heat transferred; with an m-lobed wave pattern it is possible to transfer different amounts of heat and angular momentum within certain ranges. The m-lobed wave pattern is shown to

exist only in certain ranges of the rotation and Rossby number, and when these ranges are combined with those obtained by the author in the earlier stability paper (1956) it is then possible to understand the complete stability diagram which has been obtained experimentally by Fultz (1956), and in particular to understand why there is a maximum number of waves possible in any given geometrical configuration. A result of secondary importance is that the steady solutions obtained here exist only if the ratio of the inner radius to the outer radius of the annulus is greater than a certain critical quantity. This implies that the steady wave regime cannot be maintained permanently in the open dishpan experiment.

A comparison of the theoretical absolute heat transport across either cylindrical boundary with that observed by Fultz indicates a variation with m in the correct sense, but the magnitude is considerably in error.

1. Statement of problem and method of solution

The dynamical equations of motion and the equation of heat transfer for a liquid contain terms which arise from the viscous stresses. One of the most striking features of the experiments conducted by Fultz & Riehl and by Hide is the negligible diffusion of the jet stream—a feature in which one might expect the viscous stresses to play a fundamental role. It is clear from order of magnitude arguments that the geostrophic approximation and the consequent 'thermal wind' together give results for the velocity field which are already good approximations (Davies 1953); and it would appear, although it is not possible to state this with precision, that there is probably a primary balance in the dynamical equations between the Coriolis acceleration terms and the pressure gradient (that is a geostrophic balance) and a separate but secondary balance between the viscous and inertia terms as in boundary-layer theory. Accordingly, in this non-viscous formulation of a theory of the experiments, molecular viscosity will be ignored completely.

In the absence of any heating the mean density of the liquid is taken to be ρ_0, and the small departure from this density due to a temperature increase τ above the mean is taken to be $-\alpha\tau$, where $\alpha = 2{\cdot}55 \times 10^{-4}\,\mathrm{g/cm^3}$ degree. Axes will be chosen which rotate steadily at an angular velocity ω about the fixed central z-axis, and the equations governing the motions will then be

$$\frac{du^*}{dt^*} - 2\omega v^* = -\frac{1}{\rho_0}\frac{\partial p^*}{\partial x^*}, \tag{1.1}$$

$$\frac{dv^*}{dt^*} + 2\omega u^* = -\frac{1}{\rho_0}\frac{\partial p^*}{\partial y^*}, \tag{1.2}$$

$$\rho_0\frac{dw^*}{dt^*} = -\frac{\partial p^*}{\partial z^*} + g\alpha\tau^*, \tag{1.3}$$

$$\frac{\partial u^*}{\partial x^*} + \frac{\partial v^*}{\partial y^*} + \frac{\partial w^*}{\partial z^*} = 0, \tag{1.4}$$

$$\frac{d\tau^*}{dt^*} = \kappa\nabla^2\tau^*, \tag{1.5}$$

where κ is the thermometric conductivity. Suppose that the typical temperature difference imposed externally in this problem is $(\Delta T)_H$, the suffix referring to a horizontal temperature contrast; then, if the liquid depth is h, we can introduce the non-dimensional symbols $x, y, \ldots, p$ defined by

$$\left.\begin{aligned} x^* = bx, \quad y^* = by, \quad z^* = hz; \\ u^* = 2\omega bSu, \quad v^* = 2\omega bSv, \quad w^* = 2\omega hSw; \\ t^* = t/2\omega S, \quad \tau^* = (\Delta T)_H \tau, \quad p^* = 4b^2\omega^2\rho_0 Sp; \end{aligned}\right\} \tag{1.6}$$

where the Rossby number S is defined by

$$S = \frac{gh}{4b^2\omega^2}\frac{\alpha(\Delta T)_H}{\rho_0}. \tag{1.7}$$

With these transformations the equations (1.1) to (1.5) become

$$S\frac{du}{dt} - v = -\frac{\partial p}{\partial x}, \tag{1.8}$$

$$S\frac{dv}{dt} + u = -\frac{\partial p}{\partial y}, \tag{1.9}$$

$$\frac{h^2}{b^2}S\frac{dw}{dt} = -\frac{\partial p}{\partial z} + \tau, \tag{1.10}$$

$$\frac{\partial u}{\partial x} + \frac{\partial v}{\partial y} + \frac{\partial w}{\partial z} = 0, \tag{1.11}$$

$$S\frac{d\tau}{dt} = \frac{\kappa}{2\omega}\left\{\frac{1}{b^2}\nabla_H^2\tau + \frac{1}{h^2}\frac{\partial^2\tau}{\partial z^2}\right\}, \tag{1.12}$$

where

$$\nabla_H^2 = \frac{\partial^2}{\partial x^2} + \frac{\partial^2}{\partial y^2}. \tag{1.13}$$

Now the Rossby number in jet flows is a small quantity of the order 0·1 to 0·01, and it is clear that the leading approximations to equations (1.8) to (1.12) will be as follows:

$$u_0 = -\frac{\partial p_0}{\partial y}, \quad v_0 = \frac{\partial p_0}{\partial x}, \quad w_0 = 0, \quad \tau_0 = \frac{\partial p_0}{\partial z}. \tag{1.14}$$

The first two equations represent the well-known geostrophic approximations for the horizontal motion, and combined with the fourth equation they lead to the equally well-known thermal wind equation of meteorology. The zero vertical velocity is a consequence of the vanishing of the horizontal divergence for the flow (u_0, v_0) coupled with (1.11). The heat transfer equation we treat in a more exact way, since if the conductivity is ignored it then follows that the isotherms and isobars everywhere coincide and there can be no heat transfer across the flow. We therefore retain the conductivity terms in (1.12) in order to ensure that there is a transfer of heat across the flow. On the left-hand side of (1.12), d/dt is an operator following the motion; but if we choose the angular velocity ω to be the angular velocity with which the wave system rotates relative to fixed axes in space, then the $\partial/\partial t$ term in d/dt can be omitted and the first approximation to (1.12) is

$$S\left\{u_0\frac{\partial\tau_0}{\partial x} + v_0\frac{\partial\tau_0}{\partial y}\right\} = \frac{\kappa}{2\omega}\left\{\frac{1}{b^2}\nabla_H^2\tau_0 + \frac{1}{h^2}\frac{\partial^2\tau_0}{\partial z^2}\right\}. \tag{1.15}$$

Equations (1.14) and (1.15) represent the equations of the first approximation, and the equations governing higher approximations will be developed later in this paper. When we substitute for u_0, v_0, τ_0 from (1.14) in (1.15), the resulting equation is a non-linear partial differential equation for p_0, namely

$$S\left(\frac{\partial p_0}{\partial x}\frac{\partial \tau_0}{\partial y}-\frac{\partial \rho_0}{\partial y}\frac{\partial \tau_0}{\partial x}\right)=\frac{\kappa}{2\omega}\left(\frac{1}{b^2}\nabla_H^2\tau_0+\frac{1}{h_2}\frac{\partial^2\tau_0}{\partial z^2}\right)\quad\left(\tau_0=\frac{\partial p_0}{\partial z}\right). \tag{1.16}$$

This is the equation derived originally by Miss Ruth Rogers (1959) in the investigation of the rectilinear jet.

One of the first points of interest concerning (1.16) is that to any solution found for τ_0 may be added an arbitrary linear function of z. Detailed measurements of the three-dimensional temperature field in the annulus experiment have been given by Fultz & Riehl (1957), and it is clear from these results that the mean vertical temperature field is approximately a linear function of z (except for an evaporation layer near the free surface). When this linear variation of temperature is subtracted from τ_0, the resulting temperature variation in the vertical is slow; hence if we introduce a new temperature function T_0 defined by

$$\tau_0=cz+d+T_0, \tag{1.17}$$

and a corresponding new pressure function P_0 which differs from p_0 by a quadratic function of z, then T_0 and P_0 will have a slow variation in the vertical, and it will be sufficiently accurate, in the case of a liquid whose depth is large compared with the horizontal dimension, to simplify (1.16) to the form

$$\frac{\partial P_0}{\partial x}\frac{\partial T_0}{\partial y}-\frac{\partial P_0}{\partial y}\frac{\partial T_0}{\partial x}=\epsilon\left(\frac{\partial^2 T_0}{\partial x^2}+\frac{\partial^2 T_0}{\partial y^2}\right)\quad\left(T_0=\frac{\partial P_0}{\partial z}\right), \tag{1.18}$$

where

$$\epsilon=\kappa/2\omega b^2 S. \tag{1.19}$$

The non-dimensional constant ϵ is nothing more than a scaling constant, for if we write $P_0=\epsilon P_0'$, $T_0=\epsilon T_0'$, this constant cancels out in (1.17). It is a little more convenient, however, to write $P_0=\epsilon P_0'/m$, $T_0=\epsilon T_0'/m$, where m is the wave number (see (1.22)), and we shall consider (1.18) in the form

$$\frac{\partial P_0}{\partial x}\frac{\partial T_0}{\partial y}-\frac{\partial P_0}{\partial y}\frac{\partial T_0}{\partial x}=m\left(\frac{\partial^2 T_0}{\partial x^2}+\frac{\partial^2 T_0}{\partial y^2}\right)\quad\left(T_0=\frac{\partial P_0}{\partial z}\right). \tag{1.20}$$

(The dashes have not been retained in the dependent variables of this equation.) It may be noted that, using typical experimental values for all the constants, the value of the constant ϵ is about 10^{-3}.

We shall consider equation (1.20) in terms of polar co-ordinates (r,θ), where $x=r\cos\theta$, $y=r\sin\theta$. In this case (1.20) becomes

$$\frac{\partial P_0}{\partial r}\frac{\partial T_0}{\partial \theta}-\frac{\partial P_0}{\partial \theta}\frac{\partial T_0}{\partial r}=m\left(r\frac{\partial^2 T_0}{\partial r^2}+\frac{\partial T_0}{\partial r}+\frac{1}{r}\frac{\partial^2 T_0}{\partial \theta^2}\right). \tag{1.21}$$

It may be observed that equation (1.20) is invariant with respect to a complex transformation

$$a+ib=f(x+iy),$$

since

$$\frac{\partial P_0}{\partial x}\frac{\partial T_0}{\partial y}-\frac{\partial P_0}{\partial y}\frac{\partial T_0}{\partial x}=\left|\frac{d(a+ib)}{d(x+iy)}\right|^2\left(\frac{\partial P_0}{\partial a}\frac{\partial T_0}{\partial b}-\frac{\partial P_0}{\partial b}\frac{\partial T_0}{\partial a}\right)$$

and

$$\frac{\partial^2 T_0}{\partial x^2}+\frac{\partial^2 T_0}{\partial y^2}=\left|\frac{d(a+ib)}{d(x+iy)}\right|^2\left(\frac{\partial^2 T_0}{\partial a^2}+\frac{\partial^2 T_0}{\partial b^2}\right).$$

However, no use has been made of this interesting feature in this paper, although it can be used in extending the solutions obtained by Miss Rogers.

One of the most striking features of the experimental jet flows is the existence of a periodic structure in the θ-direction in which there is one regular well-marked stable wave pattern with a particular wave number m. This suggests that we investigate a solution of (1.21) of the form

$$P_0 = f + g\sin m\theta + h\cos m\theta, \tag{1.22}$$

$$T_0 = F + G\sin m\theta + H\cos m\theta, \tag{1.23}$$

where m is an integer and where $f, g, \ldots, H$ are functions of r, z only, although the z-variation of each of these functions is slow. When we substitute (1.22) and (1.23) in the left-hand side of (1.21), this side of the equation becomes

$$\begin{aligned} m\Big\{&\frac{1}{2}\Big(G\frac{\partial h}{\partial r} - g\frac{\partial H}{\partial r} - H\frac{\partial g}{\partial r} + h\frac{\partial G}{\partial r}\Big) + \cos m\theta\Big(G\frac{\partial f}{\partial r} - g\frac{\partial F}{\partial r}\Big) \\ &+ \sin m\theta\Big(h\frac{\partial F}{\partial r} - H\frac{\partial f}{\partial r}\Big) + \tfrac{1}{2}\cos 2m\theta\Big(G\frac{\partial h}{\partial r} - h\frac{\partial G}{\partial r} - g\frac{\partial H}{\partial r} + H\frac{\partial g}{\partial r}\Big) \\ &+ \tfrac{1}{2}\sin 2m\theta\Big(G\frac{\partial g}{\partial r} - g\frac{\partial G}{\partial r} + h\frac{\partial H}{\partial r} - H\frac{\partial h}{\partial r}\Big)\Big\}. \end{aligned} \tag{1.24}$$

When we substitute (1.23) in the right-hand side of (1.21), there will be no terms in $\cos 2m\theta$ or $\sin 2m\theta$; hence we must have

$$G\frac{\partial h}{\partial r} - h\frac{\partial G}{\partial r} - g\frac{\partial H}{\partial r} + H\frac{\partial g}{\partial r} = 0, \tag{1.25}$$

$$G\frac{\partial g}{\partial r} - g\frac{\partial G}{\partial r} + h\frac{\partial H}{\partial r} - H\frac{\partial h}{\partial r} = 0. \tag{1.26}$$

Comparing the remaining terms on the right-hand side with the corresponding ones in (1.24), we obtain the following three equations:

$$\frac{1}{2}\Big(G\frac{\partial h}{\partial r} - g\frac{\partial H}{\partial r} - H\frac{\partial g}{\partial r} + h\frac{\partial G}{\partial r}\Big) = r\frac{\partial^2 F}{\partial r^2} + \frac{\partial F}{\partial r}, \tag{1.27}$$

$$G\frac{\partial f}{\partial r} - g\frac{\partial F}{\partial r} = r\frac{\partial^2 H}{\partial r^2} + \frac{\partial H}{\partial r} - \frac{m^2}{r^2}H. \tag{1.28}$$

$$h\frac{\partial F}{\partial r} - H\frac{\partial f}{\partial r} = r\frac{\partial^2 G}{\partial r^2} + \frac{\partial G}{\partial r} - \frac{m^2}{r^2}G. \tag{1.29}$$

In addition to the five equations (1.25) to (1.29), it follows also from $T_0 = \partial P_0/\partial z$ that

$$F = \frac{\partial f}{\partial z}, \tag{1.30}$$

$$G = \frac{\partial g}{\partial z}, \tag{1.31}$$

$$H = \frac{\partial h}{\partial z}. \tag{1.32}$$

If we had retained the term $\partial^2 \tau_0/\partial z^2$, the only difference to the above equations would be the addition of terms $\partial^2 F/\partial z^2$, $\partial^2 H/\partial z^2$ and $\partial^2 G/\partial z^2$ on the right-hand sides of (1.27), (1.28) and (1.29) respectively. The equations (1.25) to (1.32) are still a non-linear set, and the principal aim now will be to obtain solutions which satisfy prescribed boundary conditions at the cylindrical boundaries.

Consider first of all equations (1.25) and (1.26). These are linear equations in h and g, and if, for example, g is eliminated between these two equations a second-order equation in r will be obtained for h. Hence, the general solution for h will contain two arbitrary functions of z. It is not necessary to perform this elimination, for it may be seen that the solutions for g and h will be

$$g = A(z)H + B(z)G, \tag{1.33}$$

$$h = -A(z)G + B(z)H, \tag{1.34}$$

where A and B are arbitrary functions of z. Using (1.31) and (1.32) it now follows that G and H must satisfy the equations

$$G = \frac{\partial}{\partial z}\{A(z)H + B(z)G\}, \tag{1.35}$$

$$H = \frac{\partial}{\partial z}\{-A(z)G + B(z)H\}, \tag{1.36}$$

and it is clear that the ultimate solutions for G and H will depend upon the nature of the variation of the functions $A(z)$ and $B(z)$.

Consider now equation (1.27) which we can write in the form

$$r\frac{\partial^2 F}{\partial r^2} + \frac{\partial F}{\partial r} = \frac{1}{2}\frac{\partial}{\partial r}\{Gh - gH\};$$

using (1.33) and (1.34) this becomes

$$r\frac{\partial^2 F}{\partial r^2} + \frac{\partial F}{\partial r} = -\tfrac{1}{2}A(z)\frac{\partial}{\partial r}(G^2 + H^2),$$

which has the first integral

$$r\frac{\partial F}{\partial r} = -\tfrac{1}{2}A(z)(G^2 + H^2) + \chi(z), \tag{1.37}$$

where χ is a function of z only. It is convenient at this stage to introduce local amplitude and local phase functions Φ and Ψ respectively, in place of H and G, and we shall define these functions as follows:

$$G = \Phi \sin \Psi, \quad H = \Phi \cos \Psi. \tag{1.38}$$

In terms of these new functions, (1.37) becomes

$$r\frac{\partial F}{\partial r} = -\tfrac{1}{2}A(z)\Phi^2 + \chi(z); \tag{1.39}$$

and if for convenience we use R in place of r as independent variable, where

$$R = \log_e r, \quad r = e^R, \quad r\frac{\partial}{\partial r} = \frac{\partial}{\partial R}, \tag{1.40}$$

then (1.39) may be written in the form

$$\frac{\partial F}{\partial R} = -\tfrac{1}{2}A(z)\,\Phi^2 + \chi(z). \tag{1.41}$$

In terms of R, equations (1.28) and (1.29) may be written as follows:

$$G\frac{\partial f}{\partial R} - g\frac{\partial F}{\partial R} = \frac{\partial^2 H}{\partial R^2} - m^2 H, \tag{1.42}$$

$$h\frac{\partial F}{\partial F} - H\frac{\partial f}{\partial R} = \frac{\partial^2 G}{\partial R^2} - m^2 G. \tag{1.43}$$

If we multiply (1.42) by H, (1.43) by G and add, we obtain

$$(hG - gH)\frac{\partial F}{\partial R} = H\left(\frac{\partial^2 H}{\partial R^2} - m^2 H\right) + G\left(\frac{\partial^2 G}{\partial R^2} - m^2 G\right).$$

It is easily shown from (1.38) that

$$H\frac{\partial^2 H}{\partial R^2} + G\frac{\partial^2 G}{\partial R^2} = \Phi\frac{\partial^2 \Phi}{\partial R^2} - \Phi^2\left(\frac{\partial \Psi}{\partial R}\right)^2,$$

and thus when we make use of (1.33) and (1.34) we obtain

$$-A\Phi^2\frac{\partial F}{\partial R} = \Phi\frac{\partial^2 \Phi}{\partial R^2} - \Phi^2\left(\frac{\partial \Psi}{\partial R}\right)^2 - m^2\Phi^2. \tag{1.44}$$

Comparing (1.41) and (1.44), it now follows that Φ and Ψ are related by the equation

$$\Phi\frac{\partial^2 \Phi}{\partial R^2} - \Phi^2\left(\frac{\partial \Psi}{\partial R}\right)^2 - m^2\Phi^2 = -A\Phi^2\{-\tfrac{1}{2}A\Phi^2 + \chi\}. \tag{1.45}$$

Using (1.42) and (1.43) once more, multiplying the former by h, the latter by g and adding, we obtain

$$(hG - gH)\frac{\partial f}{\partial R} = h\left(\frac{\partial^2 H}{\partial R^2} - m^2 H\right) + g\left(\frac{\partial^2 G}{\partial R^2} - m^2 G\right).$$

Substituting in this equation for h and g from (1.33) and (1.34), we obtain

$$\begin{aligned} -A\Phi^2\frac{\partial f}{\partial R} &= (BH - AG)\left(\frac{\partial^2 H}{\partial R^2} - m^2 H\right) + (AH + BG)\left(\frac{\partial^2 G}{\partial R^2} - m^2 G\right) \\ &= B\left\{H\frac{\partial^2 H}{\partial R^2} + G\frac{\partial^2 G}{\partial R^2} - m^2(H^2 + G^2)\right\} - A\left\{G\frac{\partial^2 H}{\partial R^2} - H\frac{\partial^2 G}{\partial R^2}\right\}; \end{aligned}$$

and from (1.38) it is easily shown that

$$H\frac{\partial^2 G}{\partial R^2} - G\frac{\partial^2 H}{\partial R^2} = \Phi^2\frac{\partial^2 \Psi}{\partial R^2} + 2\Phi\frac{\partial \Phi}{\partial R}\frac{\partial \Psi}{\partial R}.$$

Hence the equation for $\partial f/\partial R$ becomes

$$-A\Phi^2\frac{\partial f}{\partial R} = B\left\{\Phi\frac{\partial^2 \Phi}{\partial R^2} - \Phi^2\left(\frac{\partial \Psi}{\partial R}\right)^2 - m^2\Phi^2\right\} + A\left\{\Phi^2\frac{\partial^2 \Psi}{\partial R^2} + 2\Phi\frac{\partial \Phi}{\partial R}\frac{\partial \Psi}{\partial R}\right\}. \tag{1.46}$$

We may note at this stage that (1.41) or (1.44) is an equation which defines $\partial F/\partial R$ in terms of Φ and Ψ, and that (1.46) defines $\partial f/\partial R$ in terms of Φ and Ψ. Bearing in mind equation (1.30), which we can write alternatively in the form

$$\frac{\partial F}{\partial R} = \frac{\partial}{\partial z}\left(\frac{\partial f}{\partial R}\right), \tag{1.47}$$

it follows that when we substitute for $\partial F/\partial R$ and $\partial f/\partial R$ we obtain a second-order partial differential relation between Φ and Ψ which, coupled with (1.45), gives a complete solution of the problem. This second relation which follows from (1.47) is

$$-\tfrac{1}{2}A\Phi^2+\chi = \frac{\partial}{\partial z}\left\{B(-\tfrac{1}{2}A\Phi^2+\chi)-\left(\frac{\partial^2\Psi}{\partial R^2}+\frac{2}{\Phi}\frac{\partial\Phi}{\partial R}\frac{\partial\Psi}{\partial R}\right)\right\}. \tag{1.48}$$

In order to exploit equations (1.45) and (1.48) it is necessary to be able to separate the variables R and z. Without going into detail, it is sufficient to state that this is possible if, and only if,

$$\Phi = \frac{1}{A(z)}\phi(R), \tag{1.49}$$

$$\chi(z) = \frac{j}{A(z)}, \tag{1.50}$$

and $\partial\Psi/\partial R$ is independent of z, where $\phi(R)$ is a function of R only and j is a constant. If one uses the above formulae, it follows that $\partial F/\partial R$ is then given by

$$\frac{\partial F}{\partial R} = \frac{1}{A(z)}\{-\tfrac{1}{2}\phi^2(R)+j\}; \tag{1.51}$$

$\phi(R)$ satisfies the equation

$$\frac{d^2\phi}{dR^2}-\phi\left(\frac{d\Psi}{dR}\right)^2-m^2\phi = -\phi(-\tfrac{1}{2}\phi^2+j); \tag{1.52}$$

$\partial f/\partial R$ is given by

$$\begin{aligned}-\phi^2\frac{\partial f}{\partial R} &= \frac{B}{A}\phi\left\{\frac{d^2\phi}{dR^2}-\phi\left(\frac{d\Psi}{dR}\right)^2-m^2\phi\right\}+\frac{d}{dR}\left\{\phi^2\frac{d\Psi}{dR}\right\}\\ &= -\frac{B}{A}\phi^2(j-\tfrac{1}{2}\phi^2)+\frac{d}{dR}\left\{\phi^2\frac{d\Psi}{dR}\right\};\end{aligned} \tag{1.53}$$

and finally, in order to satisfy (1.48) or (1.47), we must have

$$\frac{d}{dz}\left(\frac{B}{A}\right) = \frac{1}{A}. \tag{1.54}$$

Although the method of separating the variables is not along the lines of the well-known method used for linear partial differential equations, it is convenient to regard j as the separation constant.

Before proceeding further it is useful to express the temperature and pressure in terms of the amplitude and phase functions. If we substitute for G and H from (1.38) in (1.23), we obtain

$$T_0 = F+\Phi\cos(m\theta-\Psi), \tag{1.55}$$

hence

$$T_0 = F+\frac{1}{A}\phi(R)\cos(m\theta-\Psi). \tag{1.56}$$

Similarly, if we substitute for g and h from (1.33), (1.34) in (1.22), we obtain

$$P_0 = f + A(H\sin m\theta - G\cos m\theta) + B(G\sin m\theta + H\cos m\theta).$$

hence, using (1.38),

$$P_0 = f + A\Phi\sin(m\theta - \Psi) + B\Phi\cos(m\theta - \Psi). \tag{1.57}$$

Finally, making use of (1.49), we have

$$P_0 = f + \phi(R)\sin(m\theta - \Psi) + \frac{B}{A}\phi(R)\cos(m\theta - \Psi). \tag{1.58}$$

It is clear that $\phi(R)$ can be determined from (1.52) when $d\Psi/dR$ is known, and that B can be determined from (1.54) when A is known; hence, the knowledge of $d\Psi/dR$ as a function of R and of A as a function of z will be sufficient (together with the boundary conditions) to determine ϕ, B, F and f. The unknown constant j will, we shall find, be determined as an eigen-value similar to linear theory. It is important to point out that $\partial\Psi(R,z)/\partial R$ is a function of R only and the function Ψ is necessarily a function of R only, as may be verified from (1.35) or (1.36). This means that, with the present solution of the problem, that part of the temperature field which depends upon θ does not show variation in the vertical. This feature of the temperature field (not of the pressure field it may be noted) is contrary to the experiment where a phase change in the vertical is present in the temperature structure. This phase change will be discussed in greater detail in a future paper. To conclude this section we may note, from (1.51) and (1.53), that the fields of mean temperature F and mean pressure f satisfy the equation

$$\frac{\partial}{\partial R}\{f - BF\} = -\frac{1}{\phi^2}\frac{d}{dR}\left(\phi^2\frac{d\Psi}{dR}\right), \tag{1.59}$$

and thus they differ in profile as long as $\phi^2 d\Psi/dR$ is not constant. In the next section it will be shown that the horizontal transfer of westerly angular momentum is proportional to $\phi^2 d\Psi/dR$ at any level, and thus the mean temperature and mean pressure profiles will differ only when there is a transfer of westerly angular momentum.

2. The radial transfer of angular momentum and heat and the derivation of the vorticity field

In order to throw some light on the choice of the function $d\Psi/dR$ in (1.52), it is useful to calculate the transfer in the minus r direction of westerly (i.e. in the direction of θ increasing) angular momentum (M_H) across a circle of radius r at a height z. This is clearly the integral from $\theta = 0$ to $\theta = 2\pi$ of the product $-\rho_0 r^* u_0 u_r$; hence

$$M_H = 4\rho_0 b^4\omega^4 S^2\int_{\theta=0}^{2\pi}\frac{\partial p}{\partial R}\frac{\partial p}{\partial\theta}\,d\theta. \tag{2.1}$$

The leading terms in the angular momentum transfer will arise from the geostrophic flow discussed in the previous section, and, bearing in mind the transformation leading to (1.20), it follows that in terms of P_0 in (1.58) we have

$$M_H = \rho_0\kappa^2 m^{-2}\omega^2\int_0^{2\pi}\frac{\partial P_0}{\partial R}\frac{\partial P_0}{\partial\theta}\,d\theta. \tag{2.2}$$

Using (1.58), we have

$$\frac{\partial P_0}{\partial \theta} = m\phi(R)\cos(m\theta - \Psi) - \frac{mB}{A}\phi(R)\sin(m\theta - \Psi). \tag{2.3}$$

$$\frac{\partial P_0}{\partial R} = \frac{\partial f}{\partial R} + \left(\frac{d\phi}{dR} + \frac{B}{A}\phi\frac{d\Psi}{dR}\right)\sin(m\theta - \Psi) + \left(\frac{B}{A}\frac{d\phi}{dR} - \phi\frac{d\Psi}{dR}\right)\cos(m\theta - \Psi), \tag{2.4}$$

and thus

$$M_H = -\rho_0 \kappa^2 m^{-1}\omega^2 \pi M, \tag{2.5}$$

where

$$M = \left(1 + \frac{B^2}{A^2}\right)\phi^2\frac{d\Psi}{dR}. \tag{2.6}$$

We will now derive a general result concerning angular momentum transfer. The complete equation of motion in the direction of θ increasing relative to axes which are fixed in space is

$$\frac{\partial v}{\partial t} + u\frac{\partial v}{\partial r} + \frac{v}{r}\frac{\partial v}{\partial \theta} + w\frac{\partial v}{\partial z} + \frac{uv}{r} = \frac{1}{\rho}\left\{\frac{1}{r}\frac{\partial p_{\theta\theta}}{\partial \theta} + \frac{\partial p_{\theta z}}{\partial z} + \frac{1}{r^2}\frac{\partial}{\partial r}(r^2 p_{r\theta})\right\}, \tag{2.7}$$

where $p_{\theta\theta}$, $p_{\theta z}$, $p_{r\theta}$ are the viscous stresses. The appropriate continuity equation is

$$\frac{\partial \rho}{\partial t} + \frac{\partial}{\partial r}(\rho r u) + \frac{\partial}{\partial \theta}(\rho v) + \frac{\partial}{\partial z}(\rho r w) = 0, \tag{2.8}$$

and using these two equations we can deduce the Reynolds stress form of (2.7), namely

$$\frac{\partial}{\partial t}(\rho v r^2) + \frac{\partial}{\partial r}(\rho u v r^2) + \frac{\partial}{\partial \theta}(\rho v^2 r) + \frac{\partial}{\partial z}(\rho v w r^2) = r\frac{\partial p_{\theta\theta}}{\partial \theta} + r^2\frac{\partial p_{\theta z}}{\partial z} + \frac{\partial}{\partial r}(r^2 p_{r\theta}). \tag{2.9}$$

We shall write m_H and m_V for the horizontal ($-r$-direction) and vertical ($+z$-direction) transports of westerly angular momentum (about $r = 0$) across a circle of radius r at height z, so that

$$m_H = -\int_0^{2\pi} \rho u v r^2 \, d\theta, \tag{2.10}$$

$$m_V = \int_0^{2\pi} \rho w v r^2 \, d\theta. \tag{2.11}$$

We multiply (2.9) by $dr\,d\theta\,dz$ and integrate over an annular volume τ bounded by z_0, z_1 ($> z_0$), r_0 and r_1 ($> r_0$), and we then obtain after some reduction

$$\frac{\partial}{\partial t}\left\{\int_\tau \rho v r \, d\tau\right\} + \int_{z_0}^{z_1}(m_H|_{r_0} - m_H|_{r_1})\,dz + \int_{r_0}^{r_1}(m_V|_{z_1} - m_V|_{z_0})\,dr$$
$$= \int_{r_0}^{r_1} dr \int_0^{2\pi} r^2(p_{\theta z}|_{z_1} - p_{\theta z}|_{z_0})\,d\theta + \int_{z_0}^{z_1} dz \int_0^{2\pi}(r_1^2 p_{r\theta}|_{r_1} - r_0^2 p_{r\theta}|_{r_0})\,d\theta. \tag{2.12}$$

In the present problem the time average value of the first term is zero and henceforth this term will be ignored. In this case, equation (2.12) states that the total flow of westerly angular momentum outwards across the boundary S of a volume τ is equal to the moment about $r = 0$ of the viscous stresses acting on the complete surface S. Viscosity has been ignored in the formulation of the problem of the first section; but since the influence of viscosity in this angular momentum result is

equivalent to an appropriate supply of angular momentum across S, it is clear that we can simulate the effect of viscosity by an appropriate distribution of sources and sinks of angular momentum over S. I shall assume therefore that there are distributions of sources and sinks: (a) on the surface $z = \delta$ which is the plane upper boundary of the 'boundary layer' in $0 < z \leqslant \delta$, and (b) on the surfaces $r = b-\delta$, $r = a+\delta$ which are the cylindrical boundaries on the inside of the 'boundary layers' in $b-\delta \leqslant r < b$, $a < r \leqslant a+\delta$. The details of this distribution of sources and sinks in any given case can be obtained only by solving the complete Navier-Stokes equations, but here we shall assume that the distribution can be prescribed. Away from the boundary layers it is a good approximation that the total flow of angular momentum across the boundary S is zero, and assuming this to be exactly true we obtain the following result from (2.12):

$$\int_{z_0}^{z_1} (m_H|_{r_0} - m_H|_{r_1})\,dz + \int_{r_0}^{r_1} (m_V|_{z_1} - m_V|_{z_0})\,dr = 0; \tag{2.13}$$

and if we take $z_1 = z_0 + \delta z$, $r_1 = r_0 + \delta r$, we deduce that

$$\frac{\partial m_H}{\partial r} = \frac{\partial m_V}{\partial z}. \tag{2.14}$$

This will be assumed to be valid in the range $\delta < z < h$, $a+\delta < r < b-\delta$. If we introduce now the quantities M_H, M_V to represent the horizontal and vertical transports of westerly angular momentum for the relative flow (i.e. relative to axes which are rotating with angular velocity ω as in § 1), then it easily follows that

$$\frac{\partial M_H}{\partial r} = \frac{\partial M_V}{\partial z}. \tag{2.15}$$

Hence with the M_H defined in (2.5) the corresponding M_V will be given by

$$M_V = \rho_0 \int_0^{2\pi} r^{*2} u_\theta u_z \, d\theta \tag{2.16}$$

$$= -\rho_0 \kappa^2 m^{-1} \omega^2 \pi \frac{d}{dr}\left(\phi^2 \frac{d\Psi}{dR}\right) \int^z \left(1 + \frac{B^2}{A^2}\right) dz. \tag{2.17}$$

It is clear now that if either M_H or M_V is prescribed on a plane $z =$ constant, then this is equivalent to postulating the behaviour of the unknown function Ψ.

If $\phi^2(d\Psi/dR) =$ constant, it follows that $M_V = 0$, and thus the source of angular momentum can be taken at the cylindrical wall $r = b$ with an equal sink at $r = a$. If, on the other hand, there is no source or sink of angular momentum at the side walls, the whole of the angular momentum which emanates from one part of the base must be assumed to return to a sink in the remaining part of the base, so that

$$\int_a^b M_V \, dr = 0. \tag{2.18}$$

This type of angular momentum flow is the one which is similar to that of the atmosphere, and this case can be satisfied here provided

$$\left(\phi^2 \frac{d\Psi}{dR}\right)\Big|_b = \left(\phi^2 \frac{d\Psi}{dR}\right)\Big|_a. \tag{2.19}$$

We shall discuss these results further in § 4, and we now turn our attention to the radially inward transport of heat.

The radially inward transport of heat (H.T.) across a circle of radius r^* at height z^* will be obtained by integrating the product $\kappa u_r(\partial\tau^*/\partial r^*)$, hence

$$\text{H.T.} = -4\kappa\rho_0 b\omega^2 S(\Delta T)_H \int_0^{2\pi} \frac{\partial p}{\partial\theta}\frac{\partial\tau}{\partial r}\,d\theta. \tag{2.20}$$

The leading terms in this heat transfer will be given by

$$\text{H.T.} = -4\kappa\rho_0 b\omega^2 S(\Delta T)_H \epsilon^2 m^{-2} \int_0^{2\pi} \frac{\partial P_0}{\partial\theta}\frac{\partial T_0}{\partial r}\,d\theta,$$

and since, from (1.56),

$$\frac{\partial T_0}{\partial r} = \frac{\partial F}{\partial r} + \frac{1}{A}\frac{d\phi}{\partial r}\cos(m\theta - \Psi) + \frac{1}{A}\phi\frac{d\Psi}{dR}\sin(m\theta - \Psi), \tag{2.21}$$

it follows that

$$\text{H.T.} = -4\kappa\rho_0 b\omega^2 S\epsilon^2 m^{-1}(\Delta T)_H \pi H, \tag{2.22}$$

where

$$H = \frac{1}{A}\left(\phi\frac{d\phi}{d\tau} - \frac{B}{A}\phi^2\frac{d\Psi}{dr}\right). \tag{2.23}$$

It will be seen that there is an essential difference between the angular momentum and heat transport expressions, both in their z and r variations, in particular the heat transport can exist even when the momentum transport is zero.

A third quantity which will be required later in the paper is the vorticity of the two-dimensional flow of the previous section; if this is denoted by ζ_0 then we have, working with the non-dimensional symbols,

$$\zeta_0 = \frac{\partial v_0}{\partial x} - \frac{\partial u_0}{\partial y} = \frac{\partial^2 p_0}{\partial x^2} + \frac{\partial^2 p_0}{\partial y^2}, \tag{2.24}$$

hence

$$r^2\zeta_0 = r^2\frac{\partial^2 p_0}{\partial r^2} + r\frac{\partial p_0}{\partial r} + \frac{\partial^2 p_0}{\partial\theta^2}$$

$$= \epsilon^2 m^{-2}\left(\frac{\partial^2 P_0}{\partial R^2} + \frac{\partial^2 P_0}{\partial\theta^2}\right). \tag{2.25}$$

Using the expression (1.58) for P_0, we obtain after some reduction

$$r^2\zeta_0 = \epsilon^2 m^{-2}\left\{\frac{\partial^2 f}{\partial R^2} + X\sin(m\theta - \Psi) + Y\cos(m\theta - \Psi)\right\}, \tag{2.26}$$

where

$$X = \frac{d^2\phi}{dR^2} - \phi\left(\frac{d\Psi}{dR}\right)^2 - m^2\phi + \frac{B}{A}\left(\phi\frac{d^2\Psi}{dR^2} + 2\frac{d\phi}{dR}\frac{d\Psi}{dR}\right), \tag{2.27}$$

$$Y = \frac{B}{A}\left\{\frac{d^2\phi}{dR^2} - \phi\left(\frac{d\Psi}{dR}\right)^2 - m^2\phi\right\} - \left(\phi\frac{d^2\Psi}{dR^2} + 2\frac{d\phi}{dR}\frac{d\Psi}{dR}\right). \tag{2.28}$$

We shall satisfy the Helmholtz vorticity equation with the vorticity function (2.24) when we proceed to the higher approximations in the next section (see (3.13)).

3. Higher order approximations and the determination of the vertical velocity

It is possible to determine the higher order approximations in this problem by taking power series in S for the various dependent variables taking as the first approximation the equations (1.14). Thus we shall take

$$u = u_0 + Su_1 + S^2u_2 + \ldots, \tag{3.1}$$

$$v = v_0 + Sv_1 + S^2v_2 + \ldots. \tag{3.2}$$

$$w = Sw_1 + S^2w_2 + \ldots, \tag{3.3}$$

$$p = p_0 + Sp_1 + S^2p_2 + \ldots, \tag{3.4}$$

$$\tau = \tau_0 + S\tau_1 + S^2\tau_2 + \ldots, \tag{3.5}$$

where u_0, v_0, p_0, τ_0 are given by (1.14). If we substitute the above expressions in (1.8), (1.9), (1.10), (1.11) and (1.12) and equate the leading terms, (1.14) and (1.15) are obtained. Equating to zero the coefficients of the next power in S, we obtain the following equations:

$$\frac{du_0}{dt} - v_1 = -\frac{\partial p_1}{\partial x}, \tag{3.6}$$

$$\frac{dv_0}{dt} + u_1 = -\frac{\partial p_1}{\partial y}, \tag{3.7}$$

$$0 = -\frac{\partial p_1}{\partial z} + \tau_1, \tag{3.8}$$

$$\frac{\partial u_1}{\partial x} + \frac{\partial v_1}{\partial y} + \frac{\partial w_1}{\partial z} = 0, \tag{3.9}$$

$$u_0\frac{\partial \tau_1}{\partial x} + u_1\frac{\partial \tau_0}{\partial x} + v_0\frac{\partial \tau_1}{\partial y} + v_1\frac{\partial \tau_0}{\partial y} + w_1\frac{\partial \tau_0}{\partial z} = \epsilon\left(\frac{\partial^2\tau_1}{\partial x^2} + \frac{\partial^2\tau_1}{\partial y^2}\right), \tag{3.10}$$

where the term $\partial^2\tau_1/\partial z^2$ has been omitted in (3.10). From this set of five equations there are sufficient equations to solve for u_1, v_1, w_1, p_1 and τ_1. In order to determine w_1 however, it is necessary to use the three equations (3.6), (3.7) and (3.9).

The first equation (3.6) gives

$$\begin{aligned} v_1 &= \frac{\partial p_1}{\partial x} + u_0\frac{\partial u_0}{\partial x} + v_0\frac{\partial u_0}{\partial y} \\ &= \frac{\partial}{\partial x}\{p_1 + \tfrac{1}{2}u_0^2 + \tfrac{1}{2}v_0^2\} - v_0\zeta_0, \end{aligned} \tag{3.11}$$

where ζ_0 is defined in (2.24). Similarly (3.7) gives

$$\begin{aligned} u_1 &= -\frac{\partial p_1}{\partial y} - u_0\frac{\partial v_0}{\partial x} - v_0\frac{\partial v_0}{\partial y} \\ &= -\frac{\partial}{\partial y}(p_1 + \tfrac{1}{2}u_0^2 + \tfrac{1}{2}v_0^2) - u_0\zeta_0, \end{aligned} \tag{3.12}$$

and thus by substituting for u_1 and v_1 in (3.9) we obtain

$$\frac{\partial w_1}{\partial z} = \frac{\partial}{\partial x}(u_0\zeta_0) + \frac{\partial}{\partial y}(v_0\zeta_0),$$

so that, using (1.14), we have

$$\frac{\partial w_1}{\partial z} = u_0 \frac{\partial \zeta_0}{\partial x} + v_0 \frac{\partial \zeta_0}{\partial y};$$

hence the form of the Helmholtz vorticity equation is

$$\frac{\partial w_1}{\partial z} = \frac{\partial p_0}{\partial x}\frac{\partial \zeta_0}{\partial y} - \frac{\partial p_0}{\partial y}\frac{\partial \zeta_0}{\partial x}. \tag{3.13}$$

In polar co-ordinates this becomes

$$\frac{\partial w_1}{\partial z} = \frac{1}{r}\left\{\frac{\partial p_0}{\partial r}\frac{\partial \zeta_0}{\partial \theta} - \frac{\partial p_0}{\partial \theta}\frac{\partial \zeta_0}{\partial r}\right\},$$

and it may be verified that this equation can be written in the form

$$r^4 \frac{\partial w_1}{\partial z} = \epsilon m^{-1}\left\{\frac{\partial P_0}{\partial R}\frac{\partial}{\partial \theta}(r^2\zeta_0) - \frac{\partial P_0}{\partial \theta}\frac{\partial}{\partial R}(r^2\zeta_0) + 2\frac{\partial P_0}{\partial \theta}(r^2\zeta_0)\right\},$$

so that by using (2.13) we have

$$\begin{aligned}\frac{r^4(\partial w_1/\partial z)}{\epsilon^3 m^{-4}} = {} & \left\{\frac{\partial f}{\partial R} + \left(\frac{d\phi}{dR} + \frac{B}{A}\phi\frac{d\Psi}{dR}\right)s_1 + \left(-\phi\frac{d\Psi}{dR} + \frac{B}{A}\frac{d\phi}{dR}\right)c_1\right\}\{Xc_1 - Ys_1\} \\ & - \left\{\frac{\partial^3 f}{\partial R^3} + \left(\frac{\partial X}{\partial R} + Y\frac{d\Psi}{dR}\right)s_1 + \left(\frac{\partial Y}{\partial R} - X\frac{d\Psi}{dR}\right)c_1\right\}\left\{\phi c_1 - \frac{B}{A}\phi s_1\right\} \\ & + 2\left\{\frac{\partial^2 f}{\partial R^2} + Xs_1 + Yc_1\right\}\left\{\phi c_1 - \frac{B}{A}\phi s_1\right\},\end{aligned} \tag{3.14}$$

where we have written

$$s_r = \sin r(m\theta - \Psi), \quad c_r = \cos r(m\theta - \Psi). \tag{3.15}$$

In this expression for $\partial w_1/\partial z$ there will be terms independent of θ and it is clear that such terms will supply the first information concerning meridional cells in the general circulation pattern. These terms will arise from the c_1^2 and s_1^2 products and are as follows:

$$\begin{aligned}& -\tfrac{1}{2}Y\left(\frac{d\phi}{dR} + \frac{B}{A}\phi\frac{d\Psi}{dR}\right) + \tfrac{1}{2}X\left(-\phi\frac{d\Psi}{dR} + \frac{B}{A}\frac{d\phi}{dR}\right) - \tfrac{1}{2}\phi\left(\frac{\partial Y}{\partial R} - X\frac{d\Psi}{dR}\right) \\ & + \frac{1}{2}\frac{B}{A}\phi\left(\frac{\partial X}{\partial R} + Y\frac{d\Psi}{dR}\right) - \frac{B}{A}\phi X + \phi Y \\ \equiv {} & \frac{1}{2}\frac{\partial}{\partial R}\left\{\phi\left(-Y + \frac{B}{A}X\right)\right\} - \phi\left(-Y + \frac{B}{A}X\right).\end{aligned}$$

Using (2.14) and (2.15) we have

$$\frac{B}{A}X - Y = \left(1 + \frac{B^2}{A^2}\right)\left(\phi\frac{d^2\Psi}{dR^2} + 2\frac{d\phi}{dR}\frac{d\Psi}{dR}\right), \tag{3.16}$$

and thus if we denote by $\overline{w}_1$ that part of w_1 which is independent of θ when we have

$$\frac{r^4(\partial \overline{w}_1/\partial z)}{\epsilon^3 m^{-4}} = \frac{1}{2}\frac{\partial}{\partial R}\left\{\left(1 + \frac{B^2}{A^2}\right)\frac{d}{dR}\left(\phi^2\frac{d\Psi}{dR}\right)\right\} - \left(1 + \frac{B^2}{A^2}\right)\frac{d}{dR}\left(\phi^2\frac{d\Psi}{dR}\right). \tag{3.17}$$

It may be noted that the right-hand side of this expression can be written entirely in terms of M which is defined in (2.6), and in this case we have the interesting result

$$\frac{r^4(\partial\overline{w}_1/\partial z)}{\epsilon^2 m^{-4}} = \frac{1}{2}\frac{\partial^2 M}{\partial R^2} - \frac{\partial M}{\partial R}, \tag{3.18}$$

which relates the meridional part of the vertical velocity with the horizontal angular momentum transfer. Using (1.40), an alternative form of (3.18) is

$$\frac{2r^4(\partial\overline{w}_1/\partial z)}{\epsilon^3 m^{-4}} = r^2\frac{\partial^2 M}{\partial r^2} - r\frac{\partial M}{\partial r}. \tag{3.19}$$

We may note that the meridional part of the vertical velocity will be identically zero if M shows no variation with r or if M is proportional to r^2. The remaining terms in the expression for $\partial w_1/\partial z$ do not simplify in the same way as the above meridional part and in general we have from (3.14)

$$\begin{aligned}\frac{r^4(\partial w_1/\partial z)}{\epsilon^3 m^{-4}} = {} & \frac{1}{2}\frac{\partial^2 M}{\partial R^2} - \frac{\partial M}{\partial R} + \left\{X\frac{\partial f}{\partial R} - \phi\frac{\partial^3 f}{\partial R^3} + 2\phi\frac{\partial^2 f}{\partial R^2}\right\}\cos(m\theta - \Psi) \\ & - \left\{Y\frac{\partial f}{\partial R} - \frac{B}{A}\phi\frac{\partial^3 f}{\partial R^3} + \frac{2B}{A}\phi\frac{\partial^2 f}{\partial R^2}\right\}\sin(m\theta - \Psi) \\ & + \frac{1}{2}\left\{\left(Y + \frac{B}{A}X\right)\frac{d\phi}{dR} - \phi\frac{\partial}{\partial R}\left(Y + \frac{B}{A}X\right) + 2\phi\left(Y + \frac{B}{A}X\right)\right\}\cos 2(m\theta - \Psi) \\ & + \frac{1}{2}\left\{\left(X - \frac{B}{A}Y\right)\frac{d\phi}{dR} - \phi\frac{\partial}{\partial R}\left(X - \frac{B}{A}Y\right) + 2\phi\left(X - \frac{B}{A}Y\right)\right\}\sin 2(m\theta - \Psi).\end{aligned} \tag{3.20}$$

The terms which involve $\cos 2(m\theta - \Psi)$ and $\sin 2(m\theta - \Psi)$ are in general non-vanishing, thus w_1 will consist of a meridional part, a part which varies periodically with the wave and a part which varies periodically with half the fundamental wave length. To derive w_1 we can assume that $w_1 = 0$ at $z = 0$ then w_1 is the integral from 0 to z of the right-hand side of (3.20).

4. Particular examples of the foregoing theory

We consider first the boundary conditions. Since molecular viscosity is ignored, the condition of zero normal velocity has to be satisfied at each of the bounding solid surfaces. Therefore $\partial p/\partial\theta$ must vanish at the cylindrical walls, in other words the function ϕ in (1.58) must be zero at these boundaries. In the non-dimensional scheme in (1.6), the quantity b can be treated as the radius of the outer cylinder, and thus $r^* = b$ of $r = 1$ will represent the outer cylinder. If a is the radius of the inner cylinder, then $r = a/b$ will represent the inner cylinder. In terms of R introduced in (1.40) the outer and inner boundaries will be $R = 0$ and $R = -R_0$ respectively, where $R_0 = \log_e(b/a)$. Thus, the velocity conditions upon $\phi(R)$ reduce to the following:

$$\phi(0) = \phi(-R_0) = 0. \tag{4.1}$$

It is clear from (1.56) that the conditions of constancy of temperature will be satisfied on the two cylindrical boundaries due to (4.1). The only remaining

condition upon the temperature field is that the difference in temperature from one cylinder to the other must be $(\Delta T)_H$ at some level. It follows therefore that

$$\tau|_{R=0} - \tau|_{R=-R_0} = 1. \tag{4.2}$$

In terms of F in (1.56) we must therefore have, at a particular z value,

$$F|_{R=0} - F|_{R=-R_0} = \frac{m}{\epsilon}. \tag{4.3}$$

Up to the present the function $A(z)$, introduced originally in (1.33), has been left arbitrary. It will be seen from (1.51) that $\partial F/\partial R$ is proportional to $1/A$ and that the heat flow at the cylindrical boundaries, namely $\partial F/\partial r$ is also proportional to $1/A$. In order to make the problem as simple as possible, it is proposed to take uniform heat flow over the cylindrical boundaries since there is no guidance from the experiment in this matter, thus with no loss of generality we shall take

$$A = 1, \tag{4.4}$$

in which case the constant j in (1.51) is a measure of the heat flow across a section of unit length of either cylinder. Accordingly, from (1.54), we have

$$B = z + \beta, \tag{4.5}$$

where β is an arbitrary constant. With this choice of A, the solutions (1.56) and (1.58) for T_0 and P_0 become

$$T_0 = F + \phi(R)\cos(m\theta - \Psi), \tag{4.6}$$

$$P_0 = f + \phi(R)\sin(m\theta - \Psi) + (\beta + z)\,\phi(R)\cos(m\theta - \Psi). \tag{4.7}$$

The third term of P_0 evidently becomes increasingly important as z increases, hence the phase difference of the temperature and pressure fields diminishes with increasing height. The constant β is a measure of the difference in phase of the temperature and pressure waves, and the value of β, here arbitrary, can be derived from the experiment; but whether β be positive or negative, the pressure wave will be ahead of the temperature wave at all levels, the departure of the two waves diminishing with increasing height. Thus, the pressure wave has a 'backward tilt', i.e. to the west as in the case of atmospheric troughs. We may also observe that the angular momentum transfer (2.6) will have a parabolic distribution in the vertical when (4.4) and (4.5) are true, and the maximum transfer will take place at the free surface.

It is worth while noting also that we may draw a parallel with the atmosphere where the heat source in the lowest layers (troposphere) is at the equator and in the upper layers (stratosphere) at high latitudes by taking

$$\frac{1}{A} = (z_0 - z)\,e^{-\lambda z}.$$

With this choice of A, equation (1.54) gives for B the value

$$B = -\frac{1}{\lambda} + \left(\beta e^{\lambda z} + \frac{1}{\lambda^2}\right) \Big/ (z_0 - z).$$

We note that B has an infinity at the position where $1/A$ changes its sign, that is at the tropopause, and the pressure wave becomes 180° out of phase with the temperature wave in moving through this level. This will be avoided only if β is chosen appropriately.

Returning now to (4.3) and using (4.4), it then follows that the appropriate form of this condition is

$$\int_{R=-R_0}^{R=0} \frac{\partial F}{\partial R} dR = \int_{-R_0}^{0} \{j - \tfrac{1}{2}\phi^2(R)\} dR = \frac{m}{\epsilon}, \tag{4.8}$$

that is

$$jR_0 = \frac{m}{\epsilon} + \frac{1}{2}\int_{-R_0}^{0} \phi^2(R) dR. \tag{4.9}$$

Case I. Zero momentum transport; $d\Psi/dR = 0$.

This case may not have much practical significance, but so many of the technical difficulties encountered in general are also met in this simple case that it is worth while devoting considerable attention to it. The equation (1.52) now becomes

$$\frac{d^2\phi}{dR^2} = (m^2 - j)\,\phi + \tfrac{1}{2}\phi^3. \tag{4.10}$$

The first integral of (4.10) is

$$\left(\frac{d\phi}{dR}\right)^2 = (m^2 - j)\,\phi^2 + \tfrac{1}{4}\phi^4 + C, \tag{4.11}$$

where C is an arbitrary constant of integration. The function ϕ vanishes at the two end-points of the range $-R_0 \leqslant R \leqslant 0$; and, assuming that ϕ is a continuous function, it is necessary that $d\phi/dR$ should vanish within the R range. If we suppose that $d\phi/dR$ vanishes when $\phi = \phi_1$, then

$$0 = (m^2 - j)\,\phi_1^2 + \tfrac{1}{4}\phi_1^4 + C, \tag{4.12}$$

and thus

$$\left(\frac{d\phi}{dR}\right)^2 = \tfrac{1}{4}(\phi_1^2 - \phi^2)\,(4j - 4m^2 - \phi_1^2 - \phi^2). \tag{4.13}$$

Clearly it is necessary that

$$4j - 4m^2 - \phi_1^2 > 0 \tag{4.14}$$

in order for $(d\phi/dR)^2$ to be positive near $\phi = 0$; hence j is positive, or alternatively ϕ_1^2 possesses an upper bound $4(j - m^2)$. If we write

$$\phi_2^2 = 4j - 4m^2 - \phi_1^2, \tag{4.15}$$

then

$$\left(\frac{d\phi}{dR}\right)^2 = \tfrac{1}{4}(\phi_1^2 - \phi^2)\,(\phi_2^2 - \phi^2). \tag{4.16}$$

We shall take

$$\phi_2^2 > \phi_1^2, \quad k^2 = \frac{\phi_1^2}{\phi_2^2}, \tag{4.17}$$

since there is no loss of generality in doing this, and ϕ_1 will be taken to be positive. If we write

$$\phi = \phi_1 y, \quad x = \tfrac{1}{2}R\phi_2, \tag{4.18}$$

then (4.16) becomes

$$\left(\frac{dy}{dx}\right)^2 = (1 - y^2)\,(1 - k^2 y^2). \tag{4.19}$$

where k^2 is defined in (4.17) and $0 < k^2 < 1$. The solution of (4.19) which vanishes when $R = 0$ or $x = 0$ is the Jacobian elliptic function $y = \mathrm{sn}\,(x, k)$, and hence the solution of (4.16) which vanishes at $R = 0$ is

$$\phi = \phi_1 \,\mathrm{sn}\,\{-\tfrac{1}{2}R\phi_2, k\}, \tag{4.20}$$

where a slight adjustment in sign has been made in order to make $\phi > 0$ when $-R_0 < R < 0$. This elliptic function has an infinite number of zeros since we have

$$\mathrm{sn}\,(u+2K, k) = -\mathrm{sn}\,(u, k),$$
$$\mathrm{sn}\,(u+4Kn, k) = \mathrm{sn}\,(u, k) \quad (n = 0, 1, 2\ldots).$$

If that function $\phi(R)$ is chosen which vanishes at the points $R = 0$ and $R = -R_0$ and has one simple maximum in the range $-R_0 \leqslant R \leqslant 0$, then we must have

$$\tfrac{1}{2}R_0\phi_2 = 2K; \tag{4.21}$$

but there are an infinite set of solutions for ϕ, the one which possesses one maximum and one minimum being the case $\frac{1}{2}R_0\phi_2 = 4K$, and the general case is $\frac{1}{2}R_0\phi_2 = 2nK$. These different modes of solution are of course not superposable since the ϕ equation is non-linear and only one of them can exist at any one time. We shall concentrate here on the main mode which is given by (4.21). For this main mode of ϕ with a single maximum $\phi = \phi_1$ at $\frac{1}{2}R_1\phi_2 = K$ where $\mathrm{sn}\,(K, k) = 1$, it follows that the position of the maximum value is such that $R_1 = \frac{1}{2}R_0$; in terms of r, this indicates that the maximum is at r_1, where $r_1 = r_0^{\frac{1}{2}} = (a/b)^{\frac{1}{2}}$, and in terms of the original variables at $r_1^* = (ab)^{\frac{1}{2}}$, the geometric mean of the radii of the two cylinders.

The quantity K which appears in (4.21) is a function of k, and, when k is known, K can be found from tables. Since $k = \phi_1/\phi_2$ and ϕ_2 is a function of j (4.15), it follows that (4.21) is a relation between j and ϕ_1. We may observe that, since $\phi_1 < \phi_2$, then from (4.15) we obtain

$$\phi_1^2 < 2j - 2m^2 < \phi_2^2. \tag{4.22}$$

If we use (4.9), we obtain a second relation between j and ϕ_1, namely

$$jR_0 = \frac{m}{\epsilon} + \tfrac{1}{2}\phi_1^2 \int_{-R_0}^{0} \mathrm{sn}^2\,(-\tfrac{1}{2}R\phi_2, k)\,dR$$
$$= \frac{m}{\epsilon} + \frac{\phi_1^2}{\phi_2} \int_0^{2K} \mathrm{sn}^2\,(x, k)\,dx;$$

hence

$$jR_0 = \frac{m}{\epsilon} + 2k\phi_1 \int_0^{K} \mathrm{sn}^2\,(x, k)\,dx. \tag{4.23}$$

The complete elliptic integral E of the second kind is defined by

$$E = \int_0^K \mathrm{dn}^2\,(x, k)\,dx, \tag{4.24}$$

and since $\mathrm{dn}^2\,(x, k) = 1 - k^2\,\mathrm{sn}^2(x, k)$, it follows

$$\int_0^K \mathrm{sn}^2\,(x, k)\,dx = \frac{K - E}{k^2}; \tag{4.25}$$

hence, from (4.23),

$$jR_0 = \frac{m}{\epsilon} + \frac{2\phi_1}{k}(K - E). \tag{4.26}$$

Equations (4.15), (4.17), (4.21) and (4.26) now represent four independent equations between ϕ_1, ϕ_2, k and j and ϵ. Hence, this can be regarded as a one-parameter problem in the sense that if one of these five quantities is defined then, in theory, the other four can be determined; the quantity ϵ is regarded as a parameter since the quantity ω is the angular velocity of the wave system (not the angular velocity of the apparatus) and is not therefore a prescribed quantity. It is probably most convenient to treat k as the parameter at our disposal in the range $0 < k < 1$. In terms of k we have

$$\phi_2 = \frac{4K}{R_0}, \quad \phi_1 = \frac{4kK}{R_0}, \tag{4.27}$$

$$j = m^2 + \frac{4K^2}{R_0^2}(1 + k^2). \tag{4.28}$$

$$\frac{2\omega S b^2}{K} = \frac{1}{\epsilon} = mR_0 + \frac{4K\{2E - K(1-k^2)\}}{mR_0}. \tag{4.29}$$

Using these relations it is possible to throw some light on the conditions necessary for the existence of a particular wave number; their usefulness, however, is much reduced by the fact that the angular velocity ω in (4.29) is the angular velocity of the wave system with respect to fixed space axes and not the angular velocity ω_s of the apparatus as a whole. The difference between ω and ω_s is small and of the order S.

We consider first equation (4.29) which is of the form

$$\omega S = \frac{K}{2b^2}\left\{mR_0 + \frac{\mu^2}{mR_0}\right\}, \tag{4.30}$$

where $\mu^2 = 4K\{2E - K(1-k^2)\}$. For a given $R_0 (= \log b/a)$, a given m and a given k this relation between ω and S in the (ω, S)-plane is a rectangular hyperbola which we denote by Γ. As k varies from 0 to 1, it is easily shown that μ^2 moves from a minimum value of π^2 when $k = 0$ and increases monotonically to $+\infty$ as k tends to 1. Thus, if we let Γ_m denote the rectangular hyperbola

$$\omega S = \frac{K}{2b^2}\left\{mR_0 + \frac{\pi^2}{mR_0}\right\}, \tag{4.31}$$

it follows that as k moves from 0 to 1 the curve Γ in the (ω, S)-plane sweeps out that infinite area $\Gamma > \Gamma_m$ which lies on the side of the curve Γ_m remote from the origin. Since the minimum value of $mR_0 + (\pi^2/mR_0)$, considered as a function of mR_0, is attained when $mR_0 = \pi$ and its value is then 2π, it follows that the curves $\Gamma_1, \Gamma_2, \Gamma_3, \ldots$, corresponding to $m = 1, 2, 3, \ldots$, will move nearer to the origin until that integral value of $m = m^*$ is attained which makes m^*R_0 nearest π, and for m values greater than m^* the curves Γ_m will recede from the origin. For example, with $b = 2a$ ($R_0 = 0{\cdot}6931$), the successive curves Γ_s ($s = 1, 2, \ldots, 5$), approach the origin successively, but from $m = 6$ onwards the curves recede from the origin.

If we consider one of these curves, say Γ_1, then given a value of $\omega = \omega'$ and of $S = S'$ we can deduce that if the representative point (ω', S') is on the origin side of the curve Γ_1, then this particular wave number cannot exist with such a rotation and such a Rossby number. Alternatively, if the point (ω', S') is on the side of the curve Γ_1 remote from the origin, then there will be a unique k value in the range $0 < k < 1$ which will define the strength of the corresponding wave. A similar argument will apply to every curve $\Gamma_2, \Gamma_3, \ldots$, of the family Γ_m, and we then have the following overall results:

(*a*) wave number $m = 1$ cannot exist if the point (ω, S) lies on the origin side of the curve Γ_1;

(*b*) wave numbers $m = 1$, $m = 2$ cannot exist if the point (ω, S) lies on the origin side of the curve Γ_2;

(*c*) wave numbers $m = 1$, $m = 2$, $m = 3$ cannot exist if the point (ω, S) lies on the origin side of the curve Γ_3;

and so on until that particular value of $m = m^*$ is attained which makes $m^* R_0$ nearest π; and for this case and beyond we have

(*d*) no wave numbers can exist if the point (ω, S) lies on the origin side of the curve Γ_{m^*}.

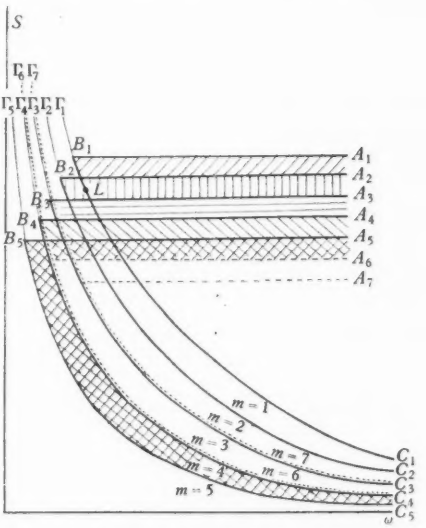

FIGURE 2. A schematic theoretical stability diagram.

In this final case (*d*) the theory does not give any indication of the particular flow pattern which will occur, but it may be inferred that the flow must be the spiral (or symmetric Hadley) type. The results stated in (*a*) to (*d*) above are summarized in diagrammatic form in figure 2.

It is of considerable interest to insert in figure 2 also the results concerning the existence of waves which were obtained by the present author in a stability investigation (1956). These results apply to infinitesimal waves, and the theory in that paper indicates that a wave number m can exist only if the Rossby number is

less than a certain critical value. For convenience, table 5 of the earlier paper is reproduced below and expressed in terms of the parameters of this paper, the Rossby number Ro_T^* of the earlier paper being related† to the present S by the formula $S = \frac{1}{2}(1-a/b)\mathrm{Ro}_T^*$ and table 1 refers to the case $b = 2a$. This table is interpreted as follows: spiral flow will exist if $S > 0{\cdot}055$, wave number $m = 1$ can also exist if $S > 0{\cdot}05$, spiral flow and wave numbers $m = 1, 2$ can exist if $S > 0{\cdot}03$ and so on. When we insert the lines $S = 0{\cdot}055$, $S = 0{\cdot}05$; $S = 0{\cdot}03$, and so on, in figure 2 we can interpret the diagram in the following way. On the origin side of the curve $A_1B_1C_1$, the wave number $m = 1$ cannot exist; on the origin side of the curve $A_2B_2C_2$ the wave number $m = 2$ cannot exist, and so on. At such a point as P in this diagram it would then appear that any one of the wave patterns $m = 1$, $m = 2$ or $m = 3$ can exist; other factors must clearly enter into the discrimination between these possible wave patterns since only one wave is known to exist at any one time.

(Mean temperature 21 °C, $\alpha = 2{\cdot}1 \times 10^{-4}$)

Wave number m	0	1	2	3	4	5
Critical value of S	0·07	0·055	0·05	0·03	0·02	0·01

TABLE 1. Annulus case $b = 2a$

We now consider the heat transported by a particular wave pattern, this being equal to the heat flow across either of the cylindrical boundary walls. The heat flow per unit axial length across $r^* = b$ is given by

$$Q = \rho_0 c_p \kappa \int_0^{2\pi} \frac{\partial \tau^*}{\partial r^*} r^* \Big|_{r^*=b} d\theta = \rho_0 c_p \kappa \frac{\epsilon}{m} (\Delta T)_H \int_0^{2\pi} \frac{\partial T}{\partial R}\Big|_{R=0} d\theta.$$

Using (1.51) and also the boundary condition $\phi = 0$ at $R = 0$, we obtain

$$Q = Q(m,k) = \frac{2\pi\kappa\rho_0 c_p j\epsilon(\Delta T)_H}{mA(z)}$$

$$= 2\pi\kappa\rho_0 c_p m^{-1}(\Delta T)_H \epsilon\left\{m^2 + \frac{4\kappa^2(1+k^2)}{R_0^2}\right\}.$$

The Nusselt number Nu (Hide 1958) for this problem may be defined by

$$\mathrm{Nu} = \frac{(b-a)Q}{2\pi b\kappa\rho_0 c_p (\Delta T)_H}; \tag{4.32}$$

and thus in the case $A = 1$ we have

$$\mathrm{Nu} = \frac{(1-a/b)}{R_0} \frac{m^2R_0^2 + 4K^2(1+k^2)}{m^2R_0^2 + 4K\{2E - K(1-k^2)\}}. \tag{4.33}$$

It is easily shown that $(1-a/b)/R_0$ is the Nusselt number for an annulus of solid but uniform material when the cylindrical boundaries are subject to a differential temperature; and if this basic Nusselt number is denoted by Nu*, it follows that

† The small error due to the angular velocity definitions being slightly different will be ignored here.

the presence of liquid in the annulus has the effect of increasing the effective Nusselt number in the ratio

$$\frac{\mathrm{Nu}}{\mathrm{Nu}^*} = \frac{m^2R_0^2 + 4K^2(1+k^2)}{m^2R_0^2 + 4K\{2E - K(1-k^2)\}}. \tag{4.34}$$

If k is near zero we have $\mathrm{Nu} \doteqdot \mathrm{Nu}^*$, but if k is near its upper limit of unity we have $K \sim \log(4/\sqrt{(1-k^2)})$, $E \sim 1$, so that

$$\frac{\mathrm{Nu}}{\mathrm{Nu}^*} \sim \frac{K}{E} = \log\left(\frac{4}{\sqrt{(1-k^2)}}\right). \tag{4.35}$$

Thus the heat flow can be increased indefinitely if k can be made to tend to unity.

It is possible to use this concept of heat transport in order to help discriminate between different regions in the (ω, S)-plane. Consider the point L in the (ω, S)-plane which lies on Γ_1, and which is in the zone between A_2B_2 and A_3B_3. At this point, waves $m = 1$ and $m = 2$ are possible. Reckoned relative to the curve Γ_1, the value of k at L is 0, and the associated Nu for this point will be

$$(\mathrm{Nu})_{L,m=1} = \mathrm{Nu}^*.$$

At this same point the value of k reckoned relative to the curve Γ_2 is k_2, where

$$\mu^2(k_2) = 2(\pi^2 - R_0^2),$$

and the corresponding value of Nu is

$$(\mathrm{Nu})_{L,m=2} = \mathrm{Nu}^* \frac{4R_0^2 + 4K^2(k_2)\,(1+k_2^2)}{4R_0^2 + 4K(k_2)\,[2E(k_2) - K(k_2)\,(1-k_2^2)]} > \mathrm{Nu}^*.$$

Hence, the $m = 2$ wave at L is capable of transporting more heat than the $m = 1$ wave. If one then assumes that the preferred liquid motion is always that one which transports the greatest amount of heat, then the point L will correspond to the $m = 2$ wave. A similar argument will apply to any point in the restricted zone between A_2B_2 and A_3B_3, and consequently this zone will correspond to the $m = 2$ wave. Kuo (1957), in a stability investigation, discusses this same zone between A_2B_2 and A_3B_3 and arrives at a similar conclusion using a different method, namely that in moving across A_2B_2 into this zone the $m = 2$ wave is the one which has maximum growth rate.

On this basis the whole of the (ω, S)-plane can be subdivided into definite regions where one can expect symmetric flow, wave number 1, wave number 2 and so on, and the complete picture is shown in figure 2.† We can look upon the lines A_1B_1, A_2B_2, ... as lines of dynamical instability, that is where the infinitesimal amplitude waves successively become resonated, and upon the curves $\Gamma_1, \Gamma_2, \ldots$ as curves of heating instability where the liquid has to change its wave pattern due to the amount of heat available being excessive or insufficient to maintain a particular wave form.

If we apply the heat transport argument to a point in the (ω, S)-plane which lies on Γ_6 and is in the zone between A_6B_6 and A_7B_7 (we deal specifically here with the

† The scales used in the schematic diagram (figure 2) may be inferred from the fact that the right-hand side of (4.30) has the order of magnitude 10^{-5}.

case $b = 2a$), it follows that, since Γ_6 is on the side of Γ_5 remote from the origin, the heat transport associated with $m = 6$ is less than that associated with $m = 5$. Thus, in such a geometrical configuration the maximum possible amount of heat can be transported by the steady wave $m = 5$, and beyond this m value the steady waves become less efficient as transporters of heat. It is of course not possible by this argument to prove that wave numbers 6, 7, 8, ..., cannot occur, but they are certainly less efficient as transporters of heat than is wave number 5.

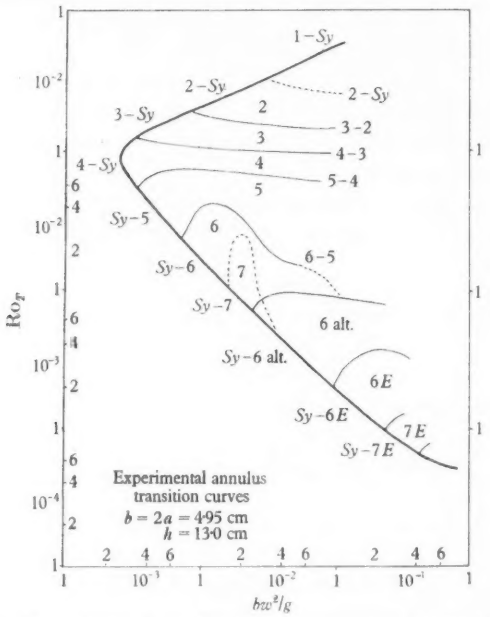

FIGURE 3. Experimental annulus transition curves obtained by Fultz.

We may compare figure 2 with one recently prepared by Fultz for the case $b = 2a$. The ordinate in the Fultz diagram, figure 3, is the Rossby number and the abscissa is a quantity proportional to ω_s^2; and it will be noted that there is a broad overall agreement between the two diagrams. There is a considerable complexity in the Fultz diagram for the lowest Rossby numbers where wave numbers 6 and 7 appear, and Fultz has described this region as containing types of instability which are inherently complicated. It is significant that this region of complicated wave features is associated in the theoretical investigation with the heat transport attaining its maximum value on Γ_5. Assuming that the value m^* gives an indication of the maximum number of steady waves in any given geometrical configuration, we have in general

$$m^* = \left[\frac{\pi}{R_0}\right] = \left[\frac{\pi}{\log(b/a)}\right], \tag{4.36}$$

where $[x]$ denotes that integral value which is closest to x. As b approaches a, $\log(b/a)$ tends to zero and m^* becomes large (this is observed experimentally; up

to 15 waves have been produced in a sufficiently narrow annulus); as a tends to zero and lies in the range $0 < a < be^{-\pi}$, it would appear that no wave motion is then possible.

For moderate values of k the typical magnitude of Nu from (4.33) is 2 or 3; Fultz in a private communication gives values of Nu which are of order 30 and over. It is clear therefore that the process of molecular conduction as assumed here cannot be the correct one for the transfer of heat in this problem. It is possible of course to postulate the existence of an eddy conductivity in order to achieve the correct order of magnitude for the heat transfer, but the more correct conclusion is probably that the bulk of the heat transfer is effected by the ageostrophic flow. In this same communication, Fultz states that 'there is a faint indication of an increase of Nu with m or some possibility of a maximum for intermediate m; it is also probable that there might be local maxima in the regions of strong vacillation'. This is in qualitative agreement with the picture described above, and it is possible to accept the present theory in as much as it provides insight into the mechanism of the change-over from one wave pattern to another. In this respect also we may compare (4.36) with an experimental result due to Hide, namely

$$\frac{m^*}{\pi}\left(\frac{b-a}{b+a}\right) = 0{\cdot}67. \tag{4.37}$$

Since
$$\log\left(\frac{b}{a}\right) = 2\left\{\left(\frac{b-a}{b+a}\right)+\frac{1}{3}\left(\frac{b-a}{b+a}\right)^3+\ldots\right\},$$

it follows from (4.36) that we have approximately

$$\frac{m^*}{\pi}\left(\frac{b-a}{b+a}\right)\left\{1+\frac{1}{3}\left(\frac{b-a}{b+a}\right)^2+\ldots\right\} = 0{\cdot}5;$$

and thus this also provides some justification for accepting (4.36) as the upper limit of the wave number.

The function ϕ being known, the functions F and f can now be determined. Using (4.4) and (1.51), we have

$$F = jR - \tfrac{1}{2}\phi_1^2\int_{-R}^{0} \mathrm{sn}^2\{-\tfrac{1}{2}R\phi_2, k\}\,dR, \tag{4.38}$$

there being no loss of generality in making $F = 0$ for $R = 0$. This gives the mean temperature field in the liquid. The mean pressure field f is given by (1.53); and in the present case $d\Psi/dR = 0$, we have

$$\frac{\partial f}{\partial R} = (\beta+z)(j-\tfrac{1}{2}\phi^2),$$

and
$$f = (\beta+z)\left\{jR - \tfrac{1}{2}\phi_1^2\int_{-R}^{0}\mathrm{sn}^2\{-\tfrac{1}{2}R\phi_2, k\}\,dR\right\} + \text{constant}. \tag{4.39}$$

As mentioned earlier the profiles of mean temperature and mean pressure at any height z are identical.

Since
$$j - \tfrac{1}{2}\phi_1^2 = m^2 + \frac{4k'^2K^2}{R_0^2}$$

from (4.27) it follows that $\partial F/\partial R$ is always positive; and thus the mean temperature and mean pressure therefore increase monotonically with r. The minimum gradient will be encountered at $r^* = (ab)^{\frac{1}{2}}$ and the maxima of the gradient and therefore the maximum mean zonal velocity at the cylindrical walls. The action of viscosity in practice may invalidate this result near the bounding walls of the annulus.

Case II. Momentum transport proportional to $\phi^2(R)$; $d\Psi/dR$ = constant

In this case we shall assume that

$$\frac{d\Psi}{dR} = m\lambda, \tag{4.40}$$

where λ is a constant. This implies that $\Psi = m\lambda \log r$, and also, from (2.5) and (2.6), that the angular momentum transport is proportional to $\phi^2(R)$. Since ϕ vanishes at the bounding cylindrical walls and attains a maximum in the liquid between, it follows that the angular momentum shows a similar type of profile, and in order to produce such a horizontal transfer there will be in this case a mechanism supplying or withdrawing westerly angular momentum in the vertical direction. The equation (1.52) in this case becomes

$$\frac{dR^2}{d^2\phi} = (m^2 + m^2\lambda^2 - j)\,\phi + \tfrac{1}{2}\phi^3; \tag{4.41}$$

and, comparing (4.41) with (4.10), it is clear that the only difference between Case I and Case II lies in the coefficient of ϕ and that all the results pertaining to this case can be deduced from Case I provided m^2 is replaced by $m^2(1+\lambda^2)$. Thus, the formulae which replace (4.27) and which apply to this case will be

$$\left.\begin{aligned} \phi_2 = \frac{4K}{R_0}, \quad \phi_1 = \frac{4kK}{R_0}, \\ j = m^2(1+\lambda^2) + \frac{4K^2}{R_0^2}\,(1+k^2), \\ \frac{1}{\epsilon} = mR_0(1+\lambda^2) + \frac{4K}{mR_0}\{2E - K(1-k^2)\}. \end{aligned}\right\} \tag{4.42}$$

The formula for F, the mean zonal temperature, will be the same as (4.29), but the formula for $\partial f/\partial R$, given by (1.53), is in this case

$$\frac{\partial f}{\partial R} = (\beta + z)\,(j - \tfrac{1}{2}\phi^2) + 2m\lambda \frac{d}{dR}(\log \phi). \tag{4.43}$$

The solution for f, the mean zonal pressure, will be

$$f = (\beta + z)\left\{jR - \tfrac{1}{2}\phi_1^2 \int_{-R}^{0} \mathrm{sn}^2\left(-\tfrac{1}{2}R\phi_2, k\right) dR\right\} + 2m\lambda \log \phi, \tag{4.44}$$

and, since ϕ vanishes at the two bounding walls it will be seen that the mean zonal pressure and mean zonal velocity have singularities at the boundaries.

Case III. Momentum transfer proportional to ϕ^3; $d\Psi/dR = \gamma\phi(R)$

One of the objections to the previous case is that the mean zonal pressure and velocity fields have singularities at the cylindrical bounding walls. Here we investigate a solution which does not suffer from this disadvantage. The formula (1.53) for $\partial f/\partial R$ indicates that the singularity in the zonal velocity arises from the term $\frac{1}{\phi^2}\frac{d}{dR}\left(\phi^2\frac{d\Psi}{dR}\right)$ on the right-hand side; and provided $d\Psi/dR$ has a simple zero at each of the bounding walls, the singularity will not arise. If, for example, Ψ is such that

$$\frac{d\Psi}{dR} = \gamma\phi^s, \tag{4.45}$$

where $s \geqslant 1$, then the singularity of $\partial f/\partial R$ is avoided. We consider here the particular case $s = 1$, and shall take

$$\frac{d\Psi}{dR} = \gamma\phi \quad (\gamma = \text{constant}); \tag{4.46}$$

but the best possible value of s to choose must await a closer comparison with experiment. Whatever the deficiencies of this choice it has the great merit that the problem can be completely solved in this case and thus we can find what modifications are introduced into the solution by the presence of an angular momentum transfer.

Equation (1.52) for ϕ now becomes

$$\frac{d^2\phi}{dR^2} = (m^2 - j)\,\phi + (\gamma^2 + \tfrac{1}{2})\,\phi^3, \tag{4.47}$$

and this case can, as before, be solved in terms of elliptic functions. The first integral of (4.47) is

$$\left(\frac{d\phi}{dR}\right)^2 = (m^2 - j)\,\phi^2 + (\tfrac{1}{4} + \tfrac{1}{2}\gamma^2)\,\phi^4 + \text{constant},$$

and if we suppose that $d\phi/dR$ vanishes when $\phi = \phi_1$, it follows that this equation can be expressed in the form

$$\left(\frac{d\phi}{dR}\right)^2 = \left(\frac{1+2\gamma^2}{4}\right)(\phi_1^2 - \phi^2)\,(\phi_2^2 - \phi^2), \tag{4.48}$$

where

$$\phi_2^2 = \frac{4(j-m^2)}{1+2\gamma^2} - \phi_1^2 > 0. \tag{4.49}$$

As before there is no loss of generality in taking $\phi_2 > \phi_1$, and we shall choose $k = \phi_1/\phi_2$, where $0 < k < 1$. The appropriate solution of (4.49) is

$$\phi = \phi_1 \operatorname{sn}\{-\tfrac{1}{2}R\phi_2\sqrt{(1+2\gamma^2)}, k\}, \tag{4.50}$$

and this will satisfy both boundary conditions (4.1) provided

$$\tfrac{1}{2}R_0\phi_2\sqrt{(1+2\gamma^2)} = 2K. \tag{4.51}$$

The solution (4.50) has its maximum at the geometrical mean value $r^* = (ab)^{\frac{1}{2}}$; thus, this result is not influenced by momentum transport. The condition (4.9) becomes

$$jR_0 = \frac{m}{\epsilon} + \frac{2\phi_2}{\sqrt{(1+2\gamma^2)}}(K-E), \tag{4.52}$$

and thus the four equations which generalize the set (4.27) to (4.29) are as follows:

$$\phi_2 = \frac{4K}{R_0\sqrt{(1+2\gamma^2)}}, \quad \phi_1 = \frac{4Kk}{R_0\sqrt{(1+2\gamma^2)}}, \tag{4.53}$$

$$j = m^2 + \frac{4K^2(1+k^2)}{R_0^2}, \tag{4.54}$$

$$\frac{m}{\epsilon} = m^2 R_0 + \frac{\nu^2}{R_0}, \tag{4.55}$$

where

$$\nu^2 = \frac{4K}{1+2\gamma^2}\{2E - K[(1-k^2) - 2\gamma^2(1+k^2)]\}. \tag{4.56}$$

These equations can be interpreted as in the first case. It is easily shown that the quantity ν^2 defined in (4.56) increases monotonically from the value π^2 at $k = 0$ to infinity as k tends to unity, and thus it follows that all the detailed features of the stability diagram are not influenced by momentum transfer, in particular the result (4.36) for the maximum number of waves remains unchanged.

The formula for the mean temperature field is similar to the previous case, and is given by

$$F = jR - \tfrac{1}{2}\phi_1^2 \int_{-R}^{0} \mathrm{sn}^2\{-\tfrac{1}{2}R\phi_2\sqrt{(1+2\gamma^2)}, k\}\, dR. \tag{4.57}$$

The mean zonal velocity field $\partial f/\partial r$ can be deduced from $\partial f/\partial R$ using (1.53) and (4.37), which give

$$\frac{\partial f}{\partial R} = \frac{B}{A}(j - \tfrac{1}{2}\phi^2) - 3\gamma\frac{d\phi}{dR}; \tag{4.58}$$

and thus the solution for the mean zonal pressure function becomes

$$f = (\beta+z)\left\{jR - \tfrac{1}{2}\phi_1^2 \int_{-R}^{0} \mathrm{sn}^2(-\tfrac{1}{2}R\phi_2\sqrt{(1+2\gamma^2)}, k)\, dR\right\} - 3\gamma\phi(R) + \text{constant}. \tag{4.59}$$

In the case of zero momentum transfer ($\gamma = 0$), it was noted that $\partial f/\partial F$ maintains the same sign for all values of R in the range $-R_0 \leqslant R \leqslant 0$, but in (4.46) it will be observed that

$$\left(\frac{\partial f}{\partial R}\right)_{R=0} = (\beta+z)j + \tfrac{3}{2}\gamma\sqrt{(1+2\gamma^2)}\,\phi_1\phi_2, \tag{4.60}$$

$$\left(\frac{\partial f}{\partial R}\right)_{R=-R_0} = (\beta+z)j - \tfrac{3}{2}\gamma\sqrt{(1+2\gamma^2)}\,\phi_1\phi_2. \tag{4.61}$$

so that if γ is negative and sufficiently large (which ensures a transfer of westerly angular momentum towards $r = 0$) or if β is sufficiently small, then the possibility exists of a reversal in the direction of the mean zonal velocity. This suggests that the presence of easterlies embedded in a westerly zonal flow implies an angular

momentum flow, as is well known to meteorologists. Using (4.48), we can say that if $\gamma < 0$ and

$$|\gamma\sqrt{(1+2\gamma^2)}\,\phi_1\phi_2| > \tfrac{2}{3}\beta, \tag{4.62}$$

then easterlies will appear near the outer (hotter) cylinder.

It is of some interest in this case to determine the meridional part of the vertical velocity which is given by (3.18). We have

$$\frac{r^4(\partial\overline{w}_1/\partial z)}{\epsilon^3 m^{-4}(1+z^2)\gamma} = \frac{1}{2}\frac{d^2}{dR^2}(\phi^3) - \frac{d}{dR}(\phi^3)$$

$$= 3\phi\left\{\tfrac{1}{2}\phi\frac{d^2\phi}{dR^2} + \left(\frac{d\phi}{dR}\right)^2 - \phi\frac{d\phi}{dR}\right\}. \tag{4.63}$$

Near the boundary walls the right-hand side behaves like $3\phi(d\phi/dR)^2$; hence the mean vertical velocity will be upwards ($w_1 = 0, z = 0$). At the position of maximum ϕ, we have $d\phi/dR = 0$; hence the right-hand side is $\frac{3}{2}\phi^2 d^2\phi/dR^2$, which is necessarily negative. Hence, in the neighbourhood of the maximum value of ϕ, the mean vertical velocity is downwards. This velocity implies the existence of at least two cells, a direct cell near the outer cylinder and an indirect cell near the inner cylinder, and by considering the changes of sign of $\frac{1}{2}\phi\phi'' + \phi'^2 - \phi\phi'$ it may be verified that there are two and only two zeros of $\overline{w}_1$ between $R = 0$ and $R_1 = -R_0$, and hence there are only two cells in the meridional structure.

Case IV. The open dishpan problem. Non-existence of a continuous solution for ϕ

In this case we assume that the inner cylinder is removed and the liquid is enclosed by one cylinder of radius b. The boundary conditions to be satisfied by the function ϕ are now as follows. At the outer cylinder the normal velocity must vanish hence as before we must have $\phi(0) = 0$. At the central axis $r = 0$, or $R = -\infty$, since there is no source along the axis it is necessary that $\partial p/\partial\theta$ should vanish along the axis, hence $\phi(-\infty) = 0$. In addition, since u_θ must vanish at $r = 0$, it is necessary that $\phi'(-\infty) = 0$. Hence we must have

$$\phi(0) = 0, \quad \phi(-\infty) = \phi'(-\infty) = 0.$$

Since two derivatives vanish at $R = -\infty$, it follows from (4.38) that all the derivatives will vanish there, hence $\phi \equiv 0$. Thus, no continuous non-zero solution exists.

REFERENCES

Davies, T. V. 1953 *Rep. Aero. Res. Coun., Lond.*, no. 15876.

Davies, T. V. 1956 *Phil. Trans.* A, **249**, 27.

Fultz, D. 1956 Studies in experimental hydrodynamics applied to large scale meteorological phenomena. *Final Report Part I, Hydrodynamics Laboratory, Dept. of Meteorology, University of Chicago, Figure B.* 84.

Fultz, D. & Riehl, H. 1957 *Quart. J. Roy. Met. Soc.* **83**, 215.

Hide, R. 1958 *Phil. Trans.* A, **250**, 441.

Kuo, H. L. 1957 *Scientific Rep. No.* 7. *General Circulation Project, Massachusetts Inst. of Tech., Dept. of Meteorology.*

Lorenz, E. 1957 *Scientific Rep. No.* 9, *General Circulation Project, Massachusetts Inst. of Tech., Dept. of Meteorology.*

Phillips, N. 1956 *Quart. J. Roy. Met. Soc.* **82**, 125.

Rogers, R. H. 1959 *J. Fluid Mech.* **5**, 41.

An unsteady turbulent boundary layer

By STURE K. F. KARLSSON

Department of Aeronautics, The Johns Hopkins University

(Received 10 September 1958)

A low speed parallel flow, whose velocity fluctuates sinusoidally in magnitude about a constant mean, has been produced in a boundary layer wind tunnel. Hot-wire measuring techniques have been developed to permit an investigation of the turbulent boundary layer developing on a flat plate with this free stream condition. The response of the layer at a Reynolds number

$$R_{\delta^*} = (\overline{U}_\infty \delta^*)/\nu = 3{\cdot}6 \times 10^3$$

was measured for free stream fluctuation amplitudes up to 34 % of the mean velocity and frequencies ranging from 0 to 48 cycles/sec. Here $\delta^* = \int_0^\infty \left(1 - \frac{\overline{U}}{\overline{U}_\infty}\right) dy$ is the boundary displacement thickness, $\overline{U}(x, y)$ the mean velocity in the boundary layer, $\overline{U}_\infty$ the mean velocity in the free stream, and ν the kinematic viscosity.

Measurements were made of the mean velocity, the amplitudes of in- and out-of-phase components of the first harmonic of the periodic fluctuations, and the intensity of higher harmonics and turbulence. It was found that non-linear effects, even at the largest fluctuation amplitudes, were so small that they were obscured by experimental errors.

Introduction

Many fluid flow problems are essentially unsteady in character. The flow over a turbine blade moving through the wakes of the guide vanes located upstream, or the flow over a rocket which accelerates from rest, are two typical examples. Problems such as these have in recent years stimulated a fair amount of interest in the behaviour of boundary layers subject to unsteady free stream conditions. In the investigation reported on here, a study was made of an unsteady turbulent boundary layer.

The ultimate goal of such a study is that it should enable one to predict the behaviour of the turbulent boundary layer at any instant, when the free stream is given as a function of time. The fact that the turbulent layer is a non-linear mechanism, however, makes this an exceedingly difficult problem. No longer can the responses due to a series of small changes of the input (free stream velocity) be superimposed to give the final response, as is the case in linear problems. In general, the unsteady turbulent boundary layer depends not only on the instantaneous value of the free stream velocity (among other things) but on its past history as well. Hence, knowledge of the response of the turbulent boundary layer to a specific kind of free stream fluctuation does not enable one, in general,

to predict the response to an arbitrary fluctuation of the free stream. Nevertheless, the best way to gain some initial understanding of this problem seems to be to study a situation, which is as simple and well defined as possible, with a specific fluctuation of free stream velocity with time.

The choice for the present experimental investigation was an incompressible two-dimensional turbulent boundary layer with a zero mean pressure gradient in the flow direction, where the free stream velocity fluctuated sinusoidally with amplitude u_∞, say, and frequency $\omega/2\pi$, about a constant mean velocity $\overline{U}_\infty$.

General considerations

In interpreting the results of our measurements it will prove helpful to have some knowledge of the behaviour of the corresponding laminar layer. This problem, restricted to small free stream oscillations, has been treated by Lighthill (1954). Here we should like to learn something about the effects of non-linearity which will appear if the free stream fluctuations are large. This can be done by studying the response of the boundary layer to very slow (quasi-steady) fluctuations of free stream velocity. Then the velocity profile at any instant can be closely approximated by the steady profile corresponding to the instantaneous free stream velocity. For the boundary layer on a flat plate, the Blasius layer, the velocity is given by

$$U = U_\infty f'\left\{y\sqrt{\left(\frac{U_\infty}{x\nu}\right)}\right\}, \tag{1}$$

where f is the Blasius function, x distance from leading edge in flow direction, y distance perpendicular to the plate, and ν kinematic viscosity.

U_∞ is the slowly varying free stream velocity $U_\infty(t)$, and the prime ($'$) denotes differentiation with respect to the argument $\left\{y\sqrt{\left(\frac{U_\infty}{x\nu}\right)}\right\}$.

Our interest is in the nature of the variations of U with time for a sinusoidal variation of U_∞ with time. To obtain an expression for this relationship which involves a minimum of other parameters, we multiply both sides of (1) by $y^2/x\nu$ and get

$$\frac{Uy^2}{x\nu} = \frac{U_\infty y^2}{x\nu} f'\left\{y\sqrt{\left(\frac{\overline{U}_\infty}{x\nu}\right)}\right\}. \tag{2}$$

We put $Uy^2/x\nu = F$ and $U_\infty y^2/x\nu = n$. These are the only variables appearing in (2) and therefore the dependence upon the varying free stream velocity for the entire boundary layer is given by a single plot of F versus n of the form $F = nf'(\sqrt{n})$. This plot is shown in figure 1. The varying free stream velocity in our case is given by

$$U_\infty = \overline{U}_\infty(1+\beta\cos\theta),$$

where θ is the slowly varying phase angle and $\overline{U}_\infty\beta$ the amplitude of the free stream fluctuations. Since U_∞ is directly proportional to n, we also have

$$n = n_\infty(1+\beta\cos\theta),$$

and consequently

$$F = F[n_\infty(1+\beta\cos\theta)]$$

is a function periodic in θ with period 2π. However, because of the non-linear nature of F the boundary layer velocity will not fluctuate sinusoidally with

a single frequency. Since F is symmetric with respect to $\theta = 0$ it can be expanded in a Fourier cosine series. For fixed values of n_∞ and β we have

$$F = \sum_{i=0}^{\infty} A_i \cos i\theta. \tag{3}$$

The first three of the Fourier coefficients A_i have been computed graphically as functions of n_∞ for $\beta = 0{\cdot}3$ and $0{\cdot}5$. After dividing both sides of (3) by $\overline{U}_\infty y^2/x\nu = n_\infty$, we get the expression for velocity in the boundary layer, i.e.

$$\frac{U}{\overline{U}_\infty} = \frac{A_0}{n_\infty} + \frac{A_1}{n_\infty}\cos\theta + \frac{A_2}{n_\infty}\cos 2\theta + \ldots.$$

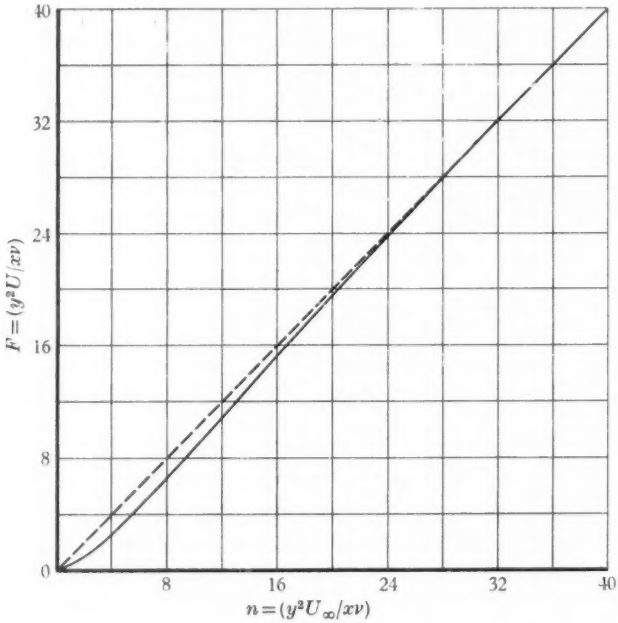

FIGURE 1. Transfer characteristic for the Blasius layer.

Using a different notation, we may write

$$\frac{U}{\overline{U}_\infty} = \frac{\overline{U}}{\overline{U}_\infty} + \frac{u^{(1)}}{\overline{U}_\infty}\cos\theta + \frac{u^{(2)}}{\overline{U}_\infty}\cos 2\theta + \ldots.$$

The quantities $\overline{U}/\overline{U}_\infty$, $u^{(1)}/\beta\overline{U}_\infty$, $u^{(2)}/\beta\overline{U}_\infty$ for $\beta = 0{\cdot}3$ and $0{\cdot}5$, and for comparison $\overline{U}/\overline{U}_\infty$ and $u^{(1)}/\beta\overline{U}_\infty$ for $\beta \to 0$, have been plotted as functions of $\eta = \sqrt{n}$ in figure 2. These curves demonstrate the non-linear behaviour of the boundary layer with respect to slow free stream fluctuations. As the amplitude of these fluctuations is increased the mean velocity profile deviates progressively from the steady one. The slope of the profile at $\eta = 0$ and therefore also the skin friction increases with increasing amplitude.

Perhaps the most striking effect of non-linearity on the velocity fluctuations in the boundary layer is to produce higher harmonics, of which only the second has been plotted. We note that the sign of the amplitude of the second harmonic changes as we proceed from the plate to the edge of the boundary layer. This represents a 180° phase shift. Simultaneously the mean velocity for the oscillating boundary layer goes from a value which is greater than the corresponding steady velocity to one which is lower. It is remarkable, however, how small an effect the fluctuations have on the mean profile even for oscillations as great as 50 % of the free stream.

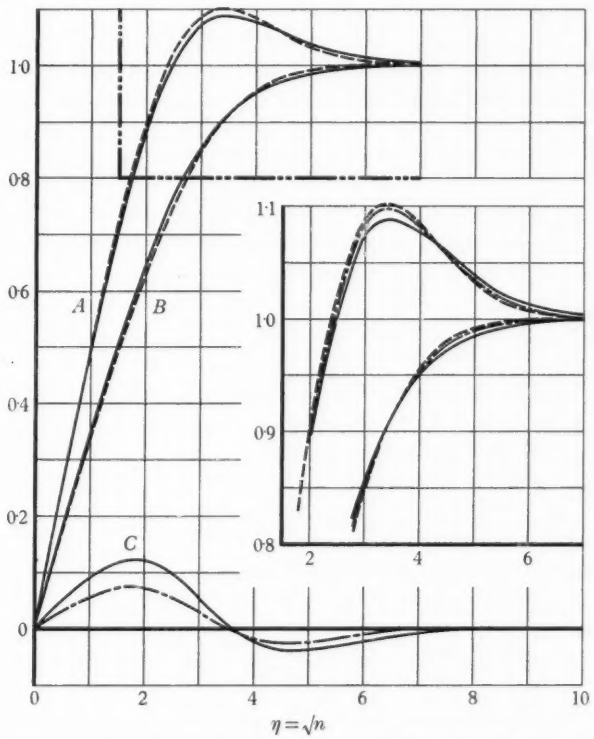

FIGURE 2. The quasi-steady Blasius layer. $A = u_1^{(1)}/\beta \overline{U}_\infty$, $B = \overline{u}/\overline{U}_\infty$, $C = u_2^{(2)}/\beta U_\infty$. ——— $\beta = 0$, – – – $\beta = 0{\cdot}3$, ——— $\beta = 0{\cdot}5$.

From this quasi-steady analysis it is not possible to predict the behaviour of the layer subjected to large free stream oscillations of arbitrary frequency. But as in the case for small amplitude oscillations (Lighthill 1954), at very high frequency the periodic and mean motions become uncoupled (if compressibility effects can be neglected), the former being governed by a linear equation. As a result the higher harmonics disappear from the fluctuations in the boundary layer and the unsteady mean velocity profile becomes identical with the steady one.

Although the turbulent boundary layer is a much more complicated mechanism than the laminar layer, they are sufficiently related that it is possible to use some

of the results of the above laminar analysis to infer the qualitative behaviour of the turbulent layer. For instance, for the quasi-steady turbulent layer we should expect the fluctuation amplitude to have a maximum greater than the free stream amplitude located near the outer edge of the layer. Non-linear interaction between the mean velocity and the periodic fluctuations takes place here also, as in the laminar layer, if the fluctuation amplitude is large enough, and should result in an increase in skin friction and production of higher harmonics. Furthermore, at very high frequencies the (incompressible) fluctuations obey a linear equation and as a consequence the mean velocity profile in that case should be identical to the corresponding steady one.

The velocity fluctuations in the turbulent boundary layer subjected to free stream oscillations can be separated into two parts: periodic and random fluctuations. If the instantaneous free stream velocity is given by

$$U_\infty(t) = \overline{U}_\infty + \mathscr{R}\left(\sum_{n=1}^{N} u_\infty^{(n)} e^{in\omega t}\right), \tag{4}$$

where $\overline{U}_\infty$ is the constant mean velocity and the amplitudes $u_\infty^{(n)}$ are in general complex to indicate relative phase shifts between different frequencies, then for the velocities inside the boundary layer we can write

$$U_k(x_1, x_2, x_3, t) = \overline{U}_k(x_1, x_2) + \mathscr{R}\left[\sum_{n=1}^{\infty} u_k^{(n)}(x_1, x_2)\, e^{in\omega t}\right] + r_k(x_1, x_2, x_3; t). \tag{5}$$

The subscripts $k = 1, 2, 3$ represent the components along the three Cartesian co-ordinate axes x_1, x_2 and x_3, respectively, where x_1 is parallel to the solid surface in the direction of the flow and x_2 is normal to the surface. $r_k(x_1, x_2, x_3, t)$ is the random part of the velocity fluctuation. The complex amplitudes are defined by

$$u_k^{(n)}(x_1, x_2) = 2\overline{U_k(x_1, x_2, x_3, t)\, e^{-in\omega t}}, \tag{6}$$

where the bar means a double averaging process: the ensemble average of the time average over a complete cycle of periodic fluctuation. That is,

$$\overline{U_k e^{-in\omega t}} \equiv \lim_{N\to\infty} \frac{1}{N} \sum_{l=1}^{N} \frac{\omega}{2\pi} \int_0^{2\pi} U_{kl} e^{-in\omega t}\, dt, \tag{7}$$

where U_{kl} is a particular realization of the velocity. By substituting (5) into the equations of motion we can obtain the boundary-layer equations for the mean velocity, periodic amplitudes and turbulence intensity. These equations are given in the author's dissertation (Karlsson 1958).

The experimental techniques used in the present experiments permitted the measurement of only the first harmonic of the periodic fluctuations. Consequently, it was necessary in the experiment to separate the fluctuations in a slightly different way than outlined above. The higher harmonics of the periodic fluctuations were added to the turbulence and the root-mean-square value of this sum was measured. This is not a serious shortcoming, since the free stream fluctuations consisted essentially of a single frequency and the higher harmonics produced in the boundary layer due to non-linear interactions (as it turned out) must have been quite small.

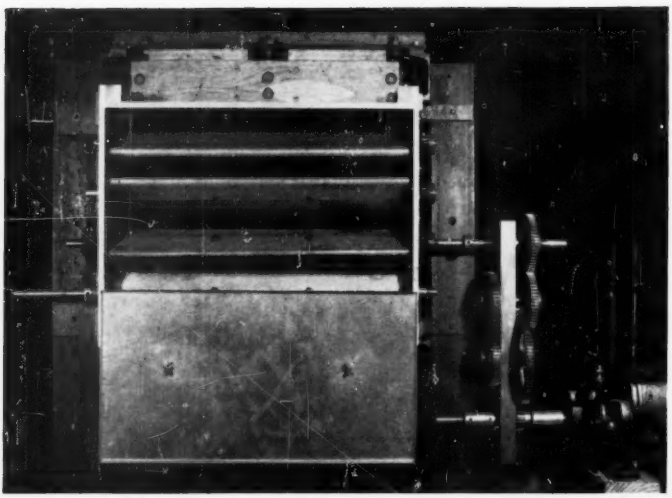

FIGURE 4 (plate 1). Shutter for producing sinusoidal fluctuations.

B

th
J
te
v
co
w
p

w
h
m
lo
w
re
w

a
n
n
s
v

n
i
t

l
n

s
s
c

Experimental equipment

The wind tunnel. The unsteady boundary-layer measurements were made in the boundary layer developing on the floor in the wind tunnel described by Johnson (1957). To accomplish the free stream fluctuations the exit area of the test section was varied by means of a shutter consisting of four parallel rotating vanes driven by an electric motor. The frequency of the free stream fluctuations could be varied continuously from $\frac{1}{3}$ to 60 cycles/sec. A schematic side view of the wind tunnel and a photograph of the shutter are shown in figure 3 and in figure 4, plate 1.

The free stream fluctuations were very nearly sinusoidal at the frequencies for which measurements were performed, except at the highest frequency, where the higher harmonics (primarily second) accounted for about 15 % of the total root-mean-square amplitude. From the acoustic point of view the fluctuations at the lower frequencies, 0·33 to 4 cycles/sec, were quasi-steady. However, as 8 cycles/sec was approached a parasitic third harmonic gained in amplitude due to acoustic reflexion. 24 cycles/sec was the fundamental frequency for the standing sound wave with pressure nodes at the beginning and end of the test section and

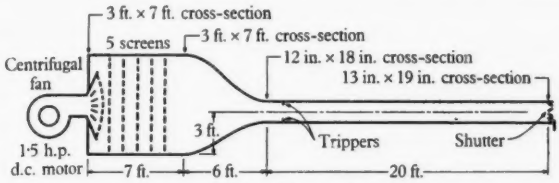

FIGURE 3. Sketch of wind tunnel.

Screen	Mesh	Solidity
1	30	0·63
2, 3	10	0·43
4	36	0·42
5	43	0·38

a velocity node in the middle. Since the measurements were performed near the middle and large fluctuations were desired, this frequency was not suitable for measurements. But measurements were performed at 48 cycles/sec, which is the second harmonic. Then there was a velocity loop in the middle of the test section with nodes on either side, halfway between the middle- and the end-points.

To remove objectionable vibration induced by the oscillating pressure it was necessary to reinforce the floor and the ceiling of the test section. After this improvement the maximum deflexion anywhere on the floor or ceiling was less than 0·001 in. relative to the externally supported hot-wire probe.

An efficient tripping device was installed, which insured transition from laminar to turbulent boundary-layer flow at the same location for the entire range of velocities used in the experiments.

The pressure gradient in the flow direction was very nearly zero in the test section for steady operation of the wind tunnel at both minimum and maximum speeds. The variation of static pressure was within $\pm 0{\cdot}4\,\%$ of $\frac{1}{2}(\rho\overline{U}_\infty^2)$, the dynamic pressure in the free stream (ρ = density of air).

Hot-wire equipment. Two hot-wire probes were used simultaneously for the unsteady boundary-layer measurements, one stationary in the free stream and one traversing the boundary layer. The traversing gear used for this probe was the same as that described by Johnson (1957). Both probes were placed centrally with respect to the side walls of the test section. Their longitudinal position could be varied over the entire 20 ft. long test section.

Throughout these experiments, 0·0001 in. diameter straight platinum hot-wires were used having a cold resistance of about 17 Ω. The heating current was adjusted so that the hot resistance was 1·8 times this value.

A new constant temperature transistor hot-wire set, recently developed by Kovasznay (1958), was employed in this work. This set has a fully compensated response from d.c. up to about 17,000 cycles/sec, which is the frequency for free oscillations, characteristic for constant temperature hot-wire sets under certain operating conditions (Kovasznay 1948). The great advantage with a constant temperature hot-wire set is that it is properly compensated even for large fluctuations in velocity. Furthermore, it is relatively easy to operate on its output signal in such a way that the final output is directly proportional to velocity.

King's equation, which expresses the heat balance in the hot-wire, can for this case be written very simply

$$U = (aI^2 - b)^2, \tag{8}$$

where U is the velocity, I the current, and a and b are dimensional constants which depend upon operating conditions and wire properties. The output voltage of the constant current hot-wire set is proportional to I. Hence, to get a signal which is proportional to the velocity it is necessary to square the output voltage, subtract a constant bias voltage, then square again. The bias is set so that the final output is zero for zero velocity. This procedure was followed here, using Philbrick multipliers for squaring circuits. Actually, equation (8) is not strictly true for very low velocities, but it was found that linear response could be obtained by this method over the range of velocity of interest.

Total head tube-manometer. For the purpose of hot-wire calibration the velocity in the wind tunnel was measured with a total head tube. The difference between total head and static pressure as sensed by a static tap in the floor was measured with a 10:1 inclined manometer. The possible error in this measurement was conservatively ± 0·0004 in. alcohol, corresponding to a maximum possible error in velocity of ± 1 % at the lowest speed measured. The pitot tube was not used for mean velocity measurements in the unsteady boundary layer, since it did not behave reliably when subjected to large velocity fluctuations.

Measuring techniques

The circuitry used for processing the linearized hot-wire signals is shown in a simplified diagram in figure 5. Since the output voltage of the hot-wire sets are proportional to the velocities, the same notation has been used for voltages as for velocities.

At low frequencies of periodic fluctuation the mean velocities could not be measured directly at the output of the hot-wire sets because of the large meter fluctuations. The necessary averaging was accomplished with a simple RC net-

work which had a time constant of about one second. Owing to the finite impedance of the vacuum tube volt meter, a correction of about $+4\%$ had to be applied to this reading.

The velocity fluctuations in the boundary layer are conveniently separated into two parts: (*a*) the fundamental frequency of the periodic fluctuation, and (*b*) the turbulence and higher harmonics generated through non-linear interaction.

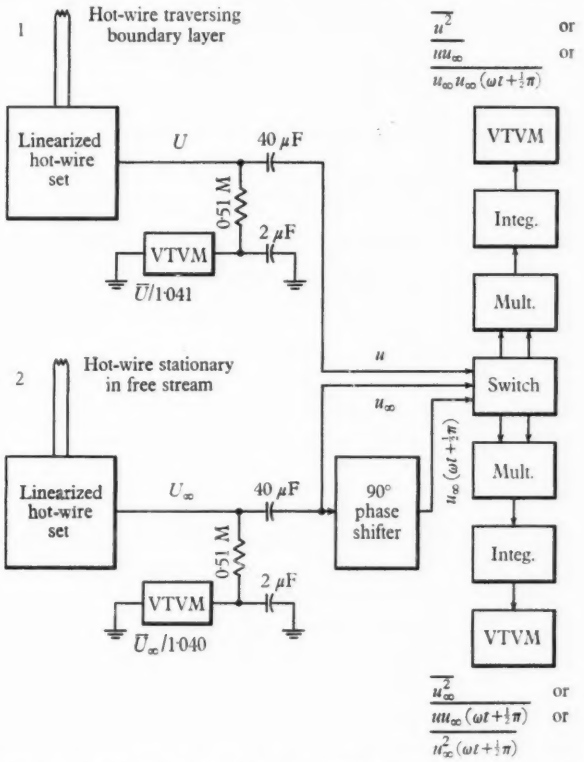

FIGURE 5. The hot-wire output circuit, VTVM = vacuum tube volt meter.

If the fluctuations in the free stream are

$$u_\infty = u_\infty^{(1)} \cos \omega t, \tag{9}$$

then inside the boundary layer the fluctuations in the x-direction are

$$\begin{aligned} u(x, y, z, t) &= u^{(1)}(x, y) \cos [\omega t + \phi(x, y)] + r(x, y, z, t) \\ &= u^{(1)} \cos \phi \cos \omega t - u^{(1)} \sin \phi \sin \omega t + r, \end{aligned} \tag{10}$$

where r contains higher harmonics as well as the random fluctuations. Multiplying with the free stream fluctuations and averaging, one gets

$$\overline{u_\infty u} = \frac{u_\infty^{(1)} u^{(1)} \cos \phi}{2}. \tag{11}$$

After shifting the free stream oscillation through 90°, multiplying and averaging, we have

$$\overline{u_\infty(\omega t + \tfrac{1}{2}\pi)\, u} = \frac{u_\infty^{(1)} u^{(1)} \sin\phi}{2}. \tag{12}$$

The amplitudes of the in- and out-of-phase components of the boundary-layer fluctuations are then respectively

$$u^{(1)} \cos\phi = \sqrt{2}\,\frac{\overline{u_\infty u}}{(\overline{u_\infty^2})^{\frac{1}{2}}} \tag{13}$$

and

$$u^{(1)} \sin\phi = \sqrt{2}\,\frac{\overline{u_\infty(\omega t + \tfrac{1}{2}\pi)\, u}}{(\overline{u_\infty^2})^{\frac{1}{2}}}. \tag{14}$$

The mean square of the total boundary-layer fluctuation is given by

$$\overline{u^2} = \frac{\overline{u^{(1)2}}}{2} + \overline{r^2}. \tag{15}$$

since r is uncorrelated with the rest of the signal. Solving for $\overline{r^2}$, we have finally

$$\overline{r^2} = \overline{u^2} - \left[\frac{(\overline{u_\infty u})^2}{\overline{u_\infty^2}} + \frac{(\overline{u_\infty(\omega t + \tfrac{1}{2}\pi)\, u})^2}{\overline{u_\infty^2}}\right]. \tag{16}$$

The mean products $\overline{u^2}$, $\overline{u_\infty^2}$, $\overline{u_\infty u}$ and $\overline{u_\infty(\omega t + \frac{1}{2}\pi)\, u}$ were computed electronically by the network shown in figure 5. The components of the computing network employed Philbrick-type, operational amplifiers and the multipliers were Philbrick GAP/R MODEL MU/DV.

Measurements

Except for preliminary surveys, the majority of the measurements were made at a distance of 98 in. from the boundary-layer tripping device. However, the 48 cycles/sec measurements were made at 114 in.

The free stream mean velocity was approximately 17·5 ft./sec for all experiments, except for 0·33 cycles/sec and the quasi-steady case, which were carried out at a mean velocity of 15 ft./sec. In either case the turbulent boundary-layer thickness was approximately 3 in. and the Reynolds number based on the free stream mean velocity and boundary displacement thickness was about $3{\cdot}6 \times 10^3$. At 17·5 ft./sec the local skin friction coefficient, c_f, was approximately 0·0034, as determined by the 'law of the wall' (Clauser 1954).

Boundary-layer measurements were carried out at the following frequencies: 0 (quasi-steady), 0·33, 0·66, 1, 1·33, 2, 4, 7·65 and 48 cycles/sec. At each frequency, except 0 and 48 cycles/sec, measurements were made at free stream fluctuation amplitudes varying from about 8 to 34 % of the free stream mean velocity. For 0 and 48 cycles/sec, results were obtained for single free stream amplitudes of 30 and 34 %, respectively. The quantities measured during each boundary layer survey were mean velocity, amplitudes of in- and out-of-phase components of the fundamental frequency and turbulence intensity level. The experimental results are plotted in figures 6 to 14.

The quasi-steady or slowly oscillating case was computed graphically from a series of steady boundary-layer measurements, following in principle the same procedures as for the laminar case discussed previously. The results for the turbu-

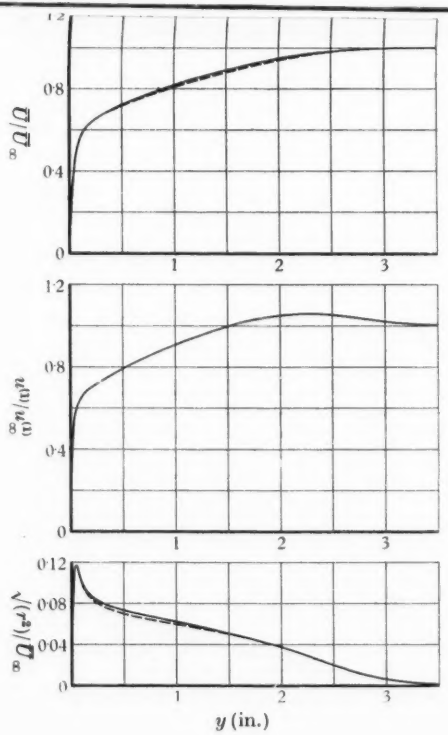

FIGURE 6

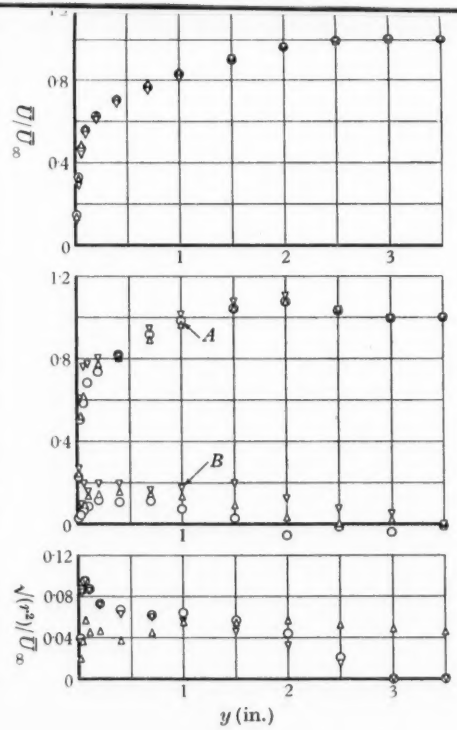

FIGURE 7

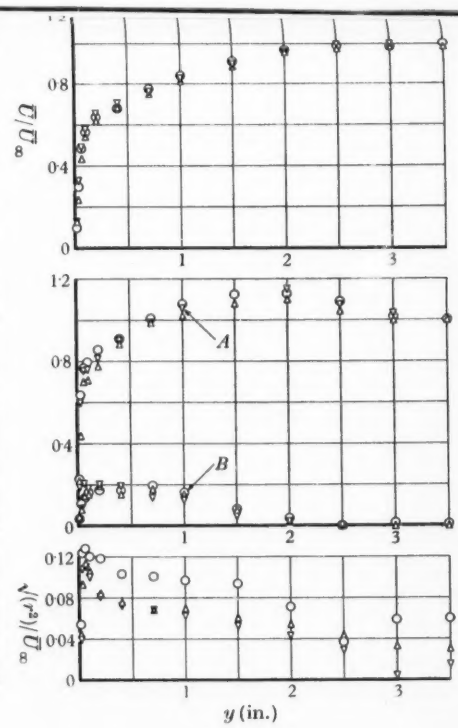

FIGURE 8

FIGURE 6. The quasi-steady (slowly varying) turbulent layer. ——— $u^{(1)}_\infty/\overline{U}_\infty = 30\,\%$, — — — $u^{(1)}_\infty/\overline{U}_\infty = 0$.

FIGURE 7. Results for the unsteady turbulent layer. $\omega/2\pi = 0{\cdot}33$ cycles/sec; $u^{(1)}_\infty/\overline{U}_\infty = 29{\cdot}2\,\%$ (○), $20{\cdot}2\,\%$ (△), $14{\cdot}7\,\%$ (▽). $A = u^{(1)}\cos\phi/u^{(1)}_\infty$, $B = u^{(1)}\sin\phi/u^{(1)}_\infty$.

FIGURE 8. Results for the unsteady turbulent layer. $\omega/2\pi = 0{\cdot}66$ cycles/sec; $u^{(1)}_\infty/\overline{U}_\infty = 34{\cdot}0\,\%$ (○), $14{\cdot}9\,\%$ (△), $11{\cdot}2\,\%$ (▽). $A = u^{(1)}\cos\phi/u^{(1)}_\infty$, $B = u^{(1)}\sin\phi/u^{(1)}_\infty$.

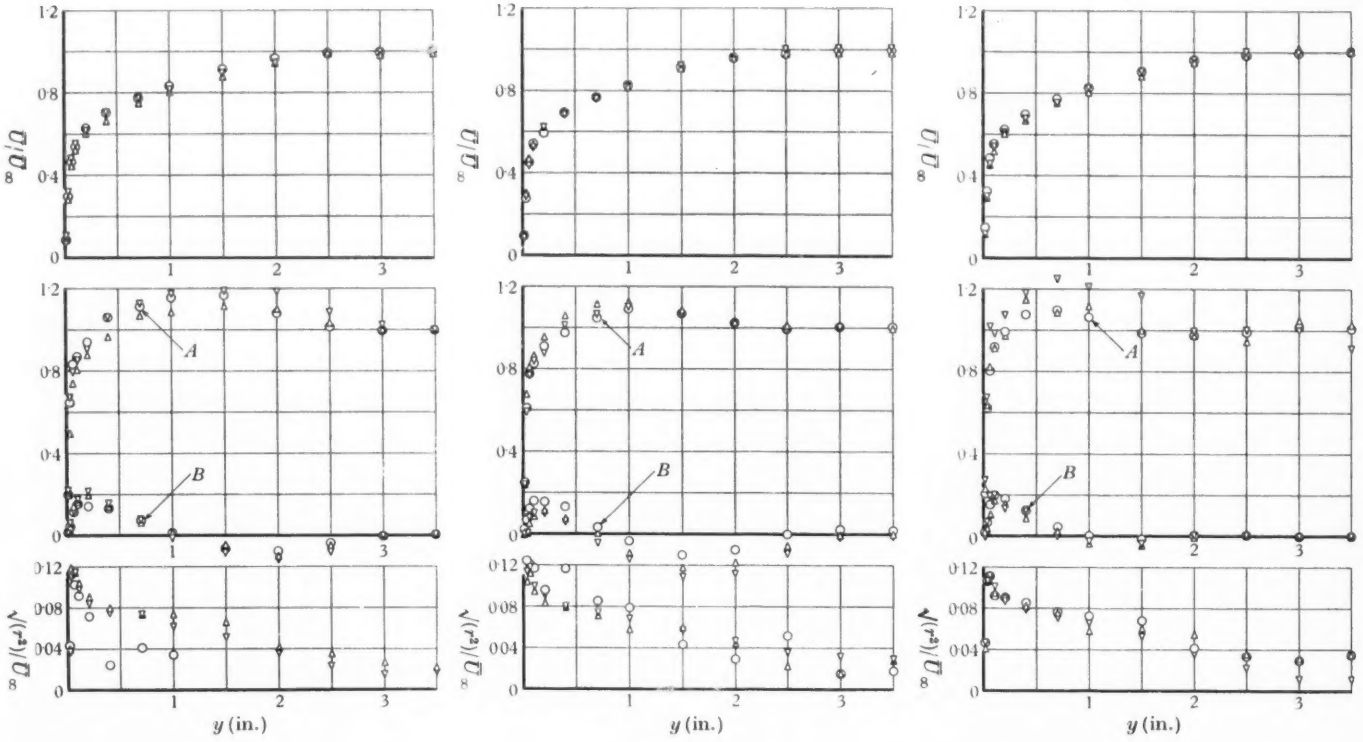

FIGURE 9

FIGURE 10

FIGURE 11

FIGURE 9. Results for the unsteady turbulent layer. $\omega/2\pi = 1{\cdot}0$ cycles/sec; $u_\infty^{(1)}/\overline{U}_\infty = 35{\cdot}2\%$ (○), $19{\cdot}5\%$ (△), $10{\cdot}7\%$ (▽). $A = u^{(1)}\cos\phi/u_\infty^{(1)}$, $B = u^{(1)}\sin\phi/u_\infty^{(1)}$.

FIGURE 10. Results for the unsteady turbulent layer. $\omega/2\pi = 1{\cdot}33$ cycles/sec; $u_\infty^{(1)}/\overline{U}_\infty = 34{\cdot}4\%$ (○), $21{\cdot}5\%$ (△), $13{\cdot}0\%$ (▽). $A = u^{(1)}\cos\phi/u_\infty^{(1)}$, $B = u^{(1)}\sin\phi/u_\infty^{(1)}$.

FIGURE 11. Results for the unsteady turbulent layer. $\omega/2\pi = 2{\cdot}0$ cycles/sec; $u_\infty^{(1)}/\overline{U}_\infty = 28{\cdot}6\%$ (○), $17{\cdot}6\%$ (△), $8{\cdot}1\%$ (▽). $A = u^{(1)}\cos\phi/u_\infty^{(1)}$. $B = u^{(1)}\sin\phi/u_\infty^{(1)}$.

$B = u^{(1)} \sin\phi/u_\infty^{(1)}$.

FIGURE 11. Results for the unsteady turbulent layer. $\omega/2\pi = 2{\cdot}0$ cycles/sec; $u_\infty^{(1)}/\overline{U}_\infty = 28{\cdot}6\%$ (○), $17{\cdot}6\%$ (△), $8{\cdot}1\%$ (▽). $A = u^{(1)}\cos\phi/u_\infty^{(1)}$. $B = u^{(1)}\sin\phi/u_\infty^{(1)}$.

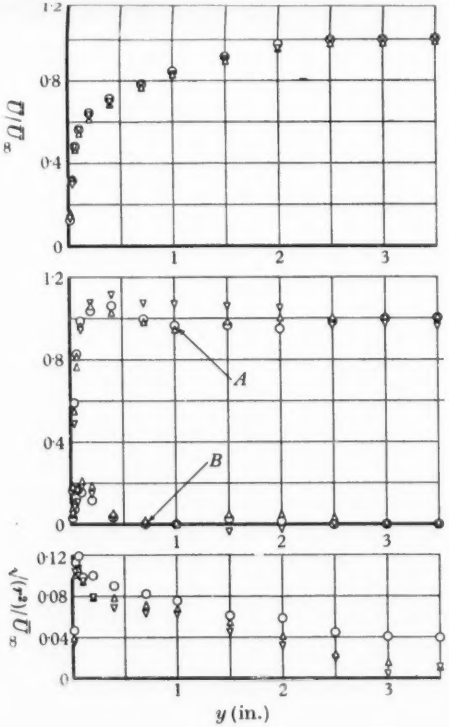

FIGURE 12

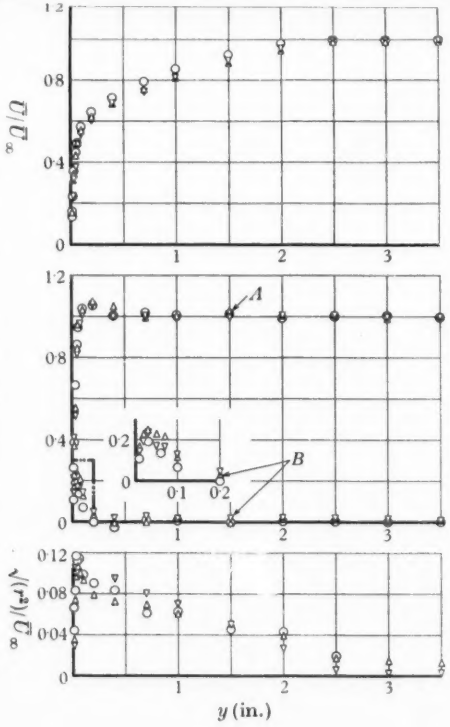

FIGURE 13

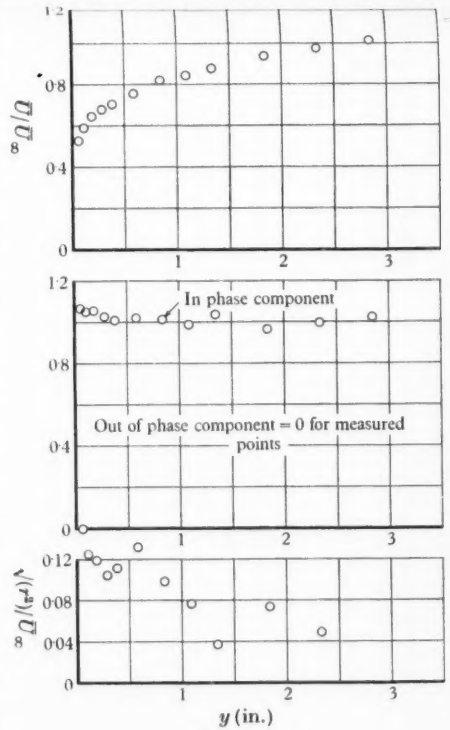

FIGURE 14

FIGURE 12. Results for the unsteady turbulent layer. $\omega/2\pi = 4{\cdot}0$ cycles/sec; $u_\infty^{(1)}/\overline{U}_\infty = 26{\cdot}4\%$ (○), $13{\cdot}6\%$ (△), $6{\cdot}2\%$ (▽). $A = u^{(1)}\cos\phi/u_\infty^{(1)}$, $B = u^{(1)}\sin\phi/u_\infty^{(1)}$.

FIGURE 13. Results for the unsteady turbulent layer. $\omega/2\pi = 7{\cdot}65$ cycles/sec; $u_\infty^{(1)}/\overline{U}_\infty = 29{\cdot}7\%$ (○), $12{\cdot}7\%$ (△), $7{\cdot}3\%$ (▽). $A = u^{(1)}\cos\phi/u_\infty^{(1)}$, $B = u^{(1)}\sin\phi/u_\infty^{(1)}$.

FIGURE 14. Results for the unsteady turbulent layer $\omega/2\pi = 48$ cycles/sec; $u_\infty^{(1)}/\overline{U}_\infty = 34\%$ (○).

lent layer are shown in figure 6 along with the profile whose free stream velocity is the same as the mean for the oscillating case. A comparison between the two profiles points out the interesting fact that the effect of non-linearity in the quasi-steady case is to *increase* the mean velocity over the major part of the profile! This gives the appearance of a thinner boundary layer and actually the displacement and momentum thicknesses are less than for the steady layer. However, although it does not show up very clearly on the graph, the mean profile is somewhat thicker and the mean shear stress at the wall is 4 % greater than in the steady case. The amplitude of the sinusoidal fluctuations increases very rapidly near the wall, then at a slower rate and reaches a maximum not far from the outer edge of the boundary layer. Non-linear effects on the fundamental frequency are almost nil at this amplitude. A slight effect is observed on the turbulence level.

For the unsteady boundary layer, figures 7 to 14, no systematic variation in the mean velocity profiles with fluctuation amplitude or frequency can be detected. This is really not so surprising, in view of the remarkably small effect on non-linearity on the quasi-steady profile.

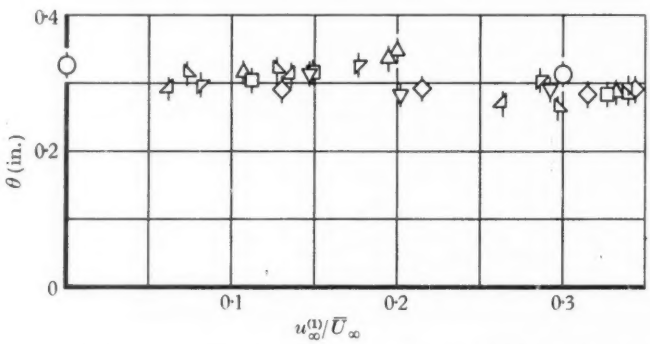

FIGURE 15. The momentum thickness (cycles/sec): ○, Quasi-steady; ▽, 0·33; □, 0·66; △, 1·0; ◇, 1·33; ▽, 2·0; ◿, 4·0; ◺, 7·65; ◹, 48·0.

Unfortunately, hot-wire measurements of this kind are plagued with sizeable random as well as systematic errors. A somewhat conservative estimate of the maximum possible error in the mean velocity profile is ± 2 %, of which half may be due to the uncertainty in the calibration of the hot-wires. The existence of this last error is in evidence at the outer edge of some of the profiles, which do not approach 1·0 exactly, although the stationary and traversing wires are measuring the same velocity.

In view of this we cannot state accurately what the effect of free stream oscillations are on the mean velocity profile. However, we can draw the following important conclusion. The change in the mean velocity profile is quite small, even when the fluctuation amplitude in the free stream is as high as 30 %.

The momentum thickness, $\theta = \int_0^\infty \frac{\overline{U}}{\overline{U}_\infty}\left(1-\frac{\overline{U}}{\overline{U}_\infty}\right)dy$, of the mean profiles has been plotted in figure 15 versus the free stream fluctuation amplitude. The vertical lines

through the points indicate the possible deviation due to a $\pm 0{\cdot}01$ systematic error in the mean profile.

The in-phase $\{(u^{(1)}/u_\infty^{(1)})\cos\phi\}$ and out-of-phase $\{(u^{(1)}/u_\infty^{(1)})\sin\phi\}$ components of the first harmonic of the boundary-layer fluctuations are also plotted in figures 7 to 14. It is estimated that the possible error in these measurements is about $\pm 5\,\%$ of the free stream fluctuation amplitude. The error is partly systematic, partly random. The reason for the large relative error for the out-of-phase component is primarily the difficulty in averaging this quantity, which has large, slow fluctuations.

Nevertheless, the measurements give a good description of the behaviour of the periodic fluctuations throughout the boundary layer and for different frequencies. At the lowest frequency of 0·33 cycle/sec, the in-phase component is very nearly the same as the amplitude of the quasi-steady oscillations. However, a positive out-of-phase component has also developed, indicating that the oscillations in the boundary layer are ahead of those in the free stream. This agrees with the behaviour of the corresponding laminar boundary layer. As pointed out by Lighthill (1954) such a phase advance in the boundary layer is to be expected, since the fluctuating pressure gradient acting on the slow moving fluid in the boundary layer is the same as the one necessary to accelerate the free stream. The same acceleration results in a greater relative change of velocity in the boundary layer than in the free stream.

The effect of increasing frequency upon the in-phase component of fluctuation amplitude is to bring the maximum value closer to the wall. The out-of-phase component becomes negative for the outer portion of the boundary layer at 1 cycle/sec, indicating that there is a lag in the fluctuations here relative to the free stream. This lag is still present at 1·33 cycles/sec, but for higher frequencies it is decreased and eventually disappears, as the region over which the fluctuations are affected by the presence of the wall becomes thinner. For the region close to the wall the out-of-phase component is positive for all the frequencies. The largest measured phase shift occurs at 7·65 cycles/sec and is approximately 35° at $y = 0{\cdot}010$ in., which is well within the laminar sublayer. A consistent effect of amplitude cannot be detected, and one must conclude that this effect is so small that it is obscured by the experimental errors.

At 48 cycles/sec the periodic fluctuations differ from those in the free stream only in a very thin layer near the wall. For this frequency the 'Rayleigh thickness', $\sqrt{(2\nu/\omega)}$, is about 0·012 in. This is less than half of the laminar sublayer thickness, which is here approximately 0·030 in. Comparing this case with that treated by Lighthill (1954), we may expect that the fluctuations are of the 'shear wave' type. It was not possible to check this experimentally, because the flow was reversed in direction during part of the period from $y = 0$ to about $y = 0{\cdot}030$ in. Since the hot-wire anemometer senses only magnitude of velocity, it cannot be used effectively to gain quantitative information about a flow that has reversals in velocity.

The measured turbulence intensity (and higher harmonics) is shown at the bottom of figures 7 to 14. The accuracy of these results is rather poor, since they are obtained by subtracting two quantities that are usually considerably larger

than the difference. This is especially true for the outer portion of the layer. In the vicinity of the wall, where the turbulence intensity is greatest, the estimated possible error is $\pm 8\%$. Within these limits the maximum turbulence level measured for the oscillating case agrees with the steady layer.

Conclusion

The experimental investigation of the zero-pressure gradient-turbulent boundary layer with a sinusoidally fluctuating free stream was intended as an initial effort in the study of unsteady turbulent boundary layers. One of the most remarkable results of this work was that the effect due to non-linear interaction was quite small, even for fluctuation amplitudes as large as 34% of the free stream velocity. Hence, transient zero-pressure gradient boundary layers, which at any given instant do not deviate very much from the steady layer, corresponding to the instantaneous free stream velocity, can be predicted using linear methods. To perform this computation it is sufficient to know the response of the layer to small sinusoidal free stream fluctuations at all frequencies. The measurements here give this response for a Reynolds number of $R_\delta^* \sim 3{\cdot}6 \times 10^3$.

The author wishes to express his appreciation to Dr F. H. Clauser, who through many helpful suggestions contributed greatly to the accomplishment of this work, and to Dr M. V. Morkovin for many stimulating discussions.

This investigation was supported by the Flight Propulsion Laboratory Department, General Electric Company, Cincinnati, Ohio.

REFERENCES

Clauser, F. H. 1954 Turbulent boundary layers in adverse pressure gradients. *J. Aero Sci.* **21**, 91.

Johnson, D. S. 1957 Velocity, temperature and heat-transfer measurements in a turbulent boundary layer downstream of a stepwise discontinuity in wall temperature. *J. Appl. Mech.* **24**, 2.

Karlsson, S. K. F. 1958 *An unsteady turbulent boundary layer.* Doctoral thesis. Department of Aeronautics, Johns Hopkins University.

Kovasznay, L. S. G. 1948 *Simple analysis of the constant temperature hot-wire anemometer.* Department of Aeronautics, Johns Hopkins University.

Kovasznay, L. S. G. 1958 SQUID project. *Semi-Annual Progress Report* (April 1, 1958). Johns Hopkins University.

Lighthill, M. J. 1954 The response of laminar skin friction and heat transfer to fluctuations in stream velocity. *Proc. Roy. Soc.* A, **224**, 1.

A cylindrical sound pulse in a rotating gas

By L. E. FRAENKEL

Aeronautics Department, Imperial College, London*

(Received 29 October 1958)

This paper deals with the propagation of a sound pulse into a gas which initially has solid-body rotation and constant temperature, the initial pressure and density increasing outwards like e^x, where x is the square of a certain dimensionless radial co-ordinate. The perturbations are due to a source-like disturbance on the axis of symmetry, which begins to act at time $t = 0$: most attention is paid to source strengths which vary in time like a Dirac pulse or a step function, but the following remarks apply generally.

Immediately behind the wave front the perturbation velocity and temperature decay like $e^{-\frac{1}{2}x}$, while the (absolute) perturbation pressure and density grow like $e^{\frac{1}{2}x}$ (the relative pressure and density increments, which are referred to local conditions in the undisturbed state, then also decay like $e^{-\frac{1}{2}x}$). The rotation also introduces oscillations in flows which, with the same disturbance at the origin and no rotation, would vary monotonically with time at a given point.

1. Introduction

The problem studied in this paper is the following. An infinite mass of perfect gas rotates with constant angular velocity about an axis of symmetry and is at constant temperature: the pressure and density increase radially. At time $t = 0$ a weak release of mass or of energy begins at the axis, or a small cylinder begins to expand there, so that cylindrical sound waves radiate outwards. This problem seems worth while for two reasons. First, interest has recently revived in all flows of a fluid with solid-body rotation: these are simple examples of flows in which vorticity plays an important role. Secondly, the problem involves the study of sound waves propagating into a variable medium.

The rotation introduces two principal effects. On a linearized theory the Coriolis force restrains radial displacements of a fluid particle in precisely the same way that a spring restrains the motion of a solid particle, and this effect would be expected to give the flow an oscillatory character. In incompressible flows of a rotating fluid with an axial velocity (see, for example, Squire 1956) this oscillatory behaviour is very evident. In addition, the variable pressure of the undisturbed medium introduces a damping effect which dominates conditions immediately behind the wave front.

* This work was done while the author was at the Guggenheim Aeronautical Laboratory, California Institute of Technology.

2. Formulation

Let (r, θ) be polar co-ordinates, (u, v) the corresponding components of velocity, (p, ρ, T) the pressure, density and temperature, c the sound speed, and γ the specific-heat ratio of a perfect gas. Conditions in the undisturbed state are denoted by suffix $(\,)_0$, and perturbations by suffix $(\,)_1$.

For the undisturbed state we take steady, solid-body rotation and constant temperature:

$$u_0 = 0, \quad v_0 = \Omega r, \quad T_0 = \text{constant}. \tag{2.1}$$

The radial momentum equation becomes

$$\frac{(\Omega r)^2}{r} = \frac{1}{\rho_0} p_{0r} = \frac{c_0^2}{\gamma} \frac{p_{0r}}{p_0},$$

where lettered suffices denote partial differentiation; hence

$$p_0(r) = p_0(0) \exp\left(\frac{\gamma \Omega^2 r^2}{2c_0^2}\right), \quad \rho_0(r) = \frac{p_0(0)\,\gamma}{c_0^2} \exp\left(\frac{\gamma \Omega^2 r^2}{2c_0^2}\right). \tag{2.2}$$

The rates of strain and viscous stresses all vanish, and there is no dissipation, no heat conduction, and no change of entropy along a streamline, so that this basic flow is an exact solution of the Navier–Stokes equations. The basic state is presumably that which would result in the laboratory from the prolonged spinning of a cylindrical container of gas.

Henceforth we neglect viscosity and heat conduction. The disturbances are to be functions of (r, t) only, and there is no velocity parallel to the axis. In writing the equations of motion, we permit the existence of weak distributed mass and heat sources of strength $Q^{(m)}$ and $Q^{(h)}$, respectively. Then

$$(r\rho)_t + (r\rho u)_r = rQ^{(m)}, \tag{2.3}$$

$$\left(\frac{\partial}{\partial t} + u\frac{\partial}{\partial r}\right) u - \frac{v^2}{r} = -\frac{1}{\rho} p_r, \tag{2.4}$$

$$\left(\frac{\partial}{\partial t} + u\frac{\partial}{\partial r}\right) (vr) = 0, \tag{2.5}$$

$$\left(\frac{\partial}{\partial t} + u\frac{\partial}{\partial r}\right) \frac{p}{\rho^\gamma} = \frac{\gamma - 1}{\rho^\gamma} Q^{(h)}. \tag{2.6}$$

Writing $p = p_0(r) + p_1(r, t)$, etc., and linearizing the disturbance terms, we obtain

$$(r\rho_1)_t + (r\rho_0 u_1)_r = rQ^{(m)}, \tag{2.7}$$

$$u_{1t} - 2\Omega v_1 = -\frac{1}{\rho_0} p_{1r} + \frac{\rho_1}{\rho_0^2} p_{0r}, \tag{2.8}$$

$$v_{1t} + 2\Omega u_1 = 0, \tag{2.9}$$

$$p_{1t} - c_0^2 \rho_{1t} - (\gamma - 1)\, p_{0r} u_1 = (\gamma - 1) Q^{(h)}. \tag{2.10}$$

If ξ is a radial displacement, such that $\xi_t = u_1$ to first order, the momentum equations (2.8) and (2.9) may be written

$$\xi_{tt} + 4\Omega^2 \xi = -\frac{1}{\rho_0} p_{1r} + \frac{\rho_1}{\rho_0^2} p_{0r},$$

which shows the spring-like effect of the Coriolis terms.

It is convenient to introduce $r\rho_0 u_1 = q$, say, in place of u_1. The function q is $1/2\pi$ times the mass flow across a circle r = constant and will be called the 'outflow'. Cross-differentiating (2.8) and (2.10) to eliminate p_1, and substituting for ρ_{1t} from (2.7) and for v_{1t} from (2.9), we obtain

$$q_{rr} - \frac{1}{r} q_r - \frac{1}{c_0^2} q_{tt} - \frac{\gamma\Omega^2}{c_0^2} r q_r - \frac{4\Omega^2}{c_0^2} q = r Q_r^{(m)} - \frac{\Omega^2 r^2}{c_0^2} Q^{(m)} + \frac{\gamma - 1}{c_0^2} r Q_r^{(h)}. \tag{2.11}$$

We have retained source terms only to show that mass and heat sources on the axis make similar contributions: hereafter we consider only sources on the axis, and incorporate their presence in boundary conditions; the equations will be written for source-free flow.

In terms of $u_1 (= u)$ equation (2.11) is then

$$u_{rr} + \frac{1}{r} u_r - \frac{1}{r^2} u - \frac{1}{c_0^2} u_{tt} + \frac{\gamma\Omega^2}{c_0^2} r u_r - (4 - \gamma) \frac{\Omega^2}{c_0^2} u = 0. \tag{2.12}$$

Alternatively, we may introduce a stream function ψ such that

$$\psi_t = r\rho_0 u_1 = q, \quad \psi_r = -r\rho_1, \tag{2.13}$$

and such that $\psi = 0$ ahead of the wave front bounding the disturbed region; ψ is then $1/2\pi$ times the perturbation mass between infinity and a circle r = constant. If (2.11) is integrated with respect to time, the arbitrary function of r which occurs is zero in view of conditions ahead of the wave front, and there results

$$\psi_{rr} - \frac{1}{r} \psi_r - \frac{1}{c_0^2} \psi_{tt} - \frac{\gamma\Omega^2}{c_0^2} r\psi_r - \frac{4\Omega^2}{c_0^2} \psi = 0. \tag{2.14}$$

u_1 and ρ_1 are given in terms of ψ by (2.13), and

$$\left.\begin{aligned} v_1 &= -\frac{2\Omega}{r\rho_0} \psi, \\ p_1 &= (\gamma - 1)\,\Omega^2 \psi - c_0^2 \frac{\psi_r}{r}, \\ c_1 &= \frac{\gamma - 1}{2} \frac{c_0}{p_0} \left(\Omega^2 \psi - \frac{c_0^2}{\gamma} \frac{\psi_r}{r} \right). \end{aligned}\right\} \tag{2.15}$$

Equations (2.12) and (2.14) involve the wave equation operator together with a damping term (of opposite sign in the two equations) and a stiffness term.

3. The propagation of weak shocks and expansion waves

The importance of the damping term immediately behind a wave front can be seen rather simply. We introduce characteristic variables $c_0 t + r = \alpha$, $c_0 t - r = \beta$, and write $\gamma\Omega^2/2c_0^2 = k$; then (2.14) becomes

$$4\psi_{\alpha\beta} + \left\{ \frac{2}{(\alpha - \beta)} + k(\alpha - \beta) \right\} (\psi_\alpha - \psi_\beta) + \frac{4\Omega^2}{c_0^2} \psi = 0. \tag{3.1}$$

If now ψ_β is discontinuous across $\beta = b$, say, while ψ, the perturbation mass, is continuous, we write

$$[\psi_\beta]_{b-}^{b+} = \frac{1}{2} \left[\frac{r\rho_0 u_1}{c_0} + r\rho_1 \right]_{b-}^{b+} = j(\alpha),$$

and obtain from (3.1)

$$4j_\alpha - \left\{\frac{2}{\alpha - b} + k(\alpha - b)\right\} j = 0,$$

which may be integrated to

$$j = \text{const.}\, r^{\frac{1}{2}} \exp\left(\tfrac{1}{2}kr^2\right).$$

Then, by (2.2),

$$\left[\frac{u_1}{c_0} + \frac{\rho_1}{\rho_0}\right]_{b-}^{b+} = \epsilon r^{-\frac{1}{2}} \exp\left(-\tfrac{1}{2}kr^2\right), \tag{3.2}$$

where ϵ is a (small) constant. Also, since ψ_α is continuous,

$$\left[\frac{u_1}{c_0} - \frac{\rho_1}{\rho_0}\right]_{b-}^{b+} = 0, \tag{3.3}$$

and since ψ is continuous, (2.15) shows that

$$[v_1]_{b-}^{b+} = 0, \quad [p_1 - c_0^2 \rho_1]_{b-}^{b+} = 0, \quad \left[\frac{c_1}{c_0} - \frac{\gamma - 1}{2}\frac{\rho_1}{\rho_0}\right]_{b-}^{b+} = 0. \tag{3.4}$$

These equations show that the strength of a shock ($\epsilon > 0$) or centred expansion wave ($\epsilon < 0$), as measured by the relative perturbations of the linear theory, decays rapidly when rotation is present ($k > 0$). Note that the Coriolis force, which is represented by the last term of (3.1), played no part in the derivation of this result. The effect is due to the fact that the shock (say) is propagating into a region of increasing pressure and density, so that compressive wavelets are continuously reflected back towards the axis along the other family of characteristics, and this reduces the relative shock strength. These reflexions are not of a conventional type. If we imagine the undisturbed gas to be divided into a large number of annular layers, in each of which the pressure and density are constant, we must also imagine that cylindrical 'membranes', representing the centrifugal force which actually balances the pressure gradient, separate the layers and support the pressure differences. It is difficult to draw conclusions from this model, because the conditions that apply across the membranes in the disturbed state are not obvious, but we may observe that the membranes are fairly 'rigid' in the following sense. Whereas they initially *support* pressure differences according to the law

$$\frac{\delta p_0}{p_0} = 2kr\,\delta r,$$

where δr is the width of an annular layer, they only *transmit* pressure behind a shock according to the law

$$\frac{\delta p_1}{p_1} = kr\,\delta r.$$

(The attenuation represented by the $r^{-\frac{1}{2}}$ in (3.2) has nothing to do with the membranes.)

To obtain a slightly more realistic picture of the propagation of a discontinuity than that given by the simple linearized theory, we apply the method of Whitham (1952). Since no real disturbance can be completely concentrated on the axis, we suppose that the perturbations are due to a cylinder $r = R(t)$ ($R' \ll c_0$). In the

linearized solution $c_0 t$ is now replaced by $\beta + r$, where β is to be interpreted as constant on a characteristic curve of a higher approximation, and is defined by

$$\frac{1}{c_0}\left(\frac{dr}{dt}\right)_{\beta \text{ const.}} = 1 + \frac{u_1 + c_1}{c_0} + \ldots, \quad \beta = c_0 t - r \quad \text{on} \quad r = R(t). \tag{3.5}$$

If the equation $r = R(\{\beta + r\}/c_0)$ is written $r = R^*(\beta)$, we then have

$$\left.\begin{aligned} u_1 &= u_1(r, \beta), \quad c_1 = c_1(r, \beta), \\ c_0 t - r &= \beta - \int_{R^*(\beta)}^{r} \frac{u_1(y, \beta) + c_1(y, \beta)}{c_0}\, dy. \end{aligned}\right\} \tag{3.6}$$

Two criticisms can be made of this representation in the present context: (i) the α-characteristics and the particle paths now also carry significant disturbances, and (ii) the algebra of the solution (u_1, c_1) is so complicated that (3.6) is not actually usable. Accordingly, we restrict attention to the case of a shock or expansion fan moving into undisturbed fluid; neither objection then is relevant. Let $R(t) = R_0$ for $t \leqslant R_0/c_0$, and let R' be discontinuous at $t = R_0/c_0$ such that

$$R'\left(\frac{R_0 + 0}{c_0}\right) = \eta.$$

Equations (3.2) to (3.4) apply, with $\beta = b = 0$, and with

$$\epsilon = \frac{2\eta}{c_0} R_0^{\frac{1}{2}} \exp\left(\tfrac{1}{2} k R_0^2\right).$$

By (3.6) the curves $\beta = 0-$ and $\beta = 0+$ become (figure 1)

$$\left.\begin{aligned} \beta = 0-: &\quad c_0 t - r = 0, \\ \beta = 0+: &\quad c_0 t - r = -\frac{\gamma + 1}{4}\, \epsilon \int_{R_0}^{r} y^{-\frac{1}{2}} \exp\left(-\tfrac{1}{2} k y^2\right) dy, \end{aligned}\right\} \tag{3.7}$$

where the integral can be expressed in terms of the incomplete gamma function. Hence for a shock ($\epsilon > 0$) the regions $\beta < 0$ and $\beta > 0$ overlap in the rt-plane, while for an expansion wave there is a gap between these domains in the rt-plane. The significant point is that, whereas with $k = 0$ the width of these regions is $O(\epsilon r^{\frac{1}{2}})$ for $r \to \infty$, it is now $O(\epsilon)$. Hence in the case of a shock, only a narrow band of characteristics $|\beta| \leqslant O(\epsilon)$ enters the overlapping region in which the shock must lie.

To fit the shock, $t = t_s(r)$ say, we note that to our approximation the shock equations are as follows ([ ] and $\overline{(\ )}$ now denote discontinuities and mean values across the shock):

$$\left[\frac{u_1}{c_0} - \frac{\rho_1}{\rho_0}\right] = 0, \quad [p_1 - c_0^2 \rho_1] = 0, \quad [v_1] = 0, \tag{3.8}$$

$$c_0 \frac{dt_s}{dr} = 1 - \frac{\overline{(u_1 + c_1)}}{c_0}. \tag{3.9}$$

If k is bounded away from zero, the shock may be drawn halfway between $\beta = 0-$ and $\beta = 0+$, so that

$$c_0 t_s = r - \frac{\gamma + 1}{8}\, \epsilon \int_{R_0}^{r} y^{-\frac{1}{2}} \exp\left(-\tfrac{1}{2} k y^2\right) dy, \tag{3.10}$$

and obtain from (3.1)

$$4j_\alpha - \left\{\frac{2}{\alpha - b} + k(\alpha - b)\right\} j = 0,$$

which may be integrated to

$$j = \text{const.}\, r^{\frac{1}{2}} \exp\left(\tfrac{1}{2}kr^2\right).$$

Then, by (2.2),

$$\left[\frac{u_1}{c_0} + \frac{\rho_1}{\rho_0}\right]_{b-}^{b+} = \epsilon r^{-\frac{1}{2}} \exp\left(-\tfrac{1}{2}kr^2\right), \tag{3.2}$$

where ϵ is a (small) constant. Also, since ψ_α is continuous,

$$\left[\frac{u_1}{c_0} - \frac{\rho_1}{\rho_0}\right]_{b-}^{b+} = 0, \tag{3.3}$$

and since ψ is continuous, (2.15) shows that

$$[v_1]_{b-}^{b+} = 0, \quad [p_1 - c_0^2 \rho_1]_{b-}^{b+} = 0, \quad \left[\frac{c_1}{c_0} - \frac{\gamma - 1}{2}\frac{\rho_1}{\rho_0}\right]_{b-}^{b+} = 0. \tag{3.4}$$

These equations show that the strength of a shock ($\epsilon > 0$) or centred expansion wave ($\epsilon < 0$), as measured by the relative perturbations of the linear theory, decays rapidly when rotation is present ($k > 0$). Note that the Coriolis force, which is represented by the last term of (3.1), played no part in the derivation of this result. The effect is due to the fact that the shock (say) is propagating into a region of increasing pressure and density, so that compressive wavelets are continuously reflected back towards the axis along the other family of characteristics, and this reduces the relative shock strength. These reflexions are not of a conventional type. If we imagine the undisturbed gas to be divided into a large number of annular layers, in each of which the pressure and density are constant, we must also imagine that cylindrical 'membranes', representing the centrifugal force which actually balances the pressure gradient, separate the layers and support the pressure differences. It is difficult to draw conclusions from this model, because the conditions that apply across the membranes in the disturbed state are not obvious, but we may observe that the membranes are fairly 'rigid' in the following sense. Whereas they initially *support* pressure differences according to the law

$$\frac{\delta p_0}{p_0} = 2kr\,\delta r,$$

where δr is the width of an annular layer, they only *transmit* pressure behind a shock according to the law

$$\frac{\delta p_1}{p_1} = kr\,\delta r.$$

(The attenuation represented by the $r^{-\frac{1}{2}}$ in (3.2) has nothing to do with the membranes.)

To obtain a slightly more realistic picture of the propagation of a discontinuity than that given by the simple linearized theory, we apply the method of Whitham (1952). Since no real disturbance can be completely concentrated on the axis, we suppose that the perturbations are due to a cylinder $r = R(t)$ ($R' \ll c_0$). In the

linearized solution $c_0 t$ is now replaced by $\beta + r$, where β is to be interpreted as constant on a characteristic curve of a higher approximation, and is defined by

$$\frac{1}{c_0}\left(\frac{dr}{dt}\right)_{\beta \text{ const.}} = 1 + \frac{u_1 + c_1}{c_0} + \ldots, \quad \beta = c_0 t - r \quad \text{on} \quad r = R(t). \tag{3.5}$$

If the equation $r = R(\{\beta + r\}/c_0)$ is written $r = R^*(\beta)$, we then have

$$\left.\begin{aligned} u_1 &= u_1(r, \beta), \quad c_1 = c_1(r, \beta), \\ c_0 t - r &= \beta - \int_{R^*(\beta)}^{r} \frac{u_1(y, \beta) + c_1(y, \beta)}{c_0}\, dy. \end{aligned}\right\} \tag{3.6}$$

Two criticisms can be made of this representation in the present context: (i) the x-characteristics and the particle paths now also carry significant disturbances, and (ii) the algebra of the solution (u_1, c_1) is so complicated that (3.6) is not actually usable. Accordingly, we restrict attention to the case of a shock or expansion fan moving into undisturbed fluid; neither objection then is relevant. Let $R(t) = R_0$ for $t \leqslant R_0/c_0$, and let R' be discontinuous at $t = R_0/c_0$ such that

$$R'\left(\frac{R_0 + 0}{c_0}\right) = \eta.$$

Equations (3.2) to (3.4) apply, with $\beta = b = 0$, and with

$$\epsilon = \frac{2\eta}{c_0} R_0^{\frac{1}{2}} \exp\left(\tfrac{1}{2} k R_0^2\right).$$

By (3.6) the curves $\beta = 0-$ and $\beta = 0+$ become (figure 1)

$$\left.\begin{aligned} \beta = 0-: &\quad c_0 t - r = 0, \\ \beta = 0+: &\quad c_0 t - r = -\frac{\gamma + 1}{4}\, \epsilon \int_{R_0}^{r} y^{-\frac{1}{2}} \exp\left(-\tfrac{1}{2} k y^2\right) dy, \end{aligned}\right\} \tag{3.7}$$

where the integral can be expressed in terms of the incomplete gamma function. Hence for a shock ($\epsilon > 0$) the regions $\beta < 0$ and $\beta > 0$ overlap in the rt-plane, while for an expansion wave there is a gap between these domains in the rt-plane. The significant point is that, whereas with $k = 0$ the width of these regions is $O(\epsilon r^{\frac{1}{2}})$ for $r \to \infty$, it is now $O(\epsilon)$. Hence in the case of a shock, only a narrow band of characteristics $|\beta| \leqslant O(\epsilon)$ enters the overlapping region in which the shock must lie.

To fit the shock, $t = t_s(r)$ say, we note that to our approximation the shock equations are as follows ([ ] and $\overline{\ }$ now denote discontinuities and mean values across the shock):

$$\left[\frac{u_1}{c_0} - \frac{\rho_1}{\rho_0}\right] = 0, \quad [p_1 - c_0^2 \rho_1] = 0, \quad [v_1] = 0, \tag{3.8}$$

$$c_0 \frac{dt_s}{dr} = 1 - \frac{\overline{(u_1 + c_1)}}{c_0}. \tag{3.9}$$

If k is bounded away from zero, the shock may be drawn halfway between $\beta = 0-$ and $\beta = 0+$, so that

$$c_0 t_s = r - \frac{\gamma + 1}{8}\, \epsilon \int_{R_0}^{r} y^{-\frac{1}{2}} \exp\left(-\tfrac{1}{2} k y^2\right) dy, \tag{3.10}$$

and the shock conditions are satisfied to sufficient accuracy. For, by (3·3) and (3.4), the equations (3.8) are satisfied exactly across $\beta = 0$; the shock now lies at $\beta = -|O(\epsilon)|$ and $\beta = |O(\epsilon)|$, and since variations with β are continuous on either side of $\beta = 0$, the equations (3.8) are still satisfied within an error of $O(\epsilon^2)$. Similarly, the characteristic slopes at the shock will be those of $\beta = 0-$ and $\beta = 0+$ within an error of $O(\epsilon^2)$, so that (3.9) is satisfied to sufficient accuracy.

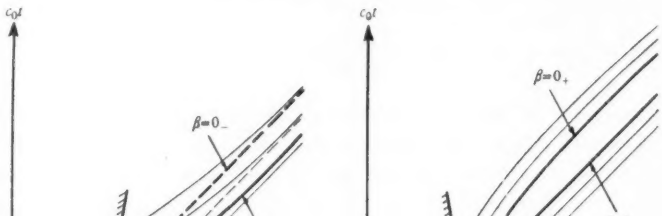

FIGURE 1. (*a*) The 'overlapping region' near a shock; (*b*) the 'gap' produced by a centred expansion wave. Some adjacent characteristics β = constant are also shown qualitatively.

The shock trajectory (3.10) could in fact have been obtained by simply inserting in (3.9) the results of the simple linearized theory for $c_0t-r = 0+$, but the shock would then lie outside the disturbed region of that theory. The advantage of the method used is that it shows how the shock fits into the general flow pattern.

In the case of a centred expansion wave, the gap may be filled by taking a linear variation of u_1 and c_1 across it: this is sufficient to our approximation.

We conclude that, as far as the propagation of discontinuities is concerned, the simple linearized theory (for $k > 0$) is uniformly valid, since the relative perturbations decay rapidly, so that the positions (c_0t-r) of characteristics and shocks are predicted correctly within an error of $O(\epsilon)$ for all r. It would therefore be surprising if the theory, applied to an expanding cylinder of finite radius, contained non-uniformities in the interior part of the field, but discussion of this point is difficult and beyond the scope of the present paper.

4. Waves propagating from the axis

We turn to the main problem of this paper. Consider sources concentrated on the axis: let their strength per unit volume be

$$Q^{(m)} + \frac{\gamma-1}{c_0^2} Q^{(h)} = 2\frac{\delta(r)}{r} f'(t), \tag{4.1}$$

where δ is the Dirac function, and $f(t) = 0$ for $t < 0$. Integration of (2.11) from $r = 0$ to $r = 0+$ shows that, equivalently, the total source strength per unit length of axis is

$$q(0+, t) = f'(t). \tag{4.2}$$

The resulting flow may be visualized as due to the mass and energy release of (4.1), or as due to a small cylinder of cross-sectional area

$$A(t) \equiv \pi R^2(t) = \frac{2\pi f(t)}{\rho_0(0)}, \tag{4.3}$$

the boundary condition $ru_1 = RR'$ being satisfied on $r = 0$ instead of on $r = R$. We shall examine in detail the solution when the source strength $f'(t)$ is a Dirac pulse (and also one or two closely related cases): in principle, all other solutions can be obtained by superposition of that for a pulse, but in practice this can be a difficult task.

The solutions to be considered are, of course, not physically valid in the immediate neighbourhood of the axis, at or near times when the source is discharging. (In the case of a cylinder, expanding and contracting for $0 \leqslant t \leqslant t_1$, $R/c_0 t_1$, R'/c_0 and $R'' t_1/c_0$ must all be $\ll 1$ and continuous if (4.3) is to lead to a physically valid solution in $r \geqslant R$ for all t.) Further, it will be found that if $f(t)$ begins more strongly than $t^{\frac{3}{2}}$ the velocity behind the wave front is infinite. However, these features are also present in the theory for irrotational flow, and therefore do little to hinder the study of rotational effects which is our main purpose here.

In place of r and t we introduce the dimensionless variables

$$x = \frac{\gamma \Omega^2 r^2}{2c_0^2} = kr^2, \quad \tau = \Omega t.$$

That x is in fact a natural co-ordinate of the problem is suggested by the fact that $p_0 = p_0(0)\, e^x$. Then (2.14) becomes

$$x\psi_{xx} - x\psi_x - \frac{1}{2\gamma}\left(\frac{\partial^2}{\partial \tau^2} + 4\right)\psi = 0. \tag{4.4}$$

The boundary conditions, which specify the perturbation mass at the axis and the absence of disturbances ahead of the wave front, are

$$\left.\begin{aligned} &\text{(i)}\ \ \psi(0, \tau) = f(t) = g(\tau), \text{ say}, \\ &\text{(ii)}\ \ \psi = 0 \quad \text{for} \quad r > c_0 t,\ x > \tfrac{1}{2}\gamma\tau^2. \end{aligned}\right\} \tag{4.5}$$

If the Laplace transform

$$\overline{\psi} = p \int_0^\infty e^{-p\tau}\, \psi(x, \tau)\, d\tau$$

is introduced, there results

$$x\overline{\psi}_{xx} - x\overline{\psi}_x - a\overline{\psi} = 0, \quad \text{where} \quad a = \frac{p^2 + 4}{2\gamma}. \tag{4.6}$$

This is a case of the confluent hypergeometric equation: in the notation of Erdélyi (1953) and Tricomi (1954) the solutions are

$$x\Phi(a+1, 2;\ x) \quad \text{and} \quad \Psi(a, 0; x) \equiv x\Psi(a+1, 2;\ x).$$

with the following properties.

For $x \to 0$,
$$\left.\begin{aligned} ax\Phi(a+1,2;x) &= ax+O(x^2),\\ \Gamma(a+1)\,\Psi(a,0;x) &= 1+O(x\log x);\end{aligned}\right\} \tag{4.7}$$

for $x \to \infty$,
$$\left.\begin{aligned} ax\Phi(a+1,2;x) &= O(e^x x^a),\\ \Gamma(a+1)\,\Psi(a,0;x) &= O(x^{-a});\end{aligned}\right\} \tag{4.8}$$

for $p \to \infty$, $\mathscr{R}p > 0$, $0 < x < \infty$,
$$\left.\begin{aligned} ax\Phi(a+1,2;x) &= \frac{e^{\frac{1}{2}x}}{2\pi^{\frac{1}{2}}}(ax)^{\frac{1}{4}}\exp\{2(ax)^{\frac{1}{2}}\}[1+O(p^{-1})],\\ \Gamma(a+1)\,\Psi(a,0;x) &= \pi^{\frac{1}{2}}e^{\frac{1}{2}x}(ax)^{\frac{1}{4}}\exp\{-2(ax)^{\frac{1}{2}}\}[1+O(p^{-1})],\\ \text{where}\quad (ax)^{\frac{1}{4}}\exp\{\pm 2(ax)^{\frac{1}{2}}\} &= \left(\frac{\Omega pr}{2c_0}\right)^{\frac{1}{2}}\exp\left(\pm\frac{\Omega pr}{c_0}\right)[1+O(p^{-1})].\end{aligned}\right\} \tag{4.9}$$

Here $\arg a = \arg p = 0$ on the positive real p-axis. Equation (4.8) suggests that the Φ-solution should be rejected here, and (4.9) confirms it. For, in view of the inversion integral of the Laplace transform, (4.9) shows that the Φ-solution represents an incoming wave, which vanishes only for $c_0t+r<0$; whereas Ψ represents an outgoing wave which vanishes for $c_0t-r<0$, as required by (4.5) (ii). Hence
$$\bar{\psi} = \Gamma(a+1)\,\Psi(a,0;x)\,\bar{g}(p),$$
and
$$\psi = \frac{1}{2\pi i}\int_{\mathscr{L}}\frac{e^{p\tau}}{p}\,\Gamma(a+1)\,\Psi(a,0;x)\,\bar{g}(p)\,dp, \tag{4.10}$$
where $\mathscr{L}$ is the Bromwich path $C-i\infty$ to $C+i\infty$ with $C>0$.

To relate this result to those of the previous section, we suppose that
$$f(t) \sim t^\nu H(t)/\nu! \quad \text{for} \quad t \to 0 \quad (\nu \geqslant 0),$$
where $H(t)$ is the Heaviside function. (In applications such an $f(t)$ must, of course, be multiplied by a small parameter ϵ.) Applying (4.9) and $\bar{g}(p) \sim (\Omega p)^{-\nu}$ for $p \to \infty$, and closing the contour of (4.10) with a large semicircle in $\mathscr{R}p > 0$, we confirm that $\psi = 0$ for $r > c_0t$; evaluating the integral for $r < c_0t$ we find that immediately behind the wave front
$$\psi \sim \frac{\pi^{\frac{1}{2}}}{(\nu-\frac{1}{2})!}e^{\frac{1}{2}x}\left(\frac{r}{2c_0}\right)^{\frac{1}{2}}\left(t-\frac{r}{c_0}\right)^{\nu-\frac{1}{2}}. \tag{4.11}$$
The case studied in §3, in which ψ_r and ψ_l have finite discontinuities, is $\nu = \frac{3}{2}$; if $\nu < \frac{3}{2}$ the theory is unrealistic near the wave front, and if $\nu > \frac{3}{2}$ the strength of the wave front is zero. The effects of rotation, however, are contained entirely in the factor $e^{\frac{1}{2}x}$, which becomes $e^{-\frac{1}{2}x}$, in the relative perturbations, and has already been discussed.

Consider now the solution
$$\psi_{(0)} = \frac{1}{2\pi i}\int_{\mathscr{L}}\frac{e^{p\tau}}{p}\,\Gamma(a+1)\,\Psi(a,0;x)\,dp, \tag{4.12}$$
for which $\psi_{(0)}(0,\tau) = H(\tau)$, $q_{(0)}(0,\tau) = \Omega\delta(\Omega t) = \delta(t)$, so that the source strength is a Dirac pulse. For any other source strength
$$\psi = \int_0^{\tau-(2x/\gamma)^{\frac{1}{2}}}\psi_{(0)}(x,\tau-\tau_1)\,g'(\tau_1)\,d\tau_1.$$

First we verify that when $x \to 0$ and $\tau \to 0$ such that x/τ^2 is finite, the irrotational solution is recovered. Let

$$\frac{r^2}{c_0^2 t^2} = \frac{2x}{\gamma\tau^2} = \theta^2, \quad p\tau = s,$$

so that $$\psi_{(0)} = \frac{1}{2\pi i}\int_{\mathscr{L}} \frac{e^s}{s}\,\Gamma(a+1)\,\Psi(a, 0; \tfrac{1}{2}\gamma\tau^2\theta^2)\,ds, \quad a = \frac{s^2+4\tau^2}{2\gamma\tau^2}.$$

Now for $\tau \to 0$ (Erdélyi, 1953, p. 266)

$$\Gamma\Psi = s\theta K_1(s\theta)\,[1+O(\tau^2)],$$

where K_1 is the modified Bessel function of the second kind and of order one. Hence

$$\begin{aligned}\psi_{(0)} &= \frac{1}{2\pi i}\int_{\mathscr{L}} e^s \theta K_1(s\theta)\,ds\,[1+O(\tau^2)] \\ &= (1-\theta^2)^{-\frac{1}{2}}\,[1+O(\tau^2)], \end{aligned} \tag{4.13}$$

and this is the irrotational solution.

A wave-front approximation which, while in principle no better than (4.11) (with $\nu = 0$), actually gives better numerical agreement with the full solution, may be obtained as follows. We observe that the Coriolis force contributed the stiffness term $-4\Omega^2\psi/c_0^2$ in (2.14), or $-2\psi/\gamma$ in (4.4), and that this is lost when the approximation $a \sim p^2/2\gamma$ for $p \to \infty$ is made in (4.9). Accordingly, this approximation is not made: then

$$\psi_{(0)} \sim \frac{\pi^{\frac{1}{2}} e^{\frac{1}{2}x}}{2\pi i}\int_{\mathscr{L}} \exp\{p\tau - 2(ax)^{\frac{1}{2}}\}\,(ax)^{\frac{1}{4}}\frac{dp}{p} \quad \left(a = \frac{p^2+4}{2\gamma}\right),$$

and the integral may be evaluated approximately by the methods of steepest descent or of stationary phase. There results

$$\begin{aligned}\psi_{(0)} &\sim e^{\frac{1}{2}x}\frac{2x}{\gamma\tau^2}\left(1-\frac{2x}{\gamma\tau^2}\right)^{-\frac{1}{4}}\cos\left\{2\left(\tau^2-\frac{2x}{\gamma}\right)^{\frac{1}{2}}\right\} \\ &\sim e^{\frac{1}{2}x}\left(1-\frac{2x}{\gamma\tau^2}\right)^{-\frac{1}{4}}\cos\left\{2\left(\tau^2-\frac{2x}{\gamma}\right)^{\frac{1}{2}}\right\}. \end{aligned} \tag{4.14}$$

This is still only valid for small values of $(\gamma\tau^2 - 2x)$, but it appears to hold over a somewhat wider range than (4.11), and it also gives a qualitative indication of the oscillatory character of the flow for $\Omega > 0$.

To obtain a series representation of $\psi_{(0)}$, we note that in (4.12) the only singularities of the integrand are simple poles at the origin and at those points on the imaginary p-axis where a is a negative integer. For $p \to \infty$ and $\mathscr{R}p < 0$,

$$\Gamma(a+1)\,\Psi(a, 0; x) \sim O[a^{\frac{1}{4}}\exp\{2(ax)^{\frac{1}{2}}\}],$$

so that the integral around a large semicircle in $\mathscr{R}p < 0$ vanishes for $c_0 t > -r$. Evaluating the residues, one finds that

$$\psi_{(0)} = \Gamma\left(\frac{2}{\gamma}+1\right)\Psi\left(\frac{2}{\gamma}, 0; x\right) - x\sum_{n=1}^{\infty}\frac{\cos\{(2\gamma n+4)^{\frac{1}{2}}\tau\}\,L_{n-1}^1(x)}{n+(2/\gamma)} \quad (x > 0), \tag{4.15}$$

where $L^1_{n-1}(x)$ is the generalized Laguerre polynomial

$$L^1_{n-1}(x) = \frac{n}{1!} - \frac{n(n-1)}{2!}\frac{x}{1!} + \ldots + (-)^{n-1}\frac{x^{n-1}}{(n-1)!},$$

with the recurrence property

$$L^1_m(x) = \left(2 - \frac{x}{m}\right) L^1_{m-1}(x) - L^1_{m-2}(x).$$

For $n \to \infty$,

$$\frac{\cos\{(2\gamma n + 4)^{\frac{1}{2}}\tau\}\, L^1_{n-1}(x)}{n + (2/\gamma)} \sim -\frac{e^{\frac{1}{2}x}}{2\pi^{\frac{1}{2}}(nx)^{\frac{3}{4}}}\left[\cos\left\{(2\gamma n)^{\frac{1}{2}}\,\Omega\left(t - \frac{r}{c_0}\right) - \tfrac{1}{4}\pi\right\}\right.$$
$$\left. + \cos\left\{(2\gamma n)^{\frac{1}{2}}\,\Omega\left(t + \frac{r}{c_0}\right) + \tfrac{1}{4}\pi\right\}\right]. \quad (4.16)$$

In (4.15) the first term is the solution obtained if in the differential equation (2.14) one lets $\Omega \to \infty$, $c_0 \to \infty$ with Ω/c_0 finite, and applies the boundary conditions $\psi = 1$ on $x = 0$, $\psi = o(e^x)$ for $x \to \infty$. Since $\psi = 1$ on $x = 0$ implies $t > 0$, this limit corresponds to $\tau \to \infty$ with x fixed; it therefore seems probable (although it has not been proved) that the second part of the solution $\to 0$ as $\tau \to \infty$, and in this case the first term can be regarded as the ultimate steady-state form of the solution. It can be shown that the series in (4.15) converges for $c_0 t > r$, although not absolutely; and that if we sum and then let $x \to 0$ the second part of the solution is $O(x)$. This last remark means that in the perturbation density, $\rho_1 = -\gamma\Omega^2 c_0^{-2}\psi_x$, the dominant term for $x \to 0$ is the logarithmic singularity implied by

$$\Gamma\left(\frac{2}{\gamma} + 1\right)\Psi\left(\frac{2}{\gamma}, 0; x\right) = 1 + \frac{2x}{\gamma}\log\frac{2x}{\gamma} + O(x).$$

The pressure is singular in the same way. This singularity (which appears for all source strengths), is due to the arrival at the axis of the wavelets reflected by the radial pressure gradient. Note that in (4.16) the high-frequency components of the solution are in fact split into outgoing and incoming waves.

5. An example

Consider the family of solutions $\psi_{(m)}$ (m an integer $\geqslant 0$) for which

$$\psi_{(m)}(0, \tau) = \tau^m H(\tau).$$

For $m = 0$ the wave-front singularity is strong, and the series in (4.15) converges very slowly throughout the field: corresponding series solutions can be written for all m, and the convergence improves as m increases, but for m large the growth of outflow with time is likely to be the dominant feature of the field. Hence $m = 1$ was chosen here; and for convenience γ was taken to be 2. The equations which correspond to (4.14) and (4.15) are then

$$\psi_{(1)} = \tfrac{1}{2}e^{\frac{1}{2}x}\sin\{2(\tau^2 - x)^{\frac{1}{2}}\} \quad (\tau^2 - x \text{ small}), \quad (5.1)$$

and

$$\psi_{(1)} = \tau\{1 + xe^x\mathrm{Ei}(-x)\} - \tfrac{1}{2}x\sum_{n=1}^{\infty}\frac{\sin\{2(n+1)^{\frac{1}{2}}\tau\}\, L^1_{n-1}(x)}{(n+1)^{\frac{3}{2}}}, \quad (5.2)$$

where Ei denotes the exponential integral.

The series was computed as follows. A large value $n = N$ was chosen, close to a zero of $\sin\{2(n+1)^{\frac{1}{2}}\tau\}$ for computations with τ constant, and close to a zero of $L^1_{n-1}(x)$ for computations with x constant. For $n \leqslant N$ the terms were computed exactly, the recurrence formula of the Laguerre polynomials being used. For $n > N$ the asymptotic forms corresponding to (4.16) were used, and to the same degree of approximation, summation could be replaced by integration. The sum for $n > N$ could then be expressed in terms of tabulated Fresnel integrals (Jahnke & Emde, 1945). Two values of N were used for each point, one near 20 and the other near 40, and the difference $\Delta\psi_{(1)}/\psi_{(1)}(0,\tau)$ was less than 2% in all cases.

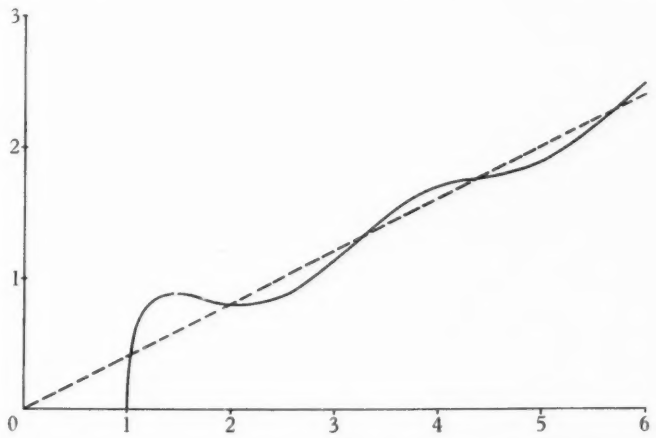

FIGURE 2. The variation of $\psi_{(1)}$ with τ at $x = 1{\cdot}0$. — — —, $\tau[1+xe^x\mathrm{Ei}(-x)]$; ——, $\psi_{(1)}(1{\cdot}0, \tau)$.

A more severe check was provided by values at $x = \tau^2$, where $\partial\psi_{(1)}/\partial x \to \infty$; here the exact value is zero, and the computations with the larger N gave:

τ	$1/\sqrt{2}$	1	$\sqrt{2}$
$\psi_{(1)}(\tau^2,\tau)/\psi_{(1)}(0,\tau)$	0·005	0·01	0·02

Because $\psi_{(m)}(x,\tau) = \partial\psi_{(m+1)}(x,\tau)/\partial\tau$, the function $\epsilon\psi_{(1)}$ can be interpreted:

(i) As a function whose time derivative (indicated by figure 2) is proportional to the solution $\psi_{(0)}$ of the previous section.

(ii) As the stream function ψ of the flow for which

$$f(t) = \epsilon\Omega t, \quad R(t) = \{2\epsilon\Omega/\rho_0(0)\}^{\frac{1}{2}}t^{\frac{1}{2}}.$$

(iii) As the outflow q of the flow for which

$$f(t) = \tfrac{1}{2}\epsilon\Omega t^2, \quad R(t) = \{\epsilon\Omega/\rho_0(0)\}^{\frac{1}{2}}t.$$

Let us adopt the second of these viewpoints and assume that $\epsilon > 0$. Figure 2 shows the variation of $\psi_{(1)}$ with time at $x = 1$, and we take $\psi = r\rho_0\int_{r/c_0}^{t} u_1\,dt$ as a measure of the radial displacement of the circle of fluid particles which lies

initially at $x = 1$. As the shock passes by, the circle surges outwards behind it (at first with infinite velocity), but this effect is soon checked by the spring-like Coriolis force, and also by a fall in density which makes the pressure gradient p_{0r} more effective, so that the circle moves inwards again. (According to the wave-front approximation (5.1), ρ_1 first becomes negative at $x = 1{\cdot}0$ when $\tau = 1{\cdot}2$.) Thereafter the particles' mean motion is outward, because of the continuing efflux from the source, but they oscillate about the mean trajectory shown by the straight line in figure 2. This line is the 'infinite rotation, infinite sound speed' solution given by the first term of (5.2).

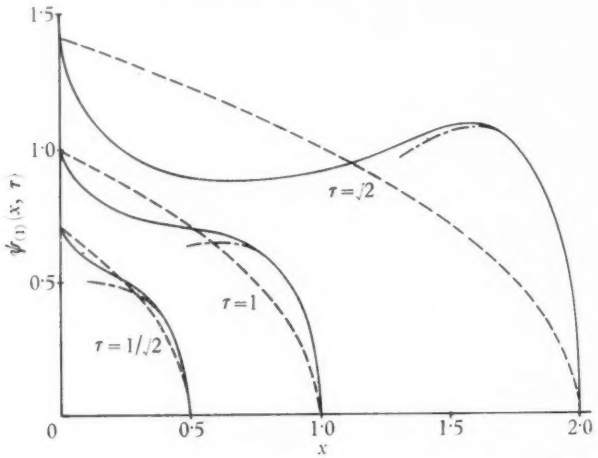

FIGURE 3. Profiles of $\psi_{(1)}$ at constant τ. ——, full solution, equation (5.2); — — —, wave-front approximation, equation (5.1); — — —, irrotational-flow solution, equation (5.3).

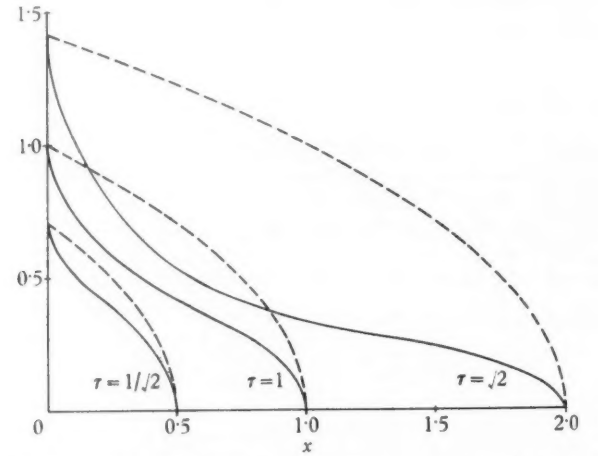

FIGURE 4. Profiles of $e^{-x}\psi_{(1)}$ at constant τ. ——, $e^{-x}\psi_{(1)}(x, \tau)$; — — —, irrotational-flow solution, equation (5.3).

Figures 3 and 4 show profiles of $\psi_{(1)}$ and $e^{-x}\psi_{(1)}$ at constant τ; the wave-front approximation (5.1) is shown also, and the shape of the irrotational solution

$$\Omega\psi^*_{(1)} = (\tau^2 - x)^{\frac{1}{2}} \tag{5.3}$$

serves as a datum. Since

$$\rho_1 = -\frac{\gamma\Omega^2}{c_0^2}\psi_x,$$

the slope of the curves in figure 3 indicates the (absolute) density perturbation: the figure also shows the effect of rotation in gradually distorting the $\psi_{(1)}$-profile from its shape in the irrotational case. The most striking feature is perhaps the appearance at $\tau = \sqrt{2}$ of a wide region of negative perturbation density (rarefaction) between the regions of strongly positive ρ_1 near the axis and the wave front. Of course, the presence of these strong condensation regions (which we attribute to the convergence on the axis of the reflected wavelets, and to the negative damping of the absolute density increment behind the wave front) makes the appearance of an intermediate rarefaction region inevitable.

The relative perturbation $e^{-x}\psi_{(1)}$ of figure 4 is a measure, not only of the area displaced by a fluid circle, but also of the loss of circulation and gain of entropy at a station x = constant. For the circles of fluid particles carry their initial circulation and entropy with them, and

$$rv_1 = -\frac{2\Omega\psi}{\rho_0}, \quad S_1 = \frac{c_v}{p_0}(p_1 - c_0^2\rho_1) = \frac{c_v(\gamma-1)\,\Omega^2}{p_0}\psi,$$

where S is the specific entropy. (Alternatively, $e^{-x}\psi_{(1)}$ may be associated with the volumetric outflow ru_1 of case (iii) above.) The figure emphasizes the resistance to small disturbances of the rotating mass of gas: the relative perturbations decay rapidly as one proceeds outwards from the axis.

I am indebted to Prof. H. W. Liepmann for suggesting this problem, to Mrs D. Diamond for the numerical computations, and to a referee for stringent and appropriate criticism of a first draft of this paper. The work was partly sponsored by the Office of Naval Research under Contract Nonr-220 (21).

REFERENCES

ERDÉLYI, A. (ed.) 1953 *Higher Transcendental Functions*, Vol. 1. New York: McGraw-Hill.

JAHNKE, E. & EMDE, F. 1945 *Tables of Functions*, 4th ed. New York: Dover.

SQUIRE, H. B. 1956 Rotating fluids. Article in *Surveys in Mechanics*, p. 139. Cambridge University Press.

TRICOMI, F. G. 1954 *Funzioni Ipergeometriche Confluenti*. Rome: Edizioni Cremonese.

WHITHAM, G. B. 1952 The flow pattern of a supersonic projectile. *Comm. Pure Appl. Math.* **5**, 30.

REVIEWS

Theorie schallnaher Strömungen. By K. G. GUDERLEY. Berlin: Springer-Verlag, 1957. 376 pp. DM. 42.

It is a real measure of the rapidity of technological progress that within the last fifteen years the transonic régime has passed from being a high-speed to a low-speed régime. The enormous body of literature on the subject is a tribute to the diligence of modern theoretical scientists. (It is an interesting question to ask if there is any connexion between the two phenomena.) In this book the author presents mainly the results of his efforts and those of his co-workers in transonic flow theory. Thus there is made available to the scientific public a substantial amount of detailed information which has appeared before only as U.S. Air Force Technical Reports. A reaction after a first glance at the book might be that a lot of mathematical heavy artillery is employed to shoot down a few pigeons, in the form of solutions to specific flow problems. Part of this impression is created by the author's desire to build up a complete mathematical background for the subject. However, the fact remains that even the simplest flow problems such as flow past an airfoil or body of revolution of arbitrary shape have resisted the barrage and furthermore there is no hint that solutions to these problems will be forthcoming by application of methods developed in the book. In spite of these comments, which are really an indication of the difficulty of solving the obvious problems for a non-linear partial differential equation, the reviewer feels that efforts along these lines are definitely worth-while. Every bit of progress in understanding details help to round out the general picture, build up the general confidence, suggest decisive experiments, etc. In the course of these investigations a surprising amount of technically useful information is obtained, such as similarity laws, asymptotic flow fields, and wind-tunnel wall effects. Also, the mathematical theory of the equations of mixed type which are studied is interesting in its own right. The advantage of having physical models to go with the equations is clearly brought out and explained by the author.

The main divisions of the book are indicated below, together with some comments:

I. *General basis.* A brief but clear introduction to inviscid compressible fluid theory.

II. *Simplification of the flow equations. Similarity law for transonic flow.* A brief treatment of the important concepts, which leads to an approximate transonic equation and the related similarity laws. The following approximate equation, and approximate boundary condition and shock relations, are obtained by a limit process in which, typically, thickness ratio $\tau \to 0$, free stream Mach number $M_\infty \to 1$ while $(1 - M_\infty^2)/\tau^2$ is kept fixed, this procedure being carried out in a modified co-ordinate system where $x, \bar{y}\ (= \tau y), \bar{z}\ (= \tau z)$ are fixed:

$$(\gamma + 1)\,\Phi_x \Phi_{xx} = \Phi_{\bar{y}\bar{y}} + \Phi_{\bar{z}\bar{z}} \quad (\Phi = \text{velocity potential}). \tag{1}$$

III. *Linearized treatment of transonic flow.* Brief discussion of the non-linear equation derived in II, showing that the solutions of the linearized version $\Phi_{\bar{y}\bar{y}} + \Phi_{zz} = 0$ cannot usually be made physically meaningful. The exception, the slender lifting wing of zero thickness, is also discussed.

IV. *Exact solutions of the potential equation of transonic flow.* Among these is a simple polynomial solution of (1), apparently new, which describes plane flow as it accelerates through sonic speed in the throat of a nozzle. This solution is used to introduce the very important concept, first noticed by Guderley, of the limiting Mach wave; this Mach wave bounds that part of the supersonic region which can influence the subsonic region. This idea, which occurred in hidden form in Tricomi's original purely mathematical treatment, here has a simple physical significance.

V. *Basis of the hodograph method.* A clear discussion is presented of the hodograph method for plane flow starting with simple incompressible examples. Tschapligin's solutions and their connexion with various asymptotic approximations, including the Tricomi approximation

$$\psi_{\eta\eta} - \eta\psi_{uu} = 0, \tag{2}$$

in which η and u are the hodograph variables, are discussed.

VI. *Discussion of transonic flow fields with the help of the hodograph.* Some simple solutions for flow over a corner and wedge in supersonic flow are presented, as well as some fairly complicated discussion of forked shock waves.

VII. *Particular solutions of the Tricomi equation.* The important solutions discovered by Guderley which have their singularity at $\eta = u = 0$ are presented in great detail. They are basically hypergeometric functions for which a special notation is introduced. The limiting Mach wave reappears as a co-ordinate and serves to separate physically meaningful solutions from the rest. The solutions of Tamada and Tomotika for singularities in the subsonic region and Falkowitsch for branch points are also discussed briefly. Certain complicated eigen-value problems are also discussed.

VIII. *Flow at Mach number* 1. This includes applications of the hodograph method to a number of problems first solved by Guderley. One of the Guderley solutions to the Tricomi equation is shown to correspond to the free stream and a special airfoil is produced by the addition of another particular solution. Too much detail is presented here. On the other hand, the solution for flow past a wedge is given a form which is brief compared with that given originally—more details could have been used here, especially with respect to the method of satisfying the boundary condition for flow around a corner. The solution for a wedge at angle of attack small compared to its thickness ratio is given, as well as that for a flat plate at angle of attack. An important practical result appears in the close agreement of the theoretical pressure distribution on the wedge at free stream Mach number 1 and that in a choked closed wind tunnel (derived later). No comment is made on whether or not the result might extend to shapes for which the sonic point can move with Mach number.

IX. *Flow fields at Mach numbers slightly different from* 1. A perturbation theory of flow at $M_\infty = 1$ is developed in detail. Choked wind tunnel problems are discussed.

X. *Further considerations of certain particular solutions, etc.*

XI. *Axi-symmetric flow.* Similarity methods are used to reduce (1) to a non-linear ordinary differential equation which describes the asymptotic flow field at a large distance from a body at $M_\infty = 1$. Group theory methods, similar to those used in blast wave theory, are used to obtain a first-order differential equation whose trajectories fix the flow. The asymptotic form is shown to be

$$\Phi = r^{-\frac{3}{7}} f\left(\frac{x}{r^{\frac{4}{7}}}\right),$$

but the scale of the solution cannot be related to any properties of the body. Unfortunately the discussion here is very brief, and so too is the following discussion of these asymptotic flows with shocks (Barish). A fairly complete list of references is presented.

As a criticism it might be said that the book does not present enough of the work of other authors. There are also some curious omissions of Guderley's own work, such as that on finite span wings. The pure mathematician would certainly find it not rigorous enough, while the engineer will no doubt find it too mathematical. There are no experimental points to mar the theoretical beauty (although transonic flow theory has produced many results in good agreement with experiment). Parts of the book are very difficult to read. Nevertheless, it is a good book representing work on a very high level and containing important practical and mathematical contributions. It is certainly a most important book for anyone who wants to try to solve transonic flow problems.

An English translation is to be made available shortly.

J. D. Cole

Rheology: Theory and Applications, volume II. Edited by F. R. Eirich. New York: Academic Press, 1958. 591 pp. $18.00.

Following a first volume which included some accounts of the theoretical analysis of various types of rheological behaviour, this second of three volumes on *Rheology: Theory and Application* lays greater emphasis on the phenomena actually observed in some real materials and on the methods available for their quantitative assessment. It is not intended to complete the picture of the present state of knowledge of deformation and flow behaviour, but is to be followed by a volume on other classes of materials of industrial importance and dealing with some technological developments in the rheological field.

The observation that in some real liquids the rate of shear is a constant multiple of the applied shear stress was noted by Newton, and this simple rule has been used by generations of physicists and applied mathematicians as a basis for their studies—experimental and theoretical—of fluid flow. Hooke's formulation of the observed proportionality of stress and strain has been similarly used as a foundation for the study of the mechanical properties of

solids. Reading the volume under review, comprising thirteen chapters, each by a different author, one is reminded how physicists and physical chemists have been stimulated to act in rather different ways by the realization that some materials are neither Newtonian liquids nor Hookean solids. The physicist seeks to determine the precise mode of response to applied stress shown by a solid or liquid to which neither of the classical laws of Hooke and Newton can be applied. The physical chemist is more interesting in knowing how some simply-defined empirical parameter which can be associated with a material—usually a 'modulus' or a 'viscosity coefficient' which gives but an imperfect characterization of the system—varies with chemical constitution and environment. The contrast is between an intensive investigation carried out on a single specimen whose properties are not changing, and the repetition of a simple measurement on many specimens which are chemically related. Behind the second approach is the desire to obtain information about microscopic structure and molecular configurations (especially in macromolecular systems) from simple physical measurements; the chemist thinks of rheology largely as a means to an end, and rarely as an interesting study in itself.

The detailed assessment of a rheologically complicated material must await the development of suitable techniques to measure more than the simple 'modulus' or 'viscosity'—i.e. more than the ratio of a stress and a strain, or rate of strain, when the ratio is neither a constant nor a simple function. The progress of rheological investigations is therefore entirely dependent on the introduction of new techniques, the subject of the last three chapters in this volume: 'Experimental techniques for rheological measurements on viscoelastic bodies' by J. D. Ferry, 'Fundamental techniques—fluids' by B. A. Toms, and 'Goniometry flow and rupture' by A. Jobling and J. E. Roberts. There is surprisingly little overlapping of subject-matter in these three articles, and the different points of view on what one should measure in various types of material are welcome and stimulating.

Jobling and Roberts include an all-too-brief description of Roberts's method of measuring normal stresses in all directions (as well as the shear stress) during a steady-shearing experiment. It is to be regretted that more experimental details and more typical results of observation on some actual liquids have not been included. Several rival theories have grown up around the existence of normal stress-differences during shearing of elastico-viscous liquids, and real progress might be made in distinguishing them if more experimental results were made available.

In other chapters, experimental techniques peculiar to the systems considered are discussed incidentally. B. Gutenberg, in describing 'Rheological problems of the earth's interior' is clearly dependent on methods of observation peculiar to his field. This author brings it forcibly to the reader's notice that it is not only new man-made materials and natural polymers that give rise to mechanical response not explainable in terms of a single coefficient. At the same time, his contribution serves to remind the reader that if a single constant is insufficient, one might be able to manage with a small number of physical constants and get a reasonable theory—without necessarily jumping from one to a continuous

infinity of parameters to characterize rheological behaviour, as is implicit in some other approaches.

Several chapters are concerned with polymer systems, and there is inevitably some overlapping, not always unwelcome, in the information presented. That the authors of different chapters do not use the same terminology or notation when writing about the same concepts is more disconcerting. The subject is introduced in a readable and informative opening chapter on 'Viscoelasticity phenomena in amorphous high polymeric systems' by H. Leaderman. Experimental results at small variable shear stresses applied to amorphous polymers can be explained in terms of a relaxation spectrum, or, for example, by functions of frequency measuring the in-phase and out-of-phase strain response to alternating stress, over the whole range of possible frequencies of application.

A closely related chapter on 'Stress relaxation studies of the viscoelastic properties of polymers' is by A. V. Tobolsky; and there follows one on 'The relaxation theory of transport phenomena' by T. Ree and H. Eyring, which might perhaps more fittingly have been found a place in volume I.

The remaining chapters in volume II each deal with a particular class of materials and with some special experimental techniques which have been developed in relation to those materials. They are 'The rheology of organic glasses' by R. Buchdahl, 'The rheology of raw elastomers' by M. Mooney, 'The rheology of cellulose derivatives' by E. B. Atkinson, 'The rheology of fibres' by R. Meredith, 'The rheology of gelatin' by A. G. Ward and P. R. Saunders, and 'Rheological Properties of Asphalts' by R. N. J. Saal and J. W. A. Labout. The emphasis on macromolecular systems, of one sort and another, is evident from the titles. In all these chapters, care has been taken to describe in sufficient detail what the systems are, as well as what their rheological properties are. Much attention is given to the variation of viscosity or stiffness with temperature, pressure, pH, degree of polymerization, breadth of polymer molecular-weight distribution curve and other aspects of physico-chemical constitution, and comparatively little space is devoted to the question of a more complete rheological investigation of any single sample.

The reader cannot but be impressed by the long lists of references to original papers throughout the volume, a high proportion of them in the literature of the last decade. Evidently, considerable selection of material has been necessary in the preparation of each chapter. The book should provide a useful introduction to the rapidly growing literature in branches of rheology which the reader is not actively engaged in, and will be a valuable work of reference for all physicists, physical chemists and applied mathematicians interested in deformation and flow problems.

The somewhat divergent lines of thought about rheological phenomena which are now current are brought together in this book, though in independent surveys with little attempt at co-ordination. The complete work might well help indirectly to bring some unity into the subject, but the work of integrating ideas put forward by different writers remains to be done.

J. G. OLDROYD

INDEX

BATCHELOR, G. K. Small-scale variation of convected quantities like temperature in turbulent fluid. Part 1. General discussion and the case of small conductivity, 113

BATCHELOR, G. K., HOWELLS, I. D. and TOWNSEND, A. A. Small-scale variation of convected quantities like temperature in turbulent fluid. Part 2. The case of large conductivity, 134

BINNIE, A. M. Instability in a slightly inclined water channel, 561

BIRD, G. A. The effect of wall shape on the degree of reinforcement of a shock wave moving into a converging channel, 60

BROGAN, T. R. *See* PATRICK and BROGAN

CORCOS, GILLES M. and SELLARS, JOHN R. On the stability of fully developed flow in a pipe, 97

DAVIES, T. V. On the forced motion due to heating of a deep rotating liquid in an annulus, 593

DEGROFF, HAROLD *See* HROMAS and DEGROFF

ELDER, J. W. Steady flow through non-uniform gauzes of arbitrary shape, 355

ELDER, J. W. The dispersion of marked fluid in turbulent shear flow, 544

FRAENKEL, L. E. A cylindrical sound pulse in a rotating gas, 637

GOLDSWORTHY, F. A. The structure of a contact region, with application to the reflexion of a shock from a heat-conducting wall, 164

HAQUE, S. M. A. The effect of eddy viscosity on the velocity profile of steady flow in a uniform rough channel, 310

HAMMITT, ANDREW G. The hypersonic viscous effect on a flat plate with finite leading edge, 242

HASIMOTO, H. On the periodic fundamental solutions of the Stokes equations and their application to viscous flow past a cubic array of spheres, 317

HOWELLS, I. D. *See* BATCHELOR, HOWELLS and TOWNSEND

HROMAS, LESLIE and DEGROFF, HAROLD Experimental search for the effect of compressibility in unsteady Couette flow, 140

KARLSSON, STURE K. F. An unsteady turbulent boundary layer, 622

KRAICHNAN, ROBERT H. The structure of isotropic turbulence at very high Reynolds numbers, 497

KYNCH, G. J. The slow motion of two or more spheres through a viscous fluid, 193

LEITE, RICHARD J. An experimental investigation of the stability of Poiseuille flow, 81

LIU, V. C. On the drag of a flat plate at zero incidence in almost-free-molecule flow, 481

LUDFORD, G. S. S. The structure of a hydromagnetic shock in steady plane motion, 67

LUDFORD, G. S. S. The propagation of small disturbances in hydromagnetics, 387

MERK, H. J. Rapid calculations for boundary-layer transfer using wedge solutions and asymptotic expansions, 460

MORTON, B. R. Forced plumes, 151

PATRICK, R. M. and BROGAN, T. R. One-dimensional flow of an ionized gas through a magnetic field, 289

PEARSON, J. R. A. The effect of uniform distortion on weak homogeneous turbulence, 274

PHILLIPS, O. M. The scattering of gravity waves by turbulence, 177

RESLER, E. L. *See* SEARS and RESLER

ROGERS, RUTH H. The structure of the jet-stream in a rotating fluid with a horizontal temperature gradient, 41

SEARS, W. R. and RESLER, E. L. Theory of thin airfoils in fluids of high electrical conductivity, 257

SELLARS, JOHN R. *See* CORCOS and SELLARS

SHARP, A. W. The supersonic flow past a leading edge separation bubble, 445

SILBERMAN, EDWARD. Experimental studies of supercavitating flow about simple two-dimensional bodies in a jet, 337

STEWARTSON, K. On the stability of a spinning top containing liquid, 577

STRATFORD, B. S. The prediction of separation of the turbulent boundary layer, 1

STRATFORD, B. S. An experimental flow with zero skin friction throughout its region of pressure rise, 17

TOOMRE, ALAR A pulsating sphere in a rotating fluid, 571

TOWNSEND, A. A. Temperature fluctuations over a heated horizontal surface, 209

TOWNSEND, A. A. *See* BATCHELOR, HOWELLS and TOWNSEND

VERONIS, G. Cellular convection with finite amplitude in a rotating fluid, 401

WHITHAM, G. B. A new approach to problems of shock dynamics. Part 2. Three-dimensional problems, 369

YIH, CHIA-SHUN Two solutions for inviscid rotational flow with corner eddies, 36

YIH, CHIA-SHUN Ring vortices generated electromagnetically, 436

REVIEWS

Collected works of Theodore von Kármán, Vols. I–IV, 329

Statistical Theory of Irreversible Processes, by R. EISENSCHITZ, 491

An Introduction to Fluid Dynamics, by G. TEMPLE, 493

Mathematical Theory of Compressible Fluid Flow, by RICHARD VON MISES, 494

Theorie schlallnaher Strömungen, by K. G. GUDERLEY, 650

Rheology: Theory and Application, Vol. II, edited by F. R. EIRICH, 652

Now in its second year

THE PHYSICS OF FLUIDS

EDITOR, F. N. FRENKIEL,

Applied Physics Lab., Johns Hopkins University, Silver Spring, Md.

ASSOCIATE EDITORS

Walker Bleakney	Jesse W. Beams	Carl Eckart
J. M. Burgers	S. Chandrasekhar	J. E. Mayer
Joseph Kaplan	Hugh L. Dryden	G. N. Patterson
John G. Kirkwood	Raymond J. Emrich	Lyman Spitzer, Jr.
Galen B. Schubauer	Arnold M. Kuethe	G. E. Uhlenbeck
Peter Wegener	Edward Teller	James A. Van Allen

Original contributions covering kinetic theory, statistical mechanics, structure and general physics of gases, plasmas, liquids and other fluids and including:

- Magneto-Fluid Dynamics
- Ionized Fluid and Plasma Physics
- Shock and Detonation Wave Phenomena
- Dynamics of Compressible Fluids
- Boundary Layer and Turbulence Phenomena
- Liquid State Physics and Superfluidity
- Hypersonic Physics
- Rarefied Gas Phenomena
- Upper Atmosphere Phenomena
- Physical Aeronomy
- Transport Phenomena
- Hydrodynamics

As well as certain basic aspects of physics of fluids bordering geophysics, astrophysics, biophysics and other fields of science.

ISSUED BI-MONTHLY—SUBSCRIPTIONS: $10.00 DOMESTIC, $11.00 FOREIGN

Subscription orders and inquiries should be sent to the Publisher:

American Institute of Physics, 335 East 45 Street, New York 17, N.Y.

ROGERS, RUTH H. The structure of the jet-stream in a rotating fluid with a horizontal temperature gradient, 41

SEARS, W. R. and RESLER, E. L. Theory of thin airfoils in fluids of high electrical conductivity, 257

SELLARS, JOHN R. *See* CORCOS and SELLARS

SHARP, A. W. The supersonic flow past a leading edge separation bubble, 445

SILBERMAN, EDWARD. Experimental studies of supercavitating flow about simple two-dimensional bodies in a jet, 337

STEWARTSON, K. On the stability of a spinning top containing liquid, 577

STRATFORD, B. S. The prediction of separation of the turbulent boundary layer, 1

STRATFORD, B. S. An experimental flow with zero skin friction throughout its region of pressure rise, 17

TOOMRE, ALAR A pulsating sphere in a rotating fluid, 571

TOWNSEND, A. A. Temperature fluctuations over a heated horizontal surface, 209

TOWNSEND, A. A. *See* BATCHELOR, HOWELLS and TOWNSEND

VERONIS, G. Cellular convection with finite amplitude in a rotating fluid, 401

WHITHAM, G. B. A new approach to problems of shock dynamics. Part 2. Three-dimensional problems, 369

YIH, CHIA-SHUN Two solutions for inviscid rotational flow with corner eddies, 36

YIH, CHIA-SHUN Ring vortices generated electromagnetically, 436

REVIEWS

Collected works of Theodore von Kármán, Vols. I–IV, 329

Statistical Theory of Irreversible Processes, by R. EISENSCHITZ, 491

An Introduction to Fluid Dynamics, by G. TEMPLE, 493

Mathematical Theory of Compressible Fluid Flow, by RICHARD VON MISES, 494

Theorie schlallnaher Strömungen, by K. G. GUDERLEY, 650

Rheology: Theory and Application, Vol. II, edited by F. R. EIRICH, 652

ontal

con-

two-

on of

men-

Now in its second year

THE PHYSICS OF FLUIDS

EDITOR, F. N. FRENKIEL,

Applied Physics Lab., Johns Hopkins University, Silver Spring, Md.

ASSOCIATE EDITORS

Walker Bleakney	Jesse W. Beams	Carl Eckart
J. M. Burgers	S. Chandrasekhar	J. E. Mayer
Joseph Kaplan	Hugh L. Dryden	G. N. Patterson
John G. Kirkwood	Raymond J. Emrich	Lyman Spitzer, Jr.
Galen B. Schubauer	Arnold M. Kuethe	G. E. Uhlenbeck
Peter Wegener	Edward Teller	James A. Van Allen

Original contributions covering kinetic theory, statistical mechanics, structure and general physics of gases, plasmas, liquids and other fluids and including:

- Magneto-Fluid Dynamics
- Ionized Fluid and Plasma Physics
- Shock and Detonation Wave Phenomena
- Dynamics of Compressible Fluids
- Boundary Layer and Turbulence Phenomena
- Liquid State Physics and Superfluidity
- Hypersonic Physics
- Rarefied Gas Phenomena
- Upper Atmosphere Phenomena
- Physical Aeronomy
- Transport Phenomena
- Hydrodynamics

As well as certain basic aspects of physics of fluids bordering geophysics, astrophysics, biophysics and other fields of science.

ISSUED BI-MONTHLY—SUBSCRIPTIONS: $10.00 DOMESTIC, $11.00 FOREIGN

Subscription orders and inquiries should be sent to the Publisher:

American Institute of Physics, 335 East 45 Street, New York 17, N.Y.

JOURNAL OF FLUID MECHANICS

Volume 5, Part 4 May 1959

CONTENTS

The structure of isotropic turbulence at very high Reynolds numbers
by ROBERT H. KRAICHNAN *page* 497

The dispersion of marked fluid in turbulent shear flow
by J. W. ELDER 544

Instability in a slightly inclined water channel
by A. M. BINNIE 561

A pulsating sphere in a rotating fluid
by ALAR TOOMRE 571

On the stability of a spinning top containing liquid
by K. STEWARTSON 577

On the forced motion due to heating of a deep rotating liquid in an annulus
by T. V. DAVIES 593

An unsteady turbulent boundary layer
by STURE K. F. KARLSSON 622

A cylindrical sound pulse in a rotating gas
by L. E. FRAENKEL 637

REVIEWS
Theorie schallnaher Strömungen 650

Rheology: Theory and Applications, vol. II 652

INDEX TO VOLUME 5 655

9363

Printed in Great Britain at the University Press, Cambridge
(Brooke Crutchley, University Printer)